CUTANEOUS C-FIBRES IN THE RAT AND THE RABBIT - HOW EFFERENT ACTIONS AND AXONAL PROPERTIES VARY WITH FUNCTIONAL CLASS

by

Michelle Debra Gee

A thesis submitted for the degree of
Doctor of Philosophy
in the University of London

Department of Physiology
University College London
October 1996

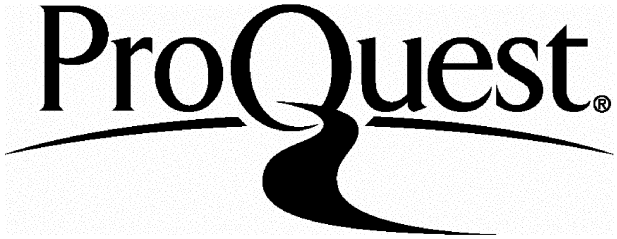

ABSTRACT

The aim of this study was to investigate further some efferent actions and axonal properties of the unmyelinated fibres innervating rabbit and rat skin.

This investigation can be separated into two parts. Firstly, single unit studies were carried out to determine which functional class(es) or sub-class(es) of C-fibre are responsible for antidromic vasodilatation in both rabbit and rat skin. The findings of these single unit studies were compared with the flare responses of the skin to noxious mechanical and heat stimuli. Secondly, activity-dependent slowing of conduction velocity and axonal spike shape were examined in identified cutaneous C-fibres in the rat in order to determine whether such axonal properties could be used to identify the different functional classes of C-fibre.

For the antidromic vasodilatation study, fine filaments were dissected from the cut proximal end of the saphenous nerve in anaesthetized rabbits and rats. Individual C-fibres (conduction velocity <2m/s) were classified into functional groups according to their responses to mechanical and thermal stimulation. The threshold for electrical stimulation of individual C-fibres was determined using the collision technique. Filaments were antidromically electrically stimulated at intensities sufficient to excite the conducting C-fibres, and skin blood flow was monitored before, during and after filament stimulation using laser Doppler perfusion imaging or laser Doppler flowmetry. In both species, the only C-fibres capable of producing a detectable vasodilator response following antidromic stimulation were nociceptive in nature, and in all cases the area of vasodilatation coincided well with the afferent receptive field. However, not all nociceptors produced a detectable

vasodilatation, and it seems that a sub-group of polymodal and heat nociceptors are responsible for the efferent action of antidromic vasodilatation in rabbit and rat skin. Flare responses in rabbit and rat skin were only detected following mechanical and heat stimuli within noxious ranges. The spread of the flare responses, together with the sizes of the afferent and efferent receptive fields of individual C-units, provide support for the axon reflex mechanism for the production of flare and antidromic vasodilatation.

The percentage slowing of conduction velocity was calculated following a standard electrical tetanus in identified C-fibres dissected from the saphenous nerve in anaesthetized rats. Nociceptive C-fibres showed a greater slowing of conduction velocity than non-nociceptive fibres, and moreover, one could separate the two classes of non-nociceptive afferent C-fibres found in the rat saphenous nerve (the mechanoreceptors and cold thermoreceptors) on the basis of their conduction velocity slowing. In addition, activity-dependent slowing of conduction velocity could be used to differentiate between the afferent and non-afferent populations of inexcitable C-fibres. Spike shapes of functionally classified C-fibres were recorded extracellularly using standardized filter settings, and some variations in spike shape in relation to receptor type were found. Polymodal nociceptors displayed wider spikes than mechanoreceptors, and cold thermoreceptor units tended to have monophasic spikes. Also, the spontaneously active sympathetic efferent C-fibres tended to have spikes of relatively long duration. The use of axonal properties such as activity-dependent slowing of conduction velocity and spike shape to differentiate nociceptors from non-nociceptors has great potential in experiments where axons are isolated from their terminals.

TABLE OF CONTENTS

LIST OF TABLES & FIGURES

ACKNOWLEDGEMENTS

My main thanks go to "the two Bruces" - to Bruce Lynn, my supervisor, for his patient and enthusiastic teaching and for his continuous encouragement, and to Bruce Cotsell for his priceless help with the experiments and for his calming influence over me.

I would like to thank the Department of Physiology at University College London for awarding me with a Bayliss Starling Scholarship, and also for providing such a friendly and helpful environment in which to work.

To my friends - you know who you are - I want to say thanks for all the good times we have had during the past few years and for all the support that your friendships have given me.

And last, but not least.....Mum, Dad and Andrew, thank you for your love and support at all times.

CHAPTER 1 INTRODUCTION

1.1 Cutaneous C-fibres - A general introduction and classification

Cutaneous C-fibres are the group of unmyelinated primary afferent nerve fibres responsible for passing sensory information from the skin to the spinal cord. In this section, I will give an overview of the different functional classes of cutaneous C-fibre that can be recorded in single-fibre studies of normal skin. Most of the studies have been carried out in whole animal *in vivo* preparations, using the teased fibre approach, whereby the nerve is repeatedly divided until single all-or-none action potentials with C-fibre conduction velocities can be recorded (Iggo 1958; Bessou and Perl 1969). Individual C-fibres can be identified using the collision technique in combination with peripheral stimulation of the afferent receptive field (Iggo 1958). By testing the responsiveness of the individual units to standard mechanical, thermal, and, in some cases, chemical stimuli, it is then possible to classify the identified C-fibres according to their sensory modality. The same approach using the teased fibre method, the collision technique and stimulation of the afferent receptive field can also be used in an *in vitro* skin-nerve preparation to study cutaneous C-fibres (Kress *et al.* 1992). The development of microneurography, whereby a microelectrode is inserted into a nerve, has allowed for the study of cutaneous C-fibres in humans (Torebjörk 1974).

Figure 1.1 shows a classification tree for the primary afferent fibres (both A- and C-fibres) innervating two frequently used preparations of mammalian skin, namely rat hairy skin and primate glabrous skin (from Lynn 1994). There are 7 main classes of C-fibre found in these two preparations, and I will briefly describe each of them. It is worth noting that the

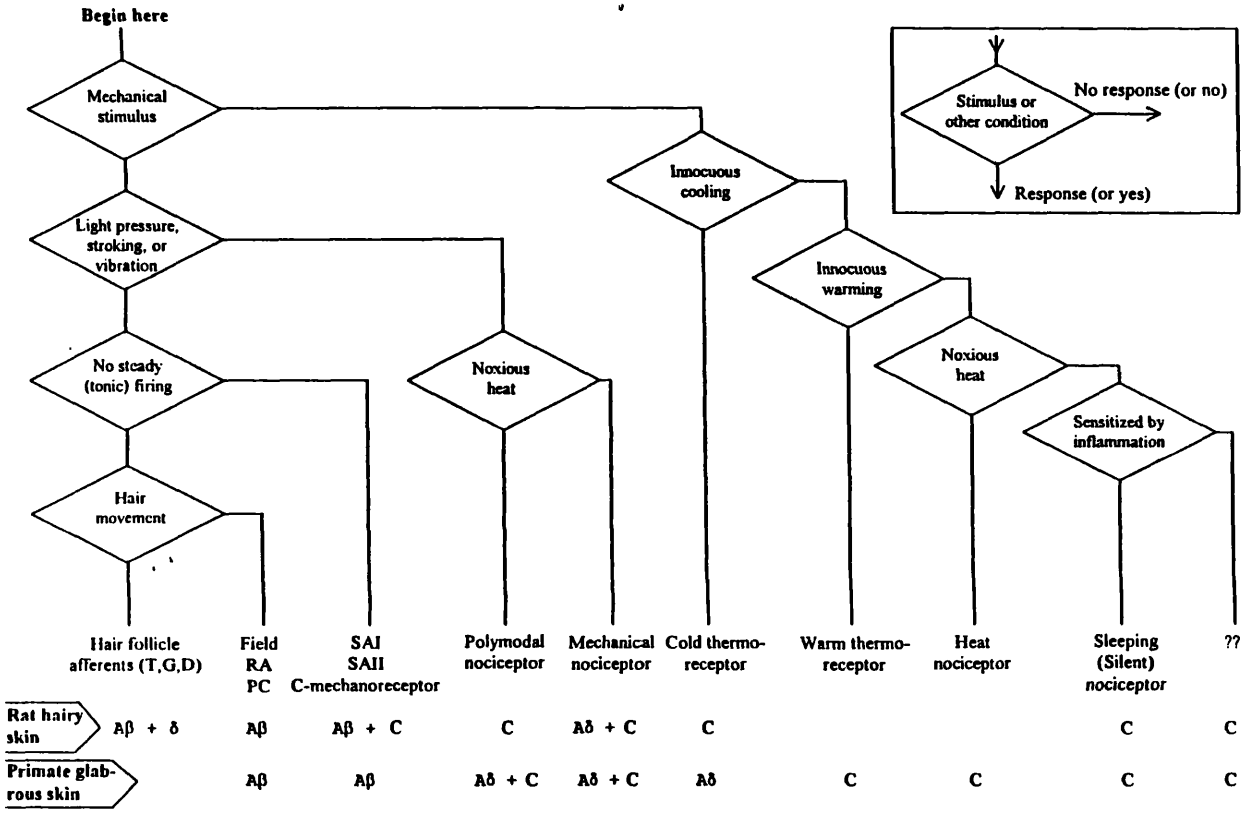

Figure 1.1 A classification tree for afferent fibres innervating mammalian skin (from Lynn, 1994). Starting at the top left corner, a series of test stimuli are applied to the skin. If a response occurs, or a condition is met, continue downwards; if no response occurs, or a condition is not met, branch to the right. Towards the bottom, the main classes of afferent units are listed. The bottom two lines indicate whether such units have been reported in significant numbers in two well studied preparations (rat hairy skin and primate glabrous skin), and if so, in which conduction velocity band they were found. Note that C-mechanoreceptors are not found in the glabrous skin of the hands or feet of primates, but they have been reported in other skin areas in primates %%464(Nordin, 1990); 465(Vallbo *et al.*, 1993)%%.

RA: rapidly adapting mechanoreceptor. PC: Pacinian corpuscle. SAI, SAII: slowly adapting type I (insensitive to lateral stretch) or type II (sensitive to lateral stretch) mechanoreceptor.

literature reveals some reluctance to agree upon a standard nomenclature (Lynn 1994, 1996b), and throughout this thesis I will use the class names presented here in the introductory section.

1. **C-polymodal nociceptors** respond to strong pressure, to heat and to irritant chemicals. They form the largest class of C-fibres innervating mammalian skin, and have been reported in the cutaneous nerves of the cat (Bessou and Perl 1969), rat (Lynn and Carpenter 1982; Fleischer *et al.* 1983), rabbit (Fitzgerald 1978, 1979; Lynn 1979), monkey (Iggo and Ogawa 1971; Beitel and Dubner 1976; Kumazawa and Perl 1977), human (Torebjörk 1974), pig (Lynn *et al.* 1995, 1996a), guinea-pig (Sugiura *et al.* 1986, 1988; Lawson 1996) and ferret (Lynn and Baranowski 1987). Such polymodal nociceptors have also been reported in lower species such as the leech and the nematode worm *Caenorhabditis elegans* (Nicholls and Baylor 1968; Belmonte *et al.* 1994; Lynn 1995). The relative proportion of C-polymodal nociceptors within a cutaneous nerve vary between species and type of nerve (e.g. nerves innervating the skin in different body areas, nerves innervating glabrous or hairy skin). Also, the electrical and afferent properties of C-polymodal nociceptors, such as their conduction velocities, mechanical thresholds and thermal thresholds, vary from unit to unit and between species and skin area. I will briefly give some indication of the properties of the C-polymodal nociceptors in the saphenous nerve of the two species studied here (i.e. the rabbit and rat).

Rat cutaneous C-polymodal nociceptors: In survey experiments carried out *in vivo* in the rat, C-polymodal nociceptors comprise between 48% and 75% of the unmyelinated fibres in the saphenous nerve (Lynn and Carpenter 1982; Fleischer *et al.* 1983; Kress *et al.* 1992), and their resting conduction velocities tend to fall in the range of 0.4-0.8m/sec (Lynn and Carpenter 1982). Rat C-polymodal nociceptors show a wide range of

mechanical sensitivity, with Lynn and Carpenter reporting thresholds ranging from 0.8mN to >50mN and Kress and colleagues reporting thresholds ranging from 8mN to >362mN (Lynn and Carpenter 1982; Kress *et al.* 1992). The mechanical thresholds vary with receptive field location and increase steadily from proximal to distal receptive fields. Lynn and Carpenter report that the average Von Frey thresholds for the rat are 7.22mN on the leg, 8.8mN on the ankle, 11.7mN on the foot and 14.8mN on the digits (Lynn and Carpenter 1982). Average heat thresholds for C-polymodal nociceptors in the rat saphenous nerve tend to be around 45°C to 47°C (Lynn and Carpenter 1982; Kress *et al.* 1992).

Rabbit cutaneous C-polymodal nociceptors: Polymodal nociceptors account for about 65% of C-fibres in the rabbit saphenous nerve, and they have resting conduction velocities in the range of 0.5m/s to 1.25m/s (Fitzgerald 1978; Shakhanbeh 1989). As in the rat, C-polymodal nociceptors in the rabbit saphenous nerve display a wide range of mechanical sensitivity, with thresholds ranging from 25mg to >5.3g and with sensitivity decreasing distally (Fitzgerald 1978). In a sample of 41 C-polymodal nociceptors from the rabbit saphenous nerve, the heat thresholds ranged from 44°C to 65°C, and had an average value of 55.2±7.1°C (mean±SD) (Fitzgerald 1978).

2. **C-mechanical nociceptors** have pressure thresholds within the noxious range, but have no heat sensitivity. They are present in cutaneous nerves of a number of species, including cat (Bessou and Perl 1969), monkey (Baumann *et al.* 1991), rat (Lynn and Carpenter 1982), rabbit (Shea and Perl 1985; Barasi and Lynn 1986; Shakhanbeh 1989), guinea pig (Sugiura *et al.* 1986, 1988), pig (Lynn *et al.* 1995) and man (Schmelz *et al.* 1994; Schmidt *et al.* 1995). In the rat saphenous nerve, mechanical nociceptors constitute only a minor class of C-fibres; in a sample of 109 characterised C-fibres dissected from the rat

saphenous nerve only 4 were mechanical nociceptors, compared to the 80 polymodal nociceptors (Lynn and Carpenter 1982). Mechanical nociceptors form only a minor class of C-fibres in rabbit cutaneous nerves too; 3-6% in the greater auricular nerve innervating the skin of the pinna (Shea and Perl 1985; Barasi and Lynn 1986) and 5% in the saphenous nerve innervating the skin of the leg and the foot (Shakhanbeh 1989).

3. **C-heat nociceptors** are excited by noxious heat stimuli, but have relatively little, or no, mechanical sensitivity. In the cases where their sensitivity to irritant chemicals (such as bradykinin and capsaicin) has been tested, they have been responsive (Baumann *et al.* 1991; Lynn *et al.* 1996a). They are reported to be present in small proportions in monkey glabrous skin (8 out of 191 = 5%; Georgopoulos 1976) and monkey hairy skin (5 out of 72 = 7%; Baumann *et al.* 1991). Microneurography studies in man reveal that heat nociceptors constitute about 6% of all C-fibres in the peroneal nerve innervating the hairy skin of the leg (Schmidt *et al.* 1995). A larger proportion (7 out of 37 = 19%) of heat nociceptors are found in the pig saphenous nerve, where they have vasodilator actions in the skin (Lynn *et al.* 1996a). However, in the rat saphenous nerve such heat nociceptors are rare (0 out of 109 characterised C-fibres, Lynn and Carpenter 1982; 0 out of 96 characterised C-fibres, Fleischer *et al.* 1983; 1 out of 89 characterised C-fibres, Kress *et al.* 1992), and no heat nociceptors have been found in rabbit cutaneous nerves, including the saphenous nerve and the greater auricular nerve (Lynn 1979; Shea and Perl 1985; Barasi and Lynn 1986; Shakhanbeh 1989).

4. **C-mechanoreceptors** are highly mechanically sensitive, responding to light stroking of the skin. In the rat saphenous nerve, they have pressure thresholds of less than or equal to 0.25mN. C-mechanoreceptors make up between 12% and 16% of the total C-fibre

population in the rat saphenous nerve (Lynn and Carpenter 1982; Kress *et al.* 1992), 21% in the rabbit saphenous nerve (Shakhanbeh 1989) and about 13% in the rabbit greater auricular nerve (Shea and Perl 1985).

5. **C-cold thermoreceptors** respond to mild skin cooling and are often spontaneously active at room temperature. In the rat, 4%-6% of C-fibres in the saphenous nerve (Lynn and Carpenter 1982; Kress *et al.* 1992) and 8% of C-fibres in the sural nerve (Handwerker *et al.* 1991) are classed as C-cold thermoreceptors. C-cold thermoreceptors also make up a small proportion of the total C-fibre population of rabbit cutaneous nerves, including the saphenous, the sural and the greater auricular nerves (Fitzgerald 1978; Lynn 1979; Shea and Perl 1985). Cold nociceptors form a separate functional class of cutaneous C-fibres in some species, although they are not present in either rat hairy skin or primate glabrous skin. Cold nociceptors are reported to innervate monkey hairy skin (Baumann *et al.* 1991) and the cat cornea (Gallar *et al.* 1993). In the skin of the guinea-pig and the rabbit, some of these cold nociceptive C-fibres are also responsive to strong pressure and are called mechanical-cold nociceptors (Shea and Perl 1985; Sugiura *et al.* 1986, 1988).

6. **C-warm thermoreceptors** respond to elevations in skin temperature of just a few degrees, and, once activated, can be silenced by cooling their afferent receptive field. Although they are not found in nerves supplying rabbit or rat hairy skin, they do innervate monkey hairy skin (LaMotte and Campbell 1978; Baumann *et al.* 1991), monkey glabrous skin (LaMotte and Campbell 1978; Darian-Smith *et al.* 1979), the skin of the upper lip, nose and limb of the dog (Iriuchijima and Zotterman 1960) and the skin of the cat limb (Hensel *et al.* 1960). Also, microneurographic recordings in man have detected small numbers of C-fibres which respond to warming of the skin within the non-noxious range of

temperatures, although these fibres also looked like they were capable of encoding thermal stimuli up to 45°C, i.e. within the lower end of the noxious range of temperatures (Konietzny and Hensel 1975).

7. Inexcitable C-fibres are the C-fibres that are insensitive to mechanical and thermal search stimuli. In a normal rat saphenous nerve, approximately 20-30% fall into this category (Pini *et al.* 1990; Pini and Lynn 1991; Kress *et al.* 1992) and in a sample of 58 C-fibres dissected from the rabbit saphenous nerve, 24% were inexcitable (Shakhanbeh 1989). Approximately half of these inexcitable units will be sympathetic efferent fibres supplying cutaneous and articular blood vessels (McMahon and Koltzenburg 1990; Kress *et al.* 1992; Karimian *et al.* 1995). The majority of the remaining inexcitable C-fibres are very high threshold afferent units called "sleeping" nociceptors. These "sleeping" nociceptors are silent under normal conditions, but they can be woken up by repeated strong stimuli or by irritant chemicals or by inflammatory events (McMahon and Koltzenburg 1990; Meyer *et al.* 1991; Cervero and Jänig 1992; Kress *et al.* 1992). Such sleeping nociceptors are also found in the knee joint and in the pelvic viscera (Schaible and Schmidt 1983, 1985; Häbler *et al.* 1988, 1990). The small remaining inexcitable C-fibres in the saphenous nerve will be non-cutaneous afferents innervating, for example, the saphenous vein (Michaelis *et al.* 1994).

As outlined above, afferent cutaneous C-fibres can be separated into highly specialized functional classes, and they have important roles in the signalling of specific sensory information about the environment. It is important to remember, however, that some of these cutaneous C-fibres have dual afferent-efferent functions. In other words, as well as providing sensory information about any mechanical, thermal or chemical stimulation of

the skin (afferent role), they are also involved in inflammation (efferent role) (see reviews by (Holzer 1988; Lynn 1988, 1996a and Section 1.2 below). An important question to be answered is which kinds of cutaneous C-fibres have such efferent roles, and in this thesis I aim to answer this question in relation to the efferent response of antidromic vasodilatation in rabbit and rat skin.

1.2 Neurogenic Inflammation

1.2.1 General introduction

The inflammatory events involving the actions of afferent nerve fibres are collectively termed "neurogenic inflammation", and comprise antidromic vasodilatation, axon reflex flare and neurogenic plasma extravasation. In this section on neurogenic inflammation, I will firstly present an historical overview of the efferent functions of afferent nerves. I will then go on to discuss in more detail which nerve fibres are thought to be involved in the generation of neurogenic inflammation. The neuropeptide content of afferent fibres will then be considered, with a view to their role in producing neurogenic inflammation. Finally, the laser Doppler techniques used here for the study of skin blood flow will be reviewed. At all times, most emphasis will be placed upon neurogenic inflammatory reactions in the skin.

1.2.2 Historical overview

The idea that sensory neurones function purely in a receptive and afferent manner was first challenged by Stricker in 1876 (see Bayliss 1901; Lynn 1996a), and was further studied at

the turn of the century by Bayliss (Bayliss 1901, 1902). Both Stricker and Bayliss demonstrated that excitation of the dorsal (sensory) roots of the spinal cord resulted in a vascular dilatation in the periphery (see Figure 1.2). The suggestion that nerve fibres with their cell bodies in the dorsal roots (i.e. sensory nerves) were capable of producing vasodilatation, which is clearly a motor effect, was an apparent contradiction to the Bell-Magendie law of separation of function, which states that sensory nerves enter the spinal cord via the dorsal roots whereas motor nerves leave via the ventral roots.

In 1913, Bruce showed that the local inflammatory responses to chemical stimulation with the irritant mustard oil were not affected by spinal cord section or by posterior root section provided that the peripheral nerve did not degenerate, but that they were reduced or abolished by chronic sensory denervation or local anaesthesia (Bruce 1913). He therefore showed that the centre for the reflex vasodilatation first studied by Stricker and Bayliss was not located in the central nervous system and was dependent upon peripheral nerve activity. Bruce went on to suggest a model which provided an explanation as to how sensory fibres could generate vasodilatation upon antidromic excitation and also how, via an axon reflex, stimulation of the sensory terminals could result in inflammation (see Figure 1.3). In his 1913 paper, Bruce also reported how chemical stimulation with mustard oil of sensory fibres innervating the conjunctiva produced swelling as well as vasodilatation, and this is the first published report of neurogenic oedema (Bruce 1913).

Thus, by 1913, two of the major signs of neurogenic inflammation (namely antidromic vasodilatation and increased vascular permeability) had been demonstrated, and a working hypothesis for the role of sensory nerve fibres in the generation of these inflammatory responses had been suggested. It was Sir Thomas Lewis in the 1920's who investigated the third mode of neurogenic inflammation - local flare around injuries (Lewis 1927).

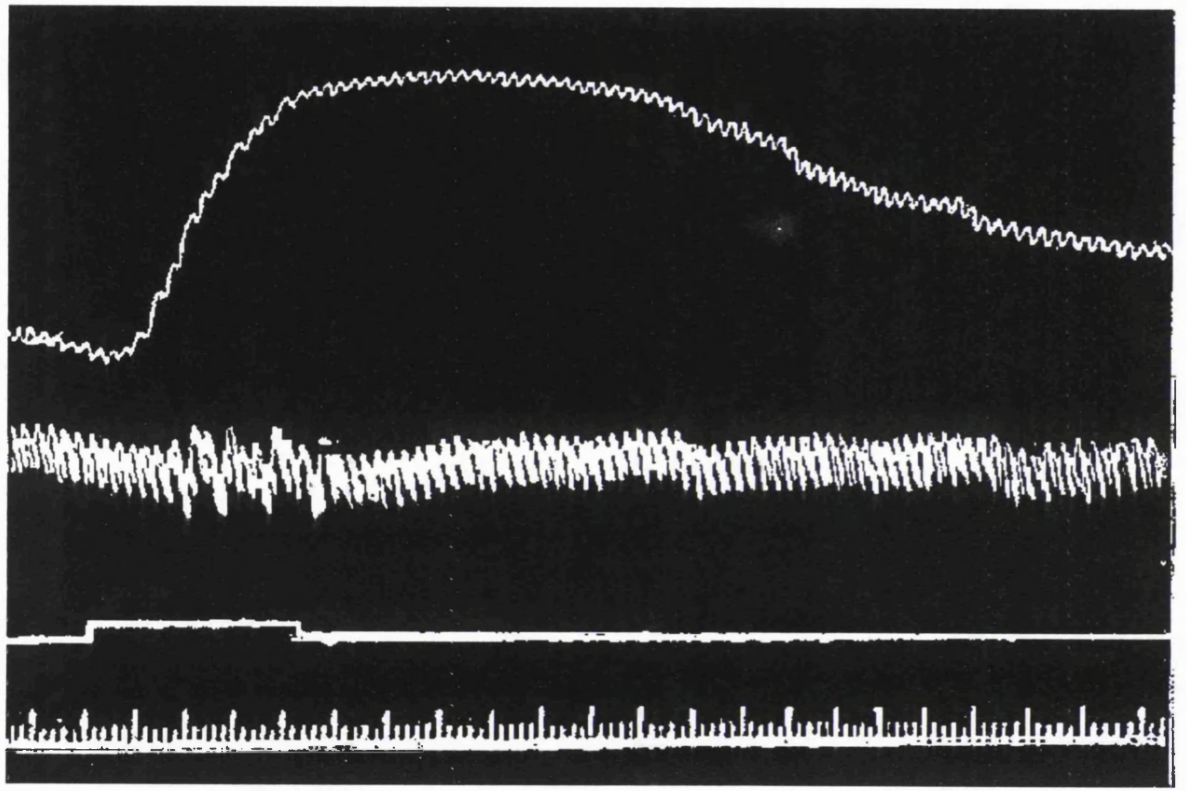

Figure 1.2 The effect of electrical stimulation at 40Hz of the L7 dorsal root on blood flow in the paw of the anaesthetized dog. From Bayliss 1901; Lynn, 1996a.

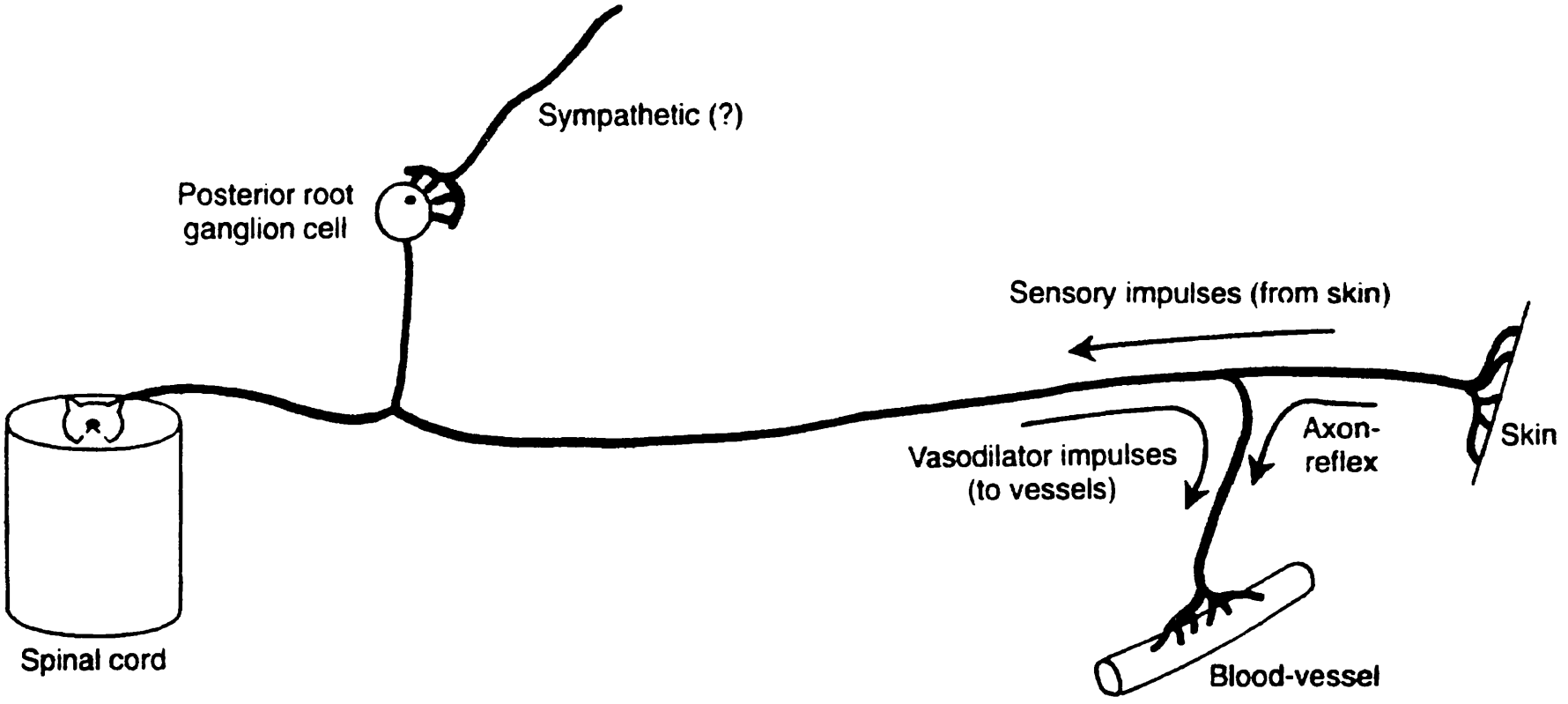

Figure 1.3 The original diagram explaining how afferent neurones can generate inflammation by axon reflexes and on antidromic stimulation. The afferent fibre, which enters the spinal cord in the posterior root, bifurcates in the periphery. One branch passes to a sensory end organ and is responsible for the conduction of sensory information from the periphery to the central nervous system. The other branch passes to blood vessels, and has an efferent effect there by bringing about vasodilatation. From Bruce, 1913.

Lewis found that the flare response around injuries was dependent upon an intact sensory innervation, and therefore it seemed likely to be due to the kind of axon reflex mechanism proposed by Bruce. Lewis, however, believed that the flare response was not due to an axon reflex in true afferent fibres, but that it was due to such a reflex in a special class of non-sensory "nocifensor" fibres arising from dorsal root ganglia. But Lewis did not provide any particularly convincing evidence to support his proposed "nocifensor" system. Likewise, since the 1920's there has also not been much support for such a system, mainly because the actions of such "nocifensor" nerves could all equally be explained by the efferent activity of regular afferent fibres achieved by way of an axon reflex. The classical axon reflex model, supported by Bruce and Lewis, where one branch has afferent properties and the other has an efferent role, was later adapted to a model where all the branches have dual receptor-effector functions (Szolcsányi 1988) (see Figure 1.4). Another mechanism that has been suggested to explain how neurogenic inflammation can result from activity in sensory nerves is the "axon response", whereby there is no peripheral branching of the afferent fibres and active neuropeptides are simply released from terminal or preterminal regions of the fibres (Lembeck 1983).

Between Bayliss, Bruce and Lewis the foundations for the concept of neurogenic inflammation had been laid. But it took many years for any significant advances to be made on understanding which nerve fibres were involved in the production of neurogenic inflammation (see Section 1.2.3 below).

So far, I have only outlined the history of antidromic vasodilatation, plasma extravasation and flare responses with respect to the skin, but the dual afferent-efferent functions of sensory neurones are not restricted to cutaneous nerves. Afferent fibres are involved in

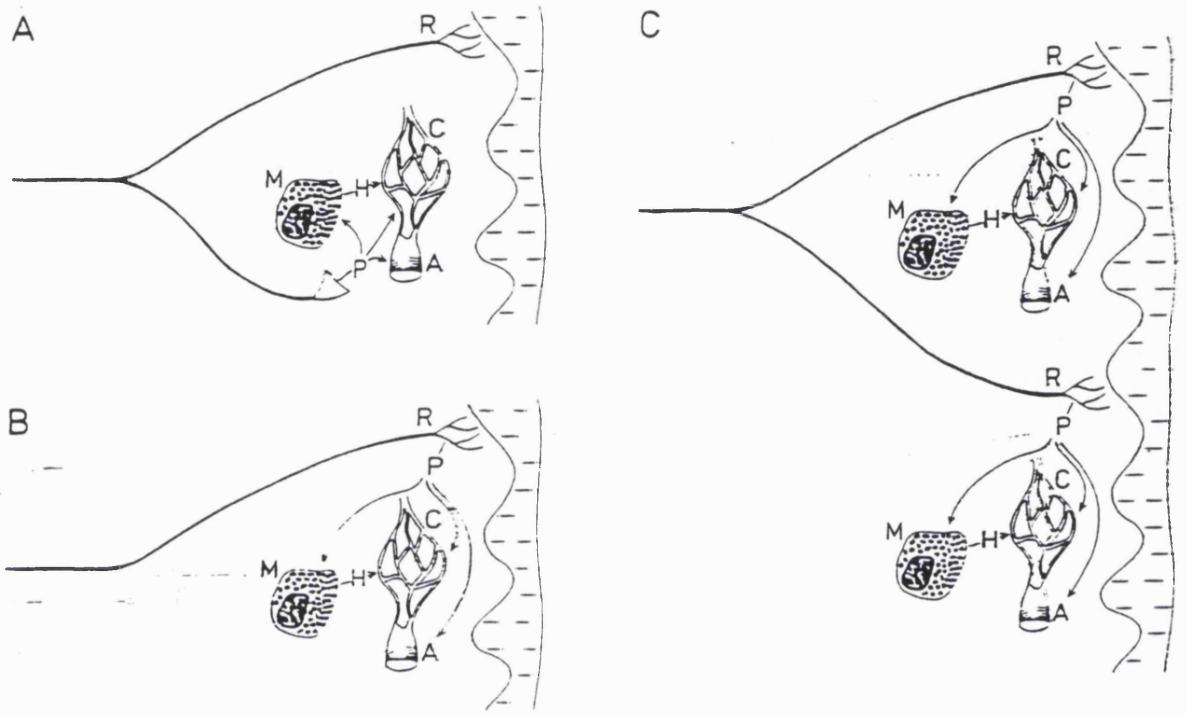

Figure 1.4 Diagrams to show possible mechanisms to account for vasodilatation, plasma extravasation and flare in skin following antidromic impulses and noxious tissue stimulation (from Bharali and Lisney, 1989).

A: Classical axon reflex proposed by Bruce (1913) and supported by Lewis (1927).

B: An "axon response" whereby the active neuropeptides are released from the terminal or pre-terminal regions of the afferent fibres %%159(Lembeck, 1983)%%.

C: The concept that afferent terminals have dual receptor-effector functions %%134(Szolcsanyi, 1988)%%.

A: arteriole. C: capillary bed. H: histamine. M: mast cell. R: sensory receptor endings. P: substance P.

neurogenic inflammatory responses to tissue injury and irritation in a number of tissues throughout the body, including the joints, the gastrointestinal tract, the respiratory tract, the eye, the gall bladder and the urogenital tract (see review by Holzer, 1988 and "Neorogenic Inflammation" by Geppetti and Holzer, 1996). In all of these tissues, increased blood flow following an injury is thought to facilitate the removal of endogenous or exogenous irritants or toxic substances (Van Hees and Gybels 1981; Lembeck 1983), and plasma extravasation is thought to aid in a faster removal of larger substances by the flow of lymph (Lembeck 1983). It is important to remember that the phenomenon of neurogenic inflammation is clinically relevant, and it has been proposed to play a role in a number of disease states, including asthma (Barnes 1986, 1989, 1990, 1996; Saria 1988), arthritis (Colpaert *et al.* 1983; Levine *et al.* 1985, 1988; Kidd *et al.* 1990; Ferrell and Lam 1996), headache and migraine (Moskowitz *et al.* 1983, 1996; Moskowitz and Buzzi 1991). Neurogenic mechanisms are also proposed to be involved in some pathophysiological conditions in the gastrointestinal tract (Holzer 1993, 1996; Holzer and Barthó 1996).

1.2.3 Which fibres are involved in neurogenic inflammation?

From as early as 1930 it has been understood that C-fibre activation results in vasodilatation (Hinsey and Gasser 1930). More specifically, it has been shown that noxious levels of stimulation are required to produce vasodilatation, thereby implicating the involvement of nociceptors (Celander and Folkow 1953). Other supporting evidence for the involvement of nociceptive C-fibres in neurogenic inflammation came from studies using capsaicin (the pungent ingredient of the red pepper, *Capsicum*). Pre-treatment of sensory nerves with capsaicin, which primarily desensitizes the C-polymodal nociceptors, leads to an inhibition of inflammation induced both by antidromic stimulation and by local

application of irritant chemicals such as mustard oil (Janscó *et al.* 1967; also see Holzer 1988; Lynn 1990). In the rat, C-fibres are also responsible for increased microvascular permeability leading to plasma extravasation (Janscó *et al.* 1967, 1968). Indeed, in rat skin, the kinds of mechanical forces required to produce flare are within the upper end of the range of mechanical thresholds of C-polymodal nociceptors (Lynn and Cotsell 1992a). Therefore, there is much evidence supporting the role of C-fibres in neurogenic inflammation, and in particular of the nociceptive C-fibres and not the non-nociceptive mechanoreceptors or thermoreceptors.

However, neurogenic inflammation is not only mediated by C-fibres. Stimulation of Aδ-fibres produces peripheral vasodilatation in rat and rabbit skin, although the vasodilatation is not as great as that seen with C-fibre stimulation (Lynn and Shakhanbeh 1988; Jänig and Lisney 1989; Kolston and Lisney 1993). An attempt at a single unit study to identify the type of Aδ-fibres with vasodilator actions in the skin was not successful (Kolston and Lisney 1993). Although Aδ-fibres produce vasodilatation in the skin, they are not capable of producing plasma extravasation (Jänig and Lisney 1989). This is also the case in the cat knee joint, where only C-fibre stimulation produces plasma extravasation (Ferrell and Russell 1986).

There have only been a few studies looking at the neurogenic inflammatory action of single identified nerve fibres (Kenins 1981; Bharali and Lisney 1992; Lynn *et al.* 1996a). Two separate groups have studied the plasma extravasation component of neurogenic inflammation at the single C-fibre level using Evan's Blue dye leakage into rat skin (Kenins 1981; Bharali and Lisney 1992). They found that upon antidromic electrical stimulation the only type of C-fibre that increased microvascular permeability were the C-polymodal

nociceptors, and that between 66% and 100% of the C-polymodal nociceptors could do so. The other successful study to identify individual afferent units with efferent actions was carried out in pig skin (Lynn *et al.* 1996a). This study revealed that the fibres with vasodilator actions in pig skin are a specialized class of C-nociceptors, called heat nociceptors, which are highly sensitive to noxious heating and irritant chemicals but which have little or no mechanical sensitivity (Lynn *et al.* 1995, 1996a).

Although neurogenic inflammation has clearly been shown to be mainly a C-nociceptor evoked process, further studies on the roles of the different kinds of C-nociceptor in cutaneous neurogenic inflammation are needed since some disparities still exist. For example, in pig skin C-heat nociceptors have been clearly shown to have vasodilator actions (Lynn *et al.* 1996a). However, although C-heat nociceptors form a major class of afferent C-fibre in the pig saphenous nerve (Lynn *et al.* 1995), they are not found in rabbit cutaneous nerves (Lynn 1979; Shea and Perl 1985; Barasi and Lynn 1986; Shakhanbeh 1989) and are very uncommon in the rat cutaneous nerves (Lynn and Carpenter 1982; Fleischer *et al.* 1983; Handwerker *et al.* 1991; Kress *et al.* 1992). Therefore, different kinds of C-fibres must be responsible for producing neurogenic vasodilatation in rabbit and rat skin than in pig skin. Could the polymodal nociceptors be responsible for antidromic vasodilatation, since they are the only C-fibres that have been shown to be capable of producing plasma extravasation in rat skin (Kenins 1981; Bharali and Lisney 1992)? Another feature of the polymodal nociceptors that makes them likely candidates for a role in antidromic vasodilatation is simply that they are the dominant nociceptive class of C-fibre innervating mammalian skin. In this study, laser Doppler techniques have been used to monitor the blood flow responses to antidromic stimulation of identified C-fibres innervating rabbit and rat skin. In addition to looking at the vasodilator response of single

identified C-fibres, the flare reaction to noxious mechanical and thermal stimulation of the skin has also been studied. Therefore, a comparison can be made between afferent and efferent receptive field sizes, and the size of flare responses, so that the validity of the axon reflex mechanism for the spread of flare can be discussed. The rabbit and rat are good animals for this study, since much is known about the relative proportions and the properties of the different classes of cutaneous afferent C-fibre in these species, and also their neurogenic inflammatory processes have been frequently studied.

1.2.4 The neurochemistry of nociceptive afferent fibres

Much interest in the question of which afferent nerve fibres are responsible for neurogenic inflammation has stemmed from studies of their neurochemistry. One of the earliest studies found that substance P, a peptide with known effects on the vasculature, was preferentially located in small dorsal root ganglion cells which have unmyelinated (C) or small myelinated (Aδ) axons (Hökfelt *et al.* 1975). Later, the vasoactive peptide, calcitonin gene-related peptide (CGRP) was characterized and its presence was demonstrated in many dorsal root ganglion neurones and afferent terminals (Rosenfeld *et al.* 1983). Other neuropeptides linked with a neurogenic inflammatory role are neurokinin A (NKA) and vasoactive intestinal polypeptide (VIP).

In order to relate the neurochemistry of specific afferent fibres to the role of these fibres in neurogenic inflammation, I will firstly discuss the evidence that nociceptive afferents contain and release neuropeptides. I will then go on to present the evidence that neuropeptides are involved in the production of vasodilatation and plasma extravasation.

1.2.4.1 The neuropeptide content of nociceptive cutaneous C-fibres

Estimates for the proportions of cutaneous neurones containing substance P and CGRP range from 20-28% and 49-60% respectively (O'Brien *et al.* 1989; Lawson 1996). By combining studies marking neuropeptides with an assessment of the morphology and the neurofilament content of the cell in question, it is possible to be more specific and to make an estimate of the percentage of C-fibres containing certain peptides. Dorsal root ganglion cells can be divided into two groups on the basis of their morphological properties (using conventional Nissl staining techniques) and of their neurofilament content (e.g. using RT97, a monoclonal antibody against the 200kDa neurofilament subunit): large, light neurones are neurofilament-rich and have fibres with A-fibre conduction velocities, whereas the small dark cells have relatively little neurofilament and have unmyelinated fibres (Lawson 1992, 1995, 1996). 61-71% of rat dorsal root ganglion cells innervating the skin were found to be negative to RT97 and therefore had C-fibre axons (O'Brien *et al.* 1989). By looking at the immunoreactivity of rat dorsal root ganglion cells to both RT97 and specific neuropeptides, O'Brien and colleagues were able to estimate the proportion of cutaneous C-fibres that contained certain peptides: 37% of small dark cells (RT97 negative, unmyelinated axons) contained substance P and 50% contained CGRP (O'Brien *et al.* 1989).

However, as discussed in section 1.2.3 above, neurogenic inflammation seems to involve mainly the nociceptive C-fibres, and the estimates of the proportions of cutaneous C-fibres containing various neuropeptides presented by O'Brien and colleagues does not distinguish between the nociceptive and non-nociceptive C-fibres. The most direct way to assess the neuropeptide content of cutaneous fibres with identified sensory receptors is to make

intracellular recordings from identified dorsal root ganglion cells combined with dye injection to allow for immunocytochemistry of the neurone (Lawson 1995, 1996). However, only a few studies of this type have been made (Leah *et al.* 1985; Zhang and Hoffert 1987; Lawson *et al.* 1993, 1994, 1996; Hoheisel *et al.* 1994). One study in the cat revealed that there is no clear correlation between the content of the neuropeptides tested (substance P, CGRP, somatostatin and VIP) and sensory receptor type (Leah *et al.* 1985). However, another study carried out in cat dorsal root ganglion cells with A-fibres reported that substance P was found in 2 of the 3 mechanical nociceptors tested, but in none of the 5 non-nociceptive A-fibre cells (Zhang and Hoffert 1987). In the rat, the majority of cells containing CGRP were small/medium sized (cross sectional area $<1200\mu m^2$) and the neurones had conduction velocities of less than 2.5m/sec; also, CGRP was preferentially located in high threshold mechanosensitive cells (Hoheisel *et al.* 1994). In the guinea-pig, both substance P and CGRP were found to be present in the dorsal root ganglia of both nociceptive and non-nociceptive A- and C-fibres, although these peptides were not located in all nociceptive cells tested (Lawson *et al.* 1994, 1996). The over-riding problem with drawing any definitive conclusions from these studies on the neuropeptide content of physiologically identified afferent fibres is that the numbers of each of the various fibre types encountered were very small. The problem is further confounded by the use of different classifications by the separate research groups, for example, Leah and colleagues have opted to divide the afferent fibres into very broad classes (Leah *et al.* 1985). The small numbers reported are due to the technical difficulties in performing these experiments and the time consuming nature of this kind of study. It would be very useful if it were possible to differentiate between nociceptive and non-nociceptive cells in the dorsal root ganglion without having to find and identify their cutaneous receptor. As reported in this thesis and in a recently published paper (Gee *et al.* 1996), the axonal property of

activity-dependent slowing of conduction velocity can be used to distinguish between nociceptive and non-nociceptive C-fibres. The use of this quick and simple method for determining the sensory modality of individual C-fibres should greatly improve the yield of information from experiments looking at the neuropeptide content of physiologically identified cutaneous afferent fibres.

1.2.4.2 Release of neuropeptides from nociceptive fibres

In the guinea-pig, it has been shown that the majority of substance P produced in sensory ganglion cells is transported axonally towards the terminals of the peripheral branches rather than in a central direction (Brimijoin *et al.* 1980). Furthermore, the neuropeptides have been shown to be localized in large granular secretory vesicles, e.g. CGRP and substance P in guinea-pig trigeminal ganglia, dorsal root ganglia and peripheral nerve fibres (Gulbenkian *et al.* 1986), and VIP in cat non-sympathetic nerve axons and terminals in the cerebral arterial walls (Lee *et al.* 1984). Neuropeptide release has been shown to be a calcium-dependent process (Hua *et al.* 1986; Franco-Cereceda *et al.* 1988; Saria *et al.* 1988; Geppetti *et al.* 1990a, b, 1991; Maggi 1991a, b, 1993; Lou *et al.* 1992; Lundberg *et al.* 1992).

Direct evidence for the release of substance P from afferent nerve fibres has been gained from several tissues and species, including cat tooth pulp (Olgart *et al.* 1977; Brodin *et al.* 1981; Gazelius *et al.* 1981), rabbit eye (Bill *et al.* 1979), rat skin (White and Helme 1985) and guinea-pig lung (Saria *et al.* 1987, 1988). There is also direct evidence for the nerve stimulation induced release of other neuropeptides, for example NKA in guinea-pig lung

(Saria *et al.* 1987, 1988) and CGRP in a number of tissues (Wahlestedt *et al.* 1986; Lundberg *et al.* 1992).

Evidence directly implicating nociceptive fibres in the release of neuropeptides comes from studies in a variety of tissues and species showing that the adequate stimuli for neuropeptide release fall within the noxious range. For example, in normal rat skin, noxious thermal stimulation at 50°C results in substance P release, and this is much reduced in denervated skin (Helme *et al.* 1986). Irritation-inducing mechanical stimulation of the rabbit eye has been shown to stimulate CGRP release (Wahlestedt *et al.* 1986). Capsaicin, which selectively excites nociceptive C-fibres, produces substance P, CGRP and NKA release from guinea-pig lung, heart and ureter (Hua *et al.* 1986; Saria *et al.* 1987, 1988; Franco-Cereceda *et al.* 1988; Martling *et al.* 1988; Lou *et al.* 1992; Lundberg *et al.* 1992) and from the glandular part of the rat stomach (Geppetti *et al.* 1991). Other chemicals that stimulate nociceptive fibres have also been shown to result in neuropeptide (specifically substance P, CGRP and NKA) release; for example bradykinin, histamine and hydrogen ions release neuropeptides in the guinea-pig lung, heart and bladder and in the rat stomach (Saria *et al.* 1987, 1988; Geppetti *et al.* 1990a, b, 1991; Lundberg *et al.* 1992). However, bradykinin, histamine, serotonin, prostaglandin E1, prostaglandin E2 and acetylcholine were all unable to stimulate neuropeptide release from the guinea-pig ureter, despite high concentrations being tested (Hua *et al.* 1986).

1.2.4.3 Neuropeptides and neurogenic inflammation

I have described the evidence for nociceptive C-fibres containing and releasing neuropeptides. The evidence that the various neuropeptides released are involved in

vasodilatation and plasma extravasation comes from a number of studies carried out in different tissues and species.

Calcitonin gene-related peptide (CGRP) is described as the most potent vasodilator of the neuropeptides and it has the longest duration of action (Lynn 1996a). In both rabbit and human skin, injection of CGRP causes significant vasodilatation (Brain *et al.* 1985, 1986). The effect of CGRP on vasodilatation has also been examined in rat knee joint (Cambridge and Brain 1992; Lam and Ferrell 1993), hamster cheek pouch (Hall and Brain 1992), rabbit eye (Wahlestedt *et al.* 1986) and rabbit skeletal muscle (Ohlen *et al.* 1987). CGRP has no direct effect on the permeability of the microvasculature of rat skin or rat trachea although it has been shown to potentiate the plasma extravasation induced by other neuropeptides (Gamse and Saria 1985; Gamse *et al.* 1987; Brokaw and White 1992). There is some dispute as to whether CGRP can directly alter microvasculature permeability in the rat knee joint (Cambridge and Brain 1992; Cruwys *et al.* 1992; Green *et al.* 1992; Karimian and Ferrell 1994). In this tissue CGRP has been shown to have a potentiating effect on histamine-induced and substance P-induced plasma extravasation (Cambridge and Brain 1992; Cruwys *et al.* 1992) and to produce plasma extravasation when co-perfused with substance P (Green *et al.* 1992).

Substance P produces no direct vasodilatation in rat skin, but it reduces the CGRP-induced vasodilatation in this tissue (Brain and Williams 1988). In rabbit skin, substance P is described as a weak vasodilator (Williams 1982). However, in other species and tissues substance P is a vasodilator (hamster cheek pouch, Hall *et al.* 1994; rabbit skeletal muscle, Ohlen *et al.* 1987; rat skeletal muscle, Baptist and Marshall 1993). There is some dispute as to whether substance P dilates vessels in the rat knee joint (Cambridge and Brain 1992;

Lam and Ferrell 1993). Substance P can increase the microvascular permeability of the skin (Hagermark *et al.* 1978; Chahl 1979; Foreman *et al.* 1983; Gamse and Saria 1985; Gamse *et al.* 1987), bladder (rat, Koltzenburg and McMahon 1986; guinea-pig, Lundberg *et al.* 1984), eye (rabbit, Bill *et al.* 1979) and airways (Saria *et al.* 1983). Substance P has also been shown to induce plasma protein extravasation in the rat knee joint and the inflammatory response to substance P is greater in the inflamed joint (Scott *et al.* 1991, 1992).

Neurokinin A (NKA) is a vasodilator (skeletal muscle, Ohlen *et al.* 1987; hamster cheek pouch, Hall *et al.* 1994) and it also produces plasma extravasation (airways, Saria *et al.* 1983; rat skin, Gamse and Saria 1985; Gamse *et al.* 1987; Andrews *et al.* 1989) although it is less potent than substance P.

Vasoactive intestinal polypeptide (VIP) is a potent vasodilator in rabbit skin (Williams 1982) and it has also been shown to dilate cerebral arteries (Lee *et al.* 1984; Edvinsson *et al.* 1985) and mesenteric vessels (Tornebrandt *et al.* 1987). Although VIP was weak in terms of increasing microvascular permeability in rabbit skin, it was potent in enhancing oedema (Williams 1982). VIP has been shown to have no effect on microvascular permeability in other species and tissues (Chahl 1979; Gamse *et al.* 1980).

Further evidence that the neuropeptides discussed above are involved in neurogenic vasodilatation and plasma extravasation come from studies using selective neuropeptide antagonists. $CGRP_{8-37}$ is the C-terminal fragment of human αCGRP, and it is a competitive antagonist at the CGRP receptor (Chiba *et al.* 1989; Han *et al.* 1990). *In vivo*, the neurogenic vasodilatation in rat and rabbit skin induced by topical capsaicin is completely

inhibited by $CGRP_{8-37}$ (Escott and Brain 1993; Hughes and Brain 1994). Also, $CGRP_{8-37}$ can inhibit the increased blood flow in rabbit skin induced by intradermal injection of capsaicin or capsaicin analogues, such as olvanil and resinferatoxin (Hughes *et al.* 1992). This antagonist produced an inhibition of the vasodilatation and plasma extravasation in rat skin following electrical stimulation of the saphenous nerve (Escott and Brain 1993). However, CGRP itself does not produce plasma extravasation in rat skin (see above), and so this effect cannot be a direct one. It has been suggested that this the effect of $CGRP_{8-37}$ on plasma extravasation is likely to be secondary to the increased blood flow (Brain and Williams 1985; Brain and Williams 1989).

There are several antagonists to the NK_1 receptor, which is the high affinity receptor for substance P. In rat and guinea-pig skin, a variety of NK_1 receptor antagonists have been shown to inhibit the formation of oedema induced by substance P, mustard oil, carrageenan and antidromic stimulation of the saphenous nerve (CP-96,345, Birch *et al.* 1992; Lembeck *et al.* 1992; Nagahisa *et al.* 1992; Xu *et al.* 1992; RP-67,580, Garret *et al.* 1991; SR-140333, Emonds-Alt *et al.* 1993). Spantide II, a tachykinin antagonist, inhibits the plasma extravasation in rat skin following stimulation of the sciatic nerve at C-fibre intensity (Xu *et al.* 1991). NK_1 antagonists also have an effect on plasma extravasation in the airways, where they greatly reduce or abolish the neurogenic response (Lembeck *et al.* 1992; Ball *et al.* 1993; Lundberg 1993).

The inhibitory effect that the NK_1 receptor antagonists have on plasma extravasation, together with the evidence that substance P produces plasma extravasation, give a good indication that substance P plays an important part in neurogenic changes of vascular permeability. And the results from the CGRP antagonist studies, taken in association with

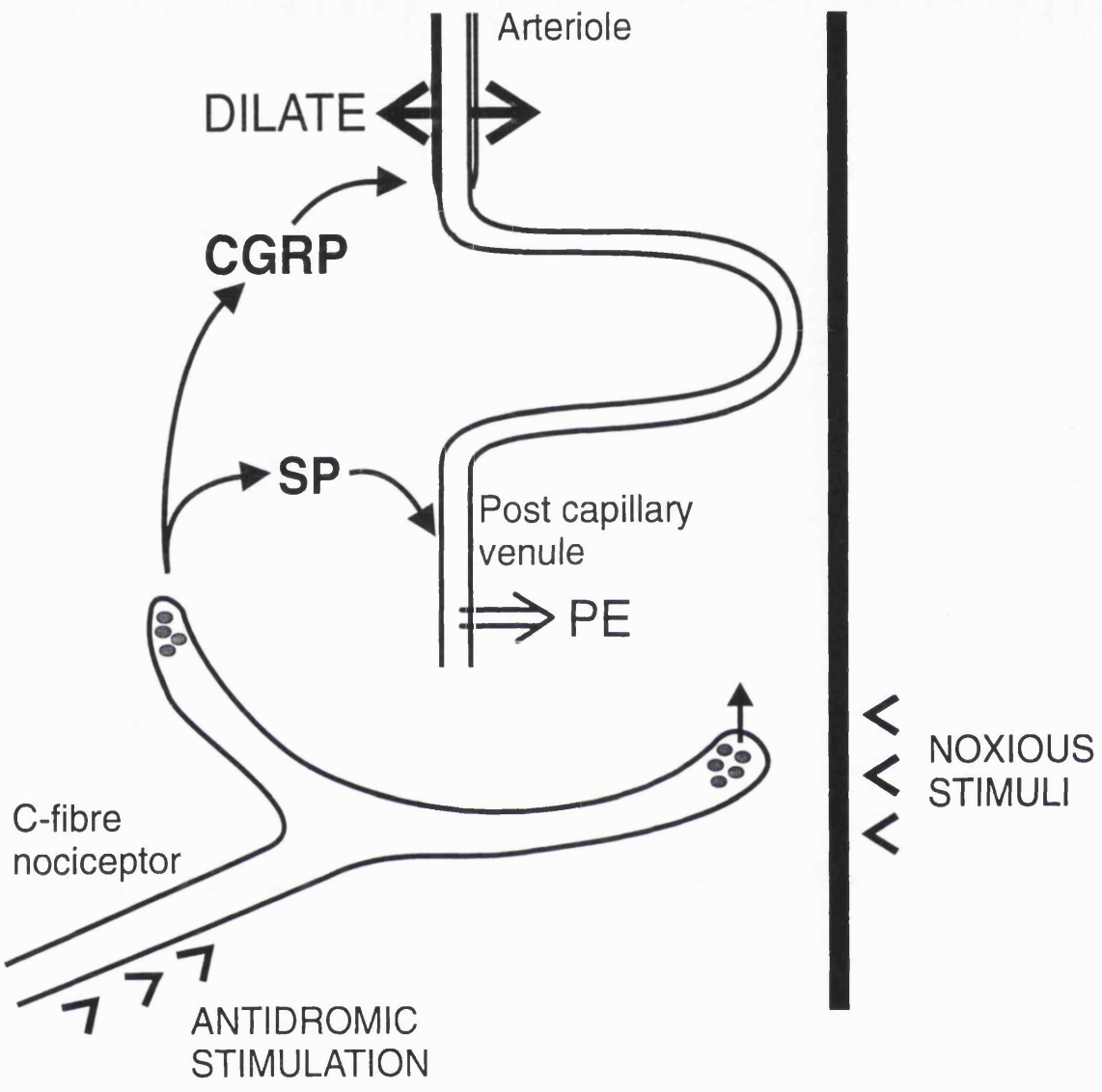

Figure 1.5 Neurogenic vasodilatation and plasma extravasation in the skin, and the mediators involved in these processes. SP, substance P; CGRP, calcitonin gene-related peptide; PE, plasma extravasation. From Lynn, 1996a.

the evidence that CGRP is a potent vasodilator, show that neurogenic vasodilatation is mainly due to the release of CGRP. The main efferent actions that substance P and CGRP have in the skin following their release from the peripheral terminals of cutaneous nociceptors are summarized in Figure 1.5 (from Lynn, 1996a).

1.2.5 Laser Doppler techniques for monitoring tissue perfusion

The methods used to monitor cutaneous antidromic vasodilatation and flare in this study are laser Doppler flowmetry and laser Doppler perfusion imaging. The use of laser Doppler techniques seems to be the preferred approach for monitoring tissue perfusion of recent years, and they have been used in a variety of species and tissues, including human skin (Brain *et al.* 1986; Lynn and Cotsell 1991; Wårdell *et al.* 1993), rat and rabbit skin (Gamse and Saria 1987; Lynn and Cotsell 1992a, b; Escott and Brain 1993), pig skin (Lynn *et al.* 1996a), rat knee joint (Lam and Ferrell 1993; Karimian *et al.* 1995) and cat dental pulp (Vongsavan and Matthews 1992; Andrew and Matthews 1996). In this section, I will briefly describe the principles of the techniques of laser Doppler flowmetry and laser Doppler perfusion imaging, and outline their advantages and disadvantages as methods for monitoring tissue perfusion.

1.2.5.1 Laser Doppler flowmetry

Laser Doppler flowmetry can provide a continuous record of blood flow in tissues. A low power (1-5mW) He-Ne laser is used as a light source and is directed at the tissue to be studied. Within the tissue, the light is scattered by the moving red blood cells and undergoes Doppler shifts in frequency, the magnitude of which depends upon the velocity of the cells. Light is guided to and from the tissue by a pair of flexible optical fibres. The intensity of the

backscattered Doppler-shifted light is detected by a photodetector and is converted into an electrical signal, so that there is a linear relationship between the electrical signal and the tissue perfusion at the point of measurement.

Laser Doppler flowmetry can be used to monitor tissue perfusion over a period of time at a given position. It has been used in a variety of tissues, including skin (Gamse and Saria 1985), bone, muscle, peripheral nerve, kidney, heart, brain, gastro-intestinal tract, oral mucosa and dental pulp (Holloway 1983; Vongsavan and Matthews 1992, 1993; Wårdell 1992). However, there are some disadvantages to the use of laser Doppler flow meters for measuring blood flow:

- The laser Doppler flow meters cannot be calibrated in absolute units of blood flow, and so the experimental protocol used must allow one to look for a change in blood flow from control conditions.
- Laser Doppler flow meters monitor temporal changes in blood flow at a single measurement site. Because of spatial variations in blood flow in a tissue, laser Doppler flowmetry is not well suited to looking at blood flow distribution over a whole area.
- The light guides are easily jogged, resulting in artefacts that can make the interpretation of results difficult.
- The probes need to be attached to, or close to, the tissue being studied. In some cases this is not very practical since it can cause pain and provides a risk of infection.

1.2.5.2 The laser Doppler perfusion imaging system

The Laser-Doppler perfusion imaging system works on the same principle as the laser Doppler flow meters, but it allows one to monitor tissue perfusion over an area and it can generate, process and display colour-coded images of tissue perfusion. The two mirrors of the scanner

are moved by two stepping motors, and this guides the low power He-Ne laser beam to the tissue surface (see Figure 1.6). The mirrors move the laser beam sequentially over the tissue, step by step and the imaging system used in this study (Lisca Developments, Linkoping, Sweden) allows a maximum of 4,096 measurements to be made. At each measurement site the laser beam penetrates the tissue to a depth of a few hundred microns. The principle of the imaging system is the same as for the laser Doppler flowmeters, in that when the beam hits red blood cells it is scattered and Doppler-shifted. The backscattered Doppler-shifted light is detected by a photodetector located in the scanner head, and this transforms the light intensity into an electrical signal. The signal processor produces an output that is proportional to tissue perfusion. When the scanning has finished, and all measurements are captured and stored in the computer, a colour-coded perfusion image is displayed on the monitor. Software allows subtraction of the images so one can perform a baseline scan (background control), then take a scan immediately after stimulation of the cutaneous nerve and subtract the images to see the change brought about by the nerve stimulation. One can continue scanning until the subtractions of the images show that there has been a complete recovery from any response.

Laser Doppler perfusion imaging overcomes some of the disadvantages of Laser Doppler flowmetry. Since laser Doppler perfusion imaging does not involve flexible optical fibres, there is no problem with movement artefacts. The imaging system is designed to look at spatial distribution of perfusion of a tissue over a certain area, rather than monitoring temporal changes in blood flow at a single site as with laser Doppler flowmetry.

Both laser Doppler flowmetry (giving temporal information about cutaneous perfusion at a single site) and the laser Doppler perfusion imaging system (giving spatial information about blood flow over an area of skin) have been successfully employed to determine the

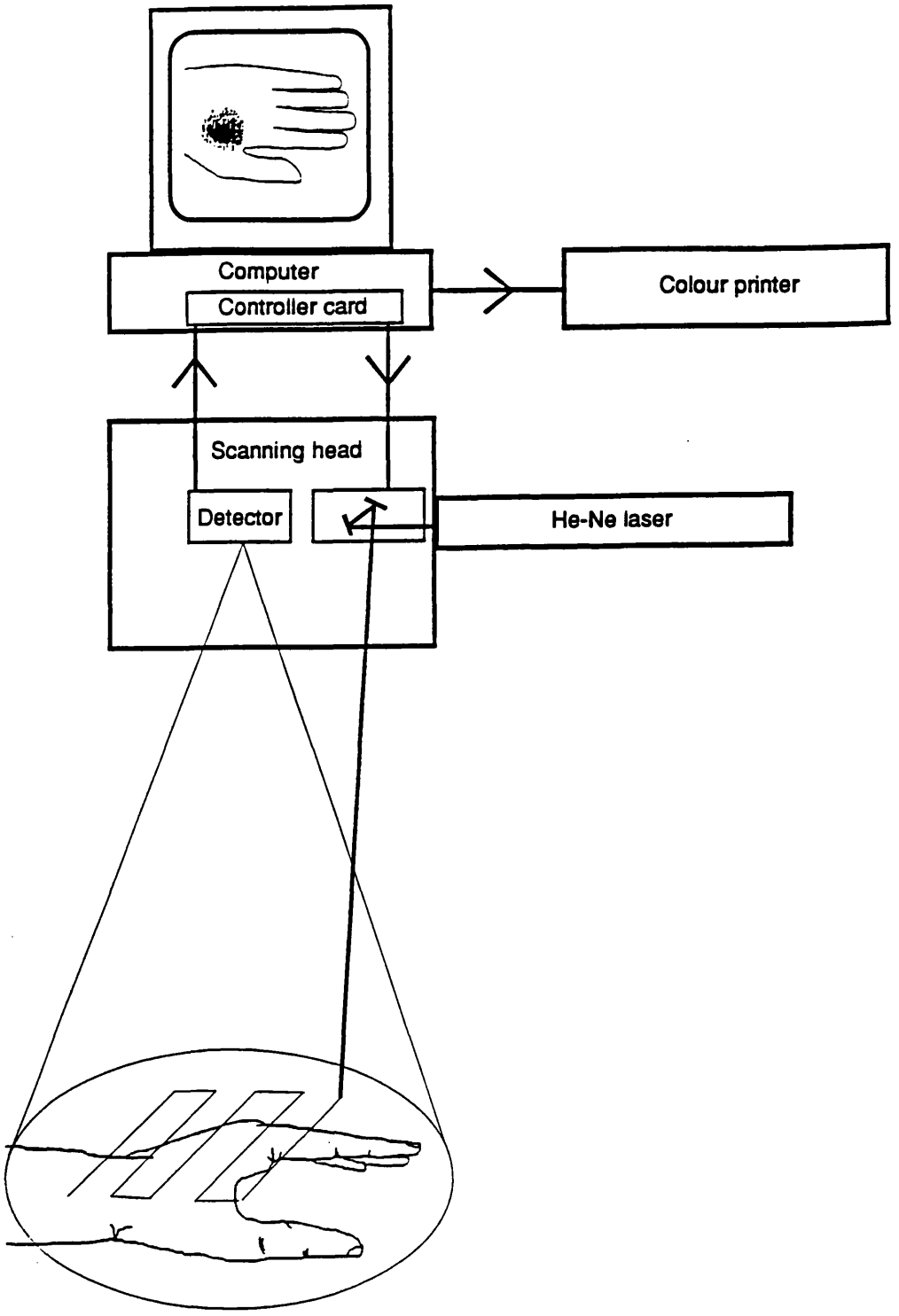

Figure 1.6 Schematic diagram of the laser Doppler perfusion imaging system.

vascular responses in rabbit and rat skin to the antidromic stimulation of single identified C-fibres (see Chapters 3, 4 and 8). Furthermore, the laser Doppler perfusion imaging system has been used to study the flare responses of rabbit and rat skin to noxious stimuli, and this system produced useful information on the intensity, extent and duration of the flares (see Chapters 5 and 8).

1.3 Some electrical properties of axons

The traditional view regarding the different functional classes of sensory neurones is that they are separated according to the adequate stimuli to which they respond. However, there are intrinsic differences between the various types of sensory neurones, e.g. differences in dorsal root ganglion spike shape (Koerber and Mendell 1992), and these differences raise the important question as to whether such variations in electrical properties can be utilized for identification purposes. In this section, I will firstly describe studies that have revealed a functional heterogeneity of somatic action potential shape. I will then discuss evidence showing that the phenomenon of activity-dependent slowing of conduction velocity varies with receptor type between cold thermoreceptive fibres and nociceptive fibres with the same conduction velocity. In this section I will also introduce the studies of the two axonal properties that are reported in this thesis; axonal spike shape and activity-dependent slowing of conduction velocity were studied in the different functional classes of cutaneous C-fibres in the rat saphenous nerve with the aim of seeing the extent to how they varied with sensory modality.

1.3.1 The functional heterogeneity of somatic spike shape

One of the earliest pieces of work investigating the relationship between action potential shape and receptor modality was carried out in the leech (Nicholls and Baylor 1968). The principle advantage of any neurophysiological studies on the leech, is that the leech has a relatively simple nervous system. For example, there are just 3 different kinds of sensory neurones in the leech, and they are located within the segmental ganglion. They are the T, P and N cells, and are excited by light touch, pressure and noxious stimuli respectively. Intracellular recordings show that the high threshold sensory neurones (i.e. the P and N cells) have larger and wider spikes than the low threshold sensory cells (i.e. the T cells). With practice, it is possible to distinguish the different kinds of sensory cell on the basis of action potential shape, and this provides neurophysiologists working on the leech with a very useful identification method.

Another interesting study on variations of spike shape with receptor modality was carried out on the pit viper snake (Terashima and Liang 1994). Intrasomal recordings from trigeminal ganglia in the snake revealed that vibrotactile neurones (which respond to vibration as well as touch) displayed larger and narrower spikes than warm thermoreceptive neurones, with the class of neurones responding only to touch having an intermediate spike shape.

Moving away from the leech and the snake and onto mammalian and avian nervous systems, there have been a number of groups who have made intracellular recordings from dorsal root ganglion cells and who report a heterogeneity in spike shape, finding some broad action potentials with an inflection on the falling phase (Yoshida *et al.* 1978; Görke

and Pierau 1980; Harper and Lawson 1985). However, in these studies, it was not possible to characterize the type of receptor innervated by the individual neurones, and so no attempt could be made at linking somatic action potential shape with peripheral receptor type.

In mammalian sensory neurones, the earliest study reporting a difference in spike shape between fibres with different receptor types was carried out in an *in vitro* preparation of the petrosal ganglion of the glossopharyngeal nerve of the cat (Belmonte and Gallego 1983). The petrosal ganglion houses the cell bodies of the sensory nerve fibres of the carotid sinus nerve, i.e. the baroreceptors from the carotid sinus and the chemoreceptors from the carotid body. Intracellular recordings were made from the petrosal ganglion and showed that chemoreceptor neurones with myelinated axons (average conduction velocity = 11m/s) had wider spikes with a hump on the falling phase. There were 2 types of baroreceptor neurones with myelinated axons. The fast baroreceptors (average conduction velocity = 33m/s) had narrow action potentials without any inflection on the falling phase. However, the slow baroreceptors (average conduction velocity = 10m/s) which had conduction velocities similar to the chemoreceptors also had spikes with similar shapes to those found in the chemoreceptors, i.e. relatively wide with an inflection on the falling phase. Therefore, in this system, there is some overlap between receptor type and spike shape, and it looks like conduction velocity is also involved in the determination of the spike shape.

The first study in a vertebrate system that allowed for a direct examination of the relationship between somatic action potential shape and receptor type, independent of any influence of conduction velocity, was carried out by Mendell and colleagues (Rose *et al.*

1986; Koerber *et al.* 1988). Recording intracellularly from dorsal root ganglion cells in anaesthetized cats, they studied the somatic spike shapes of Aß and Aδ fibres. Within both the Aß and the Aδ groups, they found cells innervating both nociceptive and non-nociceptive receptors, as well as some inexcitable cells for which peripheral receptive fields could not be located. That they found both nociceptive and non-nociceptive Aß and Aδ cells agrees with earlier studies of A-fibre afferent classes in the cat (Burgess and Perl 1967; Burgess *et al.* 1968; Perl 1968). The Aß neurones had smaller and briefer spikes than the Aδ cells. In addition to these differences in spike shape that are related to conduction velocity, variations in spike shape related to receptor type and independent of conduction velocity were also found. In both the Aß and Aδ populations, those cells innervating high threshold receptors had larger spikes with longer durations than those cells innervating low threshold peripheral receptors. The long spike duration was mainly due to an inflection on the falling phase of the action potential. The cells with Aß fibres innervating different kinds of low threshold mechanoreceptors (such as slowly adapting I units, slowly adapting II units, Pacinian corpuscles) were not distinguishable on the basis of somatic action potential shape. Therefore, this study provided conclusive evidence that for Aß and Aδ afferent fibres, somatic action potential shape varied with receptor type, with nociceptors displaying larger and wider spikes than non-nociceptors.

Mendell's group proceeded to study the relationship between somatic action potential shape and peripheral receptor type in cells with myelinated axons in the rat (Ritter and Mendell 1992). The situation in the rat was the same as in the cat, in that the cells innervating high threshold receptors responsive to noxious stimuli had long-duration spikes with a characteristic inflection on the falling phase. Those cells with A-fibre axons innervating low threshold receptors had briefer spikes with no inflections. Also, the cells

with high threshold receptors tended to have larger spikes, slower peak rates of rise and longer after-hyperpolarizations than those with low threshold receptors.

In the cat and the rat, therefore, there is a clear relationship between somatic action potential shape and A-fibre peripheral receptor type, that is independent of conduction velocity (Rose *et al.* 1986; Koerber *et al.* 1988; Ritter and Mendell 1992). There has only been one study looking at this relationship in dorsal root ganglion cells with unmyelinated (C-fibre) axons (Traub and Mendell 1988), and this work was carried out in the cat. As well as confirming earlier findings that Aδ afferents responsive to noxious stimuli had wide somal action potentials with a hump on the falling phase whereas Aδ afferents responsive to low threshold stimuli had narrow spikes without any inflections (Rose *et al.* 1986; Koerber *et al.* 1988), they also found that all the C-fibre afferents studied had broad somatic spikes with inflections on the falling phase, irrespective of modality. In contrast, a study of C-fibre axonal spike shape in the pig reveals that there is some heterogeneity of spike shape within the group of unmyelinated sensory neurones, and that this heterogeneity is related to receptor type (Lynn *et al.* 1996b). In the pig saphenous nerve C-fibre nociceptors have wider spikes than mechanoreceptors with the same conduction velocity. Also, differences in axonal spike shape exist within the group of nociceptive C-fibres, with the heat-sensitive nociceptors tending to have wider spikes than the polymodal nociceptors (Lynn *et al.* 1996a).

In this thesis, I will report on the study of axonal spike shape carried out on cutaneous C-fibres in the rat. Although, the work of Traub and Mendell revealed that all C-fibres have a similar somatic spike shape regardless of sensory modality (Traub and Mendell 1988), the finding that spike shapes vary with C-fibre class in the pig make this study in the rat most

worthwhile (Lynn *et al.* 1996a). There are clear benefits to be had if there is a relationship between axonal spike shape and sensory receptor type in the rat saphenous nerve, in that, if the differences are great enough, spike shape could be used as an tool for identifying a particular class of C-fibre. This would speed up the characterization process of individual units, which at the moment involves the testing of afferent receptive fields with a range of stimuli. In addition, the identification of particular fibre types in experiments where axons are separated from their receptive fields would become a possibility.

1.3.2 The ionic currents underlying spike shapes

A number of studies have revealed differences in cell membrane currents that can be related to the shape of the action potential, and, therefore, they can also be related to cell type. Recordings from isolated dorsal root ganglion cells from the mouse have shown that neurones can be divided into 3 main classes according to the properties of their spike (Yoshida *et al.* 1978), and the axonal conduction velocity varied between these 3 different classes of dorsal root ganglion cells (Yoshida and Matsuda 1979). 68% of the cells were classed as F neurones, and they exhibited relatively small amplitude spikes with fast peak rates of rise and brief after-hyperpolarizations. The spikes of the F neurones were sensitive to tetrodotoxin (TTX). F neurones had a large or medium sized cell body and their axons showed a fast conduction velocity, indicating A-fibres. 27% of the mouse dorsal root ganglion cells were classed as A neurones, and they had relatively broad TTX-insensitive somatic spikes with a long after-hyperpolarization. The A cells had a small cell body and they had a slow axonal conduction velocity, indicating unmyelinated (C-fibre) axons. The remaining 5% of cells were classed as H neurones. H neurones had large, broad TTX-insensitive spikes with long after-hyperpolarizations. They differed from the A neurones by

the occurrence of a distinctive hump on the falling phase of the spike. The morphological features and axonal conduction velocity of the H neurones were not uniform; some resembled F neurones whilst others were more similar to A neurones.

So, it seems that the TTX-sensitivity of the Na^+ current is an important character determining the spike shape of mouse dorsal root ganglion cells, with narrow spikes (i.e. the F neurones) being TTX-sensitive and with broader spikes (i.e. the A and H neurones) showing resistance to TTX. This is confirmed in studies in rat dorsal root ganglion cells; narrow spikes are TTX-sensitive, irrespective of axonal conduction velocity, whereas the broad somal spikes of A-fibres with inflections on the falling phase and all C-fibre spikes are TTX-resistant (Lawson *et al.* 1988; Ritter and Mendell 1990). Differences in TTX-sensitivity has also been reported between the functionally distinct cells of the petrosal ganglion in the cat, and this has been linked to the spike shape of these cells; the baroreceptors have narrow spikes and are TTX-sensitive, whereas the chemoreceptors have broad spikes and are TTX-insensitive (Gallego 1983).

Some broad somal spikes exhibit an inflection on the falling phase, and this has often been attributed to a Ca^{2+} component (Dichter and Fischbach 1977; Ransom and Holz 1977; Yoshida *et al.* 1978; Gallego 1983). However, this inflection is not solely due to Ca^{2+}, at least not in the dorsal root ganglion cells of the bullfrog (Morita and Katayama 1989). In the bullfrog, the TTX-resistant broad somal spikes of A-fibre cells were abolished in a Na^+-free solution. However, in C-fibre cells, Na^+-free solution only partially blocked the broad spikes, and the remaining Na^+-independent component could be blocked with Co^{2+}, indicating some involvement of Ca^{2+}.

The different kinds of K^+ currents found in mammalian dorsal root ganglion cells are also implicated in being involved in shaping the action potential. For example, the inward rectifying K^+ current is greater in cells with A-fibre axons/cells with narrow spikes than in those with C-fibre axons/those with broad spikes (Gallego and Eyzaguirre 1978; Koerber *et al.* 1988). The Ca^{2+}-activated K^+ current is implicated in having a role in the formation of the after-hyperpolarization and in the regulation of repetitive firing (Meech 1978; Sah 1996). In bullfrog dorsal root ganglion cells the size of this Ca^{2+}-activated K^+ current is heterogeneous, and it is greatest in the small cells with larger after-hyperpolarizations (Tokimasa *et al.* 1990). In rabbit nodose ganglion cells, a slow after-hyperpolarization lasting for a period of seconds is exhibited in a sub-population of neurones (Higashi *et al.* 1984; Fowler *et al.* 1985). This prolonged after-hyperpolarization is due to a Ca^{2+}-dependent K^+ current, and has been shown to be capable of controlling neuronal excitability and of affecting the ability of a neurone to fire in response to a period of repetitive stimulation (Weinreich and Wonderlin 1987).

Ca^{2+} channels are also differently distributed between small and large dorsal root ganglion cells (Scroggs and Fox 1991, 1992a, b). In small diameter dorsal root ganglion cells in the rat and the frog, L- and N-type Ca^{2+} currents account for most of the Ca^{2+} entry during an action potential, whereas in large diameter cells in the frog the Ca^{2+} current is carried almost entirely by N-type channels. T-type Ca^{2+} channels are expressed in small and medium sized cells in the rat but not in large diameter cells. The heterogeneous distribution of the different types of Ca^{2+} channels across the whole population of dorsal root ganglion cells, could therefore partially contribute to the different somal spike shapes of small, medium and large diameter dorsal root ganglion cells.

The studies outlined above, indicating the roles of the various kinds of Na^+, K^+ and Ca^{2+} currents in spike shape formation have all been carried out on somal spikes recorded from dorsal root ganglia. However, variations seen in somal spike shapes are not necessarily also seen in axonal spike shapes, e.g. in the cat, all C-fibres have wide somatic spike shape irrespective of sensory receptor type (Traub and Mendell 1988), whereas in the pig there is some variation of axonal spike shape in different functional classes of C-fibre (Lynn *et al.* 1996a, b). Also, the membrane properties of the cell bodies of primary afferent fibres are not mirrored in the axons, e.g. axonal spikes in all A-fibres are TTX-sensitive, independent of the TTX-sensitivity of the cell bodies (Koerber and Mendell 1992). These differences between somal and axonal spike shape and the ionic currents underlying action potential formation in the cell body and in the axon indicate the need for further experiments (see Section 9.2.3).

1.3.3 Activity-dependent changes in excitability and conduction velocity

Repetitive firing of nerve fibres produces changes in their electrical properties that result in the slowing of their conduction velocity and increases in their electrical threshold. Such "activity-dependent" effects have been studied in a variety of species, including frog, rat and man (Gilliatt and Willison 1963; Raymond and Lettvin 1978; Raymond 1979; Stöhr 1981; Carley and Raymond 1987; Shin and Raymond 1991; Thalhammer *et al.* 1994). The degree of conduction velocity slowing throughout a tetanus varies greatly between individual nerve fibres (Shin *et al.* 1994), and this variation has been shown to be related to sensory fibre type (Thalhammer *et al.* 1994). In single cutaneous afferent fibres dissected from the rat sciatic nerve and subjected to a period of electrical stimulation, impulses were found to slow less and to propagate more reliably in cold thermoreceptive fibres than in

nociceptive fibres (Thalhammer *et al.* 1994). This was true for both Aδ- and C-fibres, and was independent of resting conduction velocity.

The findings of Thalhammer and colleagues (1994) suggest the possibility that the degree of conduction slowing following a tetanus could be used to distinguish different afferent fibre types. However, if one is to use the axonal property of activity-dependent slowing of conduction velocity as an alternative to checking the afferent properties of individual units, then information is needed about conduction velocity slowing in *all* classes of afferent fibres. This prompted the study of activity-dependent slowing of conduction velocity in the different classes of C-fibre found in the rat saphenous nerve (including C-fibres identified as sympathetic efferent units), and the results from this study are presented in this thesis. The degree of conduction velocity slowing was the preferred parameter to study, since it is quicker and more simple to measure than the alternative measurements such as the threshold changes or the recovery cycle (Stys and Ashby 1990; Thalhammer *et al.* 1994). Also, by electing to measure conduction velocity slowing in this study of C-fibres of the rat saphenous nerve, it allowed a direct comparison to be made with the work of Thalhammer and colleagues from the rat sciatic nerve (Thalhammer *et al.* 1994).

So, this thesis will detail experiments looking at two axonal properties of single identified C-fibres from the rat saphenous nerve. These two axonal properties are activity-dependent slowing of conduction velocity and axonal spike shape, and they have been studied with a view to seeing if they are related to afferent class. If there are variations in axonal properties between the different functional classes of afferent C-fibres, the degree of overlap between the different classes needs to be examined, since this will determine whether these parameters can be used to identify particular sensory fibre types.

CHAPTER 2 METHODS

2.1 Anaesthesia and surgery

Experiments were carried out on adult male and female Sprague-Dawley rats from University College London breeding stock and on male New Zealand white rabbits (2.5-3.5kg). For experiments on rats, urethane anaesthesia was used (1.5g/kg i.p.), except for studies on antidromic vasodilatation when sodium pentobarbitone anaesthesia was used (60mg/kg Sagatal i.p. for induction). In all rabbit experiments sodium pentobarbitone anaesthesia was used, and induction was achieved by introducing Sagatal diluted 1:1 with 0.9% saline via the marginal ear vein. The trachea was cannulated and body temperature was maintained close to 37°C (rats) or 38°C (rabbits) using a heated underblanket controlled by a rectal thermistor probe. In experiments using pentobarbitone anaesthesia the left jugular vein was cannulated. In rats, Sagatal was infused at a rate so that the animal was areflexic to a noxious stimulus (e.g. strong pinch to the front paw, touching the eyeball with blunt glass probe). In rabbits the intravenous infusion was of a mixture of Sagatal, Gelofusine (a plasma substitute) and 0.9% saline (1:1:1), and again the infusion rate was set so as to maintain areflexia. The left carotid artery was cannulated and blood pressure was monitored throughout the experiments.

The fur on the leg was clipped prior to exposure of the saphenous nerve. A section of nerve approximately 10-15mm in length was cleared from surrounding connective tissue just distal to the point where the saphenous nerve meets the main trunk of the femoral nerve. A second length of nerve was cleared more distally for the positioning of the stimulating electrodes. The surrounding skin was stitched to a metal ring to form a pool

and this was filled with liquid paraffin oil. The foot and leg were mounted to prevent movement in the pool occurring whilst searching the saphenous territory for receptive fields.

2.2 Recording from afferent units

A pair of platinum stimulating electrodes was placed under the whole nerve at the distal end of the pool. The cut end of the nerve was placed over a fine platinum wire electrode, and a second indifferent electrode was positioned on the main nerve trunk. Figure 2.1 shows the experimental set-up for recording from afferent units in the rat.

Signals were recorded via an AC amplifier and were filtered (low frequency time constant = 1 ms, high frequency time constant = 0.1 ms). The signals were displayed on an oscilloscope (Tektronix 2230), and were logged to computer via an A/D board (Microstar Laboratories, DAP 2400).

The cut end of the nerve was placed on a mirrored platform and, working under a dissection microscope (Zeiss), the nerve was desheathed using a small piece of razor blade. Filaments were teased out using watchmakers forceps. The filaments were repeatedly split until stimulation of the whole nerve (0.5 ms pulse width) showed there to be identifiable C-fibres conducting in the filament. Although some filaments contained just one conducting C-fibre, multi-unit filaments were also used providing that individual C-fibres could be identified from the recording. C-fibres were recognised by their slow resting conduction velocity (CV); all C-fibres included in the results presented here had a resting CV of less than 2 m/s.

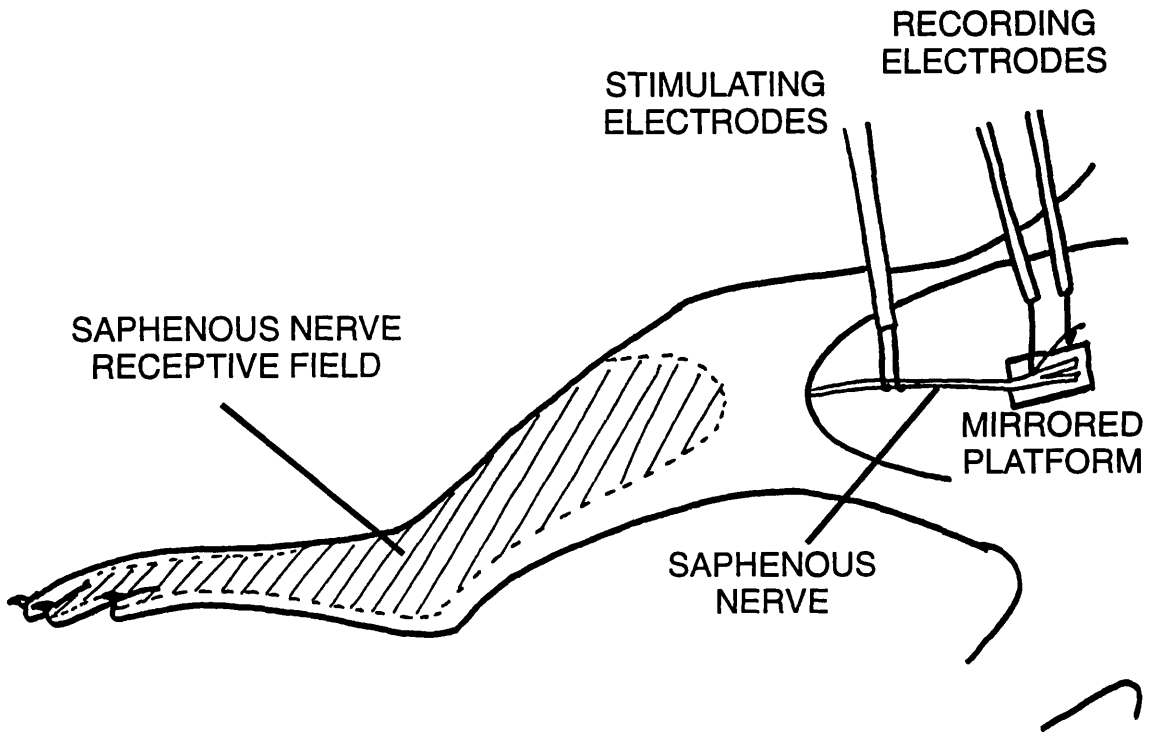

FIGURE 2.1 Schematic diagram of the experimental set-up for stimulation of and recording from afferent units in the saphenous nerve.

2.3 Identification and characterization of afferent units

When a suitable filament had been obtained the saphenous nerve receptive field was searched with mechanical stimuli (pinching the skin between finger and thumb, pressure applied with a blunt glass probe, Von Frey hairs ranging in force up to 20g). If a mechanical field was found, the mechanical threshold of the unit was determined using Von Frey hairs. The unit was then tested for heat sensitivity using a contact heat probe delivering a ramp stimulus increasing at a rate of 1°/second (35°C to 55°C in rats and 35°C to 65°C in rabbits). If no mechanical field was found the saphenous field was searched with a heat stimulus (contact heat probe at 55°C) or with innocuous cold stimuli (brief application of a cold metal ball or ice). Depending upon their responses to mechanical and thermal stimulation, individual C-fibres were classified into polymodal nociceptors, mechanical nociceptors, heat nociceptors, polymodal/mechanical nociceptors, mechanoreceptors, cold thermoreceptive units or inexcitable units, as summarised in Table 2.1. In some experiments, chemical stimulation was used in order to differentiate between afferent and non-afferent inexcitable units (see Section 2.4 below and Sections 6.5 and 9.1.5). The chemical stimulus used was a topical application of 5% or 10% mustard oil (allyl iso-thiocyanate, BDH Organics) in ethanol.

2.4 Mechanically and thermally inexcitable units - location of receptive fields using electrical skin stimulation and chemical stimulation

In some experiments in the rat, when a C-fibre had been classed as an inexcitable unit following the standard mechanical and thermal searching stimuli, electrical skin stimulation was employed to search for its electrical receptive field. The methods used were similar to

Class	Properties
Polymodal nociceptors	mechanical threshold >0.1g plus response to noxious heating[1]
Mechanical nociceptors	mechanical threshold >1.0g and insensitive to heating[1]
Heat nociceptors	sensitive to noxious heat[2] and mechanically insensitive
Mechanoreceptors	mechanical threshold <10mg
Cold thermoreceptors	sensitive to innocuous cooling
Inexcitable units	insensitive to mechanical and thermal stimuli[2]
Polymodal/mechanical nociceptors	mechanical threshold similar to that of polymodal nociceptors, but heat sensitivity not tested

[1] The standard heat stimulus applied to mechanical receptive fields was a ramp (1°C/sec) from 35°C to 55°C (rat) or 65°C (rabbit) with a contact heat probe

[2] In the absence of a mechanical receptive field, a search was carried out with the contact heat probe set at 55°C

Table 2.1 Classification of individual afferent C-fibres in the mammalian saphenous nerve.

those used previously to search for cutaneous electrical receptive fields in the monkey (Meyer *et al.* 1991), rat (Kress *et al.* 1992) and man (Schmelz *et al.* 1994). A saline soaked Q-tip was used as the cathode search electrode. One or two needle electrodes were inserted into the plantar surface of the lateral paw and these served as an anode. Electrical stimuli (up to 100V, 0.5msec duration) were applied to the skin within the territory of the saphenous nerve until the electrical receptive field had been located. As the search electrode was moved distally along the leg and foot, the latency of the unit increased. When moving the electrode more distally a point was usually reached when the latency of the unit did not increase any further. At this point, the electrical threshold of the unit usually decreased and this area was assumed to be the electrical receptive field of the unit.

In some of the activity-dependent slowing of conduction velocity experiments, an attempt to differentiate between afferent and non-afferent C-fibres which were inexcitable to mechanical and thermal stimuli, chemical stimulation using topical application of 5% or 10% mustard oil (allyl iso-thiocyanate, BDH Organics) in ethanol was carried out. In the case of units whose electrical receptive field had been established (see above), the mustard oil was painted on this area. If no response had been observed by 5 minutes, the mustard oil was removed from the skin with ethanol. In between successive applications of mustard oil, mechanical and thermal searches were carried out to see if the unit had become sensitive to these stimuli. Usually, only one or two applications of mustard oil were necessary. However, in cases where the topical mustard oil appeared to have no effect, the chemical stimulus was repeated up to 5 more times. For some C-fibres where an electrical receptive field could not be located, or where no response to successive applications of mustard oil to the electrical receptive field area had been observed, the whole saphenous field was painted with mustard oil.

2.5 Recording from spontaneously active sympathetic efferent units

In some experiments recordings were made from spontaneously active sympathetic efferent units in the rat saphenous nerve. The preparation for these experiments was similar to that for recording from afferent units. However, the saphenous nerve was cut at the distal end of the pool, and it was here that the filaments were dissected from the nerve and placed on the recording electrodes. The stimulating electrodes were placed under the whole nerve at the proximal end of the pool (see Figure 2.2). Any C-fibres displaying background spontaneous activity when recording from the nerve in this way cannot be afferent in nature and so were classed as spontaneously active sympathetic efferent units.

2.6 Antidromic filament stimulation

Electrical stimulation of fine filaments containing identified C-fibres is part of the experimental protocol for the antidromic vasodilatation study. For effective antidromic stimulation of individual C-fibres, their electrical thresholds need to be known. Two different approaches to determine the electrical threshold for antidromic stimulation of individual C-fibres were tried.

2.6.1 Averaging recordings of unitary C-potentials from the whole nerve

Firstly, the recording of C-potentials from the whole nerve trunk during antidromic filament stimulation was attempted. This approach has been used to monitor effective antidromic stimulation of A-fibres (Bharali and Lisney 1992; Kolston and Lisney 1993). The proximal electrodes (i.e. the filament electrodes) were connected to the constant

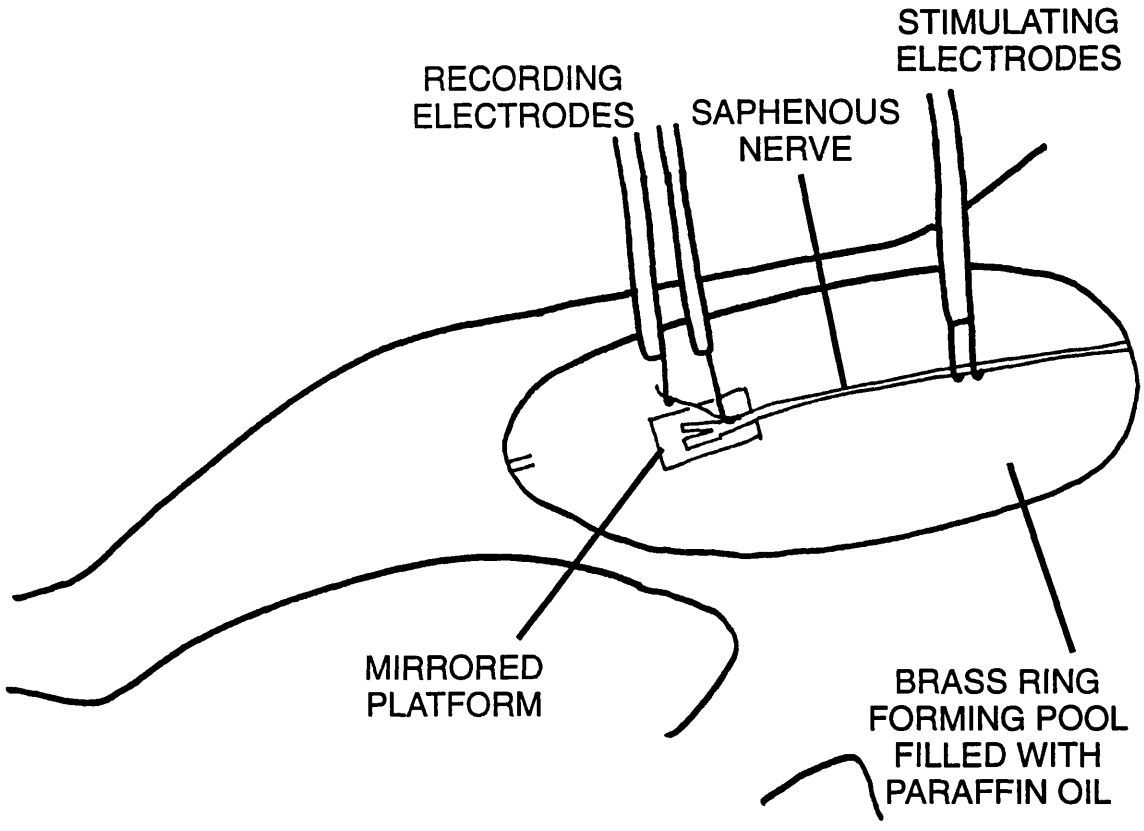

FIGURE 2.2 Schematic diagram of the experimental set-up for stimulation of and recording from spontaneously active sympathetic efferent units in the saphenous nerve.

voltage stimulator and the distal electrodes under the whole nerve were connected to the headstage amplifier for recording. The filament was stimulated using a constant voltage stimulator (0.5 ms pulse width) and activity was recorded from the whole saphenous nerve and filtered. It was not possible to resolve any C-fibre activity from the whole nerve recording unless the recordings were averaged (see Figure 2.3). Since it was vital to have evidence of effective antidromic stimulation of individual C-fibres within a filament, much time was put into trying to make this method work. However, only in a minority of cases was it possible to achieve recordings of unitary C-potentials from the whole nerve, such as the example shown in Figure 2.3, and any successful recordings were invariably noisy and gave inconsistent threshold values. The likely reason behind the failure of this method to detect single C-fibre activity from the whole nerve when it can detect individual A-fibre activity lies in the fact that for C-fibres an average record needs to be accumulated. In order to obtain an average of unitary activity from the whole nerve a stable latency is needed; a varying latency will result in a "blurred" average. However, as revealed in Chapter 6, C-fibre conduction slows during a period of repetitive stimulation. And since the different functional classes of C-fibre show varying degrees of such activity-dependent slowing of conduction velocity, it is likely that recordings of unitary activity of C-fibres from the whole nerve can be averaged successfully for some fibre types but not others. There is also the possibility that even with very low frequency stimulation, any slight temperature changes might affect conduction velocity enough to create a problem when trying to average unitary activity from the whole nerve.

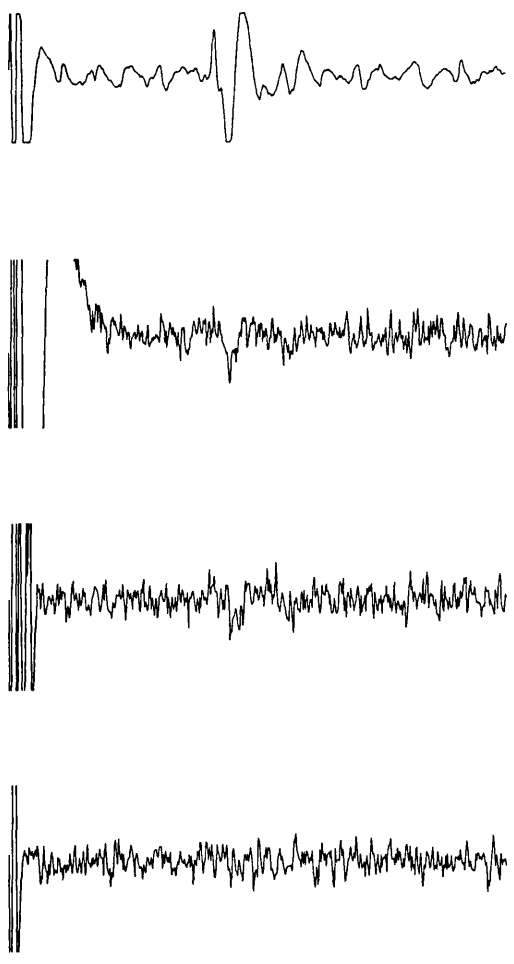

a) Recording from the filament following whole nerve stimulation (0.24mA, 1 shock, 0.5msec pulse width). There is a single C-polymodal nociceptor with a latency of 20.7msec (Unit 1).

b) The filament was stimulated at the proximal electrodes (1.4V, 30 shocks, 0.5Hz, 0.5msec pulse width). This is an average of the recording from the whole nerve at the distal electrodes, showing Unit 1 is being effectively stimulated

c) The filament was stimulated at the proximal electrodes (0.9V, 30 shocks, 0.5Hz, 0.5msec pulse width). This is an average of the recording from the whole nerve at the distal electrodes, showing Unit 1 is being effectively stimulated

d) The filament was stimulated at the proximal electrodes (0.3V, 30 shocks, 0.5Hz, 0.5msec pulse width). This is an average of the recording from the whole nerve at the distal electrodes. Unit 1 does not appear on the average; this stimulus is sub-threshold for Unit 1.

Figure 2.3 Averaging recordings from the whole nerve to establish the electrical thresholds for stimulation of individual C-fibres. A single C-max shock to the whole nerve determines the presence of C-fibres in the filament (a). The filament is given a train of shocks (30 shocks @ 5Hz) at the proximal electrodes (see Figure 2.1). The recording of activity from the whole nerve at the distal electrodes is averaged. It is possible to determine unitary activity (b,c) and thus one can conclude that the filament stimulation is supra-threshold for the unit being studied. The intensity of filament stimulation is reduced until the stimulus becomes sub-threshold for the unit in question (d). Note that this technique is very inconsistent, probably partly due to activity-dependent slowing of conduction velocity (see section 2.6.1, Chapter 6 and Chapter 9.1).

2.6.2 The use of the collision technique for establishing electrical thresholds for the antidromic stimulation of individual C-fibres

Because averaging C-fibre activity from the whole saphenous nerve following filament stimulation appeared impossible in most cases, and at best unreliable, another method for determining the electrical threshold for antidromic stimulation of identified C-fibres was needed. The second method tried was based upon the collision technique. The proximal electrodes were connected to the headstage amplifier for recording activity from the filament. A constant current stimulator was also connected to these proximal (filament) electrodes. The distal electrodes under the whole nerve were connected to a constant voltage stimulator. Figure 2.4 shows the arrangement of the electrodes used for the collision technique. The whole nerve was given a single C-max shock, and the recording from the proximal electrodes revealed the conducting C-fibres within the filament. The filament was stimulated at the same time that a single C-max shock was given to the whole nerve. The intensity of filament stimulation was increased until collision occurred and the individual C-fibres dropped out (see Figure 2.5). This method for determining the electrical threshold for single C-fibres in filaments dissected from the saphenous nerve is similar to that described by Andrew and colleagues (Andrew *et al.* 1996), but was developed independently. Our development of the collision method arose from a suggestion by Prof. David Attwell and we first presented this method at the Young Physiologists Symposium held in Bristol in 1995. The use of the collision technique to determine the electrical threshold of individual C-fibres for filament stimulation proved to be a reliable and consistent method, and gave highly repeatable threshold values.

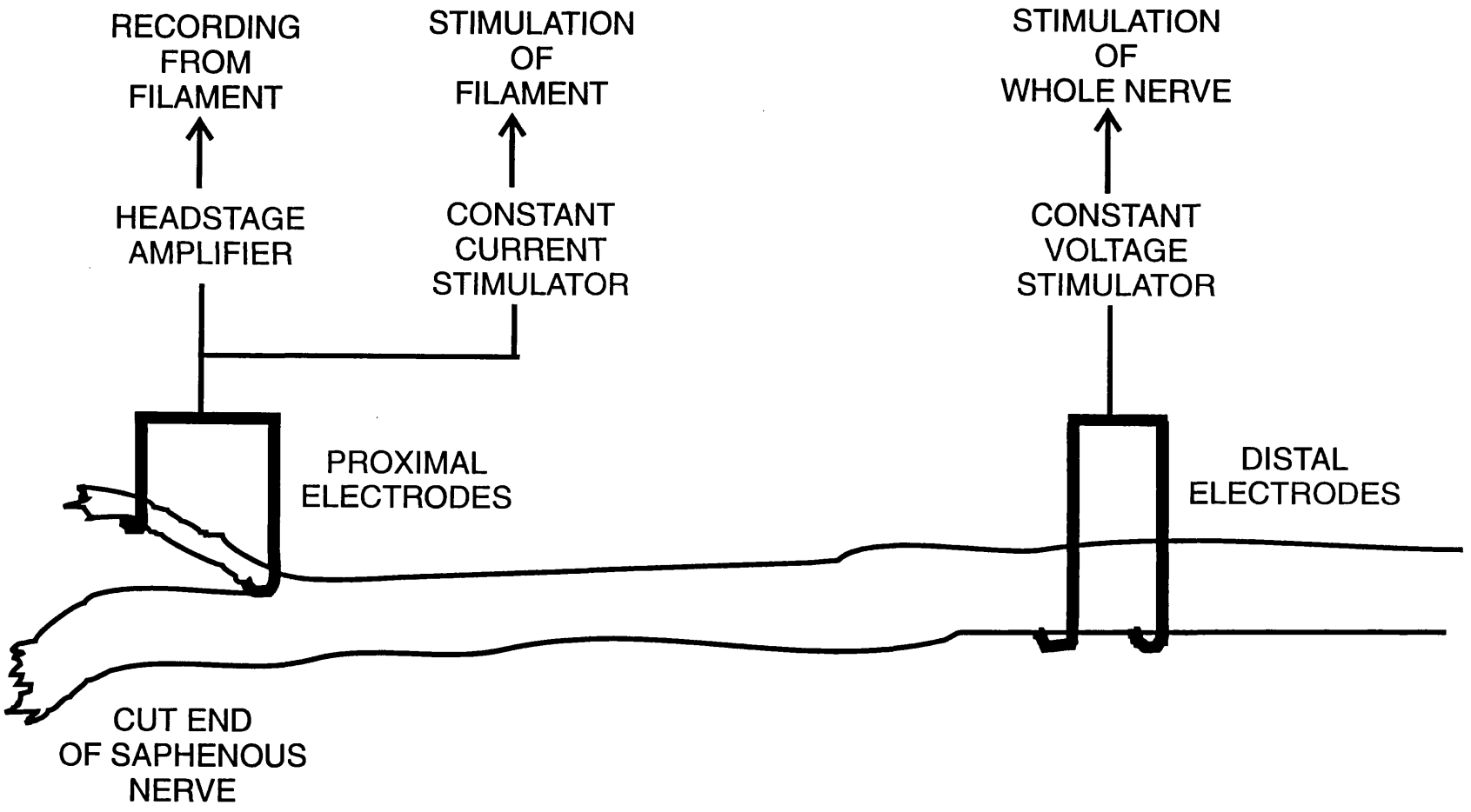

Figure 2.4 A schematic diagram showing the arrangements of the electrodes for the collision technique.

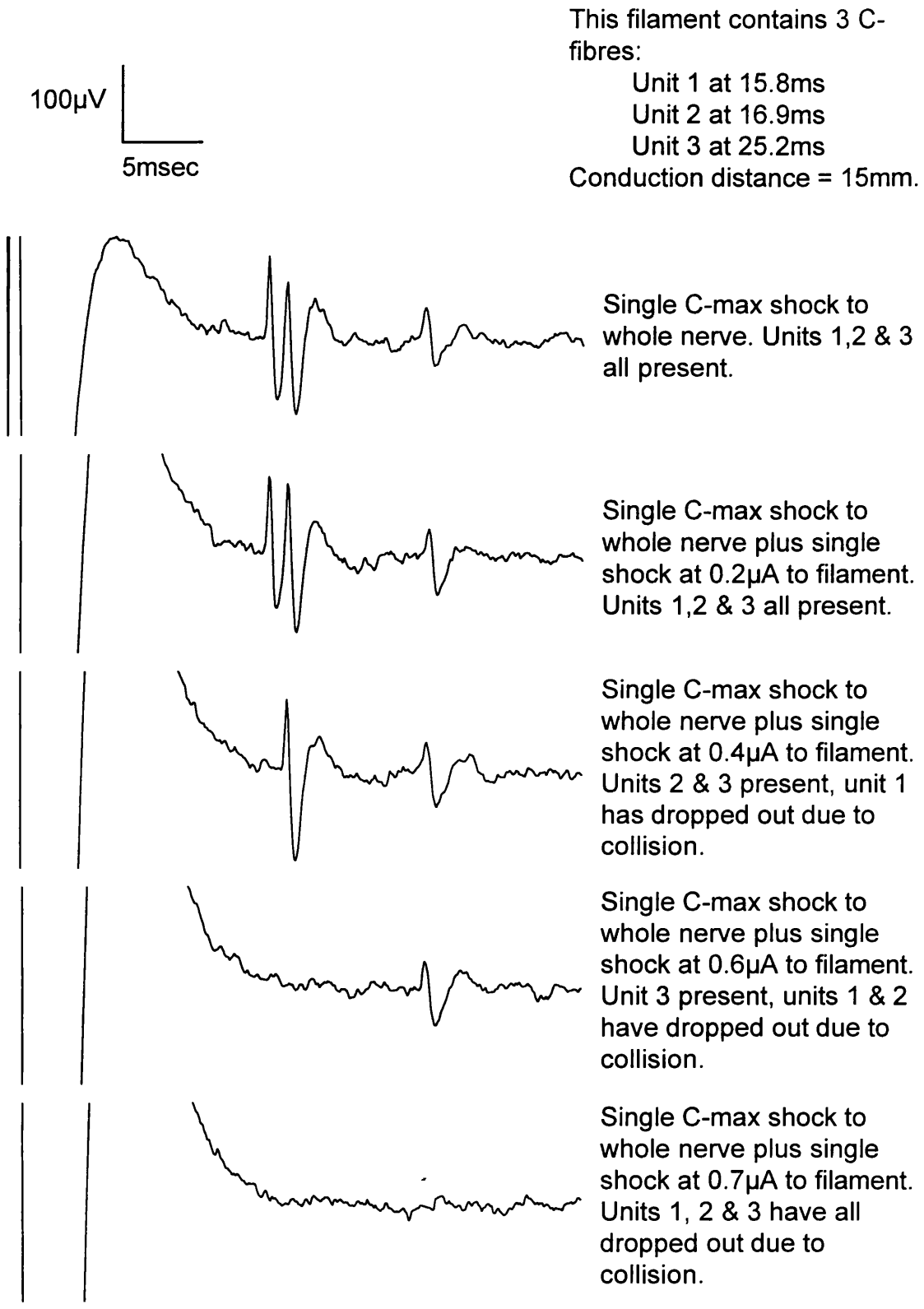

Figure 2.5 Using the collision technique to establish the electrical thresholds for stimulation of individual C-fibres in a filament. The whole nerve is given a single C-max shock at the distal electrodes. At the same time the filament is given a single shock at the proximal electrodes. The intensity of filament stimulation is increased until collision occurs and the individual C-fibres drop out.

2.7 Experimental protocols

2.7.1 Antidromic vasodilatation - single C-fibre study

This study was carried out in both anaesthetized rats and rabbits. When a suitable filament had been dissected from the saphenous nerve, the conducting C-fibres were classified and the collision technique was used to establish their electrical thresholds. The filaments were stimulated at 2-4 x threshold for 10-120 seconds at frequencies ranging from 2-10 Hz (0.5 ms pulse width), and skin blood flow was monitored before, during and after filament stimulation using laser Doppler flowmetry (MBF2 and MBF3D, Moor Instruments, UK) and/or laser Doppler perfusion imaging (Lisca Developments, Linkoping, Sweden) (see Section 1.2.5 and Appendix I). In experiments using laser Doppler flowmetry, two or three channels were used, with one or two probes positioned over the afferent receptive field(s) being studied and one probe monitoring skin blood flow in a control region within the saphenous nerve receptive field. With the laser Doppler perfusion imaging system, the scanner head was positioned so that the image included the afferent receptive fields being monitored and some surrounding control skin. Several control scans were made until a stable baseline blood flow had been established in the area being studied. In one of the control scans, the centre of the afferent fields were marked with small pieces of black adhesive tape so that their positions were visible on a control image. This allowed the position of any efferent response to be compared to the location of the identified afferents. For any units that showed a vasodilator response to antidromic stimulation, the percentage increase in blood flow from baseline was calculated. When filament stimulation did not result in any increase in skin blood flow, antidromic vasodilatation to whole nerve stimulation was checked

using a C-max intensity stimulus (0.5 msec pulse width) for 15-30 seconds at 1-2Hz (see Figure 4.7).

In rabbits, an attempt was made at comparing the extents of the afferent and efferent fields as well as comparing just their locations. This was achieved by carefully mapping the afferent receptive fields of vasodilator units with mechanical stimulation using suprathreshold (2-5 x threshold) Von Frey hairs, working with a microscope and a graticule grid. For calculation of the afferent receptive field area, the number of squares of the graticule grid overlying skin where mechanical stimulation excited the unit being studied were counted. In rats, where the afferent receptive fields were smaller, such mapping was not feasible.

2.7.2 Studying the flare responses to mechanical and heat stimuli applied to the skin.

The laser Doppler perfusion imaging system was used to study flare responses of rat and rabbit skin to mechanical and heat stimuli. All stimuli were applied to skin within the saphenous field. The imager was positioned parallel to the surface of the skin. Several scans were made until a stable baseline blood flow had been established in the area being studied. Stimuli were applied to the centre of the scanned area, and two kinds of stimuli were used

- mechanical stimulation using Von Frey hairs ranging from 0.1g to 10g (1 to 10 prods). Each mechanical stimulus lasted approximately one second, and consecutive stimuli within each trial were applied at 1 second intervals.

- heat stimulation using a contact heat probe (35°C to 50°C, 35°C to 55°C or 35°C to 60°C heat ramps at 1°C/s).

Images were then taken for up to 20 minutes following stimulation.

Any changes in skin blood flow were observed by subtracting the baseline images from the ones taken after stimulation of the skin. In any one skin area a range of mechanical stimuli were tested and the forces required to produce a flare response were noted. Only one heat test was carried out in any given skin area.

2.7.3 Activity-dependent conduction velocity slowing

The study of activity-dependent slowing of C-fibre conduction velocity was only carried out in the rat. When a suitable filament had been dissected and the C-fibres had been identified and classified, the whole nerve was stimulated electrically (pulse width = 0.5 ms) with a range of frequencies and durations. The results of preliminary experiments led to a standard electrical stimulus of 20 seconds at 20 Hz at 2-3 x threshold of the C-fibre being studied being chosen. The first of every 5 stimuli was logged to computer via the A/D board. The percentage slowing from resting conduction velocity was calculated off-line for the first and last logged response, and for every fourth logged response in between. This means that the final measurement made was after 19.75 seconds (rounded to 20 seconds for clarity).

2.7.4 Measuring spike shape

The study of the spike shapes of the different functional classes of C-fibres was only carried out in the rat. When a C-fibre had been identified and classified the filters were opened up (10 Hz to 5 kHz). Introducing some high frequency cut does have a small effect on the width of the spike, but any effect was minimized by using the same filter settings for each spike. The 10 Hz limit provided enough filtering to be able to record and measure the undershoot amplitude and width. Adequate stimuli (mechanical, thermal, cold, electrical) were used to excite non-spontaneous units, and usually several spikes were averaged before any measurements were made. For units with background activity (i.e. spontaneously active sympathetic units and most cold thermoreceptor units at room temperature) several spontaneous spikes were averaged. Four measurements of spike shape were made (see Figure 2.6): the amplitude of the first peak, the duration of the first peak at half the maximum amplitude, the undershoot amplitude and the duration of the undershoot at half its maximum amplitude.

2.8 Statistical analysis

Data are expressed as mean±SEM (n) unless otherwise stated. For comparing two groups, 2-tailed Student's *t*-tests were used, or, where appropriate, paired *t*-tests were used. For comparison of non-normally distributed data, non-parametric Mann-Whitney U tests were used. For multiple comparison across several groups, one-way analysis of variance (ANOVA) using either the Student-Newman-Keuls procedure or the Least Significant Difference method was carried out. A X^2 test was used to examine the distribution of vasoactive and non-vasoactive units within the rat saphenous nerve receptive field (see Chapter 4). P values of <0.05 were considered to be statistically significant unless stated otherwise.

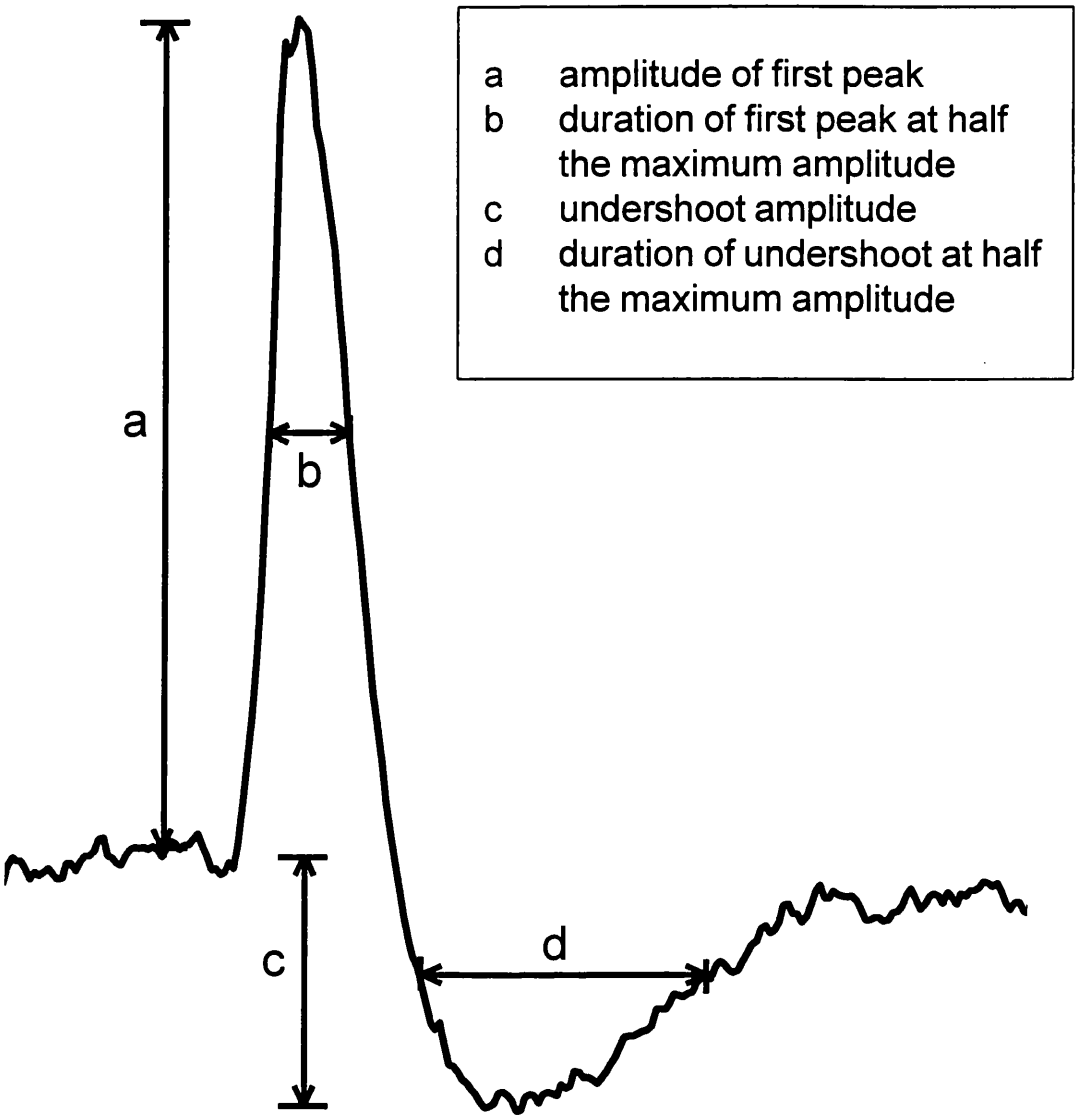

Figure 2.6 Diagram showing the spike shape measurements taken

CHAPTER 3 RESULTS: SINGLE C-FIBRE ANTIDROMIC VASODILATATION STUDY IN RABBIT SKIN

The laser Doppler perfusion imaging system was used to monitor cutaneous blood flow during electrical stimulation of identified C-fibres dissected from the saphenous nerve of Sagatal anaesthetized rabbits. The collision technique was used to establish the thresholds for electrical stimulation of the individual C-fibres, and the filaments were stimulated for 30-120 seconds at 2-4 x electrical threshold and at frequencies between 2 Hz and 10Hz (0.5 ms pulse width).

A total of 33 C-fibres from 13 rabbits were studied for their ability to produce vasodilatation upon antidromic stimulation, and they comprised 28 polymodal nociceptors, 1 mechanical nociceptor and 4 mechanoreceptors. The C-fibres did not come from a random sample and so the true proportions of the different functional classes of C-fibres present in the rabbit saphenous nerve are not represented in this population of 33 units. The afferent receptive fields of 14 polymodal nociceptors were mapped with suprathreshold mechanical stimuli (Von Frey filaments).

3.1 C-fibres with vasodilator actions

Vasodilatation was detected in 14 of the 33 (42%) C-fibres studied. All 14 vasodilator units were polymodal nociceptors, and their properties are summarised in Table 3.1. Figure 3.1 shows the mechanical and thermal thresholds, where known, of the polymodal nociceptors found in this study.

Class	Conduction velocity (m/sec)	VF threshold (g)	Heat threshold (°C)	% increase of skin blood flow above baseline
poly	0.92	0.4 - 0.6	52.5	up to 83%
poly	0.87	0.1	55.5	up to 34%
poly	0.90	0.4 - 0.6	56	up to 75%
poly	0.89	0.4 - 0.6	62.5	up to 96%
poly	0.95	0.4 - 0.6	55	up to 110%
poly	0.98	0.2 - 0.4	46	up to 39%
poly	0.95	0.1 - 0.2	50	up to 65%
poly	1.14	0.4 - 0.6	49.5	up to 46%
poly	1.10	1.0 - 2.0	54	up to 80%
poly	1.05	0.2 - 0.4	51	up to 45%
poly	0.96	0.05 - 0.1	44.5	up to 45%
poly	1.08	0.05 - 0.1	53	up to 33%
poly	0.97	0.6 - 1.0	60.5	up to 40%
poly	0.87	0.6 - 1.0	yes	up to 16%
mean±SE (n)	0.97±0.02 (14)	0.47±0.10 (14)	53.1±1.4 (13)	57.6±7.3 (14)

Table 3.1 **Properties of the vasoactive polymodal nociceptors in the rabbit saphenous nerve.**

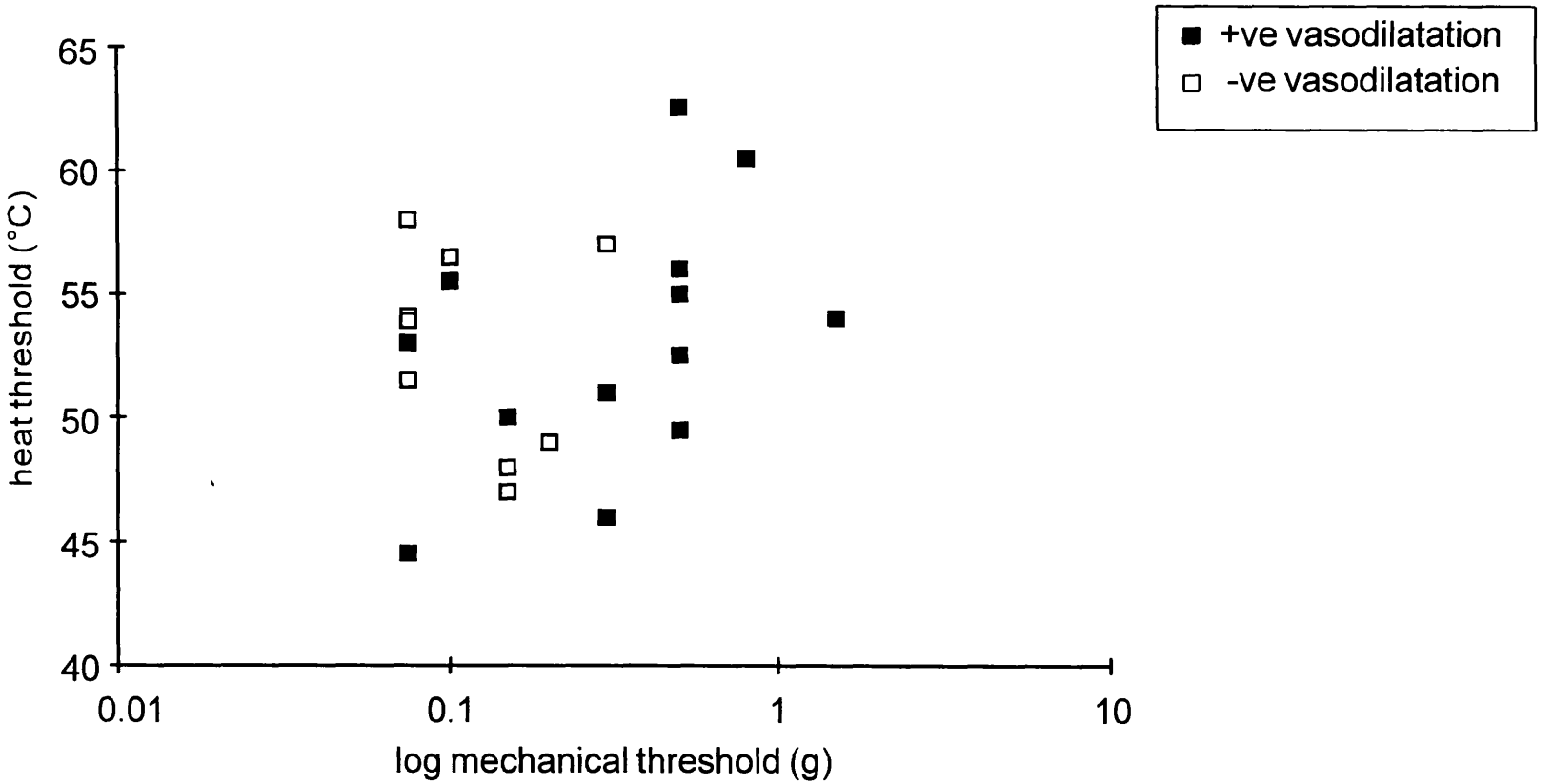

Figure 3.1 Graph showing the mechanical and heat thresholds of the polymodal nociceptors that produced vasodilatation (filled symbols) and the polymodal nociceptors that did not produce vasodilatation (open symbols) in the rabbit saphenous nerve.

3.2 Heat thresholds

The distribution of the heat thresholds of the polymodal nociceptors is shown in Figure 3.2A; the heat thresholds ranged from 44.5°C to 62.5°C and the average heat threshold was 52.9°C±0.98 (n=22; mean±SE). The average heat threshold of the vasodilator polymodal nociceptors was 53.1°C±1.42 (n=13), and the average heat threshold of the non-vasodilator polymodal nociceptors was 52.8°C±1.36 (n=9). There was no significant difference between the heat thresholds of the vasodilator and non-vasodilator polymodal nociceptors (t-test, n=22, p=0.88).

3.3 Mechanical thresholds

The distribution of the mechanical thresholds of the polymodal nociceptors is shown in Figure 3.2B; the mechanical thresholds ranged from 0.075g to 1.5g and the average mechanical threshold was 0.33g±0.06 (n=28). The average mechanical threshold of the vasodilator polymodal nociceptors was 0.47g±0.10 (n=14), and the average mechanical threshold of the non-vasodilator polymodal nociceptors was 0.18g±0.03 (n=14). Statistical comparison between these two groups shows that the vasodilator polymodal nociceptors had higher mechanical thresholds than the non-vasodilator polymodal units (Mann-Whitney U test, n=28, p=0.01).

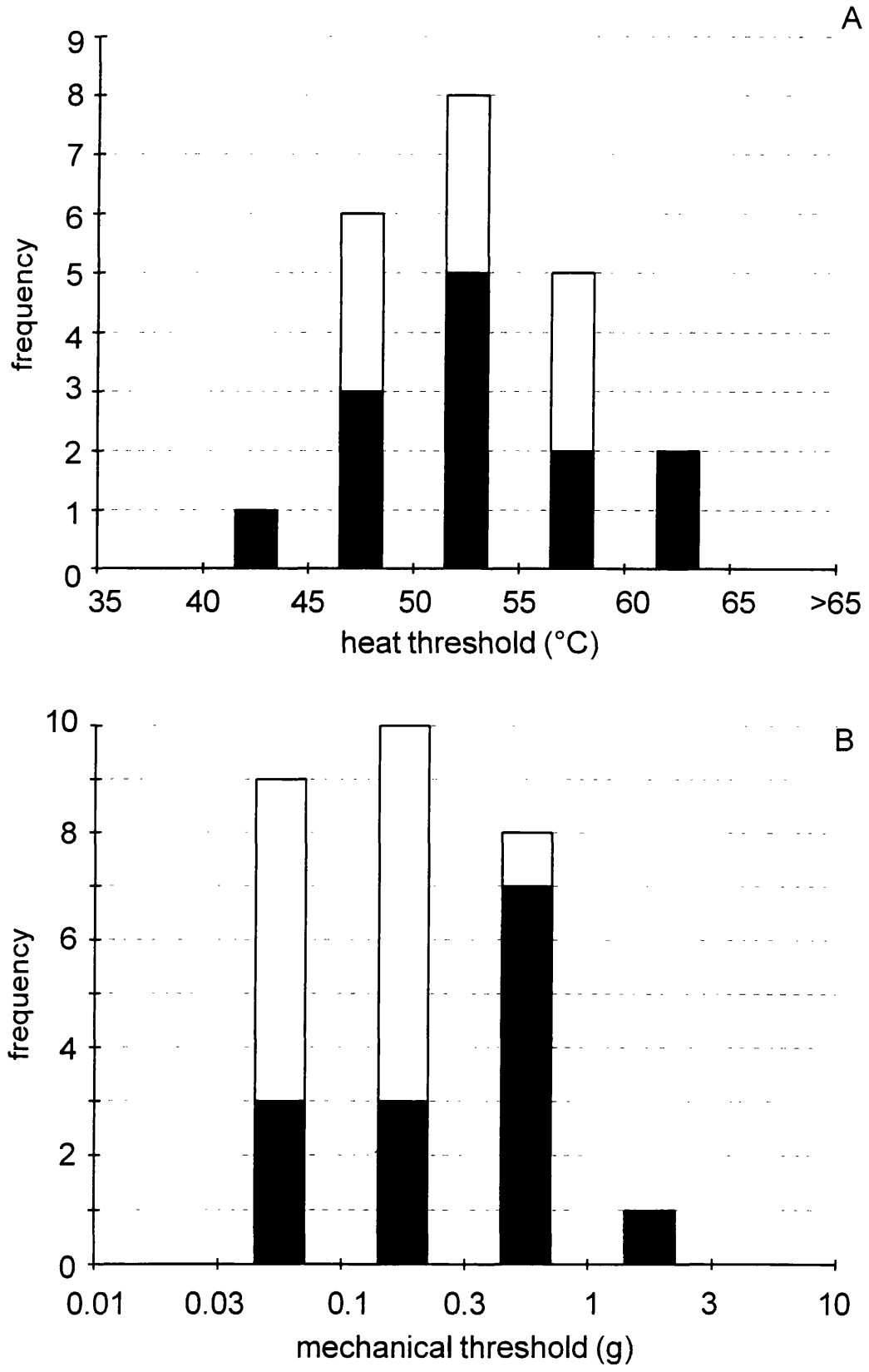

Figure 3.2 **Frequency didstribution histograms of A) the heat thresholds, and B) the mechanical thresholds, of polymodal nociceptors in the rabbit saphenous nerve.** The open bars represent all polymodal nociceptors, the closed bars represent the vasoactive polymodal nociceptors. Note the logarithmic scale in graph B.

3.4 Efferent responses

Figures 3.3 to 3.6 show images of the vasodilatation resulting from antidromic stimulation of identified polymodal nociceptive C-fibres. The images have been scaled so that the colours represent percentage increase in blood flow above the baseline. Note that in Figures 3.3 to 3.6 the blue colour represents the smallest changes in blood flow and includes any decreases in blood flow from the baseline. The 14 vasoactive polymodal nociceptors found in this study produced increases in skin blood flow ranging from 16-110% above baseline.

3.5 Comparison of the afferent and efferent receptive fields

The areas of vasodilatation were always coincident with the afferent receptive field of the polymodal units (see Figures 3.3 to 3.5). The afferent receptive fields of 13 polymodal nociceptors (including 10 of the 14 vasoactive polymodal units) were carefully mapped using suprathreshold (2-5 x threshold) Von Frey filaments (Figure 3.7). The areas of the afferent fields of these 13 units were calculated by counting the number of squares of the graticule grid that were overlying skin that responded to mechanical stimulation with a suprathreshold Von Frey filament. The afferent receptive field dimensions ranged from 3.1mm to 8.6mm in the proximal-distal direction and from 2.0mm to 5.5mm in the medial-lateral direction. There was one polymodal nociceptor where it was not possible to accurately map its afferent receptive field; however, the area of its afferent field was estimated at the time of the experiment to be approximately 3.5mm by 2.0mm. There was no significant difference between the afferent field areas and the efferent field areas (i.e. the areas of vasodilatation) (see Table 3.2; t-test, $p=0.96$, $n=28$). Figure 3.8 shows that there

is a good correlation ($r=0.72$, $p<0.01$) between the afferent and efferent receptive field areas in the 11 polymodal nociceptors where both of these measurements were made.

3.6 C-fibres without vasodilator actions

Stimulation of the remaining 19 units (14/28 polymodal nociceptors, 1/1 mechanical nociceptors and 4/4 mechanoreceptors) showed no detectable increases in skin blood flow. In all cases, stimulation of the whole saphenous nerve resulted in vasodilatation in the region of the units being studied. This showed that the skin in the area of and surrounding these 19 non-vasodilator units was capable of producing a vasodilator response. All 19 non-vasodilator units survived the period of filament stimulation. Therefore, these 19 units provided convincing negative results for antidromic vasodilatation.

3.7 Summary

- It is possible to use the laser Doppler perfusion imaging system to detect vasodilatation in rabbit skin resulting from antidromic electrical stimulation of individual C-fibres.
- In the rabbit, all of the C-fibres that produced vasodilatation were polymodal nociceptors. In this study, 14/28 (50%) of the polymodal nociceptors tested produced antidromic vasodilatation.
- The vasoactive polymodal nociceptors had significantly higher mechanical thresholds than the non-vasodilator polymodal units. There was no significant difference in the heat thresholds of the vasodilator and non-vasodilator polymodal nociceptors.
- The locations and extents of the efferent receptive fields of the vasoactive polymodal nociceptors were very similar to those of the afferent receptive fields.

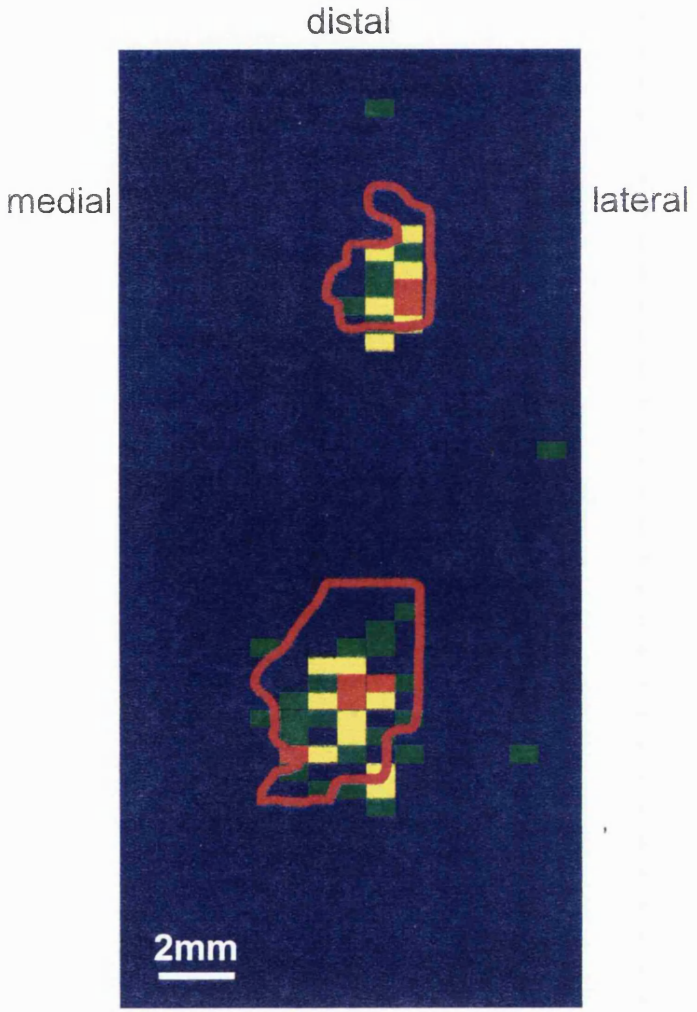

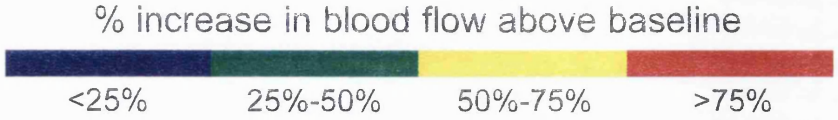

Figure 3.3 An image showing antidromic vasodilatation following electrical stimulation of a filament containing 2 C-polymodal nociceptors. The more distal (upper) unit had a conduction velocity of 0.89m/s, a Von Frey threshold of 0.4-0.6g, a heat threshold of 62.5°C and its afferent receptive field was approximately 3.9mm x 2.3mm. The more proximal unit had a conduction velocity of 0.90m/s, a Von Frey threshold of 0.4-0.6g, a heat threshold of 62.5°C and its afferent field was approximately 6.2mm x 4.7mm. Both afferent fields have been drawn on the image. In both cases, the areas of vasodilatation match well with the afferent fields. The parameters for filament stimulation were 7.0μA, 2 minutes, 5Hz, 0.5ms pulse width. Baseline scans made before stimulation have been subtracted from scans taken after stimulation. Two difference images have been averaged to make this image. The image has been scaled so that the colours represent percentage increase in blood flow above the baseline. Note that in this figure and in Figures 3.4 to 3.6, the blue colour represents the smallest changes in blood flow and includes decreases in blood flow from the baseline.

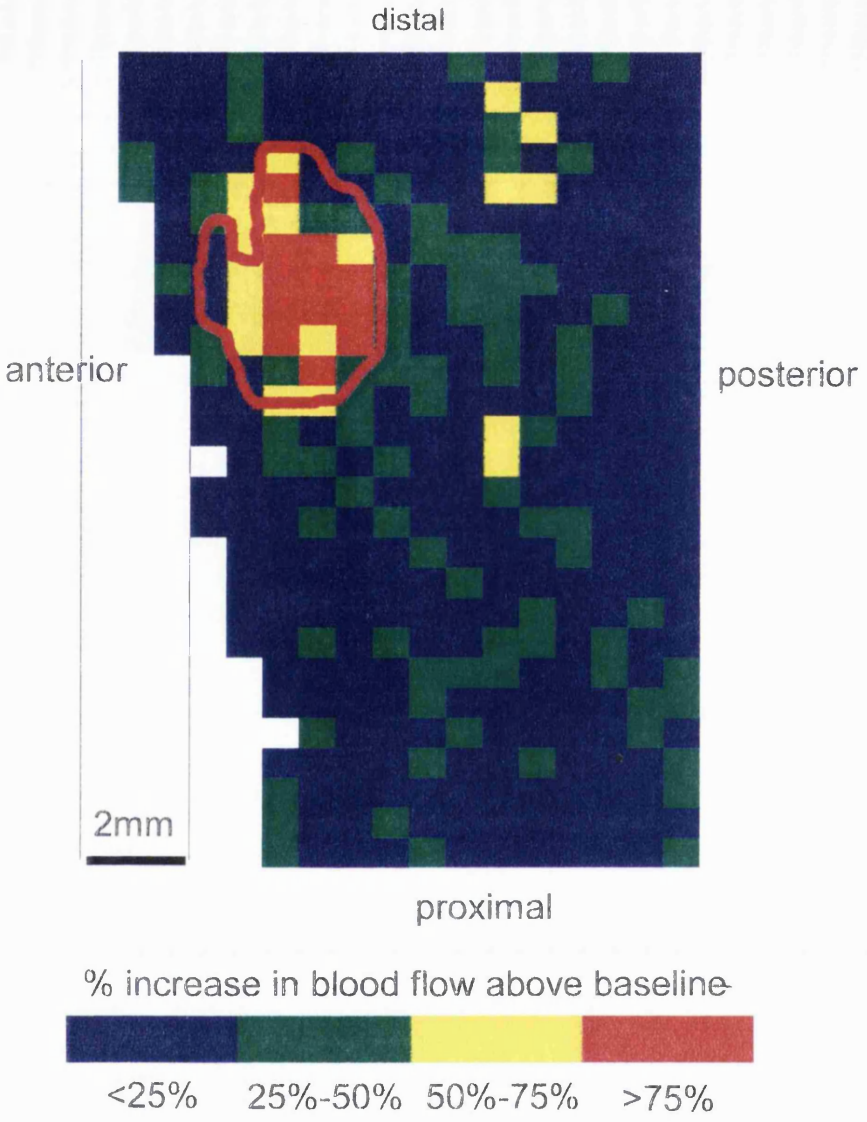

Figure 3.4 An image showing antidromic vasodilatation following electrical stimulation of a filament containing a C-polymodal nociceptor (conduction velocity = 0.95m/s, Von Frey threshold = 0.4-0.6g, heat threshold = 55°C). The afferent receptive field of this unit was approximately 6.2mm by 4.7mm, and has been drawn on the image. The area of vasodilatation matches well with the afferent receptive field. The parameters for filament stimulation were 2.0μA, 2 minutes, 5Hz, 0.5ms pulse width.
Baseline scans made before filament stimulation have been subtracted from scans taken during and after stimulation. Six difference images have been averaged to make this image. The image has been scaled so that the colours represent percentage increase in blood flow above the baseline.

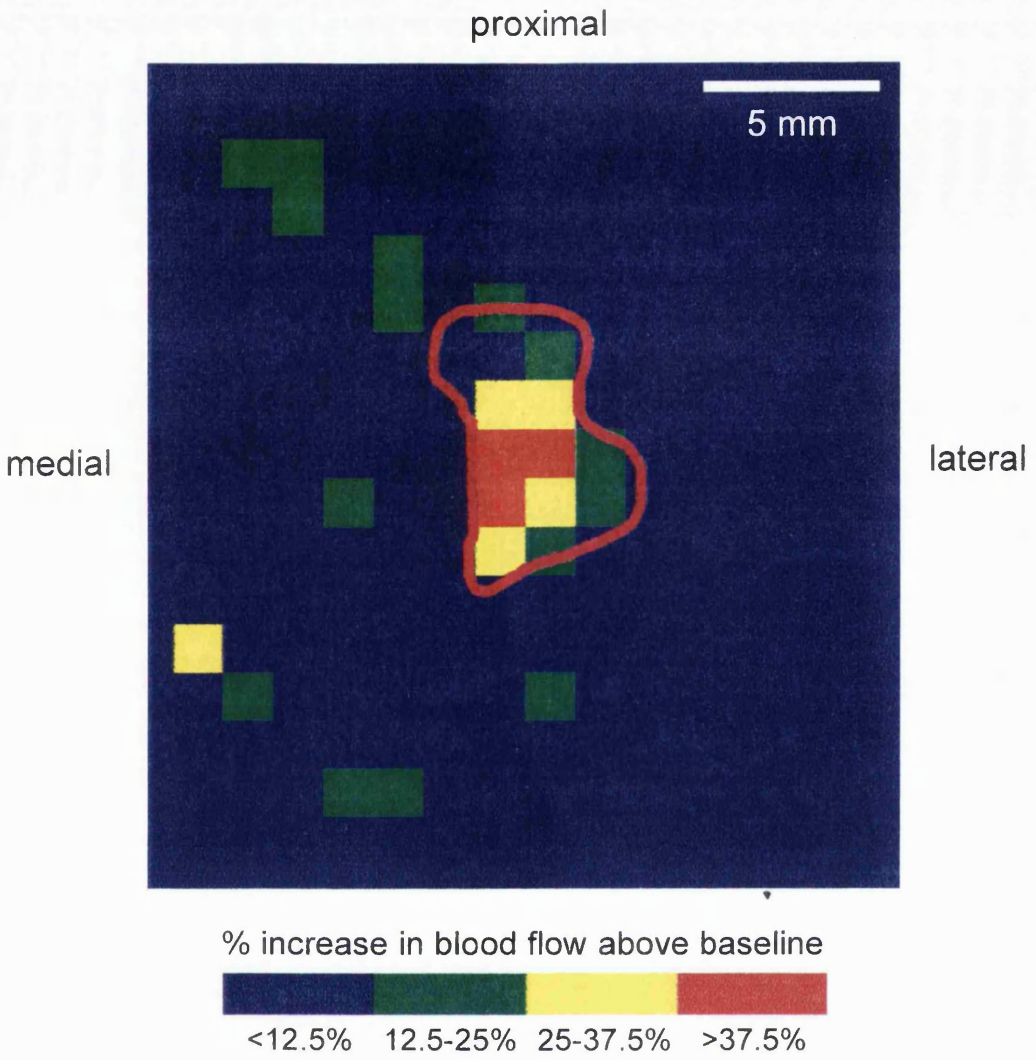

Figure 3.5 An image showing antidromic vasodilatation following electrical stimulation of a filament containing a C-polymodal nociceptor (conduction velocity = 1.14m/s, Von Frey threshold 0.4-0.6g, heat threshold = 49.5°C). The afferent receptive field of this unit was approximately 7.8mm by 4.7mm, and has been drawn on the image. The area of vasodilatation matches well with the afferent receptive field. The parameters for filament stimulation were 6.0μA, 2 minutes, 5Hz, 0.5ms pulse width.
Baseline scans made before stimulation have been subtracted from those taken during stimulation, and 3 difference images have been averaged to make this image. The image has been scaled so that the colours represent percentage increase in blood flow above the baseline.

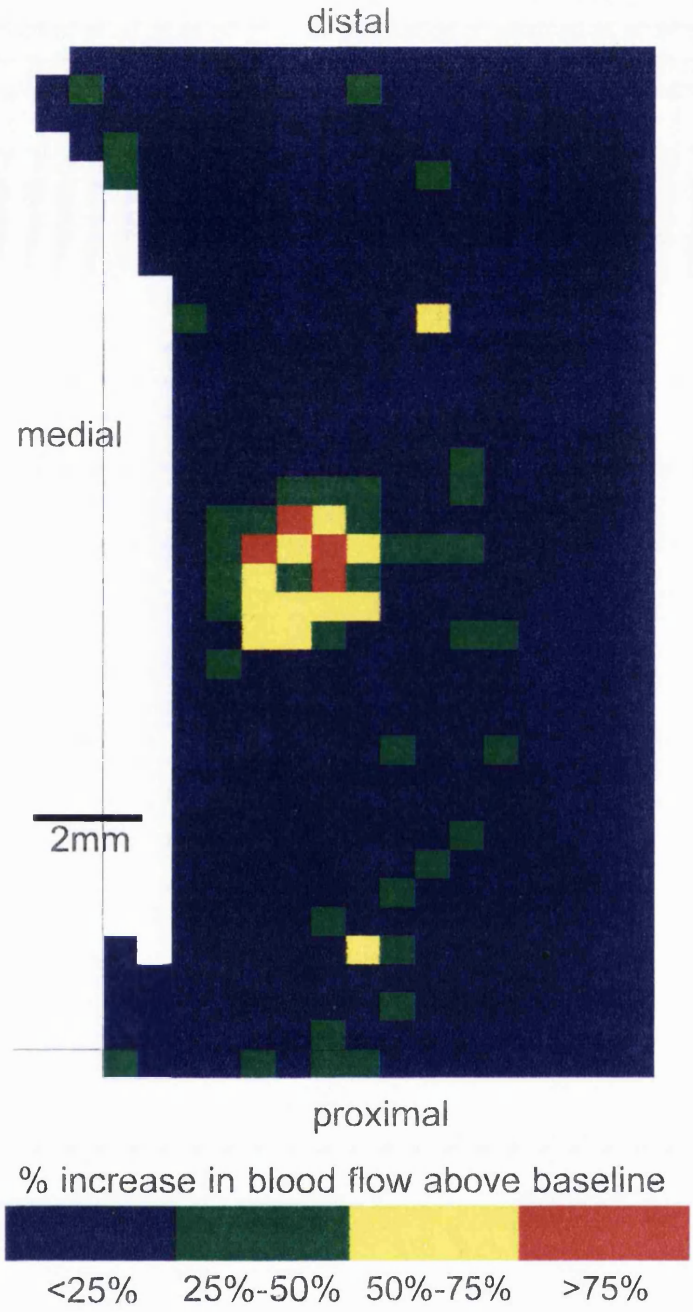

Figure 3.6 An image showing antidromic vasodilatation following electrical stimulation of a filament containing a C-polymodal nociceptor (conduction velocity = 0.92m/s, Von Frey threshold = 0.4 - 0.6g, heat threshold = 52.5°C). The centre of the afferent field coincided with the centre of the vasodilator response. The parameters for filament stimulation were 4.0μA, 60 seconds, 5Hz, 0.5ms pulse width. Baseline scans made before filament stimulation have been subtracted from those taken after stimulation, and 2 difference images have been averaged to make this image. The image has been scaled so that the colours represent percentage increase in blood flow above the baseline.

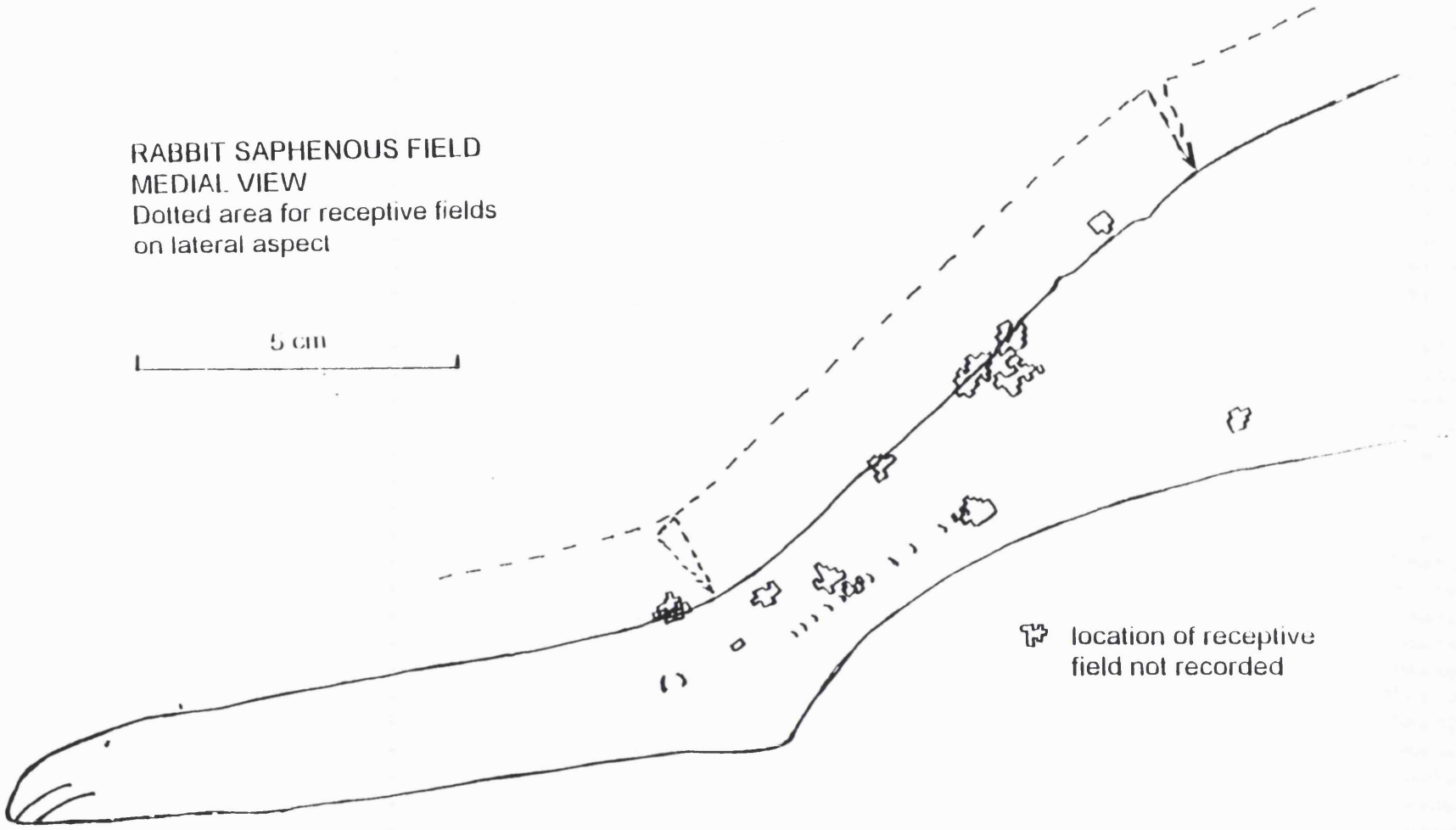

Figure 3.7 **The afferent receptive fields of 14 polymodal nociceptors in the rabbit saphenous nerve.** The fields were mapped with suprathreshold mechanical stimuli, using Von Frey filaments.

Conduction Velocity (m/s)	Mechanical threshold (g)	Heat threshold (°C)	Afferent receptive field area (mm^2)	Efferent receptive field area (mm^2)
0.87	0.1	55.5	7.0	7.7
0.89	0.4 - 0.6	62.5	5.5	5.3
0.90	0.4 - 0.6	56	19.5	14.3
0.95	0.4 - 0.6	55	18.3	23.1
0.98	0.2 - 0.4	46	5.5	2.6
1.14	0.4 - 0.6	49.5	18.9	23.5
1.10	1.0 - 2.0	54	7.9	13.7
1.05	0.2 - 0.4	51	9.0	7.0
1.08	0.05 - 0.1	53	7.9	12.1
0.97	0.6 - 1.0	60.5	10.3	13.5
0.87	0.6 - 1.0	yes	25.6	14.9
0.92	0.4 - 0.6	52.5	not mapped	8.7
0.96	0.05 - 0.1	44.5	not mapped	11.1
0.95	0.1 - 0.2	50	not mapped	6.0
0.77	0.4 - 0.6	42.5	11.5	non-vasodilator
0.70	0.2 - 0.4	47	8.3	non-vasodilator
0.75	0.05 - 0.1	51	7.0	non-vasodilator
mean±SE (n)			11.6±3.09 (14)	11.7±1.65 (14)

Table 3.2 **Conduction velocity, mechanical threshold, heat threshold and afferent and efferent receptive field areas of a sample of polymodal nociceptors from the rabbit saphenous nerve.**

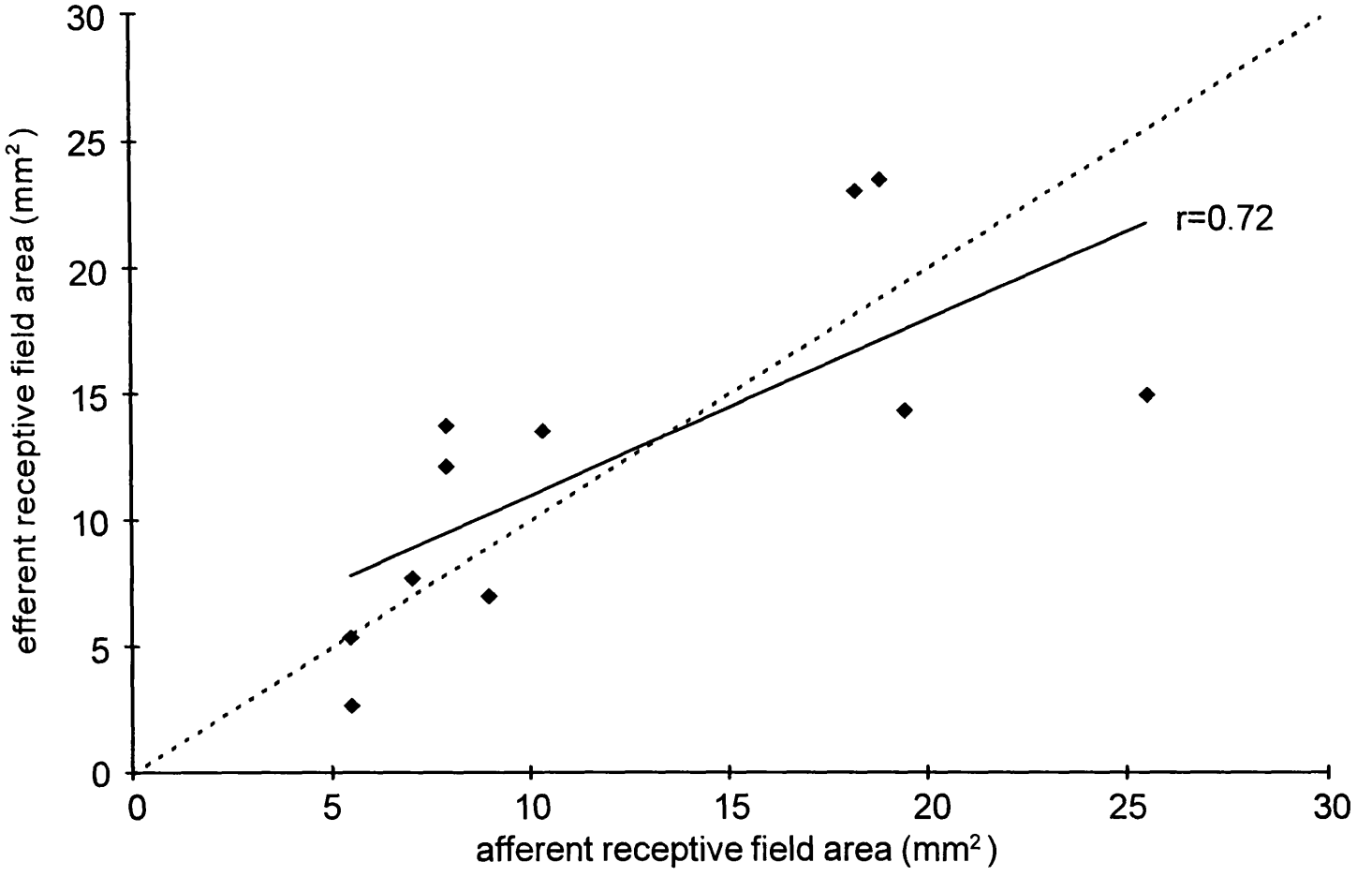

Figure 3.8 **Graph showing the relationship between the afferent and efferent receptive fields of 11 polymodal nociceptors in the rabbit saphenous nerve.** Dotted line = unity line, solid line = best fit line (r=0.72).

CHAPTER 4 RESULTS: SINGLE C-FIBRE ANTIDROMIC VASODILATATION STUDY IN RAT SKIN

Chapter 3 describes the results from the single C-fibre antidromic vasodilatation study in the rabbit. A similar study was also carried out in the rat using laser Doppler flowmetry and/or laser Doppler perfusion imaging to detect any changes in skin blood flow resulting from the electrical stimulation of identified C-fibres. As in the rabbit study, the collision technique was used to establish the thresholds for electrical stimulation of the individual C-fibres. The filaments were stimulated for 10-120 seconds at 2-3 x electrical threshold and at frequencies between 2Hz and 10Hz (0.5 ms pulse width). Some of these results have been published in abstract form (Gee *et al.* 1996b).

A total of 54 C-fibres dissected from the saphenous nerves of 35 rats were studied for their ability to produce vasodilatation upon antidromic stimulation, and they comprised 40 polymodal nociceptors, 2 heat nociceptors, 3 mechanical nociceptors, 3 polymodal/mechanical nociceptors (i.e. units responsive to noxious mechanical stimuli but not tested with heat), 2 mechanoreceptors and 4 inexcitable units. The C-fibres did not come from a random sample and so the true proportions of the different functional classes of C-fibres present in the rat saphenous nerve are not represented in this population of 54 units.

4.1 C-fibres with vasodilator actions

Of the 54 C-fibres studied, vasodilatation was detected in 11 units, all of which were nociceptors (7 polymodal, 2 heat and 2 polymodal/mechanical). The properties of these 11 units are summarized in Table 4.1. Figure 4.1 shows the mechanical and thermal thresholds of the polymodal nociceptors found in this study.

Class	Conduction velocity (m/sec)	Receptive field location	VF threshold (g)	Heat threshold (°C)	% increase of skin blood flow above baseline
poly	0.91	base of digit 1	1-2	52.5	up to 116%
poly	0.76	base of digit 1	2	49	up to 85%
poly	0.79	medial ankle	1-2	58	up to 19%
poly	0.80	anterior foot	1-2	50	up to 81%
poly	0.82	anterior/ lateral foot	1-2	44	up to 31%
poly	1.07	tip of digit 1	>20 responds to blunt probe	55	up to 17%
poly	0.79	anterior mid-leg	0.05-0.1	39	up to 70%
heat	0.82	anterior/ medial foot	-	56.5	up to 20%
heat	0.53	digit 2	-	yes	up to 160%
poly/HTM	0.58	tip of digit 1	>20 responds to blunt probe	?	up to 180%
poly/HTM	0.89	base of digit 1	1-2	?	up to 26%

Table 4.1 **Properties of the C-fibres in the rat saphenous nerve which have vasodilator actions.**

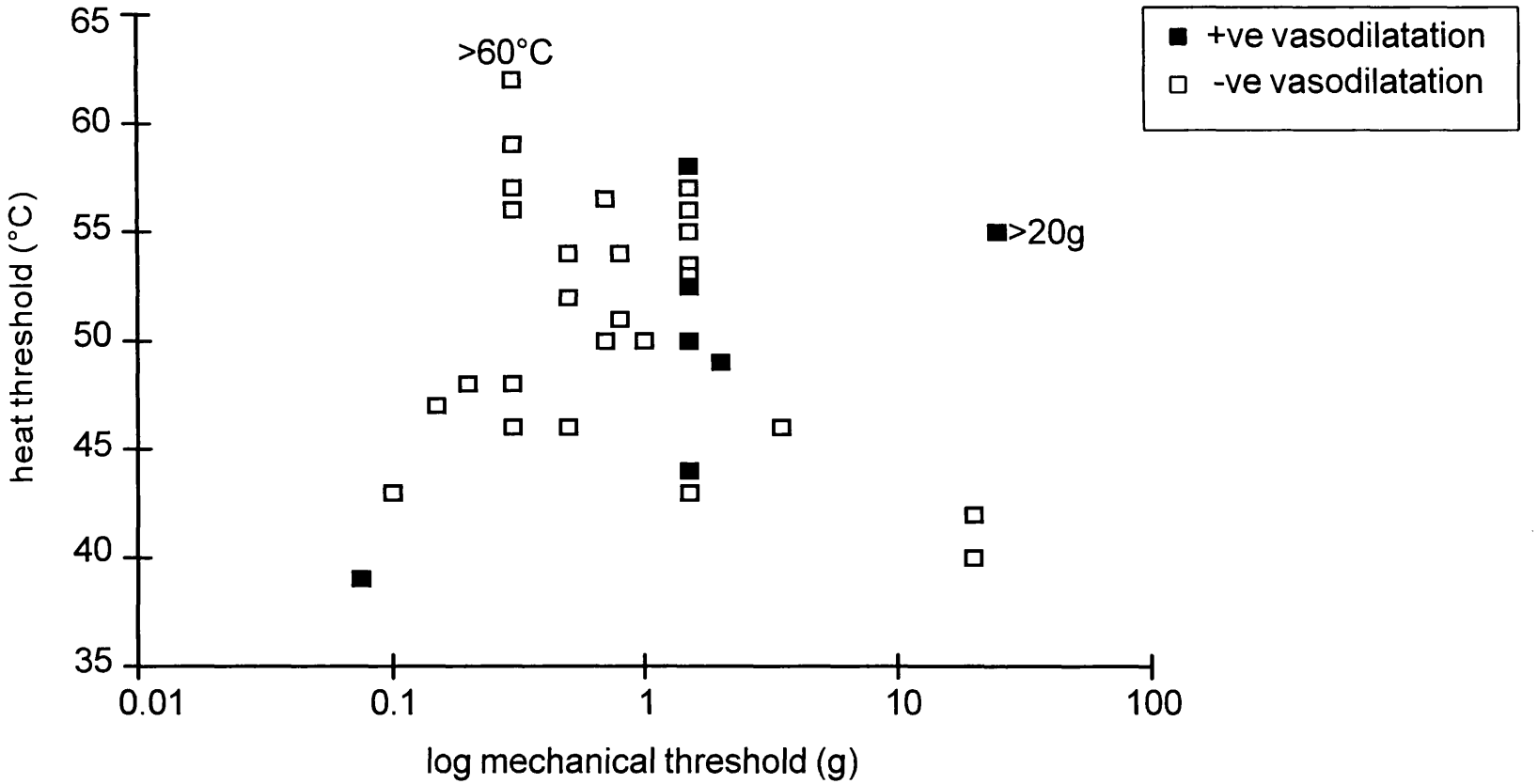

Figure 4.1 Graph showing the mechanical and heat thresholds of the polymodal nociceptors that produced vasodilatation (filled symbols) and the polymodal nociceptors that did not produce vasodilatation (open symbols) in the rat saphenous nerve.

4.2 Heat thresholds

The distribution of the heat thresholds of the polymodal nociceptors is shown in Figure 4.2A; the heat thresholds ranged from 39°C to greater than 60°C and the average heat threshold was 50.6°C±0.86 (n=37; mean±SE). Those units that produced vasodilatation had a mean heat threshold of 49.6°C±2.45 (n=7) and the non-vasodilator polymodal units had a mean heat threshold of 50.8°C±0.9 (n=30). The vasodilator polymodal units did not have significantly different heat thresholds from the non-vasodilator units (t-test, n=37, p=0.60).

4.3 Mechanical thresholds

The distribution of the mechanical thresholds of the polymodal nociceptors is shown in Figure 4.2B; the mechanical thresholds ranged from 75mg to greater than 20g and the average mechanical threshold was 2.0g±0.69 (n=39). With the exception of one unit, the polymodal nociceptors that produced antidromic vasodilatation had mechanical thresholds of greater than 1g. However, although the polymodal units with vasodilator actions tended to have mechanical thresholds towards the higher end of the range, the pressure thresholds of these units were not significantly different to those of the non-vasodilator polymodal units (Mann-Whitney U test, n=39, p=0.27).

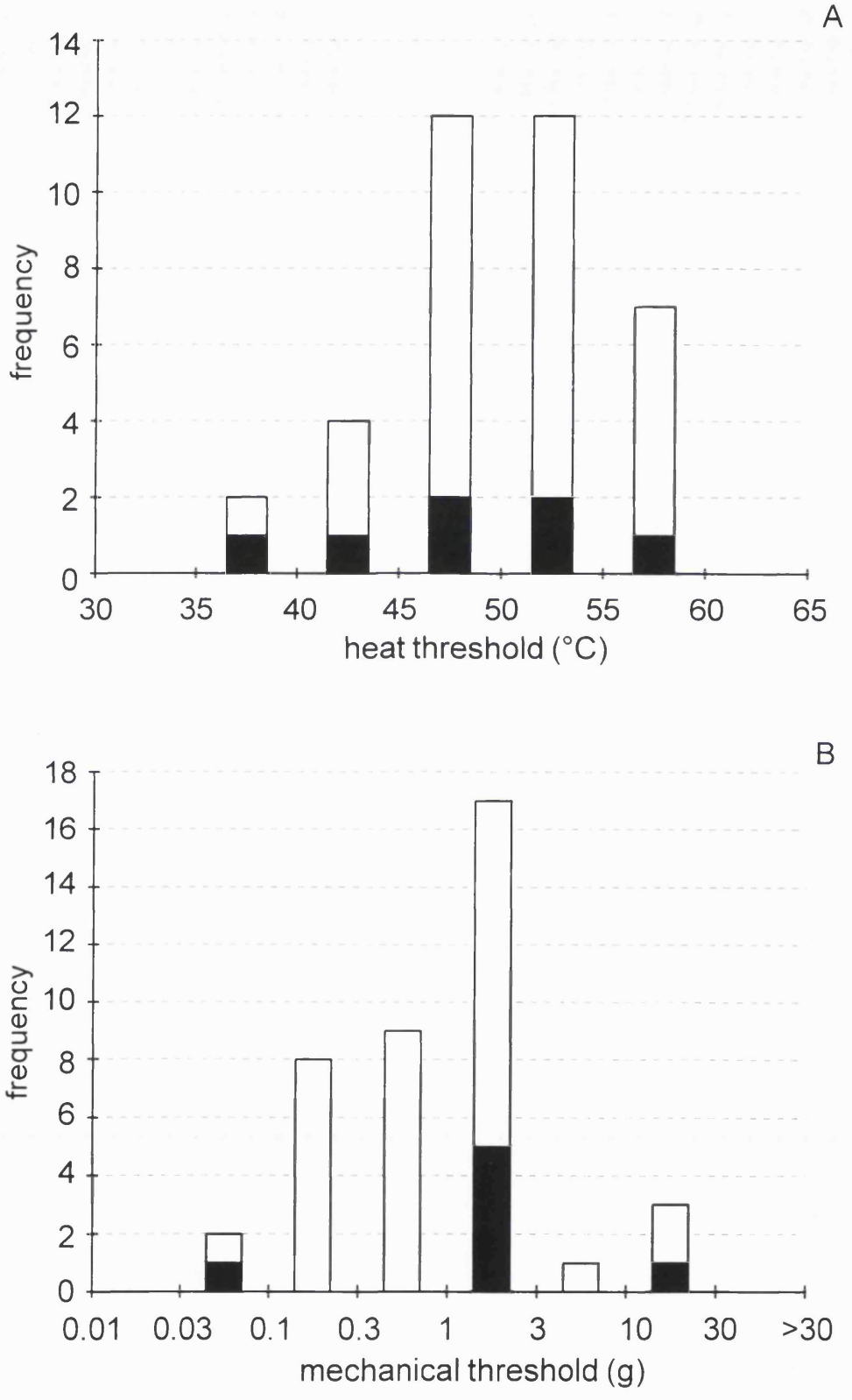

Figure 4.2 **Frequency distribution histograms of A) the heat thresholds, and B) the mechanical thresholds, of polymodal nociceptors in the rat saphenous nerve.** The open bars represent all polymodal nociceptors, the closed bars represent the vasoactive polymodal nociceptors. Note the logarithmic scale in graph B.

4.4 *Efferent responses*

Figures 4.3 to 4.5 show images of the vasodilatation resulting from antidromic stimulation of nociceptive C-fibres. The images have been scaled so that the colours represent percentage increase in blood flow above the baseline. Note that in Figures 4.3 to 4.5 the blue colour represents the smallest changes in blood flow and includes any decreases in blood flow from the baseline. Figure 4.6 shows laser Doppler flowmeter traces illustrating the skin blood flow at three sites before, during and after stimulation of a fine filament. The filament contained 2 identified C-fibres - both classified as polymodal/mechanical nociceptors. Only one of these 2 C-fibres demonstrated detectable vasodilatation. The 11 vasodilator units found in this study produced increased blood flow ranging from 17-180% above baseline. The areas of vasodilatation were always coincident with the afferent receptive field of the units (see Figure 4.5). Nine of the 11 vasodilator units had receptive fields on the foot or digits. Statistical analysis shows that the vasodilator units were not distributed evenly between the foot (including the digits) and the ankle/leg regions of the saphenous field (χ^2= 6.7, P=0.025).

4.5 *C-fibres without vasodilator actions*

Stimulation of the remaining 43 units showed no detectable increases in skin blood flow. However, stimulation of the whole saphenous nerve always resulted in antidromic vasodilatation, thereby showing that the skin was capable of producing a vasodilator response (see Figure 4.7). Also, only units that survived the period of filament stimulation are included in these results. Thus, these 43 units provided convincing negative results for antidromic vasodilatation.

4.6 Summary

- It is possible to detect vasodilatation in the skin of the rat resulting from antidromic stimulation of single C-fibres using laser Doppler flowmetry and laser Doppler perfusion imaging.
- All the fibres that produced increased skin blood flow in the rat were nociceptive. In this study, only a small proportion of the polymodal and polymodal/mechanical nociceptors (21%) were able to produce a detectable vasodilatation, although both of the heat nociceptors were vasodilators.
- The polymodal nociceptors with vasodilator actions tended to have relatively high mechanical thresholds and to be located on the foot or digits.

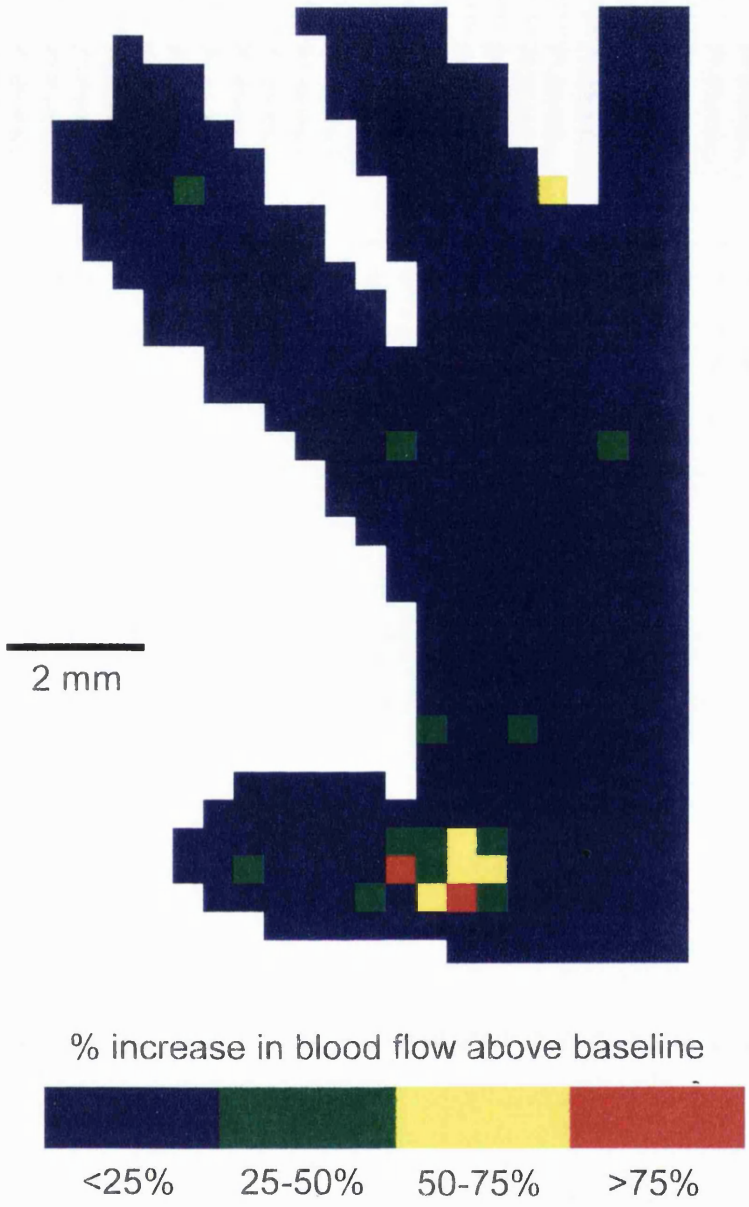

Figure 4.3 An image showing antidromic vasodilatation following electrical stimulation of a filament containing a C-polymodal nociceptor (conduction velocity = 0.91m/s, Von Frey threshold = 1-2g, heat threshold = 52.5°C) whose afferent receptive field was a small zone at the base of digit 1. The centre of the afferent field coincided with the centre of the vasodilator response. The parameters for filament stimulation were 1.0μA, 2mins, 5Hz, 0.5ms pulse width. Baseline scans made before stimulation have been subtracted from those taken during stimulation, and 5 difference images have been averaged to make this image. The image has been scaled so that the colours represent percentage increase in blood flow above the baseline. Note that in this figure and in Figures 4.4 and 4.5, the blue colour represents the smallest changes in blood flow and includes decreases in blood flow from the baseline.

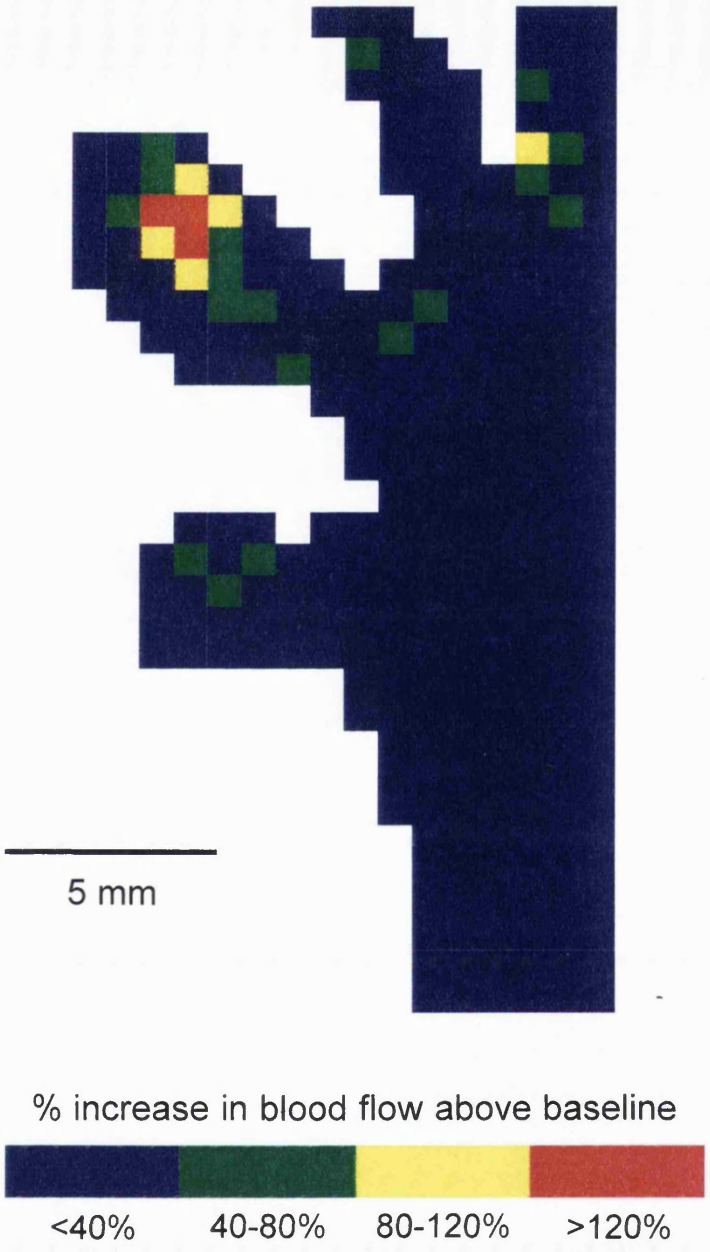

Figure 4.4 An image showing antidromic vasodilatation following electrical stimulation of a filament containing a C-heat nociceptor (conduction velocity = 0.53m/s, heat threshold = 53°C) whose afferent receptive field was on the anterior surface of digit 2. The centre of the afferent field coincided with the centre of the vasodilator response. The parameters for filament stimulation were 1.4μA, 30 seconds, 5Hz, 0.5ms pulse width.
Baseline scans made before stimulation have been subtracted from those taken during stimulation, and 3 difference images have been averaged to make this image. The image has been scaled so that the colours represent percentage increase in blood flow above the baseline.

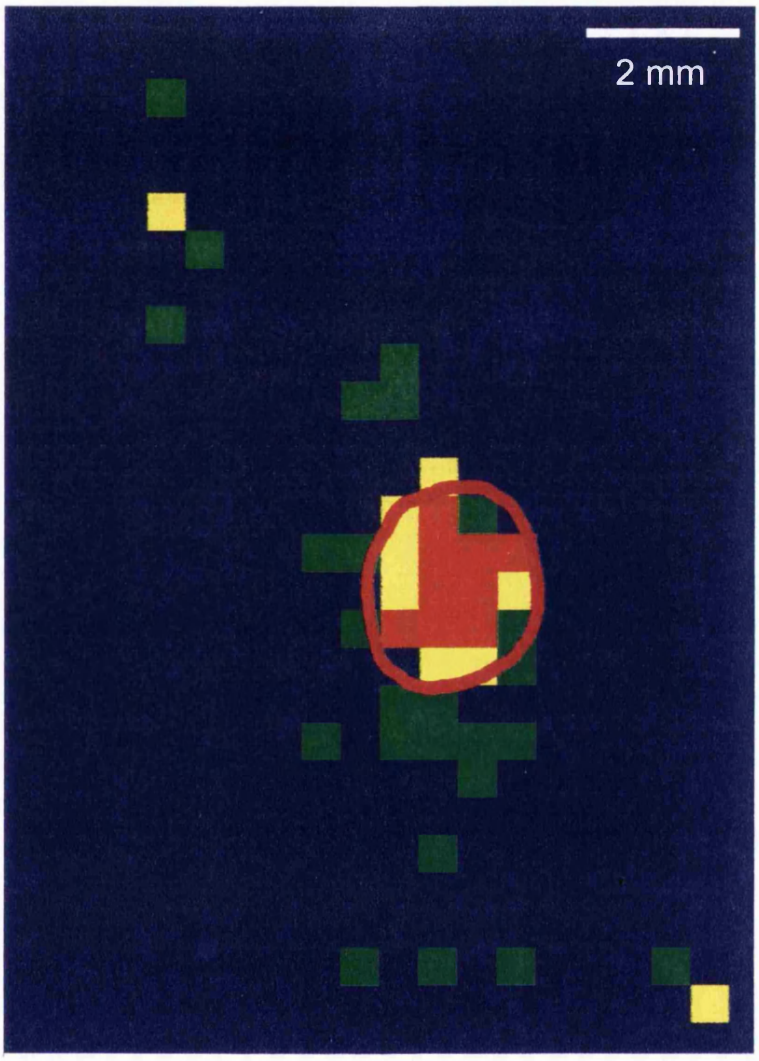

Figure 4.5 An image showing antidromic vasodilatation following electrical stimulation of a filament containing a single C-polymodal nociceptor (conduction velocity = 0.79m/s, Von Frey threshold = 1-2g, heat threshold = 53°C) whose afferent receptive field was located on the anterior foot near the ankle. The afferent receptive field of this unit was approximately 2.5mm by 2mm, and has been drawn on the image. The area of vasodilatation is slightly larger than the afferent field. The parameters for filament stimulation were 0.9μA, 1 minute, 5Hz, 0.5ms pulse width.
Baseline scans made before stimulation have been subtracted from those taken during stimulation, and 3 difference images have been averaged to make this image. The image has been scaled so that the colours represent percentage increase in blood flow above the baseline.

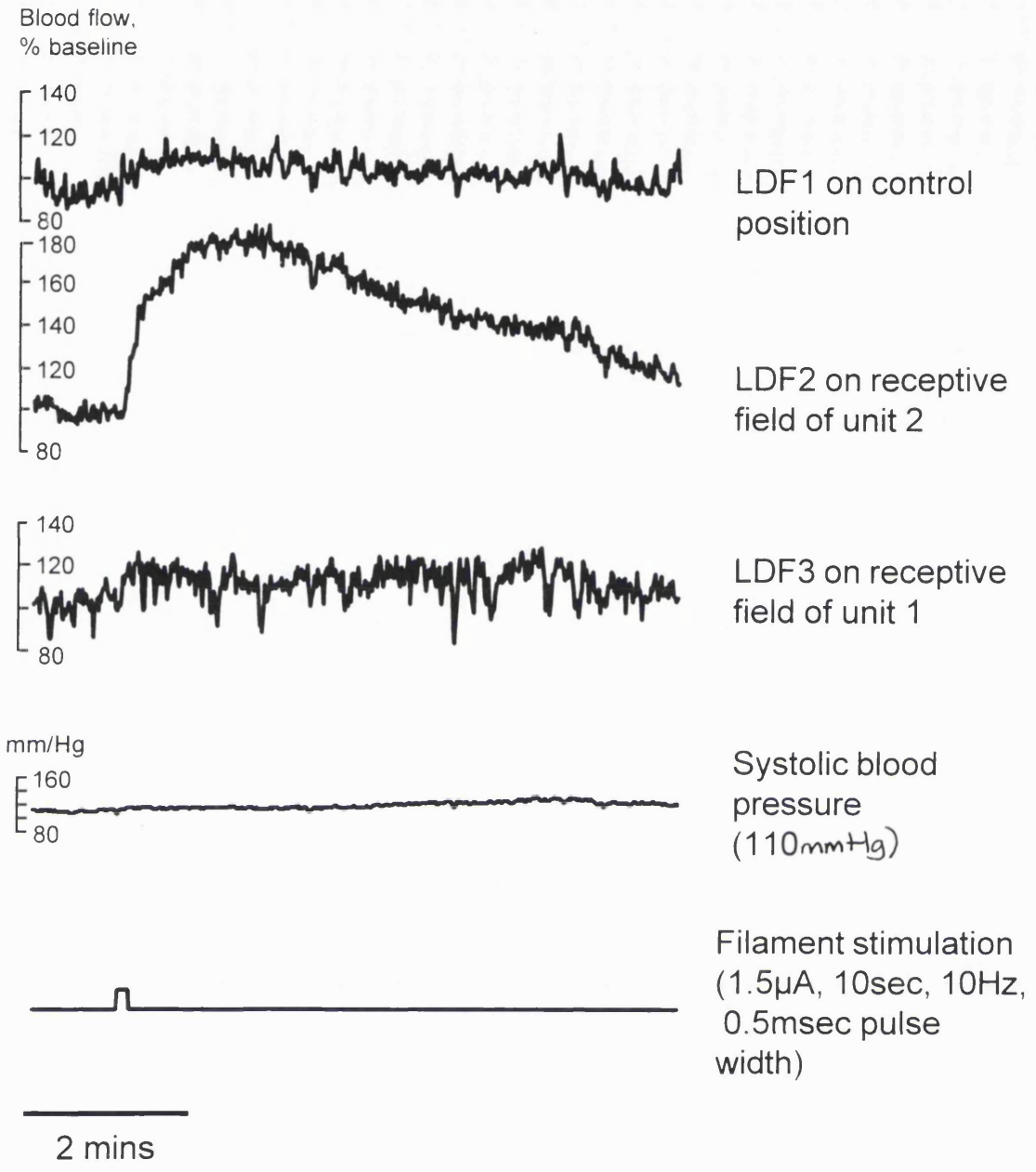

Figure 4.6 Laser Doppler flowmeter traces during filament stimulation (1.5 μA, 10 secs, 10 Hz, 0.5 ms pulse width). This filament contained 2 C-fibres. Unit 1 was a polymodal/mechanical nociceptor located on the medial lower leg near the ankle; no vasodilatation was detected at its receptive field. Unit 2 was a polymodal/mechanical nociceptor located on the tip of digit 1. Electrical stimulation resulted in a great increase of skin blood flow at the receptive field of unit 2 (145% increase above baseline). A laser Doppler flowmeter probe placed in a control position (on the anterior mid-foot) did not record any vasodilatation. The blood pressure remained constant at around 110/80mmHg (systolic/diastolic).

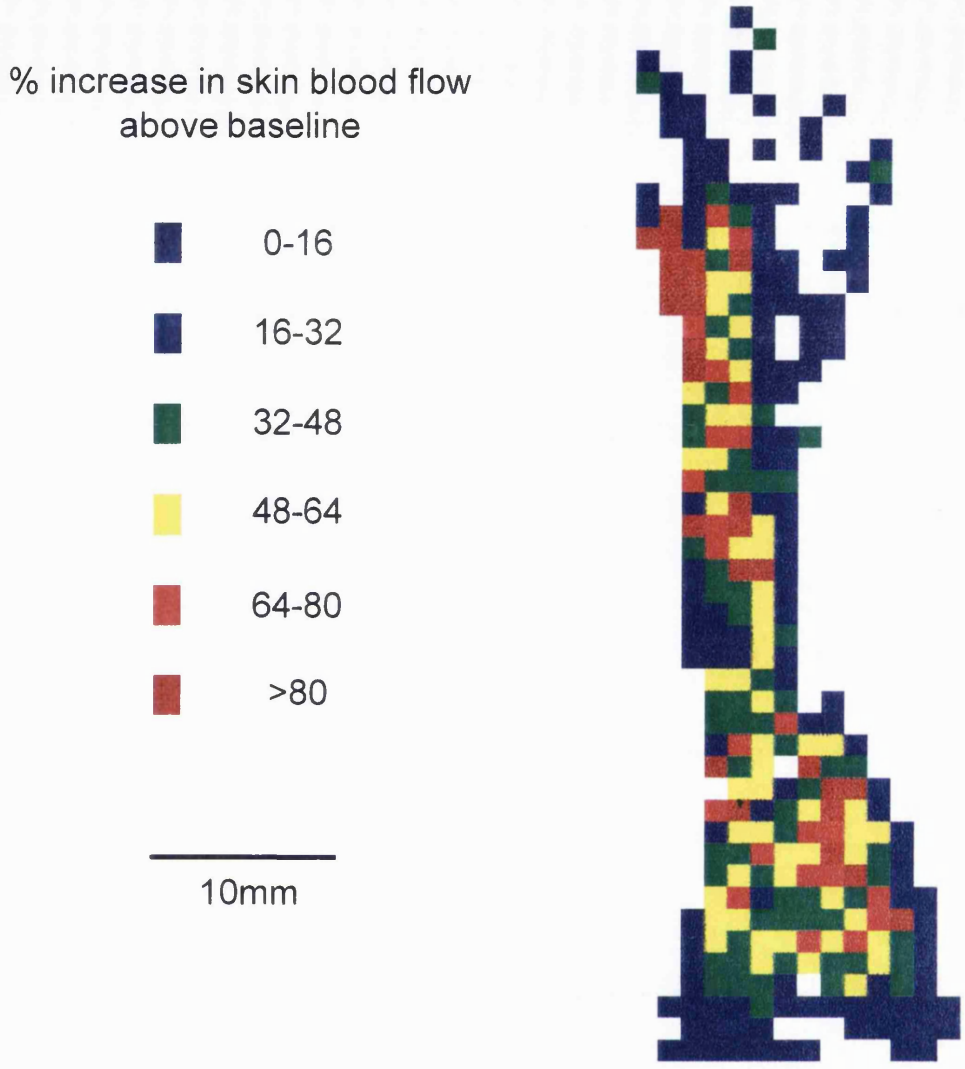

Figure 4.7 **An image showing antidromic vasodilatation following electrical stimulation (1.5mA, 15 seconds, 2Hz, 0.5msec pulse width) of the rat saphenous nerve.**
This image was created by subtracting the scan taken before electrical stimulation from the scan taken approximately 1 minute after stimulation. Skin blood flow has clearly risen in the saphenous field.

CHAPTER 5 RESULTS: THE FLARE RESPONSES OF RABBIT AND RAT SKIN TO MECHANICAL AND HEAT STIMULI

The flare responses following mechanical stimulation of rabbit and rat skin, and heat stimulation of rabbit skin, were studied using the laser Doppler perfusion imaging system. These flare studies were all carried out on skin within the saphenous receptive field. Of interest in this study were the thresholds required to produce a flare response, and the maximum intensity, duration and extent of the flares.

Each mechanical stimulus consisted of 1-10 applications of a Von Frey filament. A range of Von Frey filaments were tried (from 0.1g to 10g) with diameters from 0.15mm to 0.40mm, in 9 locations in the rabbit (3 animals) and in 6 locations in the rat (1 animal). Any changes in skin blood flow that exceeded a 15% increase from the baseline and were outside the small zone of local injury were considered to be flare responses. The mechanical thresholds to produce a flare response were noted.

Heat stimuli were applied to rabbit skin using a circular contact heat probe (diameter = 7mm) and consisted of heat ramps from 35°C to 50°C, 55°C or 60°C. The temperatures of all the heat ramps were raised at a rate of 1°C/second. Any changes in skin blood flow that exceeded a 15% increase from the baseline and were outside the region of local injury (i.e. the circular area of the heat probe) were considered to be flare responses. The flare responses were imaged for up to 32 minutes after stimulation.

5.1 Flare responses following mechanical stimulation of rabbit skin

In the rabbit, the forces required to produce a flare response to mechanical stimulation were investigated in 9 different skin areas within the saphenous receptive field. The thresholds for flare to mechanical stimulation ranged from 0.4g to 1.0g, with the average threshold being 0.60±0.06g (mean±SE, n=9). Figure 5.1 shows the imaged flare responses 10 seconds and 90 seconds after mechanical stimulation with a range of Von Frey filaments. The greatest forces resulted in the largest, most intense and most long-lasting flare responses. Figures 5.2 and 5.3 show the blood flow changes that occurred for up to 3 minutes following mechanical stimulation with a range of Von Frey filaments, in two different locations. The greatest flare response resulted from 3 applications of a 5g Von Frey filament. The maximum increase in skin blood flow 1mm away from this stimulus was 114% (see Figure 5.2), and the response lasted for about 16 minutes. The maximum extent of this flare was 17.6mm in the proximal-distal direction and 9.4mm in the medial-lateral direction.

5.2 Flare responses following mechanical stimulation of rat skin

In the rat, flare following mechanical stimulation with a range of Von Frey filaments was studied in 6 different skin areas within the saphenous receptive field. There was a wide range of threshold forces required to produce a flare response in rat skin. The thresholds ranged from 2g to 10g, with an average value of 7.0±1.41g (mean±SE; n=6). Figure 5.4 shows the images taken up to 8 minutes after mechanical stimulation with a range of Von Frey filaments. Figure 5.4 demonstrates that the largest, most intense and most long-lasting flares were those that resulted from mechanical stimulation using the greatest force.

Figures 5.5 and 5.6 show the blood flow changes that occurred for up to 4 minutes after mechanical stimulation in two different areas of rat skin. The greatest flare response seen after 3 applications of a Von Frey filament to rat skin was seen with the 10g Von Frey hair. The change in blood flow measured 1mm away from this stimulus was a 74% increase above the baseline, and this flare lasted for about 7 minutes. The maximum extent of a flare response to mechanical stimulation of rat skin was 6.1mm in the proximal-distal direction, and 3.4mm in the medial-lateral direction.

5.3 Flare responses following heat stimulation of rabbit skin

In the rabbit, a total of 6 heat ramp stimuli were applied to different areas of skin within the saphenous receptive field. Three different heat ramps were used - 2 each of 35-50°C, 35-55°C and 35-60°C, all increased at a rate of 1°C/second. Skin blood flow was monitored for up to 32 minutes after the heat tests. All 6 heat ramp stimuli produced a flare response in rabbit skin. Figure 5.7 shows the flare responses imaged up to 14 minutes after heat ramps from 35°C to 50°C, 55°C and 60°C. The heat ramp that reached the highest maximum temperature (i.e. the 35-60°C ramp) produced the most intense flares, the largest flares and the flares of the longest duration. The relationship between the maximum temperature reached in the heat ramp and the intensity, size and duration of the resulting flare response is summarized in Figures 5.8 to 5.11. Note the similarity of the flare responses following the pairs of heat stimuli (Figures 5.8 to 5.11). The greatest flare response was seen following one of the 35-60°C heat ramps. This stimulus produced a flare response that, 1mm away from the edge of the heat probe, showed a 125% increase in skin blood flow and lasted for longer than 32 minutes (see Figures 5.7 and 5.8). The

maximum radius of this flare measured from the edge of the heat probe was 8.2mm in the proximal-distal direction, and 3.5mm in the medial-lateral direction.

5.4 Summary

- Flare responses to localized noxious mechanical and thermal stimulation of rabbit and rat skin can be observed using the laser Doppler perfusion imaging system. Measurements of the size, intensity and duration of the flares can be made.
- Flare responses following mechanical stimulation of rat skin were variable. There was a wide range (2 - 10g) of threshold forces required to produce a flare response to mechanical stimulation (n=6).
- The maximum extent of the flare resulting from mechanical stimulation of rat skin was 6.1mm by 3.4mm.
- Flare responses in rabbit skin were more consistent than in rat skin (note the similarity of the flares following pairs of heat stimuli in Figures 5.8 to 5.11). The threshold temperature required to produce a flare in rabbit skin was <50°C. The mechanical thresholds required to produce a flare in rabbit skin ranged from 0.4g to 1.0g (n=9).
- The maximum extent of the flare resulting from mechanical stimulation of rabbit skin was 17.6mm by 9.4mm.

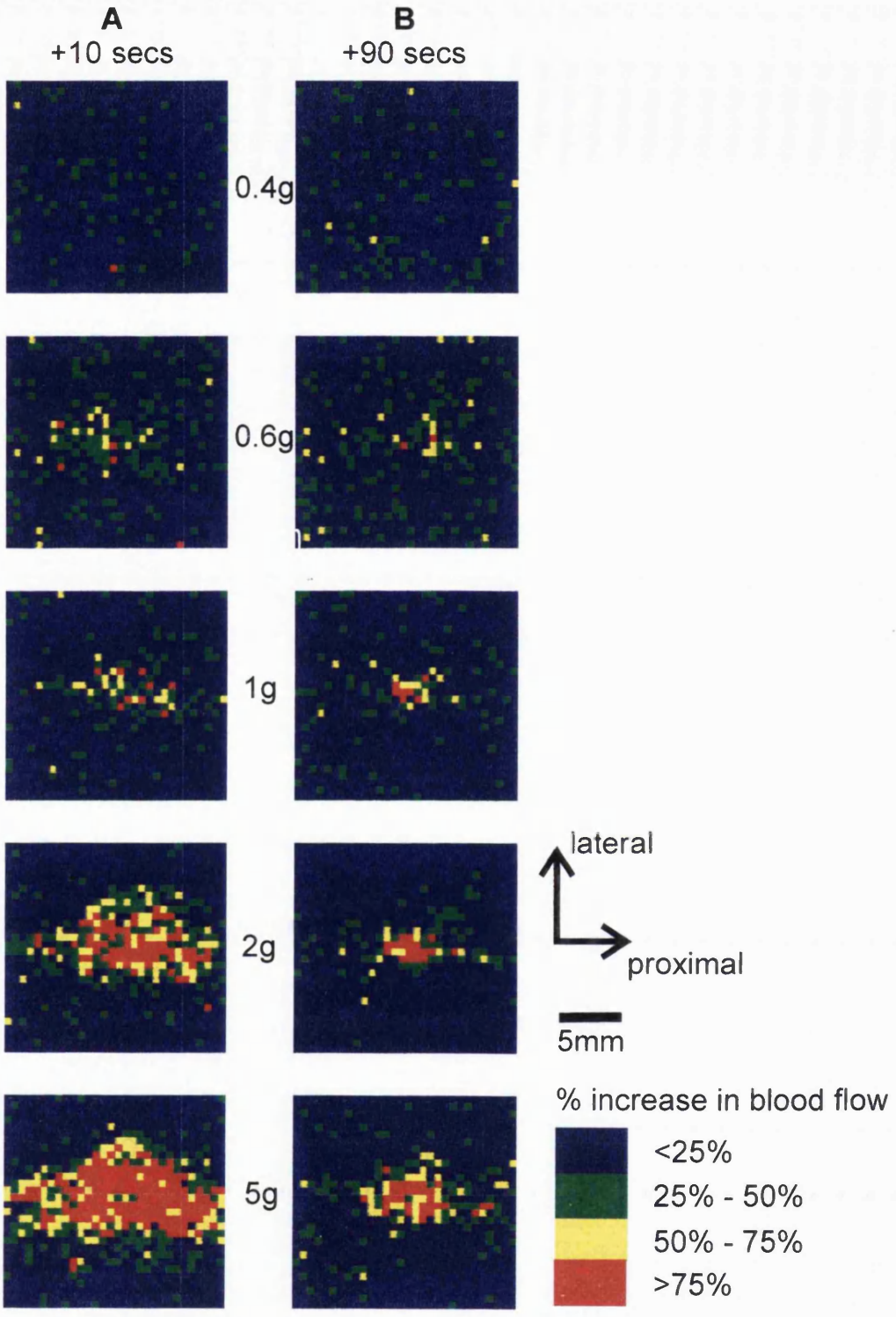

Figure 5.1 Images showing flare responses in rabbit skin, A) 10 secs, and B) 90 secs, after mechanical stimulation with a range of Von Frey filaments. Each mechanical stimulus consisted of 3 applications of a Von Frey filament, each lasting approximately 1 second.
Baseline scans taken before the mechanical stimulation have been subtracted from those taken after the stimulation. The images have been scaled so that the colours represent percentage increase in skin blood flow above the baseline.

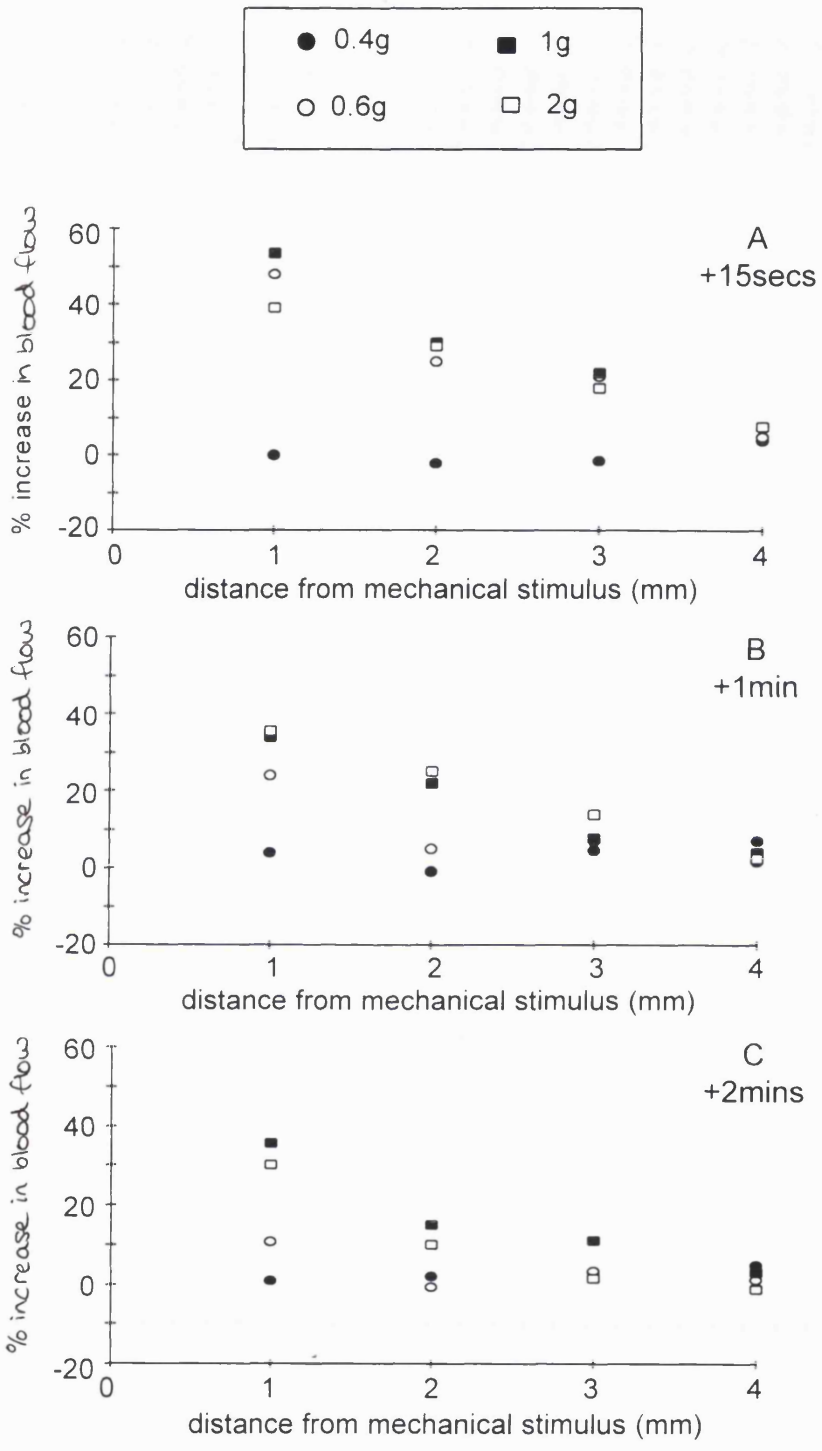

Figure 5.2 Graphs showing the percentage increase in skin blood flow A) 15secs, B) 1min, and C) 2mins, after mechanical stimulation of the skin on the medial upper leg of the rabbit. A range of Von Frey filaments were used. Each mechanical stimulus consisted of 3 applications of a Von Frey filament.

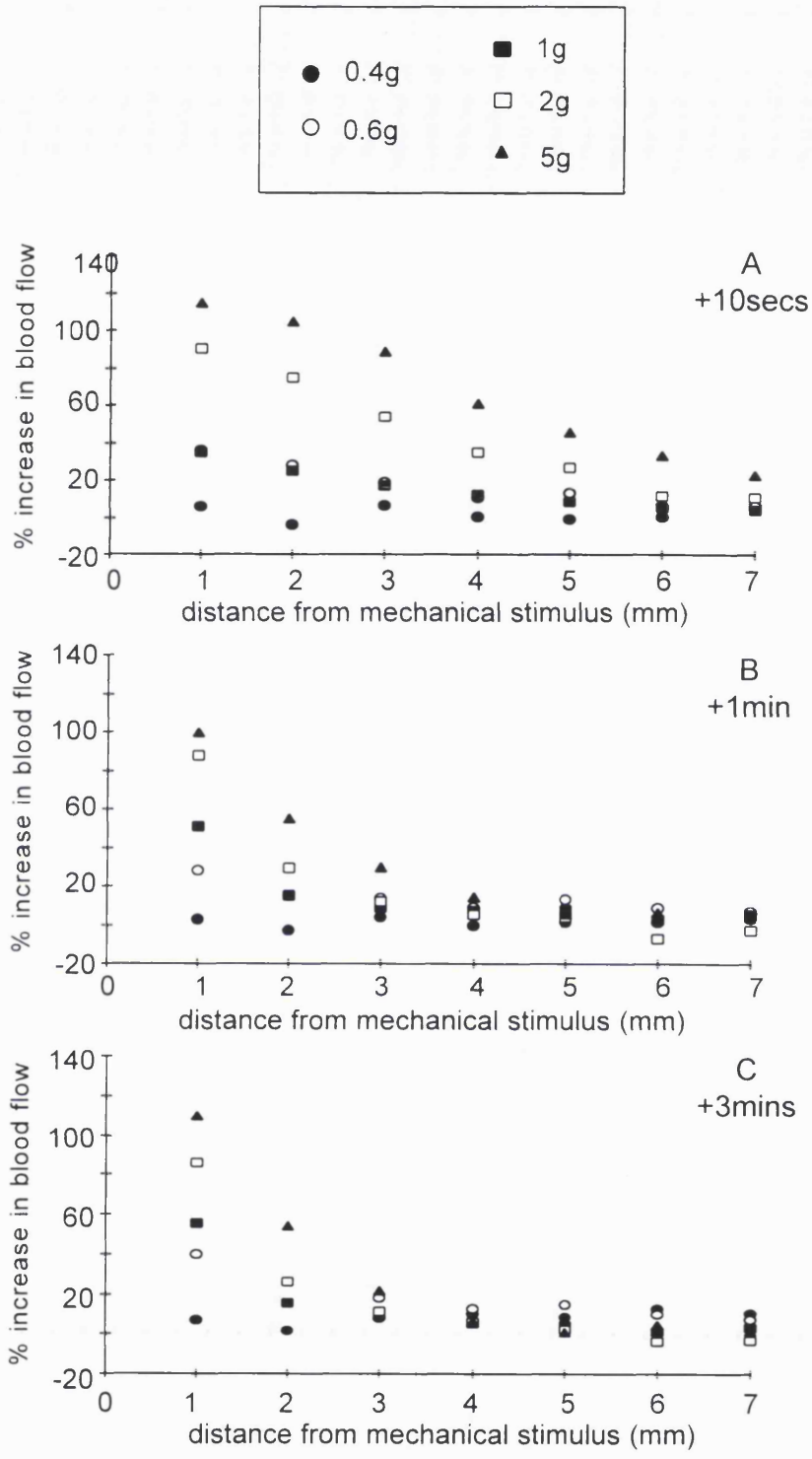

Figure 5.3 Graphs showing the percentage increase in skin blood flow A) 10secs, B) 1min, and C) 3mins, after mechanical stimulation of the skin on the medial mid-leg of the rabbit. A range of Von Frey filaments were used. Each mechanical stimulus consisted of 3 applications of a Von Frey filament.

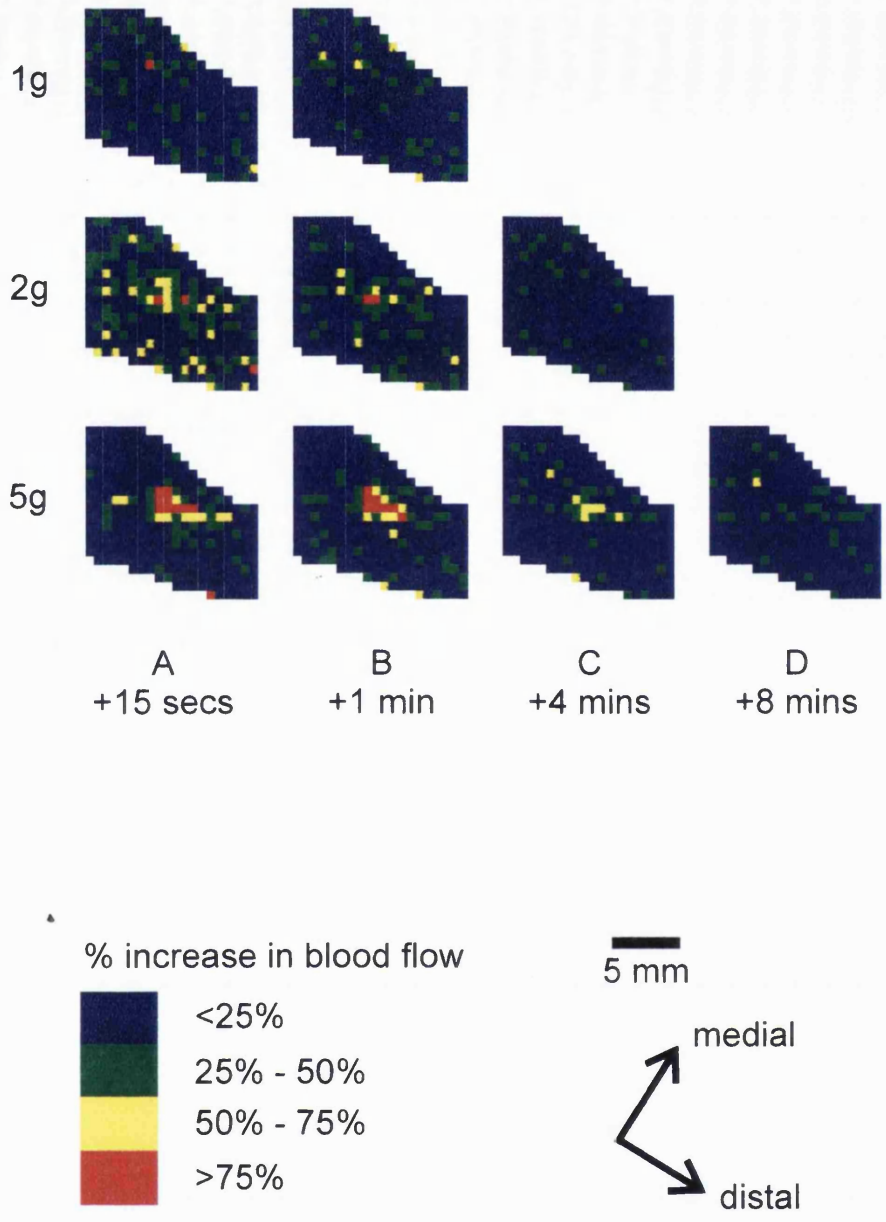

Figure 5.4 Images showing flare responses in rat skin, A) 15secs, B) 1 min, C) 4 mins, and D) 8 mins, after mechanical stimulation with a range of Von Frey filaments. Each mechanical stimulus consisted of 3 applications of a Von Frey filament.
Baseline scans taken before the mechanical stimulation have been subtracted from those taken after the stimulation. The images have been scaled so that the colours represent percentage increase in skin blood flow above the baseline.

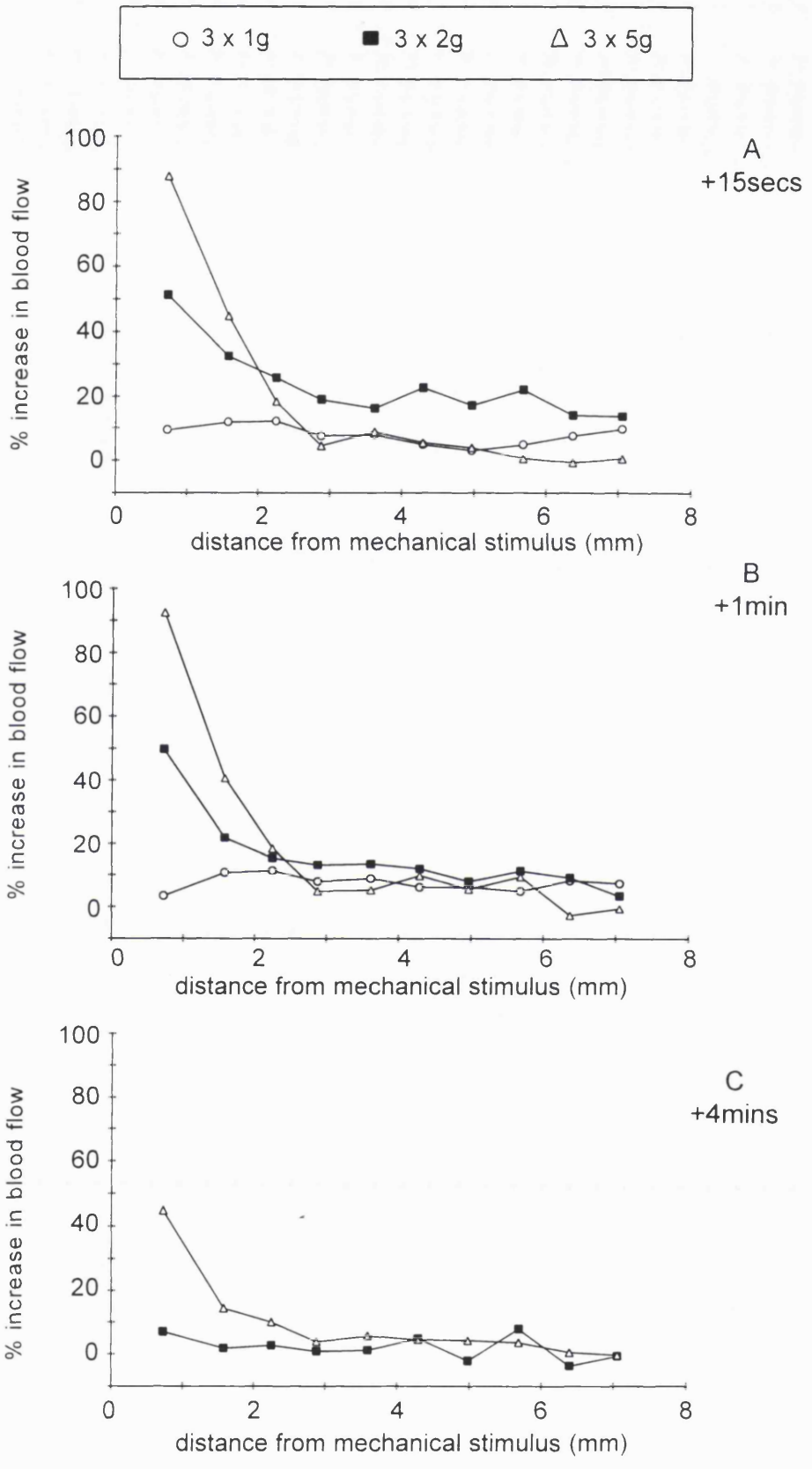

Figure 5.5 Graphs showing the percentage increase in skin blood flow A) 15secs, B) 1min, and C) 4mins, after mechanical stimulation of the skin on the anterior foot of the rat. A range of Von Frey filaments were used.

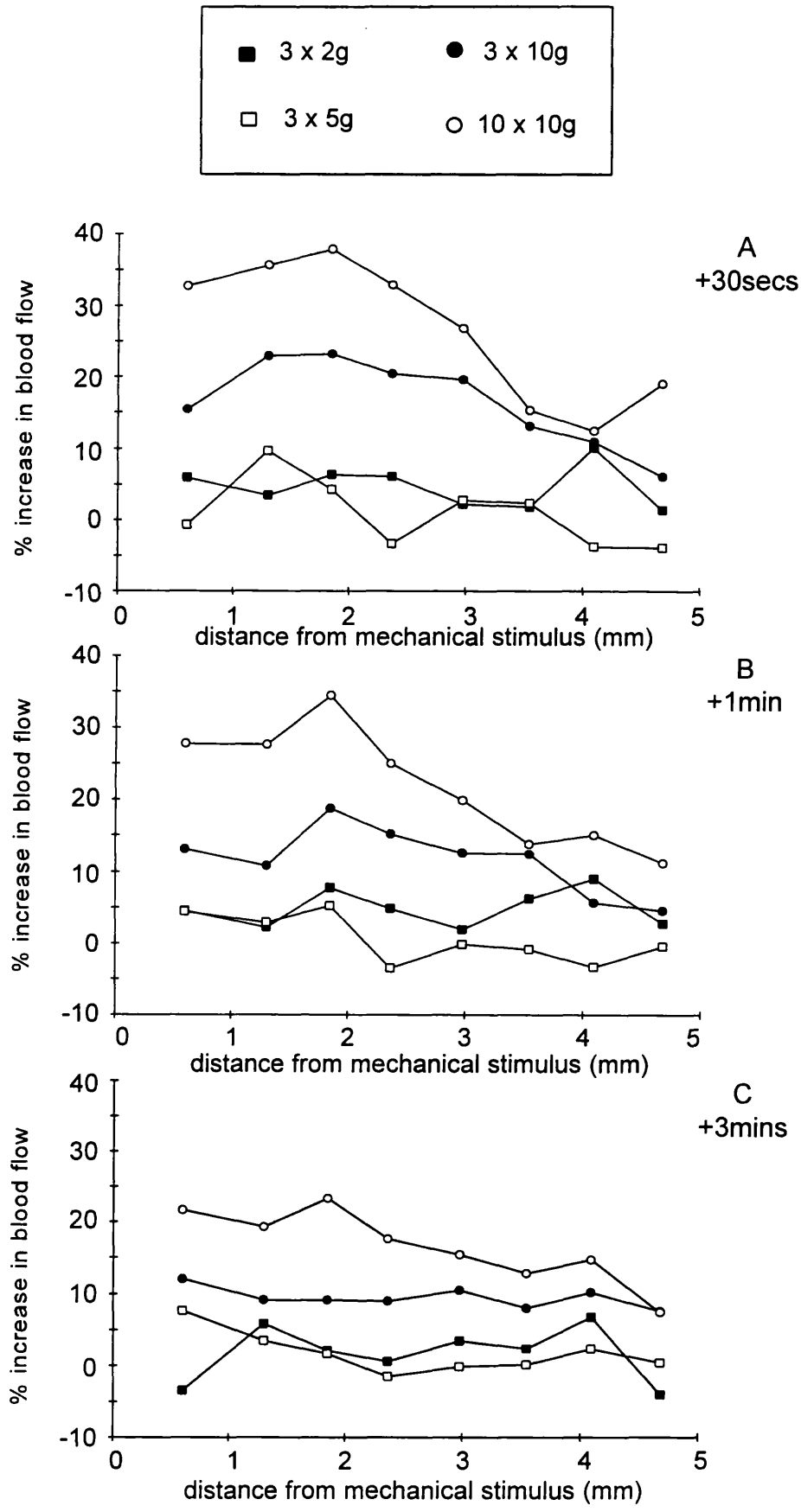

Figure 5.6 Graphs showing the percentage increase in skin blood flow A) 30secs, B) 1min, and C) 3mins, after mechanical stimulation of the skin on the anterior ankle of the rat. A range of Von Frey filaments were used.

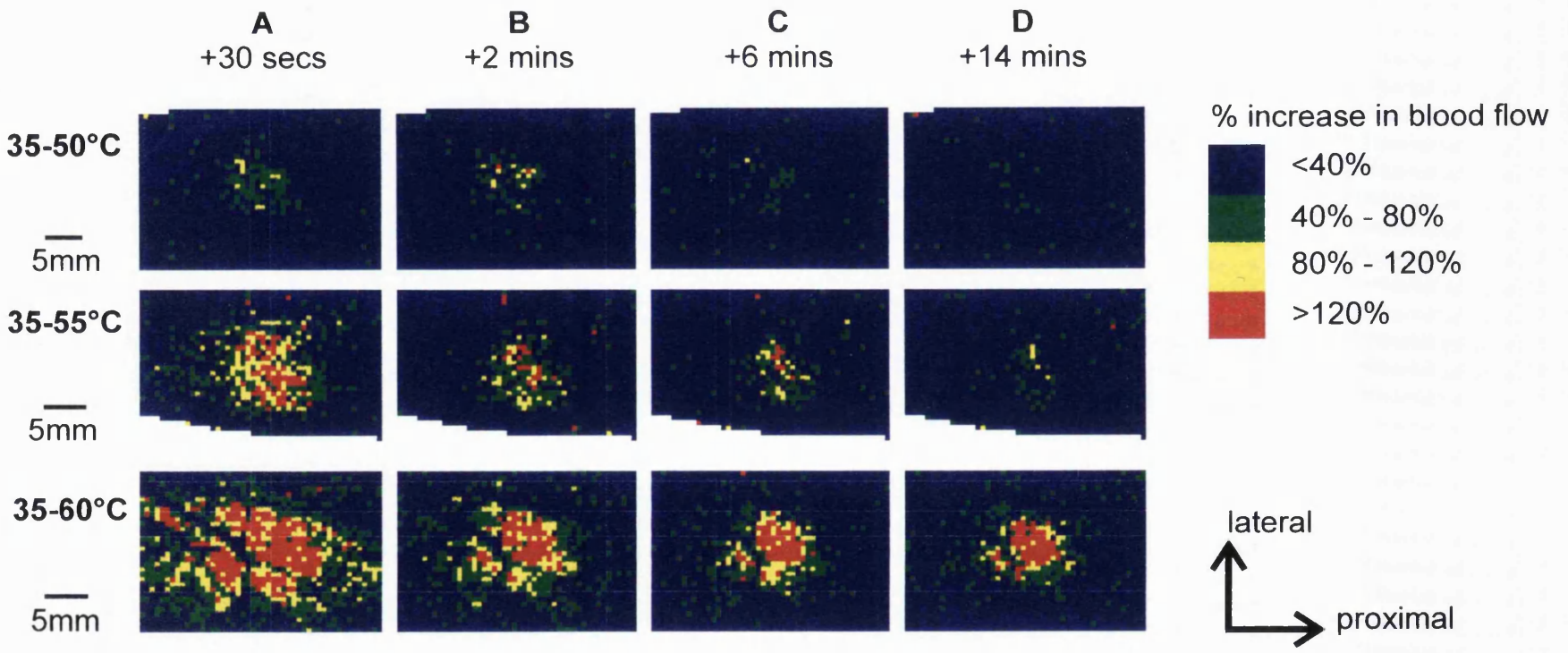

Figure 5.7 Images showing flare responses in rabbit skin, A) 30 secs, B) 2 mins, C) 6 mins, and D) 14 mins, after heat stimulation. Three different ramped heat stimuli were used - 35-50°C, 35-55°C and 35-60°C from top to bottom respectively. All ramps were increased at a rate of 1°C/sec. The 3 different heat stimuli were tested in different locations. The heat stimuli were applied using a circular contact heat probe (diameter = 7mm). Baseline scans taken before the heat stimulation have been subtracted from those scans taken after the stimulation. The images have been scaled so that the colours represent percentage increase in skin blood flow above the baseline. Note that the strip showing low percentage increase in the 35-60°C scans marks the course of a blood vessel, with high resting flow.

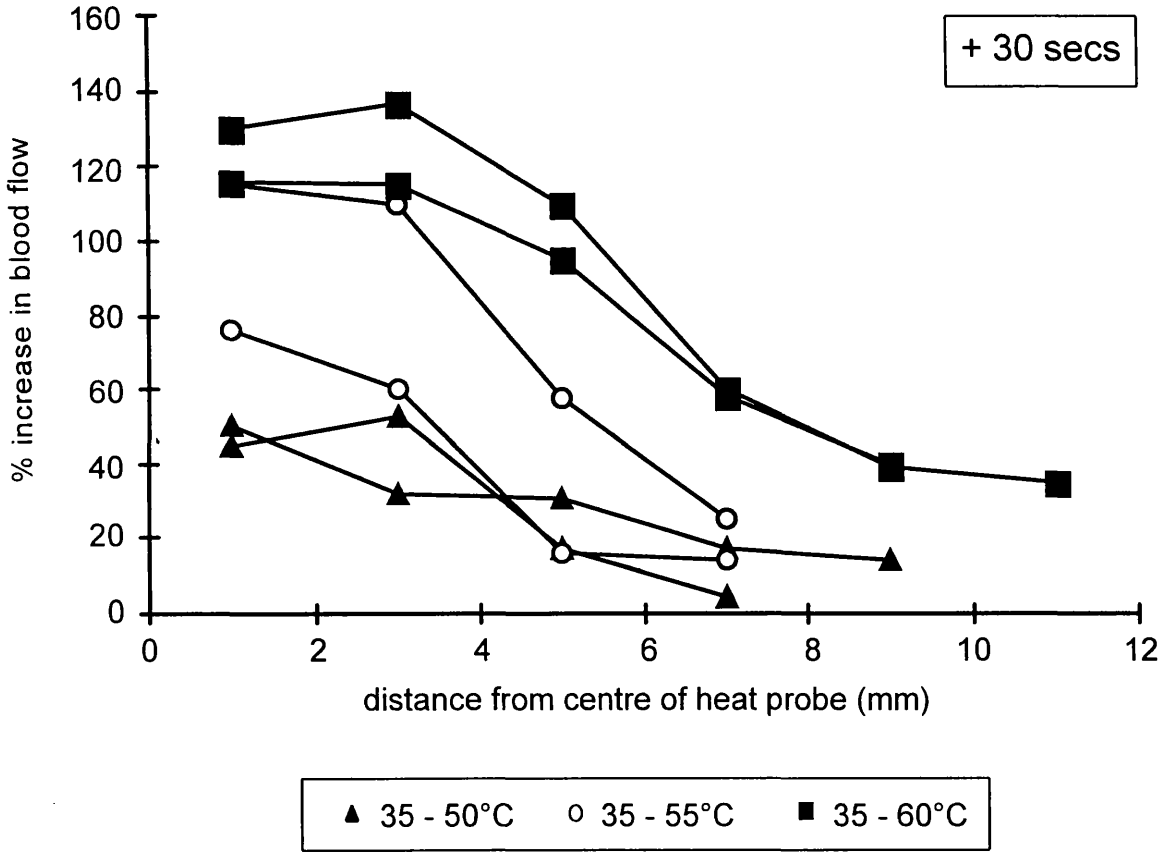

Figure 5.8 Graph showing the percentage increase in skin blood flow 30 seconds after heat stimulation of rabbit skin. Six ramped heat stimuli were used - two each of 35-50°C, 35-55°C and 35-60°C (all increased at a rate of 1°C/sec). The heat stimuli were applied using a contact heat probe (diameter = 7mm). Note the similarity of the flare responses to the pairs of heat tests.

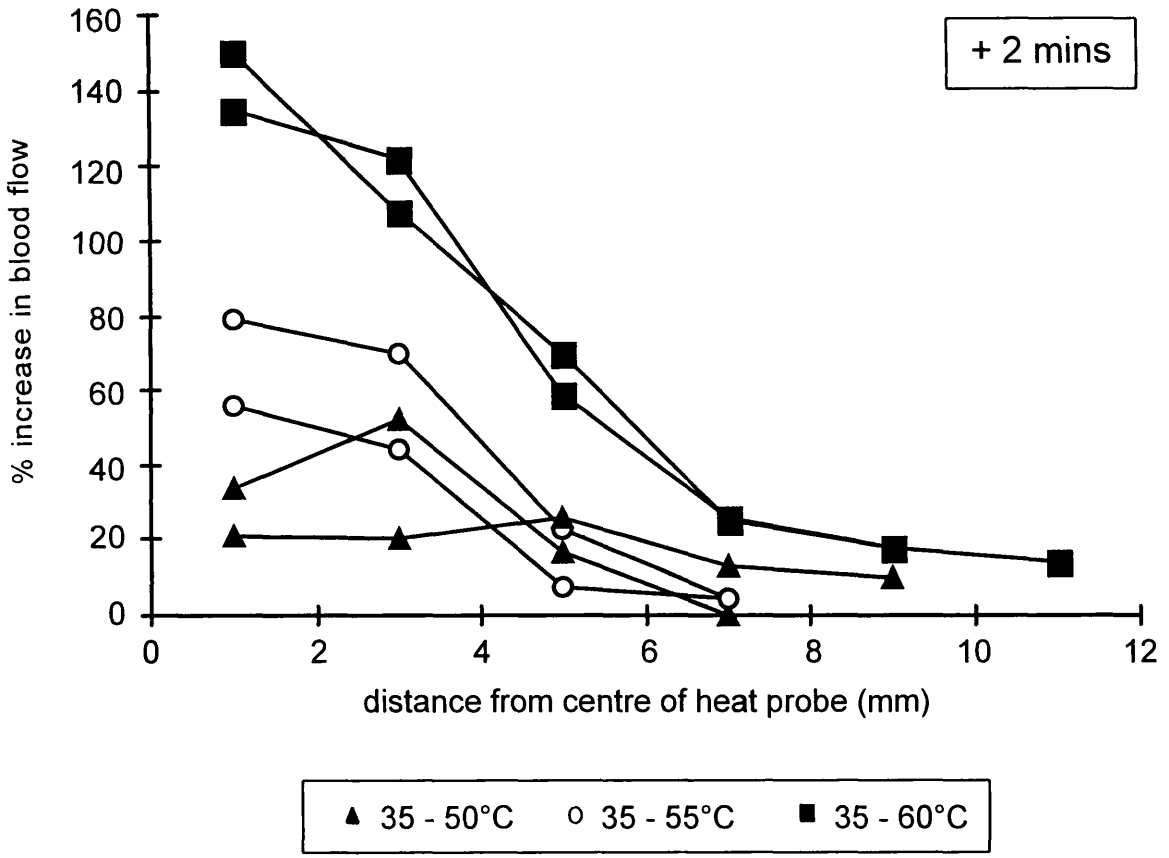

Figure 5.9 Graph showing the percentage increase in skin blood flow 2 minutes after heat stimulation of rabbit skin. Six ramped heat stimuli were used - two each of 35-50°C, 35-55°C and 35-60°C (all increased at a rate of 1°C/sec). The heat stimuli were applied using a contact heat probe (diameter = 7mm). Note the similarity of the flare responses to the pairs of heat tests.

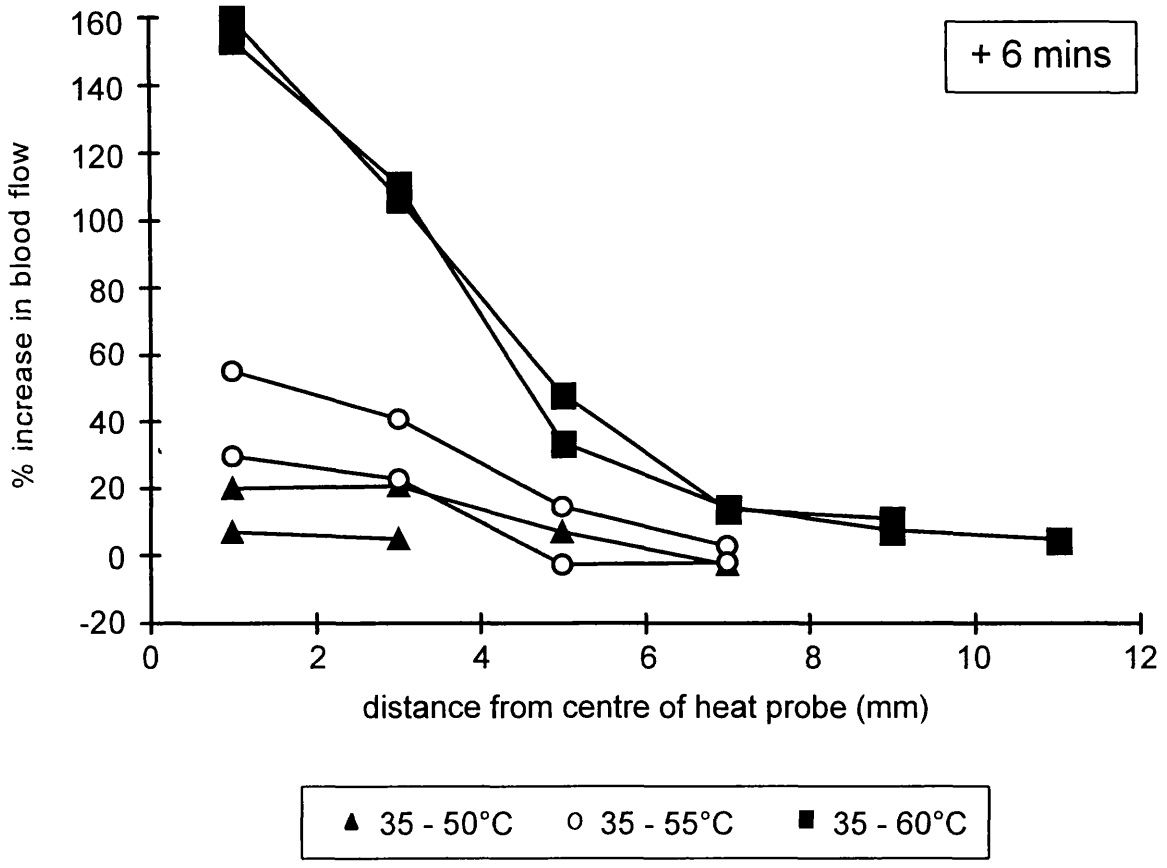

Figure 5.10 **Graph showing the percentage increase in skin blood flow 6 minutes after heat stimulation of rabbit skin.** Six ramped heat stimuli were used - two each of 35-50°C, 35-55°C and 35-60°C (all increased at a rate of 1°C/sec). The heat stimuli were applied using a contact heat probe (diameter = 7mm). Note the similarity of the flare responses to the pairs of heat tests.

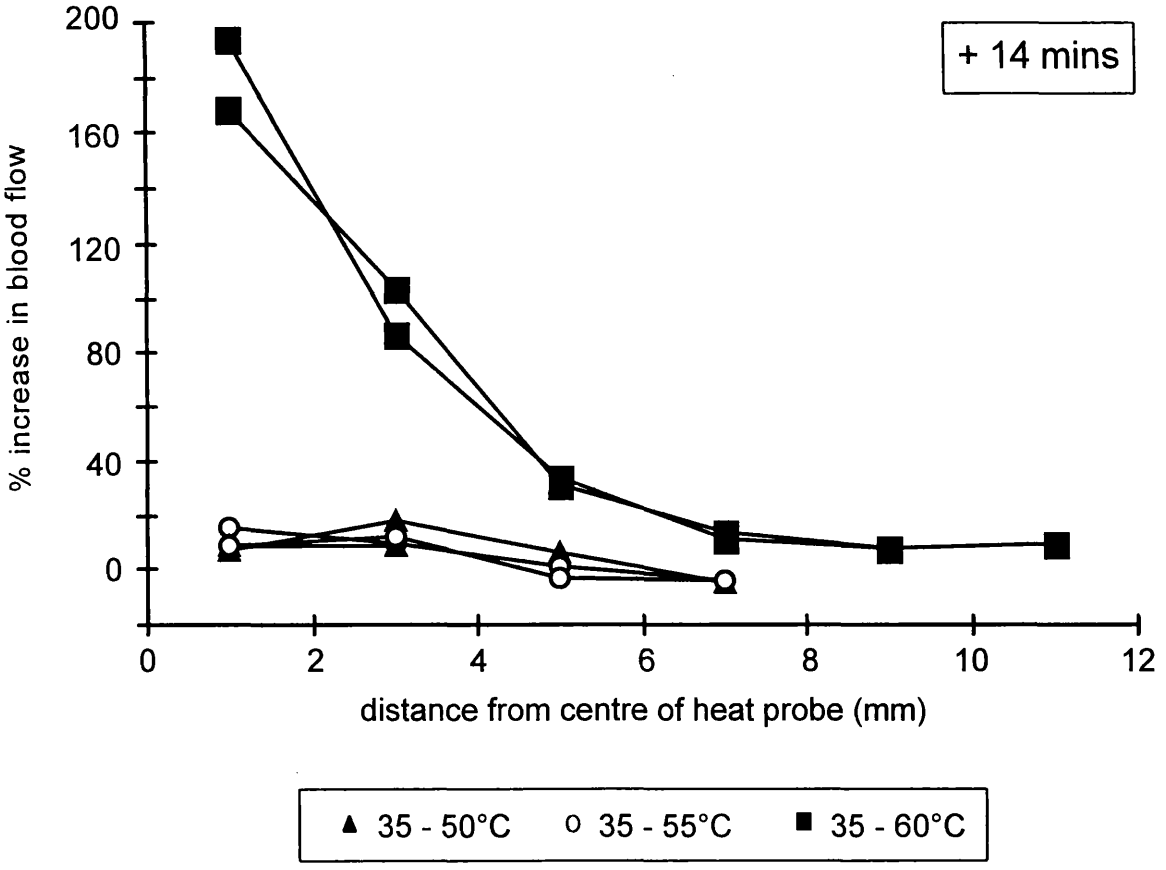

Figure 5.11 **Graph showing the percentage increase in skin blood flow 14 minutes after heat stimulation of rabbit skin.** Six ramped heat stimuli were used - two each of 35-50°C, 35-55°C and 35-60°C (all increased at a rate of 1°C/sec). The heat stimuli were applied using a contact heat probe (diameter = 7mm). Note the similarity of the flare responses to the pairs of heat tests.

CHAPTER 6 RESULTS: ACTIVITY-DEPENDENT SLOWING OF C-FIBRE CONDUCTION VELOCITY

Conduction velocity was measured in single unmyelinated fibres of the rat saphenous nerve throughout tetani at frequencies up to 33 Hz. A total of 178 C-fibres from 52 rats were studied (Gee *et al.* 1996a).

6.1 Response of C-fibres to tetani of different frequencies and durations

During periods of repetitive stimulation the conduction velocity of all fibres slowed, resulting in increased conduction delay (Figures 6.1 to 6.3). The greater the frequency of stimulation, the greater the degree of conduction velocity slowing (Figure 6.4). Likewise a longer stimulus duration resulted in a greater degree of conduction velocity slowing. Stimulating at 33 Hz, or at 20 Hz for longer than 20 seconds, resulted in conduction failure in many polymodal nociceptors (Table 6.1). Based on these findings the standard electrical stimulus was chosen as 20 seconds at 20 Hz. Stimulation with these parameters resulted in a large degree of conduction velocity slowing, but did not cause failure of conduction in the majority of fibres.

The pattern of conduction velocity slowing throughout the standard electrical stimulus of 20 Hz for 20 seconds varied from unit to unit. Most units showed a steady slowing of conduction velocity (see Figures 6.4a and 6.5), whereas some units (mainly the mechanoreceptors) tended to plateau (see Figures 6.4b and 6.5).

6.2 Conduction velocity slowing in different classes of afferent C-fibre

Following the standard electrical stimulus of 20 Hz for 20 seconds, the degree of conduction velocity slowing varied between the different classes of afferent unit, and this is demonstrated by the examples in Figures 6.1 to 6.3. Overall, the nociceptive units showed a greater degree of conduction velocity slowing (mean ± SEM; polymodal and heat nociceptors = 29.2% ± 0.7, n=53; mechanical nociceptors = 27.7% ± 1.7, n=13) than the cold units (10.8% ± 0.6, n=10), with the mechanoreceptors showing an intermediate change (14.4% ± 0.8, n=17) (see Figures 6.5 and 6.6). ANOVA (using the Student-Newman-Keuls procedure) shows significant differences ($p<0.05$) in the percentage slowing from resting conduction velocity between the different classes of nociceptors and the mechanoreceptors, between the different classes of nociceptors and the cold units, and between the mechanoreceptors and the cold units, although there is no significant difference among the different classes of nociceptive fibres. The cumulative frequency distributions for the nociceptive units, the mechanoreceptors and the cold units are shown in Figure 6.6. There was almost no overlap of the degree of conduction velocity slowing between the polymodal nociceptors and the mechanoreceptors. Only 2/17 mechanoreceptors showed a greater than 20% slowing from resting conduction velocity following 20 seconds at 20 Hz, whereas all 51/51 polymodal nociceptors slowed by greater than 20%. There was no overlap of the degree of conduction velocity slowing between the polymodal nociceptors and the cold units after 20 seconds at 20 Hz.

As noted above, there is a significant difference between the degree of conduction velocity slowing of the cold units and the mechanoreceptors following 20 seconds at 20 Hz. However, as can be seen from Figure 6.5, the conduction velocity slowing of

mechanoreceptors plateaus within the 20 second period, whereas this does not happen for cold units. In consequence, there is a greater difference between the degree of conduction velocity slowing of the cold units and the mechanoreceptors after just 6 seconds than after the full 20 seconds. Figure 6.7 shows that there is very little overlap between these two classes after 6 seconds at 20 Hz; 0/10 cold units slow in conduction velocity by greater than 10%, whereas 14/17 mechanoreceptors show a greater than 10% slowing of conduction velocity.

The percentage slowing of conduction velocity following 20 seconds at 20 Hz is not correlated with the resting conduction velocity of the units. ANOVA shows no significant differences between the resting conduction velocity of the different classes of afferent unit (mean ± SEM; polymodal and heat nociceptors 0.80 m/s ± 0.03, n=53; mechanical nociceptors 0.91 m/s ± 0.08, n=13; mechanoreceptors 0.78 m/s ± 0.04, n=17; cold units 0.87 m/s ± 0.06, n=10).

6.3 Conduction velocity slowing in C-fibres without mechanical or thermal fields

Those C-fibres for which no mechanical or thermal field could be found showed a wide range of conduction velocity slowing (Figure 6.8a). Figure 6.8b shows the conduction velocity slowing of the polymodal nociceptors and the spontaneously active sympathetic units after the standard electrical stimulus. Comparison of Figures 6.8a and 6.8b reveals that the results are consistent with there being two populations of inexcitable units. Those inexcitable units that show a greater than 20% slowing from resting conduction velocity following stimulation at 20 Hz for 20 seconds have a similar distribution to the polymodal

nociceptors (compare Figures 6.8a and 6.8b). Those inexcitable units that show a less than 20% slowing of conduction velocity have a similar profile to the spontaneously active sympathetic units (see below). There is no significant difference between the resting conduction velocity of those inexcitable units that slowed by greater than 20% (0.85 m/s ± 0.05, n=27; mean ± SEM) and those that slowed by less than 20% (0.74 m/s ± 0.03, n=34; mean ± SEM).

6.4 Conduction velocity slowing in spontaneously active C-fibres recorded from the cut distal end of the saphenous nerve

The slowing of conduction velocity following the standard electrical stimulus of 20 seconds at 20 Hz was measured in 24 spontaneously active C-fibres recorded from the cut distal end of the saphenous nerve. The spontaneous firing of these units was often related to the respiration of the rat. In 18 of these fibres, the frequency of spontaneous firing ranged from 0.1 Hz to >4 Hz, with only 3 of them displaying spontaneous firing at less than 1 Hz. The spontaneously active units showed a mean slowing of conduction velocity of 14.9% ± 0.8 (n=24), and the distribution of conduction velocity slowing of the sampled population is shown in Figure 6.6 and Figure 6.8b. The spontaneously active sympathetic efferent fibres had significantly slower resting conduction velocities (0.66 m/s ± 0.02, n=21; mean ± SEM) than the afferent units (0.82 m/s ± 0.02, n=93) ($p<0.01$). This is consistent with published data from cat sural nerve (Lisney 1988) and is also a consistent finding in the rat saphenous nerve (see Chapter 7 of the Results).

6.5 More detailed investigation of mechanically and thermally insensitive units

Twenty three units without mechanical or thermal receptive fields were investigated using electrical skin stimulation and topical application of 5% or 10% mustard oil. Of these 23 units, 9 showed a less than 20% slowing of conduction velocity following the standard electrical stimulus of 20 seconds at 20 Hz. Afferent fields could not be found for any of these 9 units, even after these more extensive searching procedures. Electrical receptive fields could not be found for 4 of these 9 units.

Electrical receptive fields were located for 13 of the remaining 14 units, which all showed a greater than 20% slowing of conduction velocity. Of these 14 units, 11 were found to have afferent properties following either the electrical skin stimulation or the topical application of mustard oil. Of these 11 units, 6 were found to have mechanical and/or thermal fields after electrical skin stimulation had been used to locate their electrical receptive fields (4 of which were excited by mustard oil), 3 were excited by mustard oil (one of which later became mechanically and thermally sensitive) and 2 did not respond to mustard oil but became mechanically sensitized following the chemical stimulus.

The responses of 12 polymodal nociceptors to topical mustard oil were also examined. Eight polymodal nociceptors responded to the mustard oil. The remaining four were not excited (and 1 of these 4 lost all of its afferent properties).

The pattern of firing in response to topical mustard oil varied greatly, and this wide range of firing behaviour was observed in both insensitive units and polymodal nociceptors.

Some units responded to the mustard oil with constant firing of 1-2 Hz throughout the period that the mustard oil remained on the skin, whereas other units fired just a few spikes (or in one case, a single spike) in response to the mustard oil.

6.6 Summary

- Repetitive firing of nerve fibres results in the slowing of their conduction velocity.
- The degree of conduction velocity slowing shown by a unit was not correlated with its resting conduction velocity .
- Following 20 seconds of stimulation at 20 Hz, nociceptive C-fibres showed a significantly greater slowing of conduction velocity than cold thermoreceptive fibres, mechanoreceptors and spontaneously active sympathetic efferent units.
- There was little overlap of the degree of conduction velocity slowing between the nociceptive and non-nociceptive fibres, therefore allowing one to distinguish nociceptive and non-nociceptive afferent fibres simply by looking at the axonal property of activity-dependent slowing of conduction velocity.
- Since there was little overlap of conduction velocity slowing between the mechanoreceptors and the cold units, particularly after just 6 seconds of stimulation at 20 Hz, it is possible to use this axonal property to separate these two classes of non-nociceptive afferent C-fibre.
- It was not possible to differentiate the sub-classes of nociceptive C-fibres on the basis of activity-dependent slowing of conduction velocity.
- Units for which no receptive field to mechanical or thermal stimuli could be found showed a bimodal distribution of conduction velocity slowing. Those inexcitable units slowing in conduction velocity by greater than 20% showed a similar distribution to

the polymodal nociceptors, and those inexcitable units slowing by less than 20% showed a similar distribution to the spontaneously active sympathetic units. It therefore seems that one can use activity-dependent slowing of conduction velocity to differentiate between the afferent and non-afferent populations of inexcitable C-fibres.

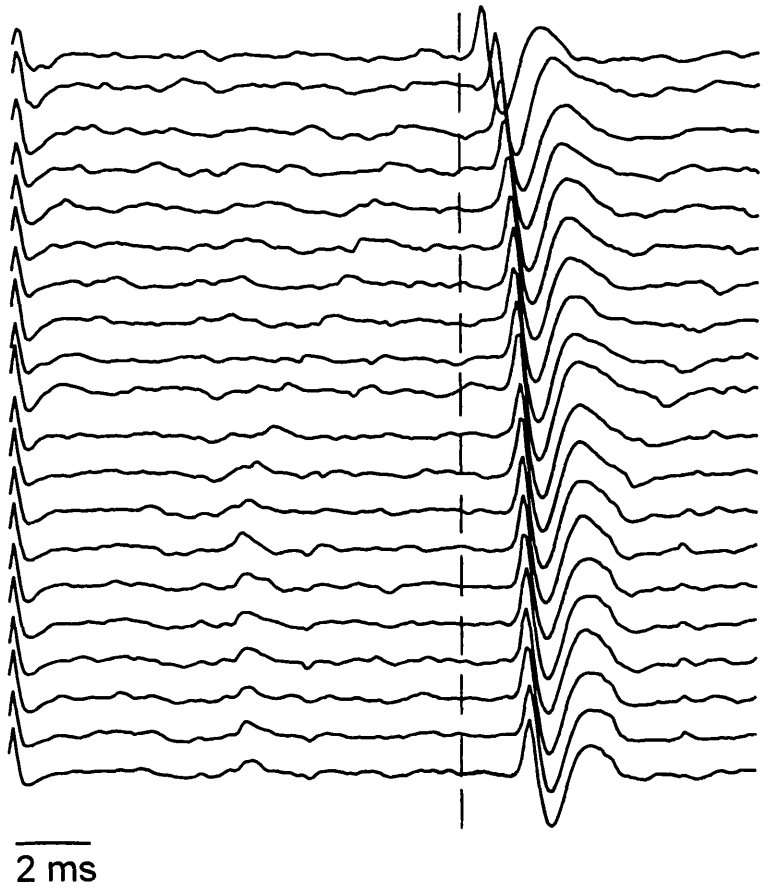

Figure 6.1 **Electrical stimulation of a single cold thermoreceptor C-fibre (20 Hz, 20 sec, 2 x electrical threshold).** Every 20th sweep is shown (i.e. consecutive sweeps are at 1 sec intervals), and they are displayed from top to bottom. Conduction distance = 15mm, resting conduction velocity = 1.23 m/s, final conduction velocity = 1.11 m/s, 9.8% slowing from resting conduction velocity.

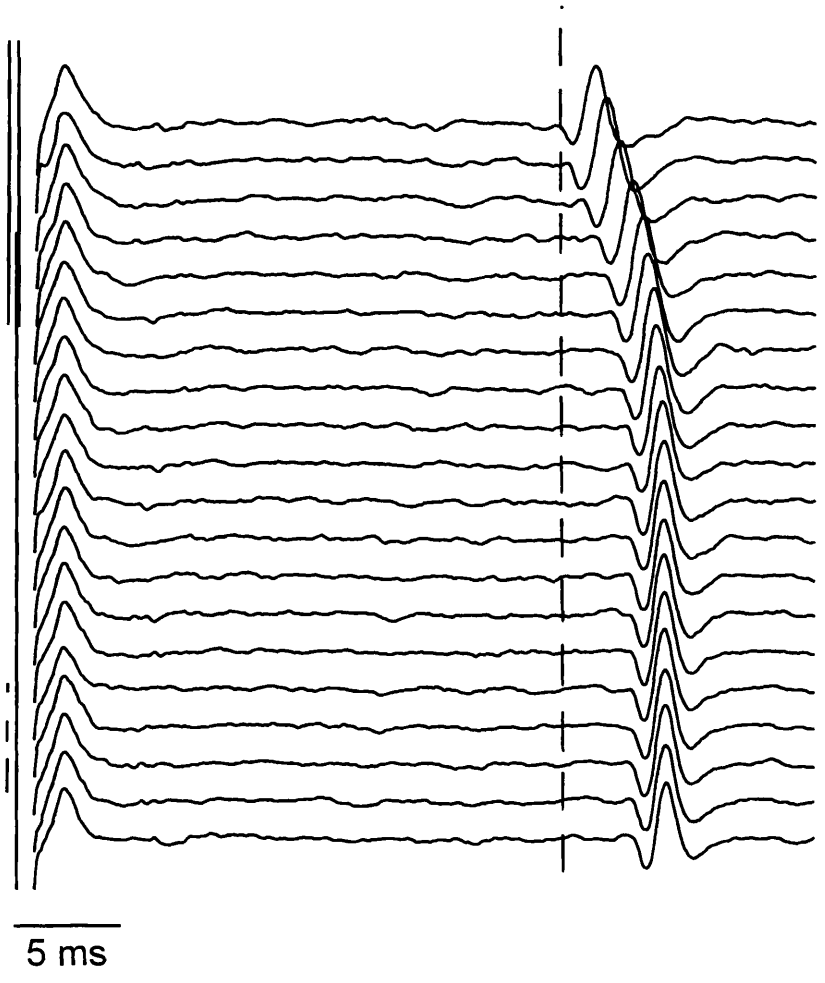

Figure 6.2 **Electrical stimulation of a single mechanoreceptor C-fibre (20 Hz, 20 sec, 2 x electrical threshold).** Every 20th sweep is shown (i.e. consecutive sweeps are at 1 sec intervals), and they are displayed from top to bottom. Conduction distance = 21mm, resting conduction velocity = 0.81 m/s, final conduction velocity = 0.72 m/s, 11.1% slowing from resting conduction velocity.

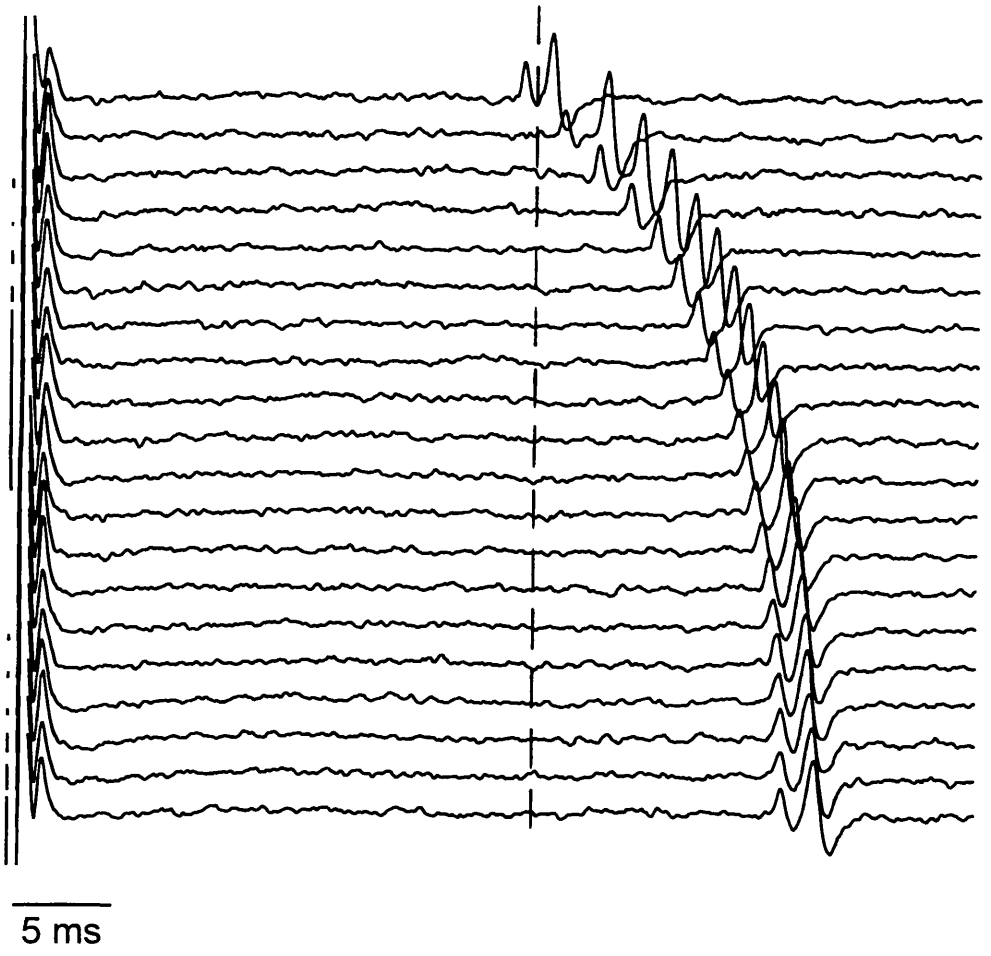

Figure 6.3 **Electrical stimulation of C-fibres (20 Hz, 20 sec, 2 x electrical threshold).** Every 20th sweep is shown (i.e. consecutive sweeps are at 1 sec intervals), and they are displayed from top to bottom. This filament contained two C-fibres. The smaller, earlier unit was not characterised. The larger, later unit was a polymodal nociceptor (conduction distance = 21mm, resting conduction velocity = 0.78 m/s, final conduction velocity = 0.52 m/s, 33.3% slowing from resting conduction velocity).

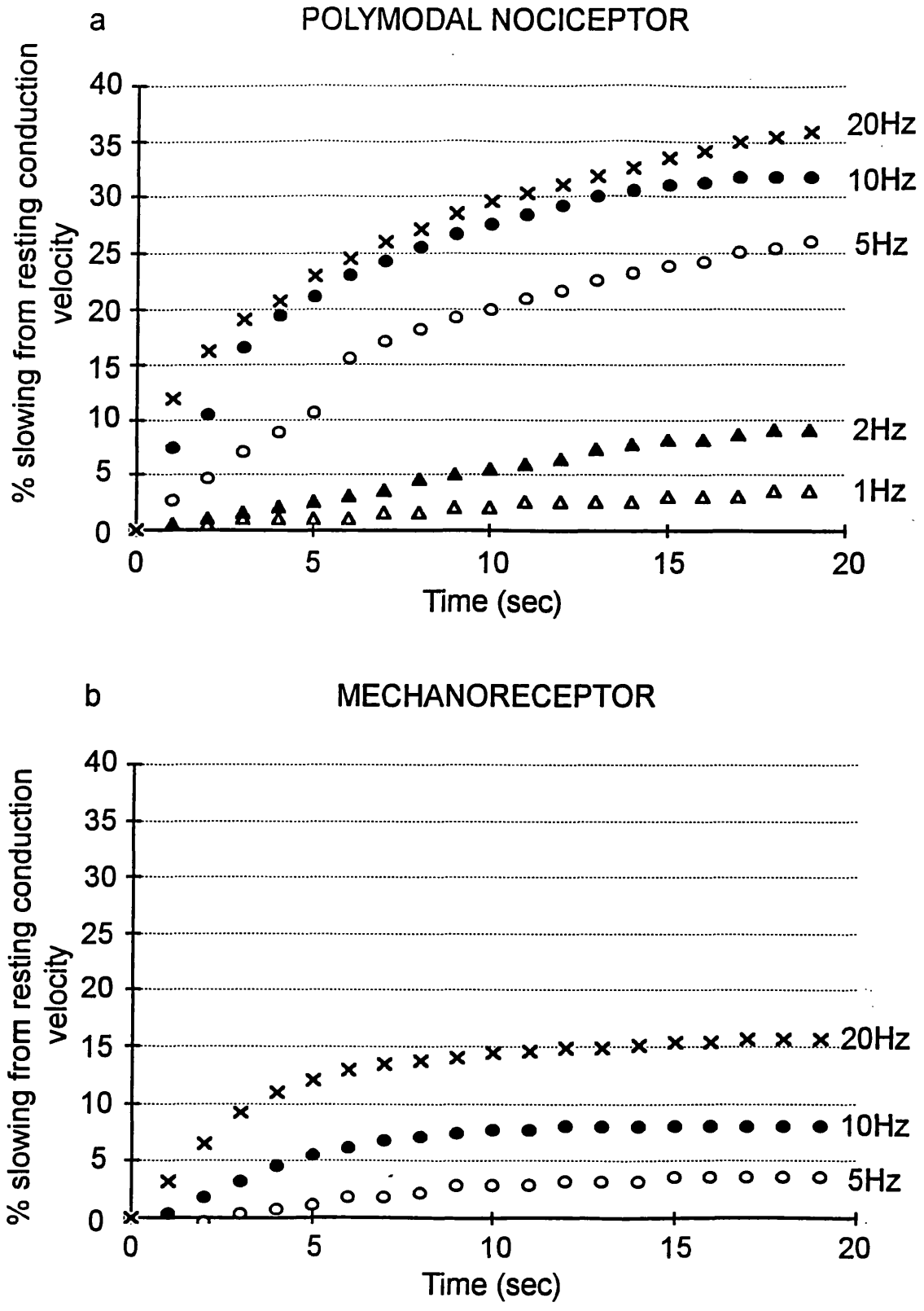

Figure 6.4 **The relationship between conduction velocity slowing and stimulus frequency.** The percentage conduction velocity slowing of (a) a single polymodal nociceptor (resting conduction velocity = 0.68 m/sec), and (b) a single mechanoreceptor (resting conduction velocity = 0.68 m/sec), throughout 20 seconds of stimulation at frequencies up to 20 Hz.

Stimulus frequency (Hz)	Stimulus duration (sec)	Polymodal nociceptors	Cold units	Mechanoreceptors
33	20	1/4	2/2	3/3
20	60	1/8	2/2	2/3
20	40	2/8	2/2	3/3
20	20	46/53	10/10	17/17

TABLE 6.1 Proportion of C-fibres conducting every impulse throughout tetani of different frequencies and durations. Stimulus strength was set at 2 x electrical threshold at low frequency (<1 Hz) stimulation.

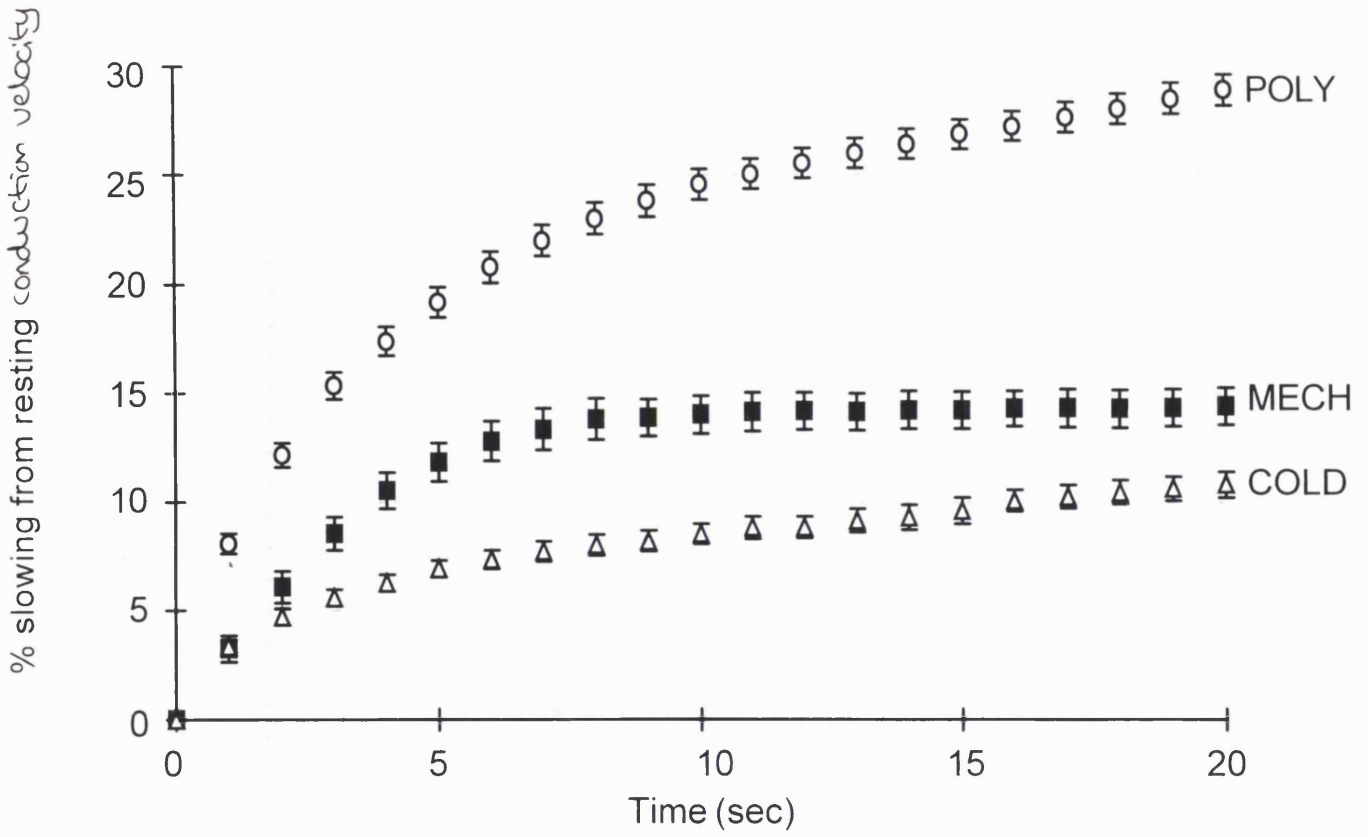

Figure 6.5 **The average time course (mean±SE) of the percentage slowing from resting conduction velocity of the three major classes of afferent C-fibre during electrical stimulation at 20 Hz.**

POLY = polymodal nociceptors, n=51; MECH = mechanoreceptors, n=17; COLD = cold thermoreceptive units, n=10.

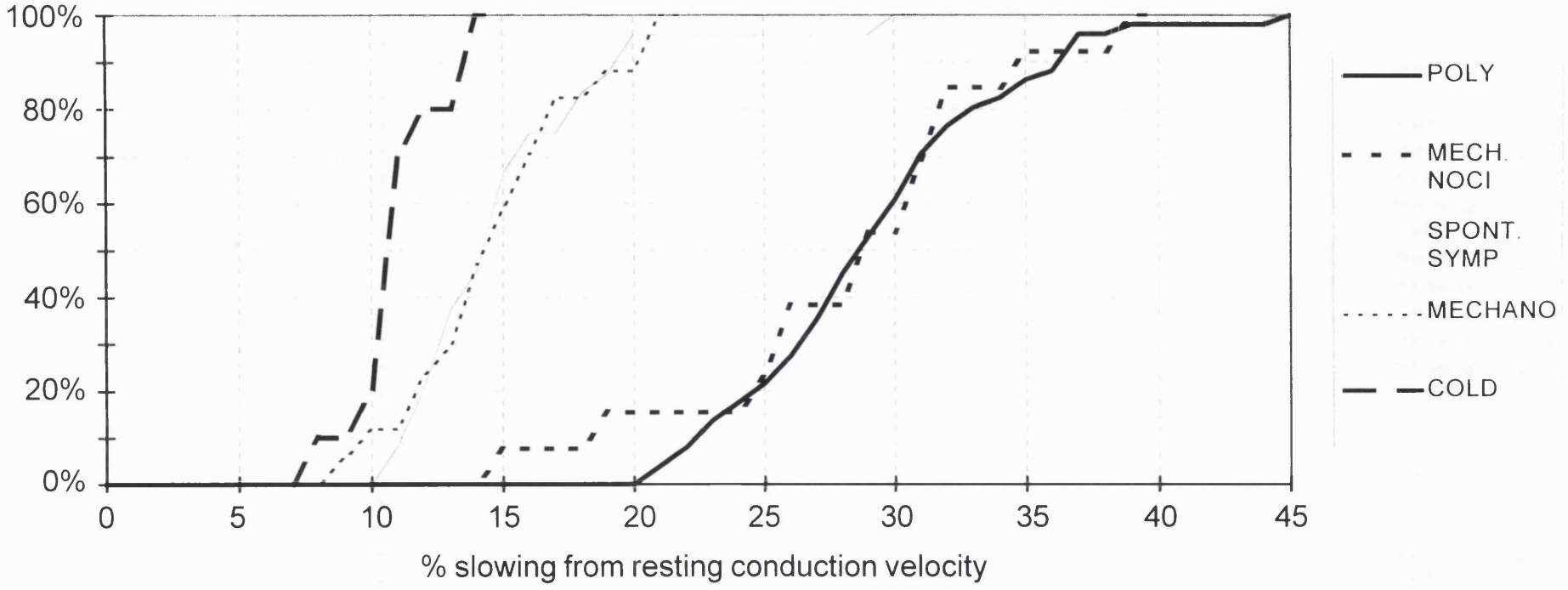

Figure 6.6 Cumulative frequency distribution histograms for the % slowing from resting conduction velocity after 20 seconds at 20 Hz of the different classes of afferent C-fibre and of the spontaneously active sympathetic efferent units. Note that there is very little overlap between the polymodal nociceptors and the mechanoreceptors, and no overlap between the polymodal nociceptors and the cold units.

POLY = polymodal nociceptors (n=51), MECH. NOCI = mechanical nociceptors (n=13), SPONT. SYMP = spontaneously active sympathetic efferents (n=24), MECHANO = mechanoreceptors (n=17), COLD = cold thermoreceptive units (n=10). In addition to these units, two heat nociceptors were studied; they slowed by 33.4% and 40.1% from their resting CV following stimulation at 20 Hz for 20 seconds.

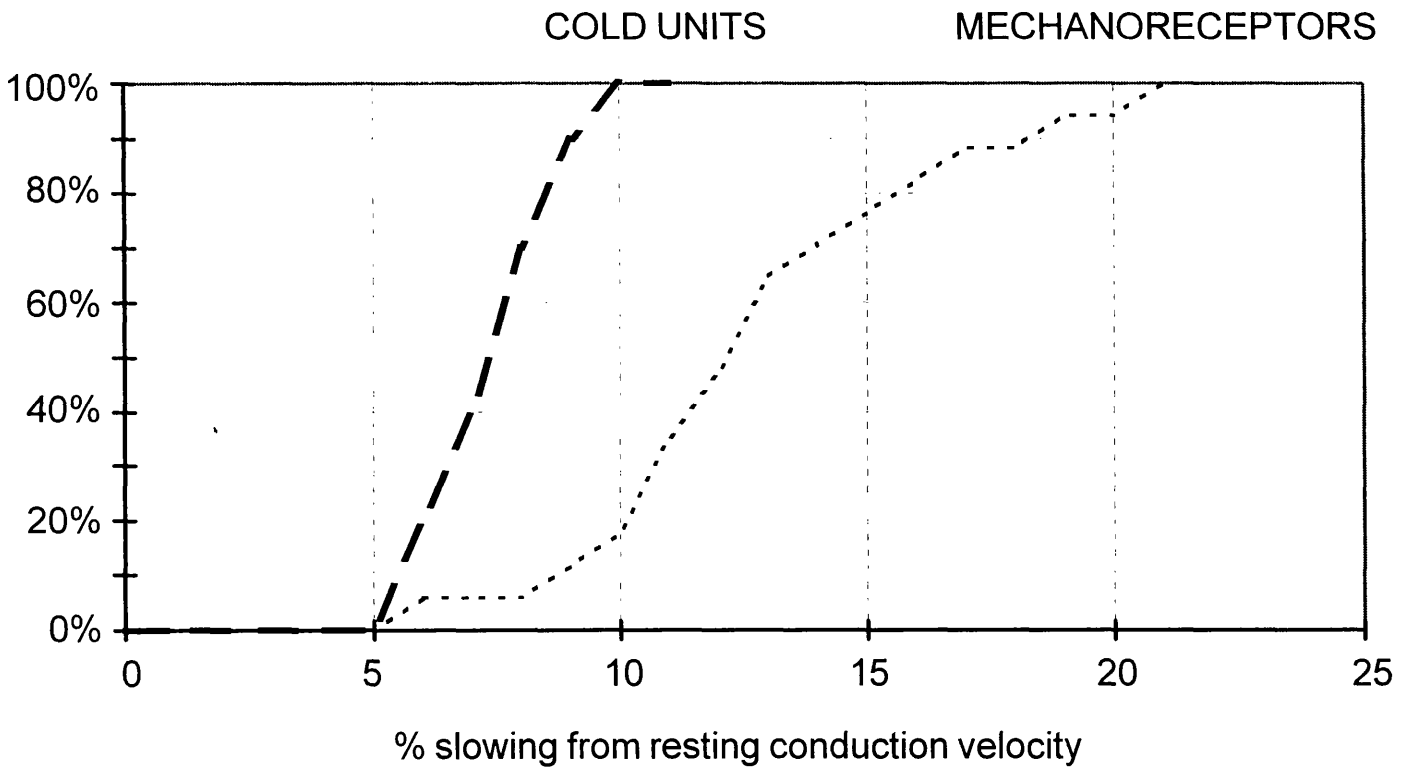

Figure 6.7 Cumulative frequency distribution histograms for the percentage slowing from resting conduction velocity of the cold units (dashed line, n=10) and the mechanoreceptors (dotted line, n=17) after 6 seconds at 20 Hz. Note that there is very little overlap between the cold units and mechanoreceptors after just 6 seconds at 20 Hz.

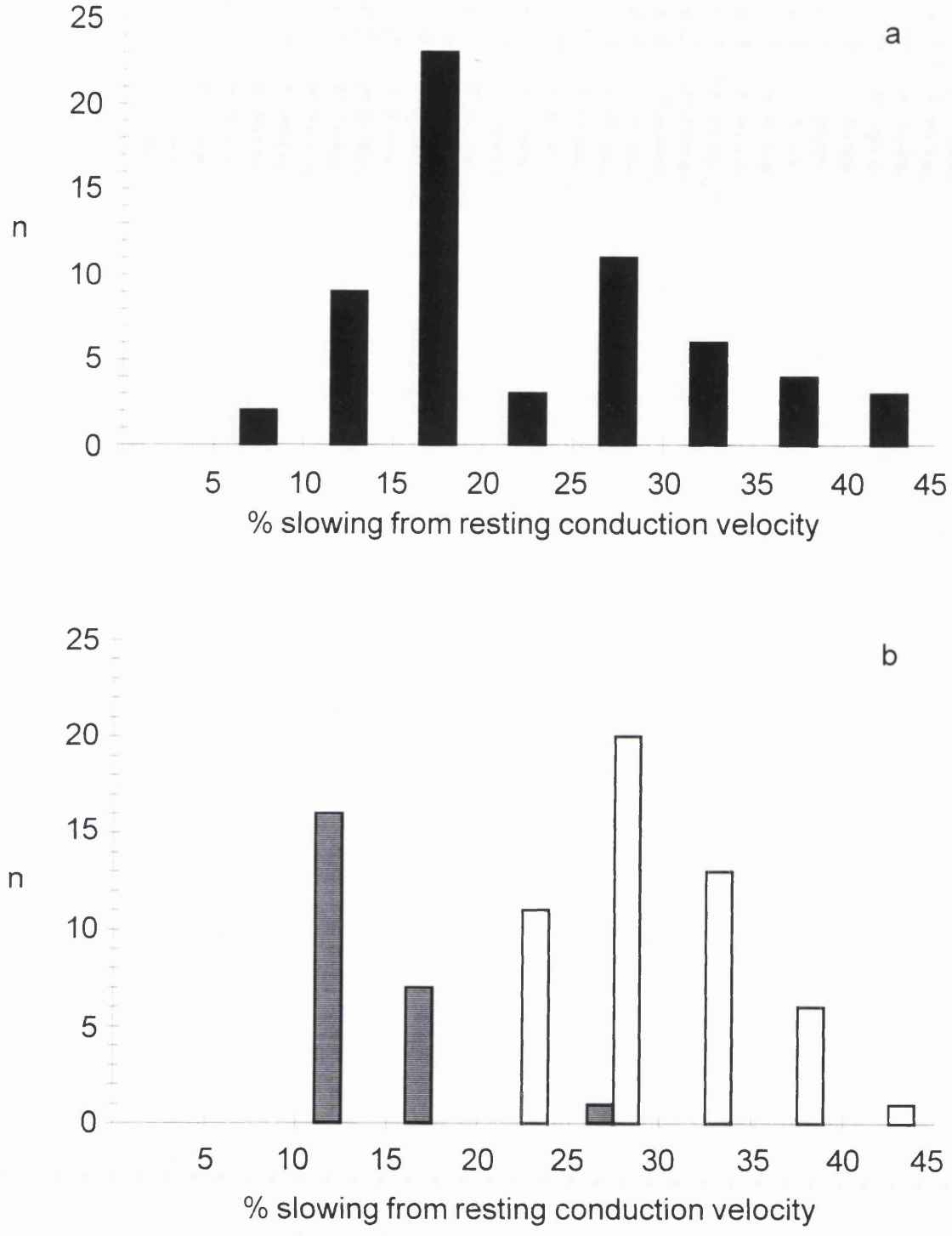

Figure 6.8 a) Histogram of the percentage slowing from resting conduction velocity following 20 seconds at 20 Hz of 61 C units that had no mechanical or thermal receptive fields with the standard search procedures.
b) Histogram of the percentage slowing from resting conduction velocity following 20 seconds at 20 Hz of the 51 polymodal nociceptors (open bars) and the 24 spontaneously active sympathetic units (striped bars). Note the bimodal distribution of the conduction velocity slowing of the inexcitable population (Figure 6.8a) and its similarity to the combined distribution of the two classes of C-fibre in Figure 6.8b.

CHAPTER 7 RESULTS: SPIKE SHAPE

7.1 General information

The average spike shapes of 180 C-fibres dissected from the rat saphenous nerve were recorded using standardized filter settings (10 Hz to 5kHz). This population comprised of 70 polymodal nociceptors, 14 mechanical nociceptors, 3 heat nociceptors, 23 mechanoreceptors, 20 cold thermoreceptors, 28 inexcitable units and 22 spontaneously active sympathetic efferent units. It must be noted that this population of C-fibres did not come from a random sample, and in some experiments units from a particular class were actively sought for. Therefore, the true proportions of the different functional classes of C-fibres present in the rat saphenous nerve are not represented in this population of 180 units.

Figures 7.1-7.4 show representative spike shapes of some polymodal nociceptors, some mechanoreceptors, some cold thermoreceptors and some spontaneously active sympathetic efferent units. In Figure 7.5, the units from Figures 7.1-7.4 have been taken and they have all been plotted on the same scale for an easier comparison of their spike shapes.

Measurements of resting conduction velocity, amplitude of the first peak, duration of the first peak at half the maximum amplitude, undershoot amplitude and duration of the undershoot at half its maximum amplitude were made, and the ratio of undershoot amplitude to first peak amplitude was calculated (see Table 7.1; Figures 7.6-7.11).

7.2 Statistical analysis

ANOVA was carried out on the resting conduction velocities of the polymodal nociceptors, mechanical nociceptors, mechanoreceptors, cold units, inexcitable units and spontaneously active sympathetic units. ANOVA was also carried out on the spike shape measurements taken from the polymodal nociceptors, mechanical nociceptors, mechanoreceptors, cold units and inexcitable units. The spike shapes of the spontaneously active sympathetic units varied greatly (see Table 7.1). Due to the non-homogeneity of the variances of the spike shape measurements of the sympathetic units, these units were excluded from the ANOVA carried out on the spike shape measurements. Student t-tests were performed to compare the spike shapes of the spontaneously active sympathetic efferents with all the excitable afferent units. The heat nociceptors were excluded from both the ANOVA tests (conduction velocity and spike shape measurements) because of their small number (n=3). However, in general, the heat nociceptors had similar resting conduction velocities and spike measurements to the polymodal nociceptors (see Table 7.1).

7.3 Conduction velocity measurements

ANOVA (using the Student-Newman-Keuls procedure) revealed that the spontaneously active sympathetic efferents and the inexcitable units had significantly slower resting conduction velocities than the other C-fibre classes ($p<0.05$), although there was no significant difference in conduction velocity between the sympathetic and inexcitable units (see Figure 7.6). For the values of resting conduction velocity for the different classes of C-fibre, refer to Table 7.1 and Figure 7.6. Activity-dependent slowing of conduction

velocity was studied in 17 of the 28 inexcitable units. Eleven of the 17 units showed a less than 20% slowing of conduction velocity following 20 seconds of stimulation at 20 Hz.

7.4 Spike height measurements

Although there was no significant difference between the different C-fibre classes in terms of the amplitude of the first peak (see Figure 7.7), ANOVA (Least Significant Difference; $p<0.05$) did reveal that the cold units displayed significantly smaller undershoots than the polymodal nociceptors, the mechanical nociceptors and the mechanoreceptors (see Figure 7.9). The undershoot/first peak ratio of the cold fibres was significantly less than that of the polymodal nociceptors, the mechanical nociceptors, the mechanoreceptors and the inexcitable units (see Figure 7.11). In other words, cold units tended to have more monophasic spikes than the other afferent fibre types.

7.5 Spike width measurements

ANOVA (Student-Newman-Keuls procedure) showed no significant differences overall between the different classes of afferent C-fibre in terms of the width of the first peak and the width of the undershoot ($p>0.05$; see Figures 7.8 and 7.10). There was, however, a clear trend for the polymodal nociceptors to have wider spikes than the other sub-classes of excitable afferent units.

When recording extracellularly, much of the variability in spike shape will come from the differing extent to which spikes conduct into a filament. To minimize this effect on spike

shape, recordings were made from more than one unit from within the same filament as often as possible.

There were 10 filaments containing at least one polymodal nociceptor and one mechanoreceptor unit. Overall, these filaments contained 16 polymodal nociceptors and 11 mechanoreceptors. In all 10 filaments, the polymodal nociceptors consistently displayed the wider spikes (see Figure 7.12). The average width of the first peak of the nociceptors was 0.86±0.09ms (mean±SEM; n=16) and their average undershoot width was 2.07±0.13ms (n=14). The average first peak width of the 11 mechanoreceptors was 0.59±0.05 ms and their average undershoot width was 1.25±0.17ms. A two-tailed paired t-test for units within the same filament shows that the polymodal nociceptors had significantly wider first peaks than the mechanoreceptors (n=10 pairs; p=0.001) and that they also had significantly wider undershoots than the mechanoreceptors (n=8 pairs; p=0.02). Where more than one unit of each of the two classes was present, the average width was used. A t-test performed on first peak width for all the polymodal nociceptors (n=70) and all the mechanoreceptors (n=23) shows that within the whole population this difference still holds (p=0.03). However, it must be noted that in an overall comparison between all of the afferent classes this trend was not significant (see above). Within the whole population there is no significant difference in undershoot width between the polymodal nociceptors (n=59) and the mechanoreceptors (n=23) (t-test, p=0.11). A two-tailed paired t-test performed on polymodal nociceptors and inexcitable units from within the same filament shows no significant difference between their first peak widths (p=0.25, 9 pairs) or their undershoot widths (p=0.51, 5 pairs). No spike shape measurements were made from polymodal nociceptors and cold units from within the same filament.

7.6 Spontaneously active sympathetic efferent units

The non-parametric Mann-Whitney test revealed no significant differences between the sympathetic efferent units (n=22) and all the afferent units (n=130 comprising 70 polymodal nociceptors, 14 mechanical nociceptors, 3 heat nociceptors, 23 mechanoreceptors and 20 cold units) in terms of the amplitude of the first peak, the undershoot amplitude and the undershoot/first peak ratio. However, the sympathetic units had significantly wider first peaks ($p<0.02$) and significantly wider undershoots ($p<0.01$) than the afferent units. The undershoot width of the sympathetic units varied greatly (see Figure 7.10), with some sympathetic units, but not all of them, displaying prolonged undershoots lasting several milliseconds.

7.7 Summary

- The spontaneously active sympathetic and inexcitable units had slower resting conduction velocities than the other C-fibre types.
- In filaments containing both polymodal nociceptors and mechanoreceptors, and also across the population as a whole, the polymodal nociceptors had wider first peaks than the mechanoreceptors.
- The spontaneously active sympathetic units had wider spikes (both first peak and undershoot widths) than the afferent units.
- Cold units tended to have monophasic spike shapes.

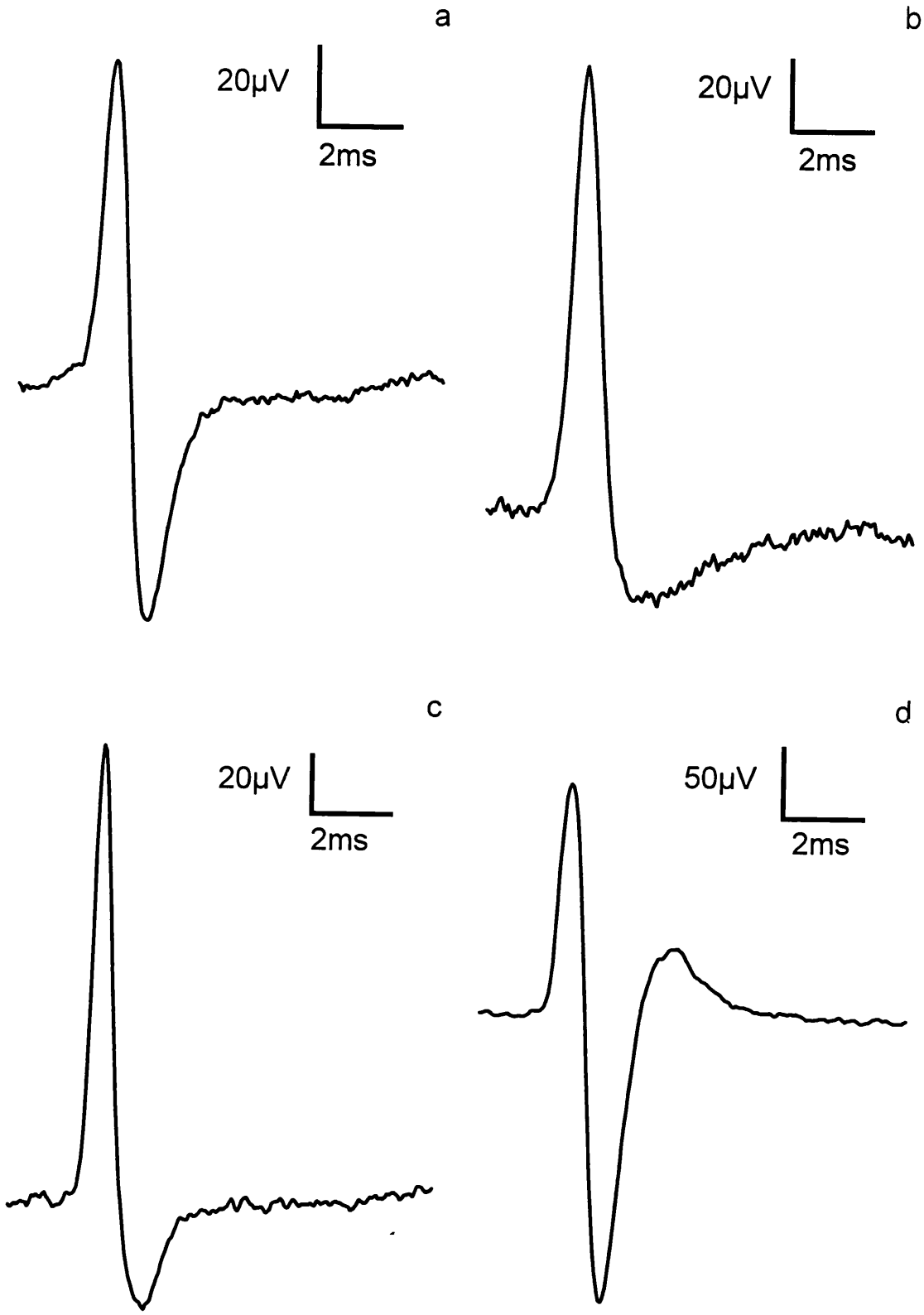

Figure 7.1a-d **Four examples of polymodal nociceptor spikes.**

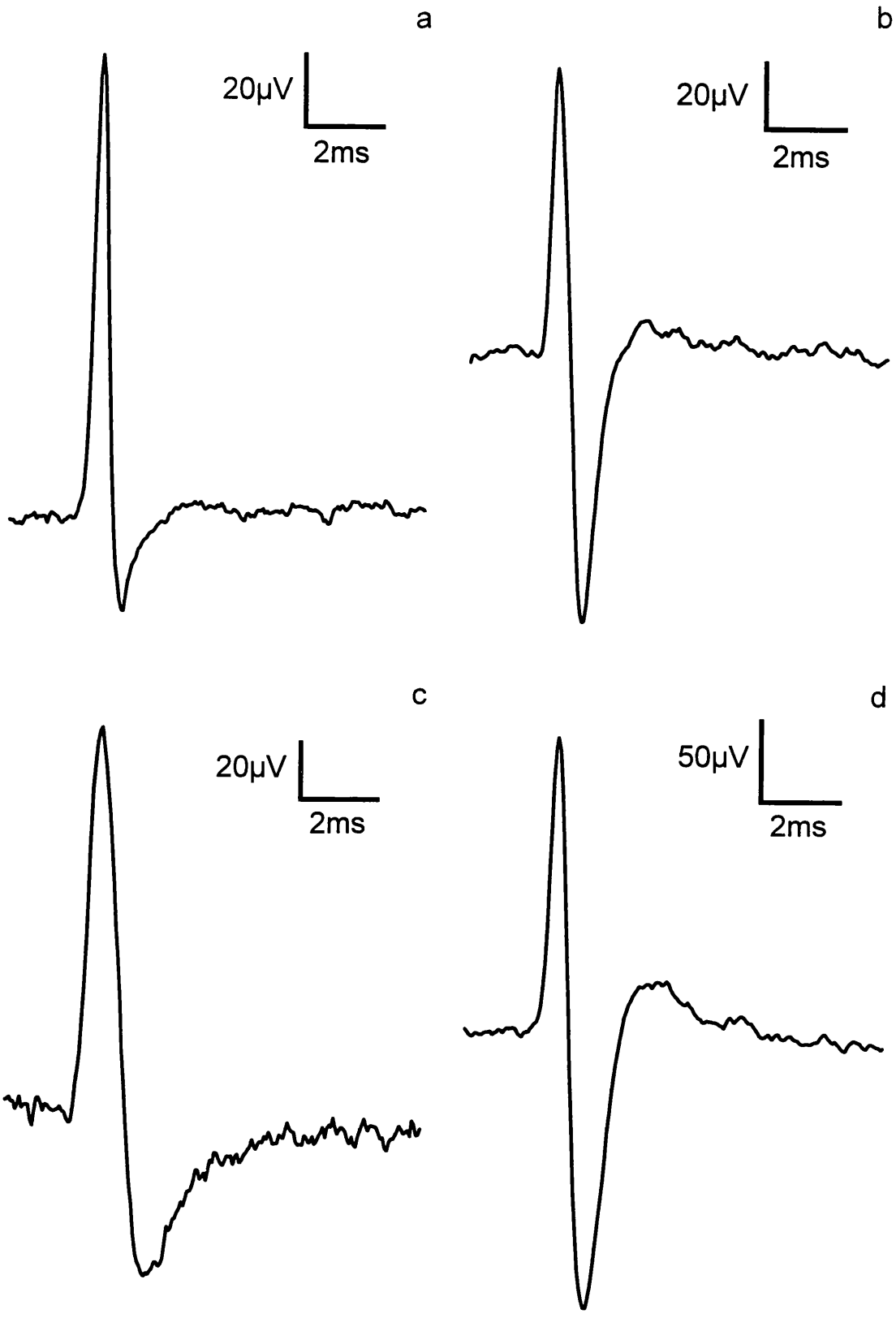

Figure 7.2a-d **Four examples of mechanoreceptor spikes.**

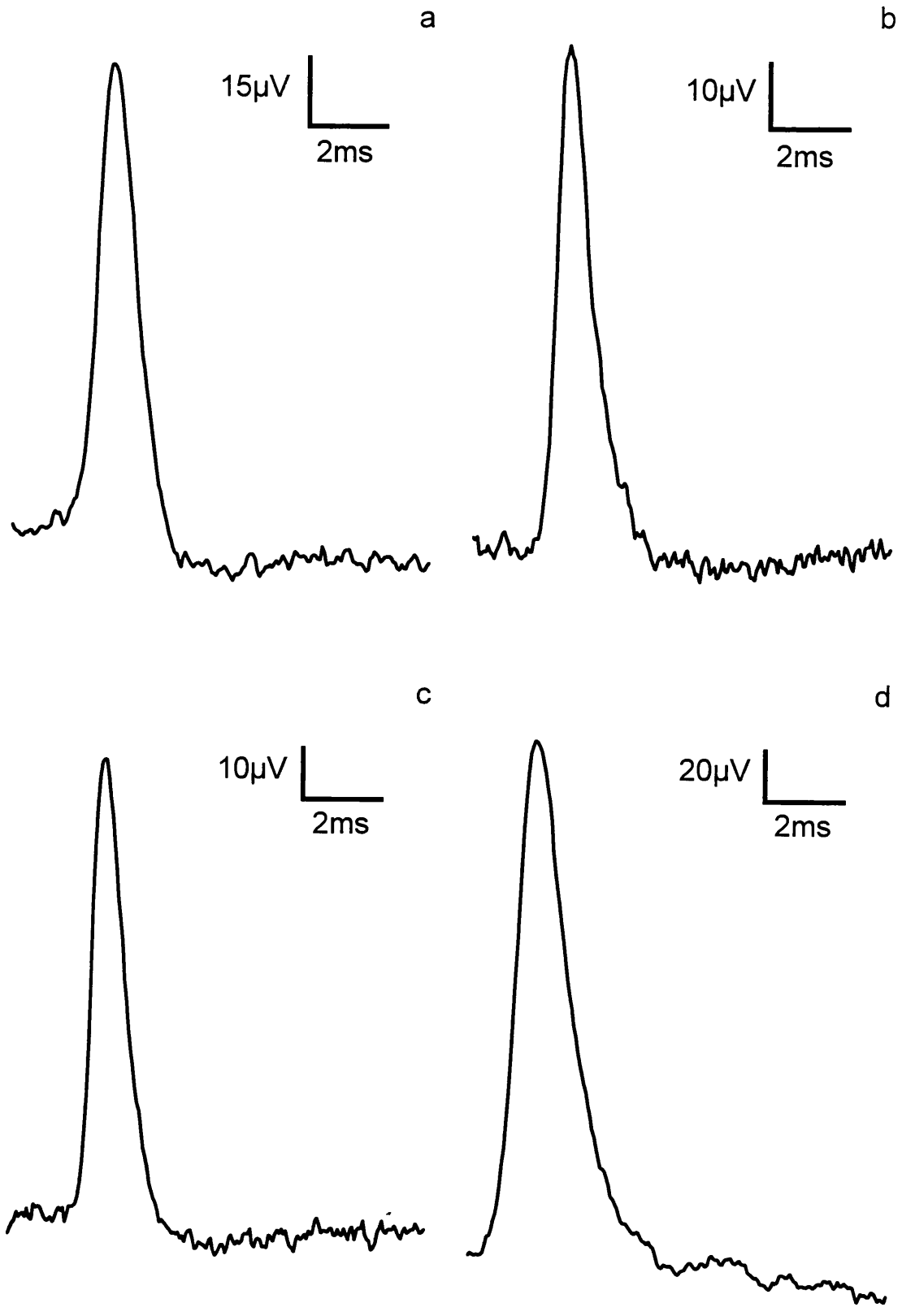

Figure 7.3a-d **Four examples of cold unit spikes.** Note their monophasic shape.

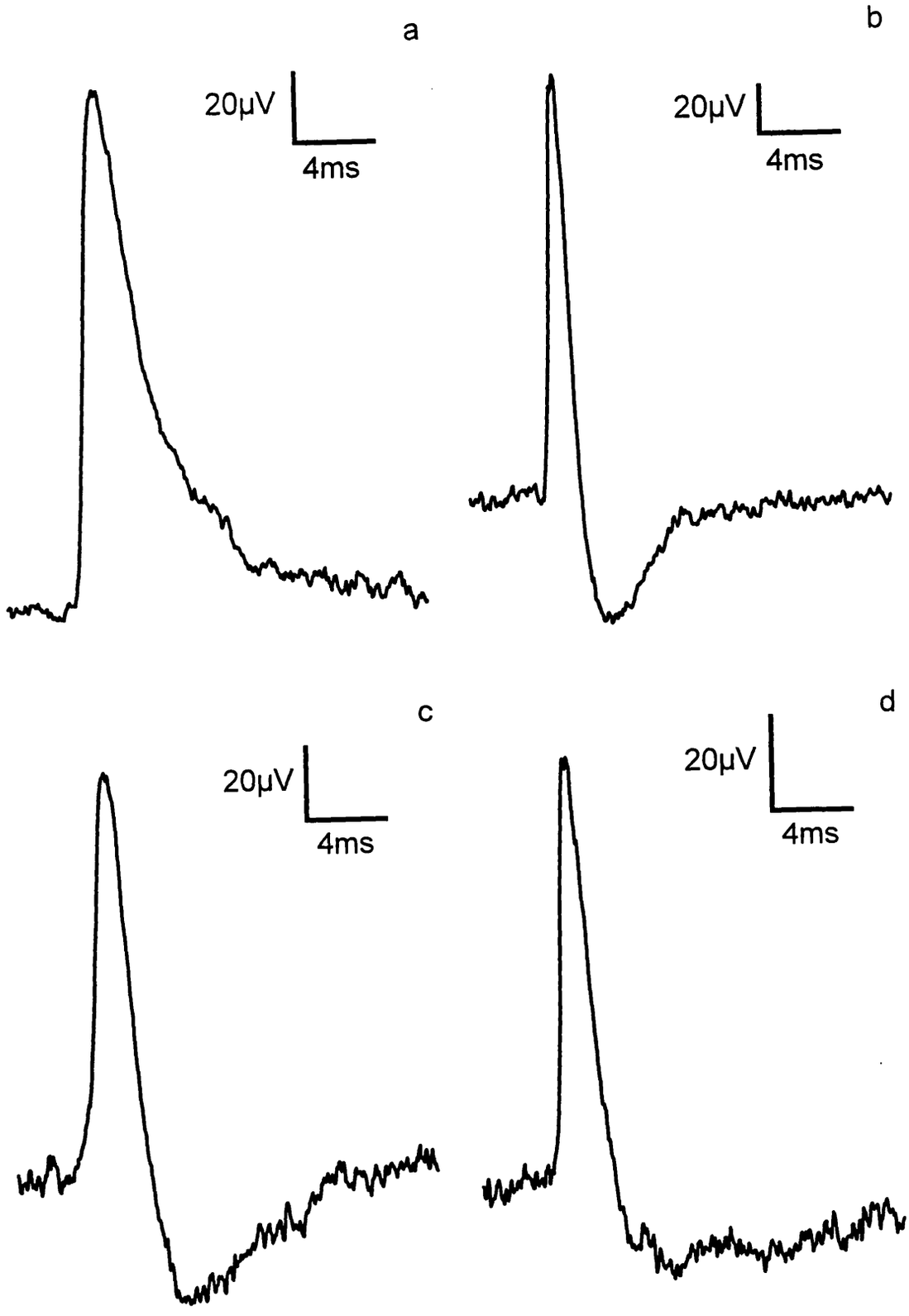

Figure 7.4a-d **Four examples of spontaneously active sympathetic efferent spikes.**

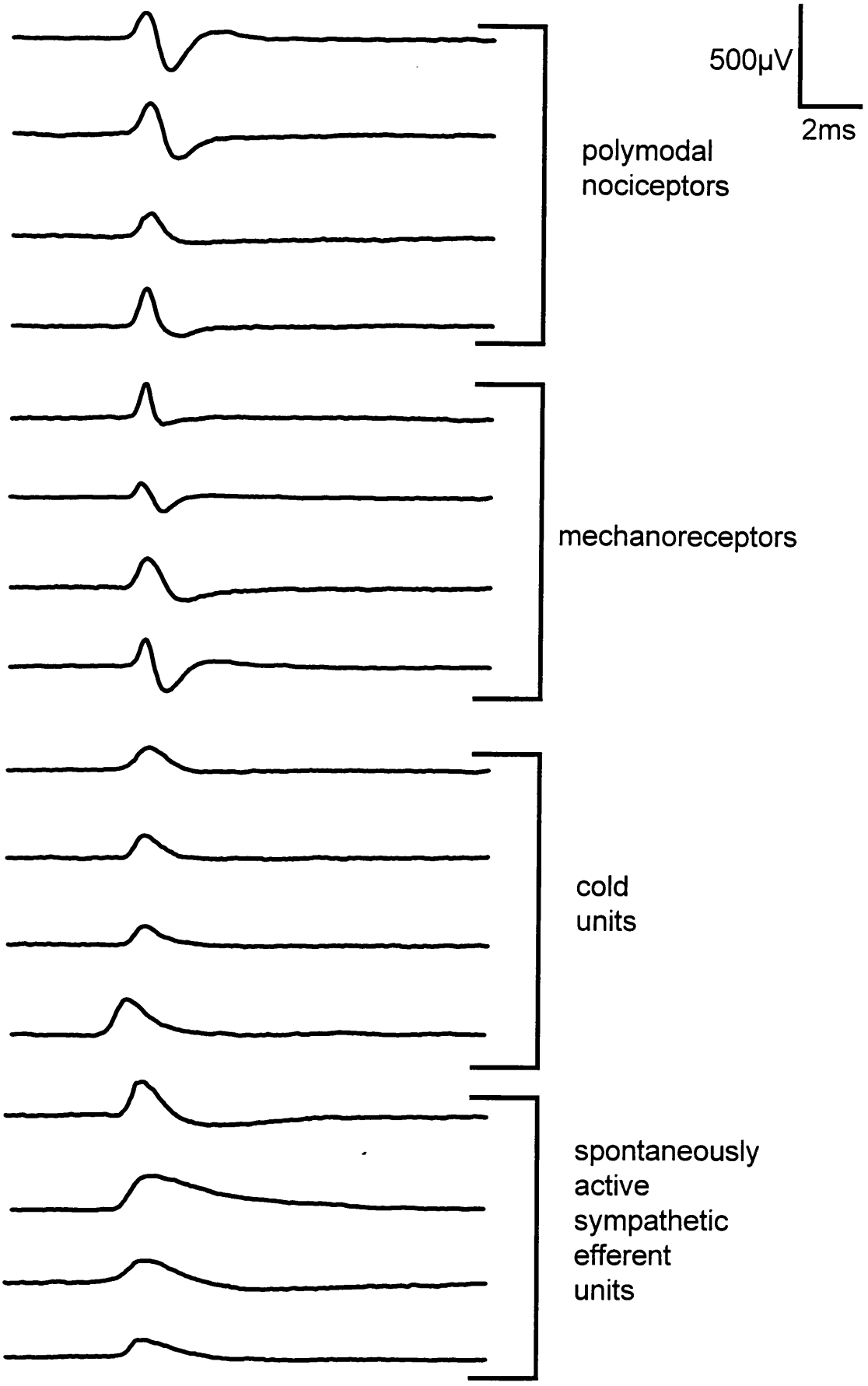

Figure 7.5 **Examples of spike shapes of some polymodal nociceptors, mechanoreceptors, cold units and spontaneously active sympathetic units.**

Class	CV (m/s)	Spike amplitude (μV)	Half amplitude width (ms)	Spike undershoot (μV)	Half undershoot width (ms)	Undershoot /amplitude
Polymodal nociceptors	0.81±0.02 (69)	126.5±7.9 (70)	0.75±0.05 (70)	51.5±4.6 (70)	1.62±0.14 (59)	42.59±3.16 (70)
HTMs	0.87±0.07 (14)	108.3±13.5 (14)	0.63±0.08 (14)	54.2±10.3 (14)	1.17±0.13 (13)	51.32±6.63 (14)
Heat nociceptors	0.64±0.05 (3)	138.0±25.9 (3)	0.77±0.44 (3)	44.0±21.0 (2)	0.80±0.18 (2)	28.46±15.5 (2)
Mechanoreceptors	0.79±0.02 (21)	113.1±10.0 (23)	0.60±0.04 (23)	46.9±8.5 (23)	1.29±0.14 (23)	41.06±5.27 (23)
Cold units	0.85±0.05 (18)	108.9±10.3 (20)	0.60±0.05 (20)	22.5±5.0 (20)	1.04±0.14 (14)	22.87±5.18 (20)
Inexcitable units	0.68±0.02 (27)	118.3±15.1 (28)	0.72±0.06 (28)	40.3±5.0 (28)	1.57±0.18 (22)	38.30±4.20 (28)
Spontaneous sympathetic units	0.62±0.02 (21)	146.9±27.0 (22)	1.01±0.12 (22)	54.0±11.5 (22)	4.10±1.23 (20)	38.35±6.02 (22)

TABLE 7.1 **Conduction velocity and spike shape measurements of the different classes of C-fibre in the rat saphenous nerve (mean±SEM (n)).** Recordings were made using filtering ranging from 10 Hz to 5 kHz.

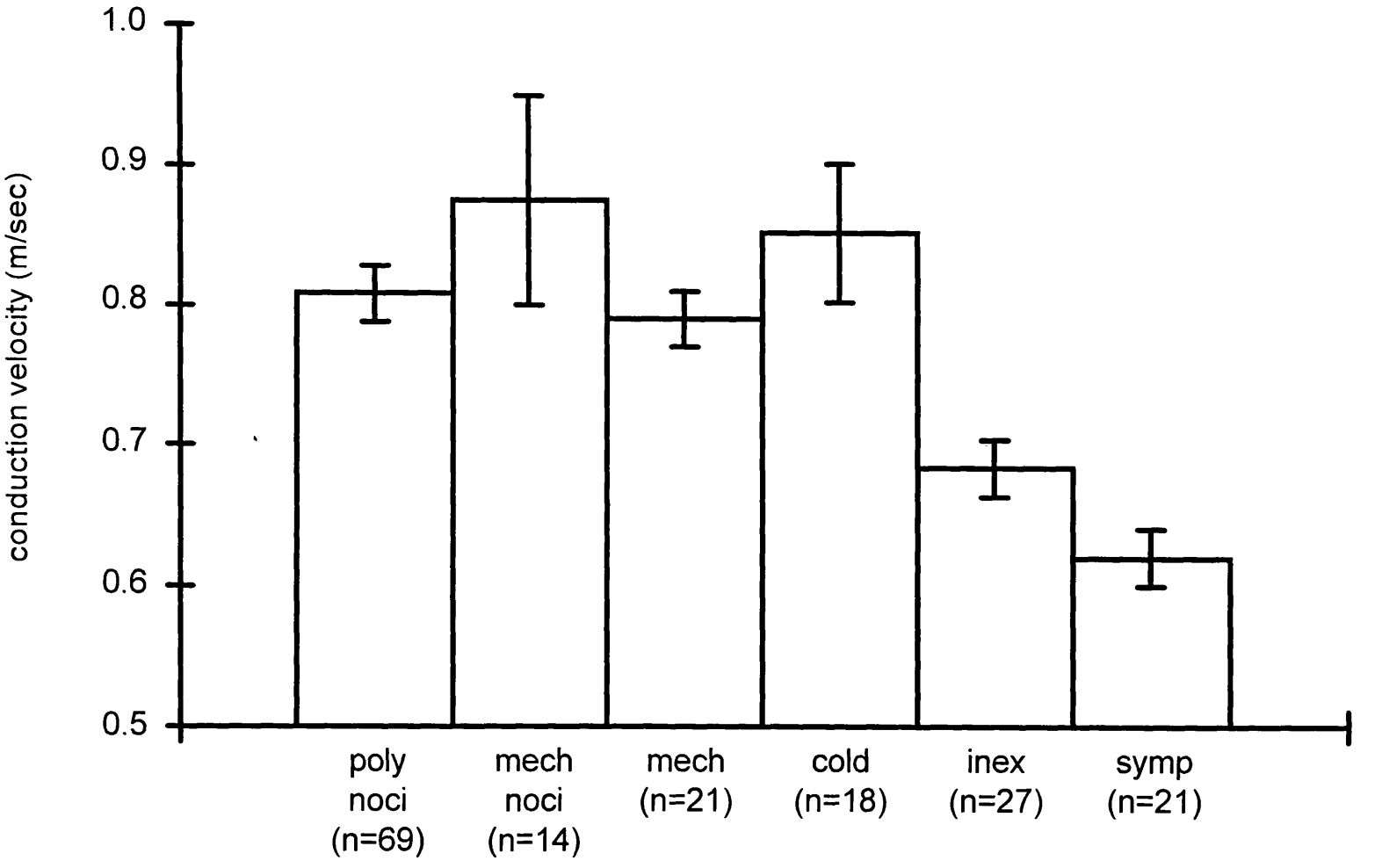

Figure 7.6 Bar chart showing the resting conduction velocities (mean±SE) of the different classes of C-fibre.
poly noci = polymodal nociceptors; mech noci = mechanical nociceptors; mech = mechanoreceptors; cold = cold thermoreceptors; inex = inexcitable units; symp = spontaneously active sympathetic efferents

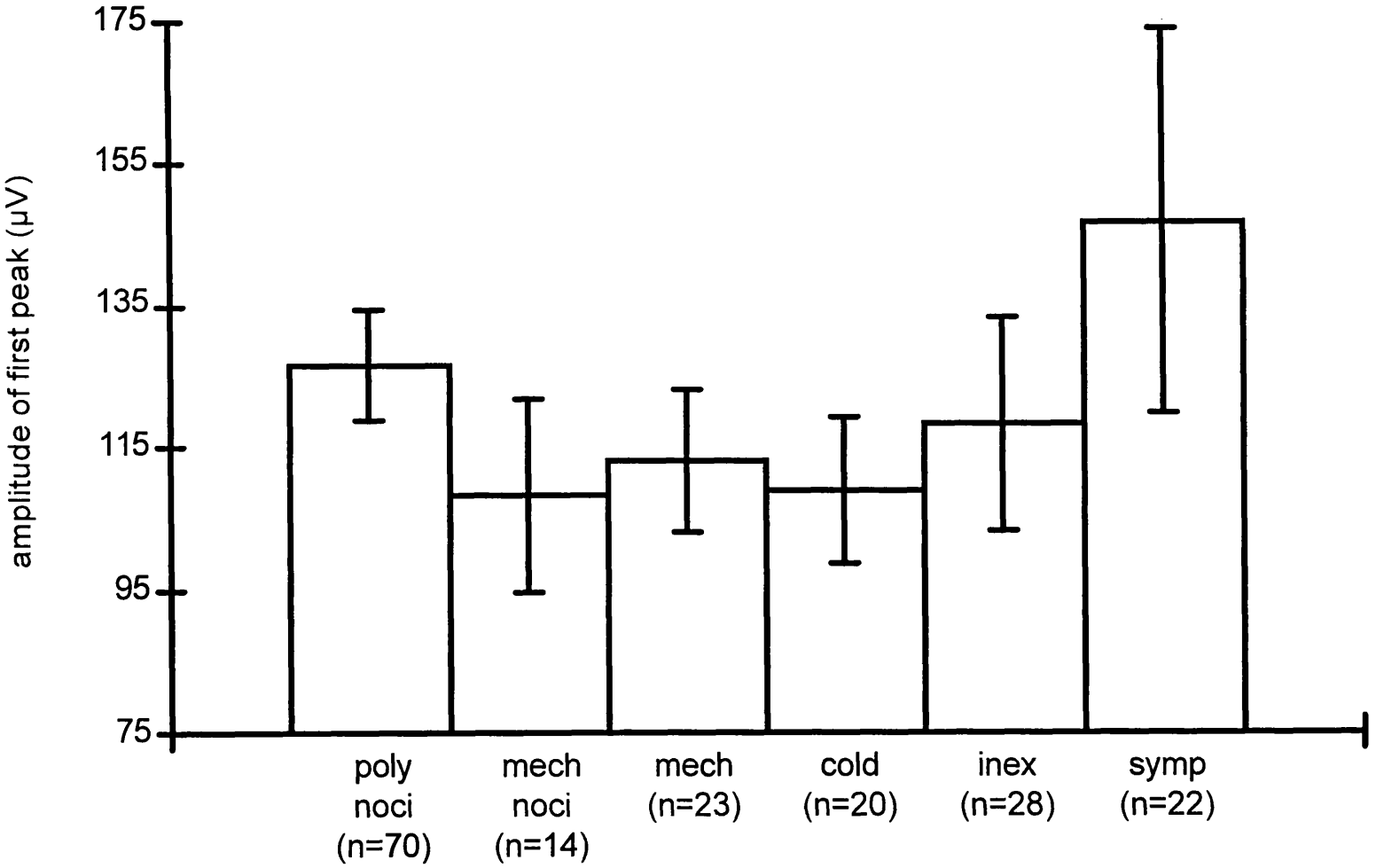

Figure 7.7 **Bar chart showing the amplitude of the first peak (mean±SE) of the different classes of C-fibre.** poly noci = polymodal nociceptors; mech noci = mechanical nociceptors; mech = mechanoreceptors; cold = cold thermoreceptors; inex = inexcitable units; symp = spontaneously active sympathetic efferents

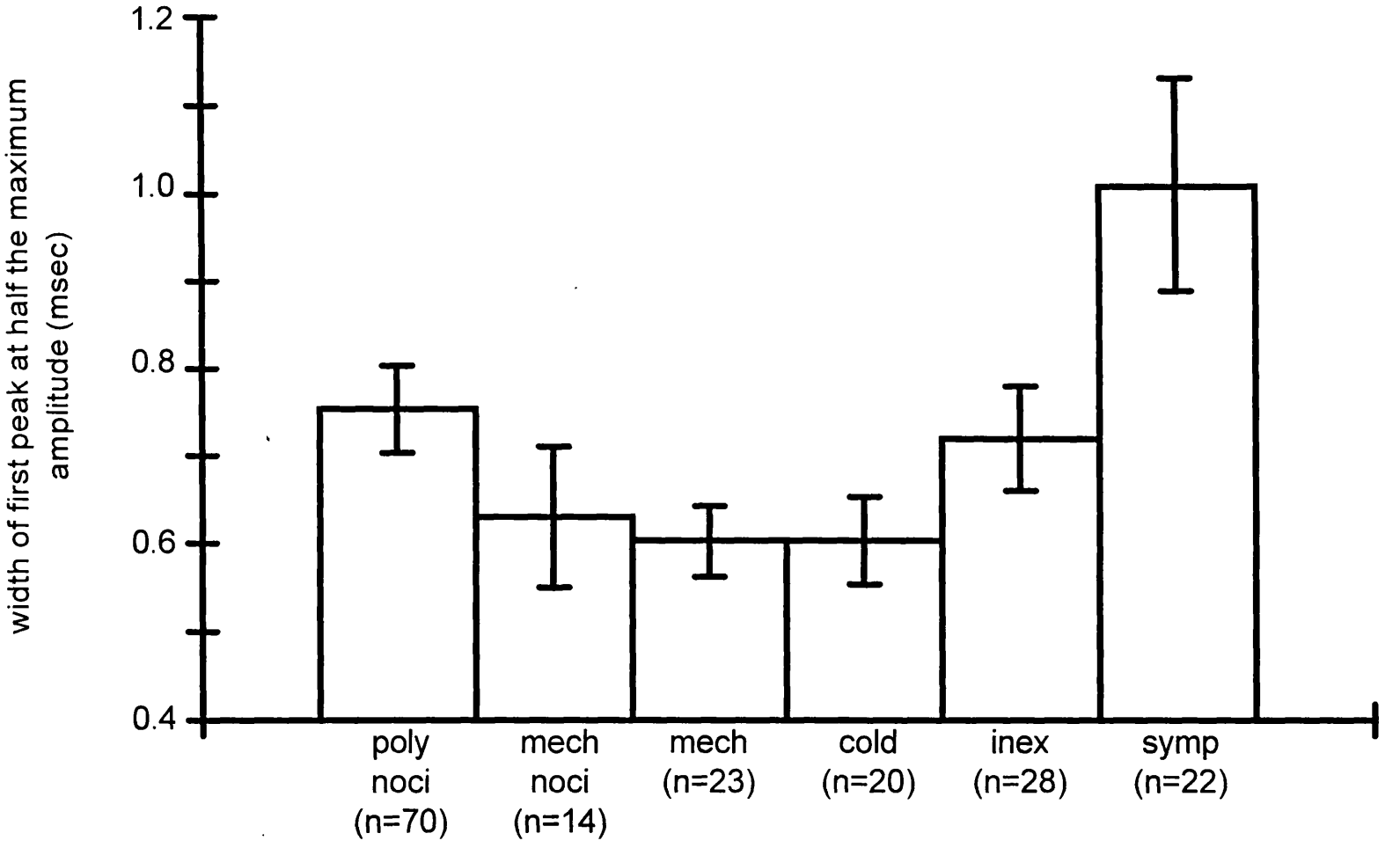

Figure 7.8 **Bar chart showing the widths of the first peak at half the maximum amplitude (mean±SE) of the different classes of C-fibre.**

poly noci = polymodal nociceptors; mech noci = mechanical nociceptors; mech = mechanoreceptors; cold = cold thermoreceptors; inex = inexcitable units; symp = spontaneously active sympathetic efferents

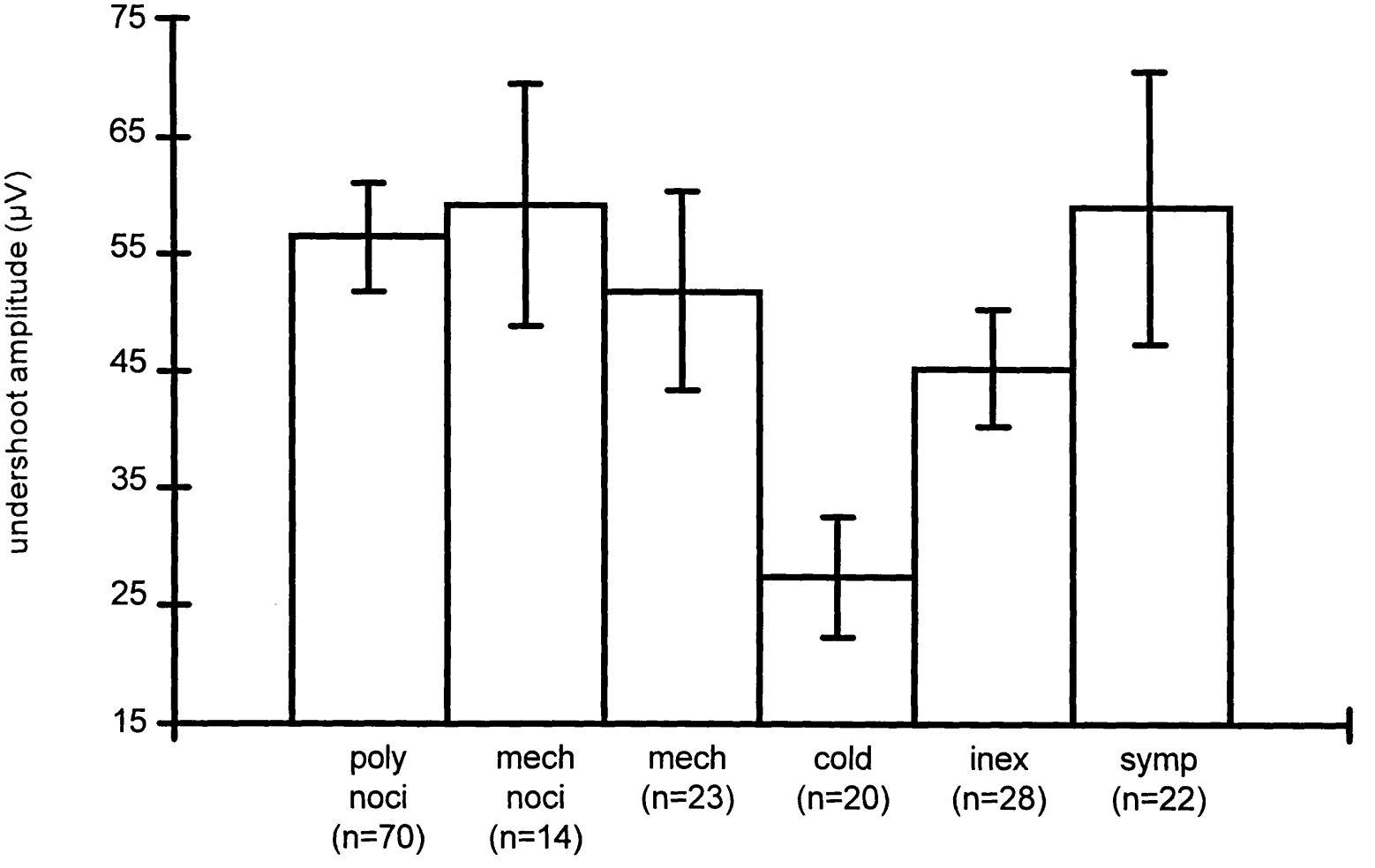

Figure 7.9 **Bar chart showing the undershoot amplitude (mean±SE) of the different classes of C-fibre.**
poly noci = polymodal nociceptors; mech noci = mechanical nociceptors; mech = mechanoreceptors; cold = cold thermoreceptors; inex = inexcitable units; symp = spontaneously active sympathetic efferents

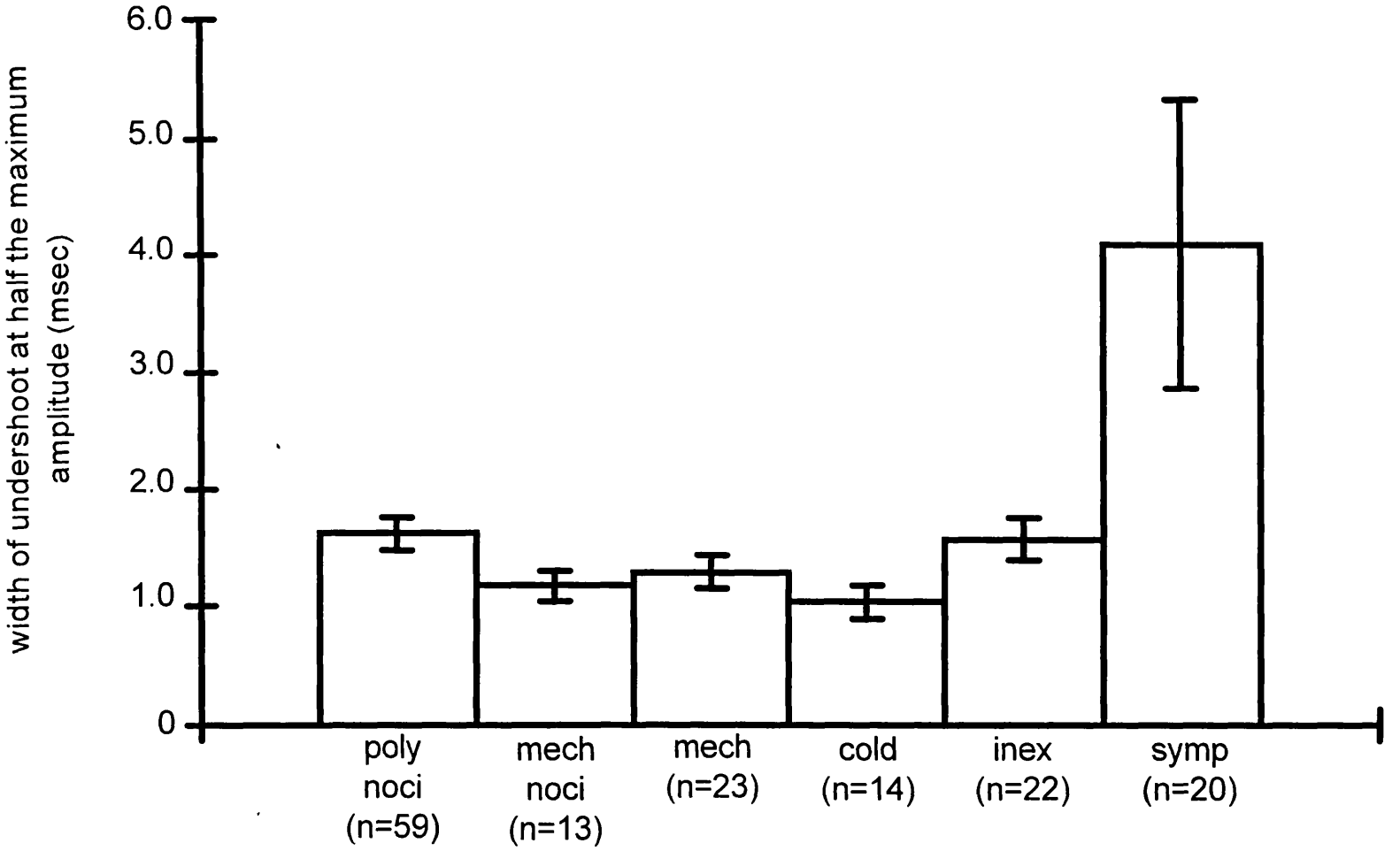

Figure 7.10 **Bar chart showing the widths of the undershoot at half the maximum amplitude (mean±SE) of the different classes of C-fibre.**

poly noci = polymodal nociceptors; mech noci = mechanical nociceptors; mech = mechanoreceptors; cold = cold thermoreceptors; inex = inexcitable units; symp = spontaneously active sympathetic efferents

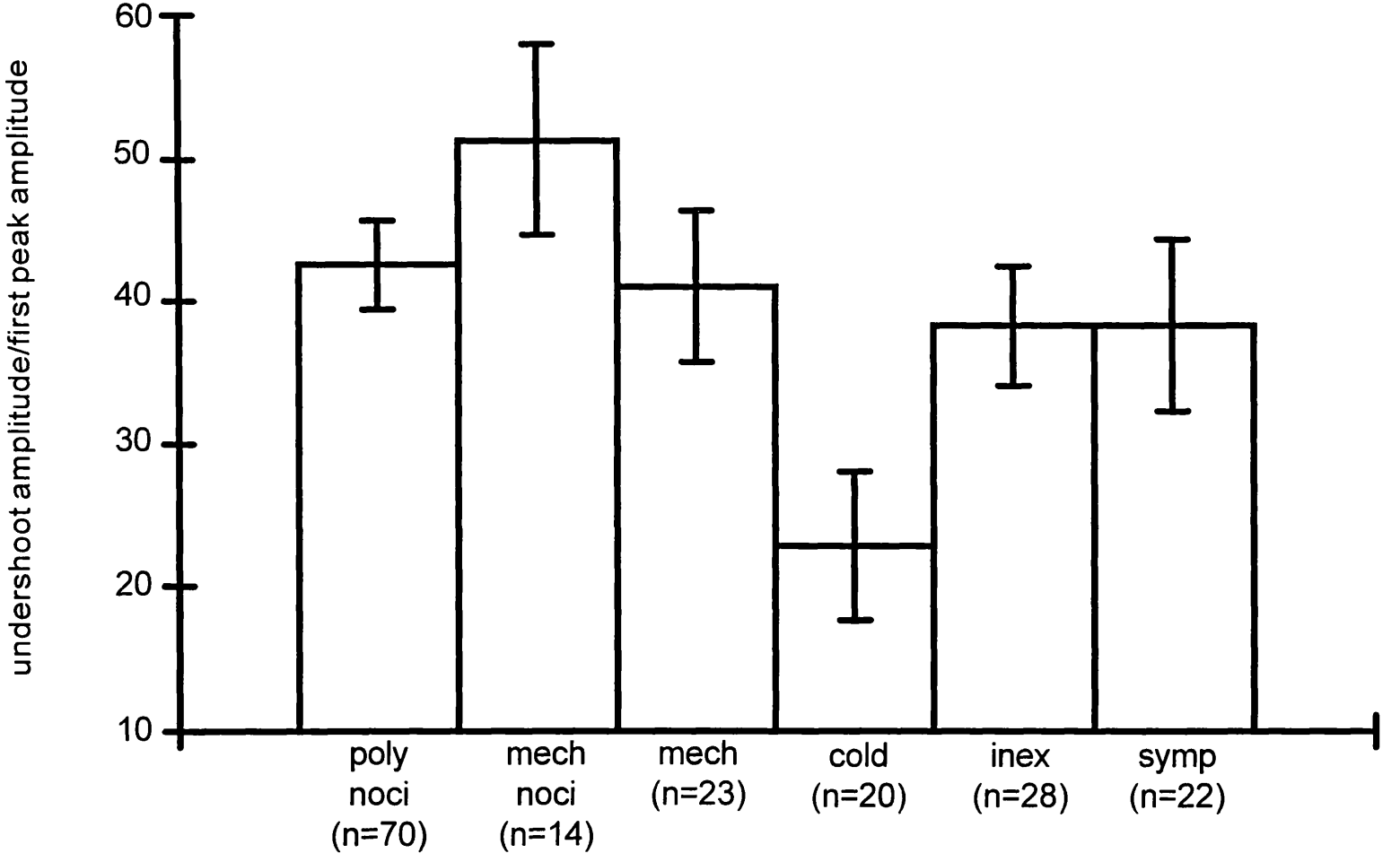

Figure 7.11 **Bar chart showing the undershoot amplitude/first peak amplitude (mean±SE) of the different classes of C-fibre.**

poly noci = polymodal nociceptors; mech noci = mechanical nociceptors; mech = mechanoreceptors; cold = cold thermoreceptors; inex = inexcitable units; symp = spontaneously active sympathetic efferents

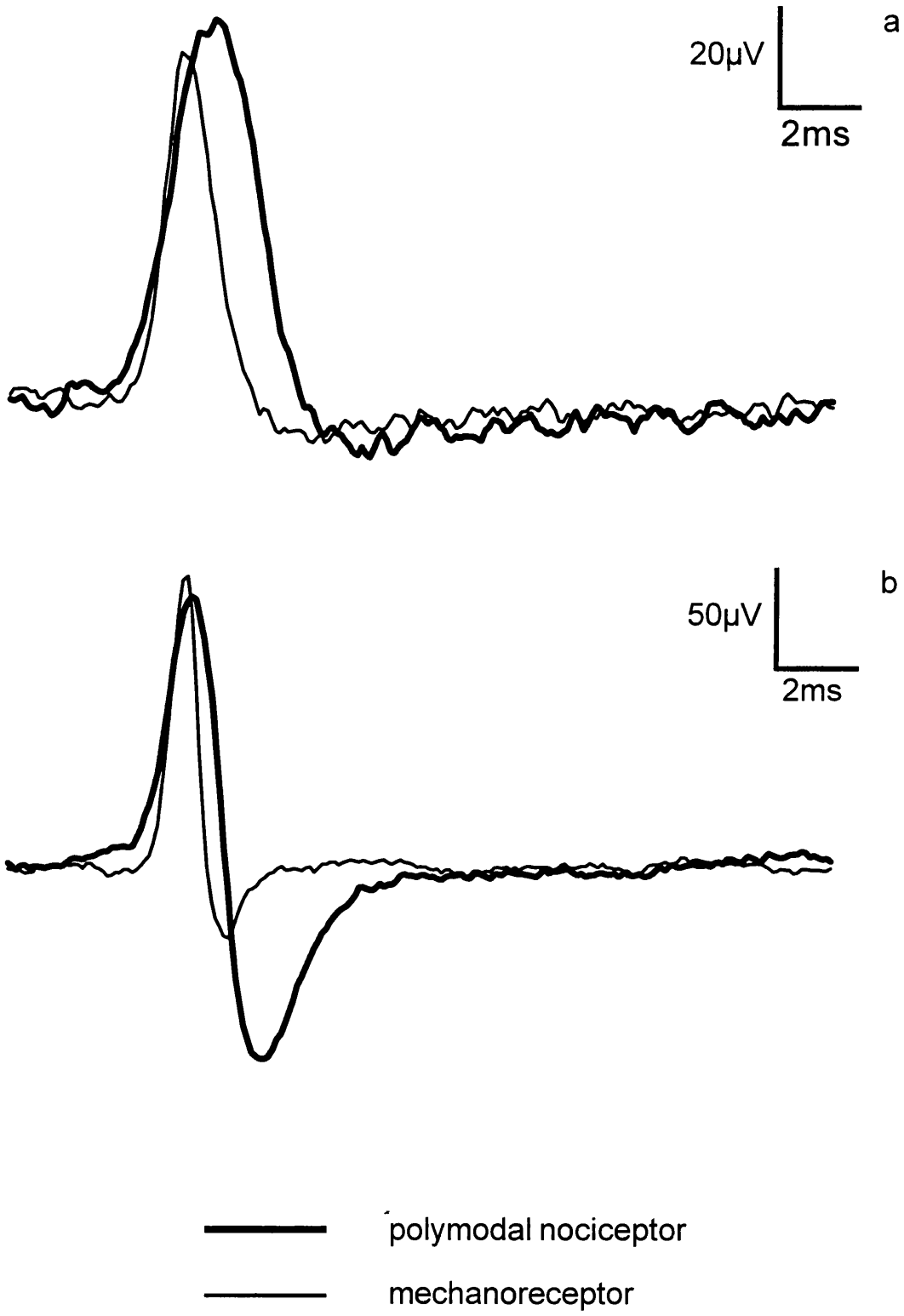

Figure 7.12a,b **Two examples of filaments containing both a polymodal nociceptor and a mechanoreceptor.** Note that in all 10 cases where both types of fibre were present in a single filament, the polymodal nociceptor always had a wider spike than the mechanoreceptor.

CHAPTER 8 DISCUSSION: EFFERENT ACTIONS OF CUTANEOUS C-FIBRES

I have shown that by combining the use of laser Doppler perfusion imaging and/or laser Doppler flowmetry with controlled electrical stimulation of identified C-fibres of the rabbit and rat saphenous nerve, it is possible to directly examine which types of C-fibre have vasodilator actions in the skin of these animals. Some of the results from these studies have been published in abstract form (Gee *et al.* 1996b). Also, using the laser Doppler perfusion imaging system to study the flare reactions of the skin to noxious stimuli, I can compare the kinds of stimuli required to produce flare with the kinds of stimuli that excite the vasoactive C-fibres.

8.1 Improvements over previous single unit studies on neurogenic inflammation

This study has three main advantages over similar single unit studies of neurogenic inflammation in mammalian skin (Kenins 1981; Bharali and Lisney 1992; Kolston and Lisney 1993). The first, and I think the most important improvement made in this study, was that good control was applied over the antidromic electrical stimulation of the filaments. In these experiments, efficient filament stimulation is necessary in order to provide convincing evidence that in the case of those units that did not produce any vasodilatation, the lack of any vascular response was not merely due to insufficient stimulation. In previous studies, filament stimulation was monitored by averaging the activity from "en passant" recordings taken from the whole nerve. However, with this approach it is only possible to record unitary activity of Aß and Aδ fibres, and not of C-

fibres (Bharali and Lisney 1992; Kolston and Lisney 1993; also see Methods section). In the experiments reported here, a modification of the collision technique was used to establish the electrical threshold for antidromic stimulation of individual C-fibres (Andrew *et al.* 1996; see Figure 2.5 in the Methods section). The collision technique provided repeatable threshold values, which ensured that the stimulus intensity could be set at a level which would be sufficient to excite the units, but at the same time not too great so as to risk damaging or killing the filaments. Therefore, by using the collision technique, evidence of adequate filament stimulation was attained, and such evidence is essential in order to prove the negative results.

Secondly, when studying neurogenic inflammation there are clear advantages to choosing to study the vasodilatation response as opposed to plasma extravasation. Using laser Doppler flowmetry and/or laser Doppler perfusion imaging to study neurogenic vasodilatation allows individual units to be repeatedly tested. In contrast, with single unit experiments involving the use of extravasation of Evans blue dye there is only one chance to get a result with each unit. Another advantage that studies of neurogenic vasodilatation have over studies of plasma extravasation is that local increases in skin blood flow can still be detected even when there is some background vasodilatation. However, background leakage of Evans blue dye into the skin is a serious problem in single unit studies of plasma extravasation.

The third major advantage that this study had over previous attempts to identify single units involved in neurogenic inflammation is that the laser Doppler perfusion imaging system was used. Laser Doppler perfusion imaging is the most sophisticated technique presently available to monitor tissue perfusion and offers many advantages over other,

older, techniques (Wårdell 1992). Although laser Doppler flowmetry can, and indeed did, provide information on skin blood flow changes in response to the antidromic stimulation of single identified C-fibres (Figure 4.6), the laser Doppler perfusion imaging system has several advantages over the single channel system:

1. With the single channel laser Doppler flowmetry technique, skin blood flow in one position can be monitored over a period of time. However, the laser Doppler perfusion imaging system provides spatial, as well as temporal, information about tissue blood flow.

2. Because the single channel technique monitors blood flow from one particular position, there is no scope for inaccurate location of receptive fields. However, since the imaging system provides information of skin blood flow in an area of tissue, it allows one to test units where it is not possible to accurately locate receptive fields (e.g. inexcitable units). One can check if inexcitable units are vasoactive either by scanning and imaging the whole saphenous field, or, if its electrical receptive field can be determined by electrical skin stimulation, by imaging the region around the electrical receptive field.

3. Imaging blood flow in an area of skin allows one to gather information about the vasoactive properties of many C-fibres within a multi-unit preparation.

8.2 Vasodilator units in the rabbit and rat

In both the rabbit and rat, the only type of C-fibres shown to have vasodilator actions when individually stimulated were nociceptors. In the rabbit, all the vasodilator nociceptive C-fibres found were of the polymodal type, sensitive to both noxious mechanical and thermal stimuli. In the rat, the majority of the vasoactive C-fibres were polymodal nociceptors (7 of 11, i.e. 63.6%), and the other vasoactive units were heat nociceptors

(n=2) and polymodal/mechanical nociceptors (i.e. incompletely classified nociceptors, n=2). It could be argued that the two incompletely classified nociceptors were likely to be polymodal nociceptors, since they had mechanical thresholds within the polymodal range and also because, in the rat, mechanical nociceptors constitute only a minor class of cutaneous C-fibres (Lynn 1994).

These findings in the rabbit and rat differ from the results of a recent study of neurogenic vasodilatation in pig skin (Lynn *et al.* 1996a). Twenty-eight identified cutaneous C-fibres were dissected from the saphenous nerve of the anaesthetized pig, comprising 9 polymodal nociceptors, 11 heat nociceptors, 1 mechanical nociceptor, 2 mechanoreceptors, 1 warm unit and 4 inexcitable units. Using the laser Doppler perfusion imaging system, these fibres were studied for their ability to produce vasodilatation upon antidromic electrical stimulation. Increases in skin blood flow were only detected after stimulation of heat nociceptors, and 10 of the 11 heat nociceptors studied produced a vasodilator response. Vasodilatation was not seen following stimulation of any other type of C-fibre, including the polymodal nociceptors.

So, it appears that in pig skin, the vasodilator component of neurogenic inflammation is caused by heat nociceptors. This is clearly not the case in the rabbit, where there are no reports of C-heat nociceptors being found in cutaneous nerves (Lynn 1979; Shea and Perl 1985; Barasi and Lynn 1986; Shakhanbeh 1989). Instead, in rabbit skin, a proportion of the polymodal nociceptors are responsible for producing antidromic vasodilatation. But it is interesting to note that not all the polymodal nociceptors are involved, and the polymodal units which had vasodilator actions were the least mechanically sensitive ones.

There was no significant difference in the sensitivity to heat of the vasodilator and non-vasodilator polymodal nociceptors of the rabbit saphenous nerve.

The situation in rat skin also differs from that in the pig. In the rat, the majority of vasoactive C-fibres belong to the polymodal nociceptor class. But again, as in the rabbit, the vasoactive units had mechanical thresholds towards the higher end of the range for C-polymodal nociceptors (Lynn and Carpenter 1982). There was however no difference between the vasodilator and non-vasodilator units in terms of their heat thresholds. It must be pointed out that although heat nociceptors constitute 11.3% of C-fibres in the pig saphenous nerve (Lynn *et al.* 1995), such heat nociceptors are very uncommon in the rat saphenous nerve (Lynn and Carpenter 1982; Fleischer *et al.* 1983; Kress *et al.* 1992). Therefore, although both of the heat nociceptors found and tested in this study were capable of producing a vasodilator response, it is difficult to critically assess the role that this small class of C-fibres play in neurogenic inflammation in rat skin.

Heat nociceptors are reported to be present in significant numbers in primate cutaneous nerves. In man, microneurography studies in the peroneal nerve have shown that 6% of C-fibre afferents are heat nociceptors (Schmidt *et al.* 1995). In monkey hairy skin, it is reported that heat nociceptors make up 7% of C-fibre afferents (Baumann *et al.* 1991), and in monkey glabrous skin they make up 5.5% of nociceptive C-fibres (Georgopoulos 1976). It will be of interest to see the relative roles that the heat and polymodal nociceptors play in generating neurogenic inflammation in primate skin.

8.3 Vasodilatation resulting from stimulation of single C-fibres innervating rabbit skin

The vasoactive polymodal nociceptors innervating rabbit skin showed a wide range of efferent responses (16-110% increases in skin blood flow above the baseline). Such a range was also seen in the study carried out in the pig (up to 176% increase above the baseline; Lynn *et al.* 1996a).

The efferent response was always coincident with the afferent receptive field. Furthermore, in the rabbit data presented here, the average area of vasodilatation resulting from stimulation of a single polymodal nociceptor (mean±SE, 11.7mm^2±1.65, n=14) was very similar to the average polymodal nociceptor afferent receptive field (11.6mm^2±3.09, n=14). This close similarity of afferent and efferent receptive field size is consistent with the terminals of cutaneous C-fibres having dual afferent and efferent functions, rather than there being separate afferent and efferent terminals (Szolcsányi 1988; Lisney and Bharali 1989).

8.4 Vasodilatation resulting from stimulation of single C-fibres innervating rat skin

As in the rabbit, there was a wide range of efferent vasodilator responses (17-180% increase in skin blood flow above the baseline), and the responses were always coincident with the afferent receptive fields.

A striking observation from the single unit study in the rat was that the vasodilator units were not distributed evenly throughout the saphenous nerve receptive field. The majority (9 of 11) of the vasodilator units were located on the foot/digits, with the remaining 2 units being located on the ankle/leg. This provides an interesting correlation with the finding that the vasodilatation brought about by antidromic stimulation of the whole saphenous nerve at C-fibre intensity is also not evenly distributed throughout the saphenous receptive field. Most published work involving extravasation of Evan's Blue dye following stimulation of the rat saphenous nerve at C-fibre intensity, shows results that are restricted to the skin on the foot (Brenan 1986; Brenan *et al.* 1988; Wiesenfeld-Hallin 1988; Wiesenfeld-Hallin *et al.* 1988, 1989; Kinnman and Wiesenfeld-Hallin 1993). However, those that do show C-fibre induced extravasation of Evan's Blue dye in the *whole* saphenous field, show that the response on the leg is more patchy than on the foot (Lisney 1987; Bharali and Lisney 1988). In fact, the variation of Aδ-fibre evoked vasodilatation in different parts of the rat saphenous nerve has been offered as a suggestion to explain why no vasodilatation could be detected from antidromic stimulation of single Aδ fibres (Kolston and Lisney 1993). As well as looking at antidromic vasodilatation, I have also carried out some experiments looking at plasma extravasation of Evan's Blue dye following stimulation of the saphenous nerve at C-fibre intensity. I found that both the vasodilatation and the extravasation responses in the rat show considerable animal to animal variation. However, in general, I have found that both the vasodilatation and the dye leakage are more consistent and more intense on the foot, and more patchy on the leg. The finding that there were fewer vasodilator units on the leg than on the foot and digits provides an explanation for the relatively poor neurogenic effects (both antidromic vasodilatation and plasma extravasation) that are seen on the leg.

8.5 Non-vasodilator units in the rabbit and rat

In this study, rigorous controls have been applied so as to provide convincing evidence that any units that did not produce detectable vasodilatation were true non-vasodilator units. These controls were threefold:

1. The use of the collision technique to establish the thresholds for electrical antidromic stimulation of individual C-fibres ensured that any negative results were not due to insufficient stimulation.

2. Only units which survived the period of filament stimulation were included in this study, i.e. units were only included if orthodromic activity could be evoked after the period of antidromic filament stimulation, indicating that no conduction block developed during the period of antidromic stimulation.

3. Following the antidromic stimulation of units that were unsuccessful in producing vasodilatation, the vasodilatation response to whole nerve stimulation was checked. Only those units whose receptive fields were in areas of skin that were clearly capable of producing vasodilatation were included in the results.

Despite these controls, I think that it is still necessary to question whether the approaches employed in this study are sophisticated enough to detect all of the vasoactive units. This is because, to me, there seems to be some disparity between the vasodilator response seen when the whole nerve is antidromically stimulated and the low proportion of individual units found to have vasodilator properties. This is particularly so in the rat, where the proportion of vasoactive nociceptors was very low (22.9% of the nociceptors tested were vasoactive). In both the rabbit and the rat, it could be that C-fibre evoked antidromic vasodilatation is brought about by the actions of a small proportion of nociceptors.

However, there was a great range of magnitude of blood flow changes brought about by the activity of single units (16-110% in the rabbit and 17-180% in the rat; for values refer to Tables 3.1 and 4.1), i.e. some units are more effective than others at producing vasodilatation. Based on the fact that the vasoactive C-fibres clearly vary in the degree of their ability to produce vasodilatation, I think that the likely situation is that there are some vasoactive units whose single contribution is not great enough to be detected by the methods used in this study. Also, I think that the level of a 15% increase in blood flow which has been used as the lower limit for a true vasodilator response is a conservative limit. The use of a conservative limit, such as 15%, probably conceals some genuine vasodilator responses within the 5-10% increase in skin blood flow range. However, I think that the variability in the background blood flow in any given preparation and the great animal to animal variability in antidromic vasodilatation responses justifies the use of a conservative limit. I therefore think that it is likely that the proportion of vasoactive units as revealed in this study has been underestimated. Even if a less conservative lower limit had been used, it is a possibility that there are some very weak vasoactive units whose individual effects would still have remained undetected. In the case of these weaker units, perhaps more than one fibre needs to be excited before a detectable response is produced (Kolston and Lisney 1993).

8.6 Comparison with single unit plasma extravasation studies in the rat

Although the neurogenic inflammation that has been described in many tissues of several species has been linked to the efferent actions of nociceptive C-fibres, and to a lesser extent, of Aδ fibres (Ferrell and Russell 1986; Holzer 1988; Lynn 1988, 1996a), there have only been a few successful studies on the contribution of single identified units to

neurogenic vasodilatation and plasma extravasation (Kenins 1981; Bharali and Lisney 1992; Lynn *et al.* 1996a).

Two separate research groups have used Evan's Blue dye leakage in to rat skin to study the plasma extravasation component of neurogenic inflammation at the single C-fibre level (Kenins 1981; Bharali and Lisney 1992). Both groups found that the only type of C-fibres capable of producing extravasation upon antidromic electrical stimulation were the polymodal nociceptors. Kenins (1981) found that all 12 polymodal nociceptors tested produced extravasation, whereas Bharali and Lisney (1992) reported that only 12 of the 18 (i.e. 66%) polymodal nociceptors tested produced extravasation. One possible explanation of the lower percentage of vasoactive polymodal nociceptors found by Bharali and Lisney (1992) is that the antidromic stimulation was not effective in all cases, because, apart from a positive extravasation response, there was no further evidence that the stimulus parameters used were sufficient to excite the individual units.

In this study, only a proportion (17.5%) of rat C-polymodal nociceptors were found to be vasodilators. Thus, even if one takes the more conservative estimate that 66% of C-polymodal nociceptors are involved in plasma extravasation in rat skin, it is unlikely that all of the C-fibres responsible for extravasation are also vasoactive. The possibility that the group of vasoactive C-fibres does not completely overlap with the group of C-fibres responsible for plasma extravasation is not an unrealistic one, since different neuropeptides have been implicated in these two forms of neurogenic inflammation and different sites of action within the microvasculature are involved. In the skin, neurogenic vasodilatation is thought to be mostly due to the action of CGRP on the arterioles, and plasma extravasation is thought to be mainly due to the effect of substance P on the postcapillary

venules (see Lynn, 1996; see Figure 1.5). The role of heat nociceptors in the plasma extravasation component of neurogenic inflammation has yet to be assessed (Kenins 1981; Bharali and Lisney 1992), and so it remains possible that the small number of heat nociceptors present in the rat saphenous nerve are involved in plasma extravasation as well as antidromic vasodilatation.

Neurogenic inflammation is not a purely C-fibre evoked process. In the skin, the finely myelinated Aδ fibres also have efferent actions. Aδ fibres can produce a vasodilator response in rabbit and rat skin (Lynn and Shakhanbeh 1988; Jänig and Lisney 1989; Kolston and Lisney 1993), although their actions are weak in comparison to that brought about by C-fibres. It is not yet known which type of Aδ fibre contributes to the antidromic vasodilatation response in rat skin (Kolston and Lisney 1993). Although cutaneous Aδ fibres possess vasodilator properties, they do not cause any plasma extravasation (Jänig and Lisney 1989). Also, the Aδ fibres innervating the knee joint of the cat do not produce any plasma extravasation (Ferrell and Russell 1986).

8.7 Relationship with the neurochemistry of cutaneous afferent fibres

As discussed in the introductory chapter, there is much evidence that neurogenic inflammatory responses are brought about by the release of neuropeptides from nociceptive neurones. The main neuropeptides linked with neurogenic inflammation are substance P, calcitonin gene-related peptide (CGRP), neurokinin A (NKA) and vasoactive intestinal polypeptide (VIP), but there is very little direct evidence of the neuropeptide content of cutaneous afferents with identified sensory receptor types (Lawson 1996).

Using RT97 (an anti-neurofilament antibody), the neurofilament content of dorsal root ganglion cells can be used to identify fibre type in the rat - the small, dark cells with unmyelinated axons are neurofilament-poor and the light cells with myelinated axons are neurofilament-rich, although there is some overlap in the C/Aδ-fibre group (Lawson and Waddell 1991). Immunocytochemistry studies carried out in the rat show that of the RT97-negative cells (i.e. C-fibres) retrogradely labeled from the skin 50% contained CGRP and 37% contained substance P (O'Brien *et al.* 1989). Also, in the rat, substance P is known to co-exist with CGRP in up to 20% of small and medium sized dorsal root ganglion neurones and in about 20% of trigeminal ganglion cells (Lee,Y *et al.* 1985a, b).

As discussed above, neurogenic vasodilatation in the skin is thought to be mostly due to the action of CGRP on the arterioles, and plasma extravasation is thought to be mainly due to the effect of substance P on the postcapillary venules (see Lynn, 1996; see Figure 1.5). Therefore, we can compare the results of the single unit studies on neurogenic inflammation and the estimates of CGRP- and substance P-containing cutaneous C-fibres in the rat. In this study, 24.4% of the C-fibres classified as polymodal nociceptors, polymodal/mechanical nociceptors or heat nociceptors were found to have vasoactive properties. Polymodal nociceptors account for between 48% and 75% of the total C-fibre population in the rat saphenous nerve (Lynn and Carpenter 1982; Fleischer *et al.* 1983; Kress *et al.* 1992). This means that between 11.7% and 18.3% of cutaneous C-fibres can produce vasodilatation, and should therefore contain the potent vasodilator CGRP. This is a much lower proportion than the 50% which are said to contain CGRP (O'Brien *et al.* 1989). This contrast between the percentage of C-fibres shown to have vasodilator properties and the percentage said to contain CGRP lends some support to my opinion that the proportion of vasoactive C-fibres in the rat saphenous nerve revealed in this study

is probably an underestimate and that there are C-fibres with weaker vasodilator actions that have not been detected in this study (as discussed in Section 8.5 above). However, the much lower proportion of vasoactive C-fibres compared to the proportion of C-fibres containing CGRP can also be explained by the fact that CGRP has other actions besides producing vasodilatation. For example, CGRP has been shown to modulate some macrophage functions, including antigen presentation (Nong *et al.* 1989). Also, the terminals of some CGRP-containing nerve fibres are located in the epidermis, which is an avascular structure, and so this clearly indicates other roles for CGRP besides its action as a vasodilator (Dalsgaard *et al.* 1989; Garcia-Caballero *et al.* 1989). In human epidermis, there is a close anatomical association between the macrophage-like Langerhans cells and CGRP-containing nerve fibres, and CGRP has been found at the surface of some Langerhans cells (Hosoi *et al.* 1993; Asahina *et al.* 1995). One effect of CGRP on the epidermal Langerhans cells is an inhibition of antigen presentation (Hosoi *et al.* 1993).

It is suggested that between 66% and 100% of C-polymodal nociceptors (i.e. between 32% and 75% of cutaneous C-fibres) in the rat saphenous nerve are involved in neurogenic plasma extravasation (Kenins 1981; Bharali and Lisney 1992). The estimate that 37% of cutaneous C-fibres in the rat contain substance P falls within this range (O'Brien *et al.* 1989). However, it is worth noting that substance P has other actions besides increasing microvascular permeability. Substance P has been shown to enhance the phagocytic activity of macrophages and polymorphonuclear leukocytes (Bar-Shavit *et al.* 1980; Hartung and Toyka 1983; Payan *et al.* 1984), and substance P is in fact chemotactic for these cells (Ruff *et al.* 1985). Substance P has been shown to stimulate human T-lymphocyte proliferation (Payan *et al.* 1983) and it also induces mast cell degranulation (Fewtrell *et al.* 1982).

8.8 Flare responses of rabbit and rat skin to noxious stimuli

The single unit studies discussed above provided clear results about the kinds of afferent C-fibres involved in antidromic vasodilatation. The study of the flare responses of rabbit and rat skin to noxious stimuli was carried out so that the results from the single unit studies could be related to the classical neurogenic vasodilatation response of flare. In other words, this study allowed for a direct comparison of mechanical and thermal thresholds and of spatial organization to be made between single C-units and flare. The flare responses were measured using the laser Doppler perfusion imaging system.

8.8.1 Flare responses to heat stimulation of rabbit skin

Using a ramped heat stimulus, the temperature that needed to be reached in order to produce a flare response in rabbit skin was less than 50°C. In the rabbit, the flare responses of the skin to pairs of heat stimuli were remarkably consistent (see Figures 5.8 to 5.11). The heat thresholds of the rabbit polymodal nociceptors found in this study ranged from 44.5°C to 62.5°C, with a mean heat threshold of 52.9°C±0.98°C (mean±SE; n=22). In a larger sample of 69 rabbit polymodal nociceptors, the heat thresholds ranged from 41°C to 65°C (with an average heat threshold of 54.1°C). It therefore seems that the temperatures required to produce flare in rabbit skin fall in the lower end of the range of heat thresholds of polymodal nociceptors. Thus there is a good fit between the thresholds of single units and the flare threshold.

8.8.2 Mechanical thresholds for flare responses in rabbit and rat skin.

In the rabbit, the thresholds for a flare response to mechanical stimulation ranged from 0.4g to 1.0g, with an average threshold value of 0.6±0.06g (mean±SE; n=9). The average mechanical threshold of the rabbit polymodal nociceptors found in this study was 0.33g±0.066 (n=28), and this is similar to the average threshold value of 0.46g found in a sample of 148 rabbit polymodal nociceptors (Lynn and Baranowski 1987). Therefore, it seems that the pressure required to produce a flare response in rabbit skin is greater than that required to excite a typical cutaneous polymodal nociceptor. This is consistent with the results from the single unit study on antidromic vasodilatation in rabbit skin which showed that the vasoactive polymodal nociceptors had significantly greater mechanical thresholds (0.47±0.10g, n=14) than the non-vasodilator polymodal units (0.18±0.03g, n=14) (p=0.01, Mann-Whitney U test).

The flare responses following mechanical stimulation of rat skin were generally weak and inconsistent (see Chapter 5), and this is in agreement with a previous study of mechanically evoked flare in the rat (Lynn and Cotsell 1992a). In this study, the threshold pressures required to produce flare in rat skin ranged from 2g to 10g, with an average value of 7.0±1.41g (n=6). Again, this is in agreement with the previous study by Lynn and Cotsell (1992a) who found that the lowest Von Frey filament that produced a flare response was 2g, and that 6.5g and 10g stimuli produced flares at most of the locations tested. The mechanical thresholds of the 39 polymodal nociceptors dissected from the rat saphenous nerve in this study ranged from 75mg to >20g, with an average value of 2.0±0.69g. Thus, the kinds of pressures that excite most rat cutaneous polymodal nociceptors do not necessarily result in flare. This is consistent with the tendency for the cutaneous afferent

units with neurogenic vasoactive properties to have greater mechanical thresholds than the non-vasodilator units. However, it is worth pointing out that one of the vasoactive C-fibres in the rat had a relatively low mechanical threshold (0.05-0.1g), and therefore one should occasionally expect to see a flare response in rat skin following relatively weak mechanical stimuli.

The results from this study of the flare responses of rabbit and rat skin to mechanical and heat stimuli therefore lend support to the results of the single unit antidromic vasodilatation studies in these two species, in that they both point towards the conclusion that neurogenic vasodilatation is brought about by a sub-population of cutaneous nociceptors with low mechanical sensitivity but typical heat sensitivity.

8.8.3 The spread of flare in rabbit and rat skin

In order to see whether the flare response of rabbit skin generated by noxious stimuli can be explained by the axon reflex model (Lewis 1927), it is necessary to examine in detail the relationship between flare size and afferent receptive field size. Figure 8.1 demonstrates that stimulation of the skin will activate several afferent units with overlapping receptive fields. The maximum spread of a flare response from the site of stimulation (i.e. the "radius" of the flare) will be similar to the maximum extent of a typical afferent receptive field (i.e. the "diameter" of a unitary receptive field). The spread of flare from the stimulation site is going to be greater in the proximal-distal direction than in the medial-lateral direction, since the afferent receptive fields tend to be elongated in the proximal-distal direction.

The maximum extents of the receptive fields of the rabbit polymodal nociceptors mapped with suprathreshold mechanical stimuli ranged from 3.1mm to 8.6mm in the proximal-distal direction and from 2.0mm to 5.5mm in the medial-lateral direction (n=14). Using the model of flare illustrated in Figure 8.1, a maximum flare response of 17.2mm by 11.0mm would be predicted. This predicted value is very close to the observed maximum flare response following mechanical stimulation of rabbit skin which was a roughly elliptical shape spreading about 17.6mm in the proximal-distal direction and 9.4mm in the medial-lateral direction (see Figures 5.1 and 5.2). In the study of the vasodilator component of neurogenic inflammation in pig skin (Lynn *et al.* 1996a) there was also a good fit between the maximum spread of flare following noxious stimulation (15mm using an intradermal injection of capsaicin as the noxious stimulus) and the maximum extent of the afferent receptive fields of single heat nociceptors (13mm). Therefore, in both rabbit and pig skin, the spread of a flare response does appear to be limited by the extent of the terminals of single cutaneous nociceptive afferents and this provides direct support for the axon reflex model (Lewis 1927).

The results of the study of the flare responses in rat skin need to be treated with more care, since the small distances involved make it difficult to present a convincing argument. In this study, the afferent receptive fields in the rat were not mapped. However, in a previous study, the receptive fields of C-fibre polymodal nociceptors to punctate pressure ranged in maximum extent from 1.3mm to 5.7mm (n=11), with most units measuring about 2.5mm in maximum extent (Lynn and Cotsell 1993). Afferent receptive fields measuring a maximum of 2.5mm would correspond to flares extending to about 5mm, and indeed, the maximum flare resulting from mechanical stimulation of rat skin measured 6.1mm in the proximal-distal direction and 3.4mm in the medial-lateral direction.

Although these results from the rat need to be treated with caution, when taken in conjunction with the results from the rabbit presented here and with the results from the study in the pig (Lynn *et al.* 1996a), it does seem that there is a good correlation between the maximum spread of flare responses (the flare "radius") and the maximum extent of C-nociceptor afferent receptive fields (the receptive field "diameter"). Both the extent of flare and C-nociceptor receptive field size increase with body size to a similar extent, and thus give good support to Lewis' axon reflex model of flare (Lewis 1927; Lynn *et al.* 1992; Lynn and Cotsell 1993).

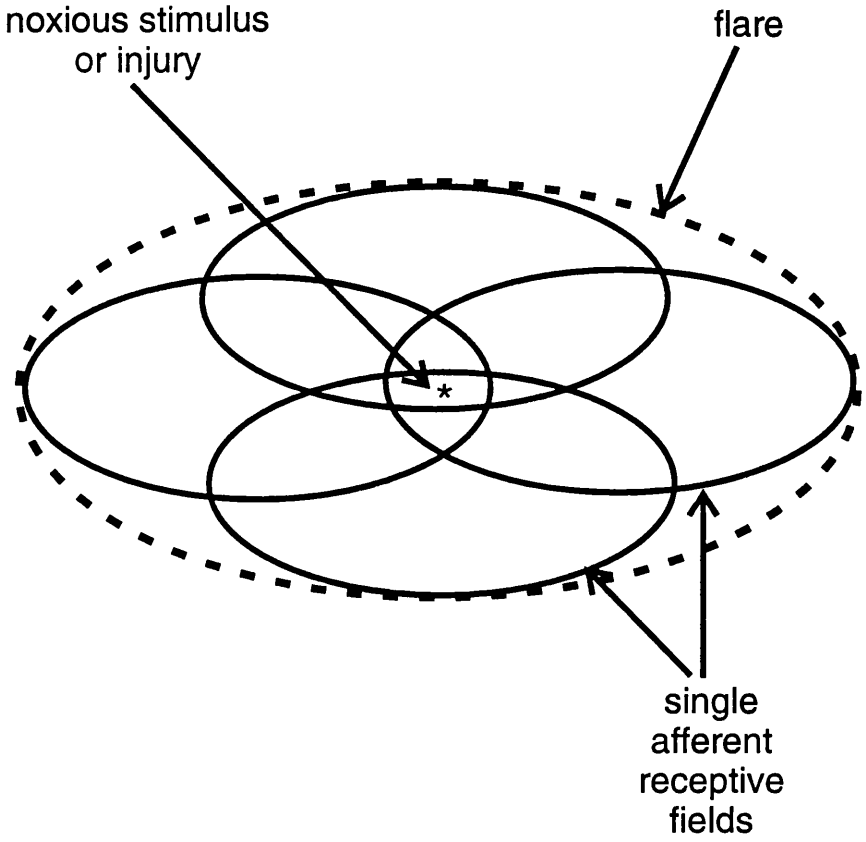

Figure 8.1 Diagram showing the relationship between the size of the flare response following a noxious stimulus or injury and the size of the receptive fields of afferent units.
Noxious stimulation or an injury will excite several cutaneous nociceptors with overlapping afferent receptive fields. The maximum spread of the flare response from the site of stimulation or injury (i.e. the "radius" of the flare) will be similar to the maximum extent of individual afferent receptive fields (i.e. the "diameter" of the receptive field). Note that afferent receptive fields and flare responses to noxious stimulation both tend to be roughly elliptical in shape and elongated in the proximal-distal direction, shown here as left/right..

CHAPTER 9 DISCUSSION: AXONAL PROPERTIES OF CUTANEOUS C-FIBRES

The discussion about axonal properties of the different classes of cutaneous C-fibre in the rat saphenous nerve will be presented in two sections. Firstly, I will discuss the phenomenon of activity-dependent slowing of conduction velocity. I will then go on to discuss the heterogeneity of C-fibre axonal spike shapes.

9.1 Activity-dependent slowing of conduction velocity in cutaneous C-fibres

9.1.1 Ubiquity of activity-dependent variations in excitability and conduction velocity

Activity-dependent changes in excitability and conduction velocity of peripheral nerve fibres have been studied in a variety of species (Gilliatt and Willison 1963; Raymond and Lettvin 1978; Raymond 1979; Stohr 1981; Carley and Raymond 1987; Shin and Raymond 1991; Thalhammer *et al.* 1994). Raymond and Lettvin (1978) studied the degree of correlation between threshold and latency changes in frog peripheral nerve by making simultaneous measurements of latency and threshold following activity. Their results showed that latency and threshold were closely associated, and that as the latency increased so did the threshold. The main reason for electing to measure latency changes was that they are simple and quick to measure compared to tracking threshold changes (Stys and Ashby 1990). In addition, a previous study in the rat sciatic nerve had

demonstrated marked differences between nociceptive and cold thermoreceptive fibres, and latency increases had been measured in this study (Thalhammer *et al.* 1994).

9.1.2 Mechanisms underlying activity-dependent slowing of conduction velocity

There are several possible mechanisms for the activity-dependent slowing of conduction velocity studied here. One possible mechanism involves the activity of the electrogenic Na^+/K^+ pump which will hyperpolarize the axon following activity. Raymond and Lettvin (1978) demonstrated in frog peripheral nerves that ouabain (which inhibits the Na^+/K^+ pump) eliminates the period of increased latency that follow tetani. Another possible explanation for the activity-dependent changes in excitability and conduction velocity that occur is the presence of prolonged after-hyperpolarizations involving K^+ currents. A sub-population of neurones in the rabbit nodose ganglion exhibit a slow after-hyperpolarization which lasts for a period of seconds (Higashi *et al.* 1984; Fowler *et al.* 1985). This prolonged after-hyperpolarization is due to a Ca^{2+}-dependent K^+ current, and is capable of controlling neuronal excitability and of affecting the ability of a neurone to fire in response to a period of repetitive stimulation (Weinreich and Wonderlin 1987). It is an attractive possibility that similar, long-lasting after-hyperpolarizations could be present in nociceptive axons and could therefore account for the great degree of conduction velocity slowing shown by nociceptors following a tetanus and also for their inability to fire at high frequencies for a prolonged period. This hypothesis for the mechanisms underlying activity-dependent slowing of conduction velocity in the different functional classes of C-fibres is currently being investigated.

9.1.3 Correlation of activity-dependent slowing of conduction velocity with natural firing pattern

Thalhammer *et al.* (1994) reported that cold fibres fire at higher frequencies than nociceptors during natural stimulation. On the basis of this finding, they suggested that axonal excitability could account for the different and distinct firing patterns that the various classes of C-fibre show in response to their adequate stimulation. Our findings support this suggestion, in that we consistently find that mechanoreceptor activation by light stroking of the skin results in a higher frequency discharge than activation of nociceptors, and mechanoreceptors, like cold units, show relatively little activity-dependent slowing of conduction velocity.

9.1.4 Recordings from afferent units with mechanical or thermal receptive fields

The finding that the vast majority of afferent C-fibres were capable of conducting every impulse throughout 20 seconds of stimulation at 20 Hz was an unexpected one for the following two reasons, (1) although polymodal nociceptors can fire at frequencies exceeding 20 Hz, such high firing frequencies are not maintained throughout periods of sustained mechanical stimulation (Handwerker *et al.* 1987), and, (2) Thalhammer and colleagues (1994) observed failure of impulse conduction in nociceptive axons during periods of stimulation at 10 Hz.

The results show a clear difference between the average conduction velocity slowing shown by nociceptive and non-nociceptive C-fibres following 20 seconds of stimulation at

20 Hz. This supports the work of Thalhammer and colleagues (1994), although we have also included mechanoreceptors in this study and in the saphenous nerve the differences are more marked than in their work using the sciatic. One possible explanation for the more marked differences found in this study than in the work by Thalhammer and colleagues (1994) is that different preparations were used. Thalhammer and colleagues worked on the rat sciatic nerve, which is a mixed nerve innervating muscle, hairy skin and glabrous skin. Cutaneous nociceptive C-fibres in the sciatic nerve would therefore be expected to be more heterogeneous than those in the saphenous nerve which innervates only a restricted area of hairy skin. The cold units and mechanoreceptors show significantly different degrees of conduction velocity slowing after 20 seconds of stimulation at 20 Hz. However, the mechanoreceptors show an unusual time course of conduction velocity slowing in that their conduction velocity slowing plateaus within 10 seconds. This results in there being a greater difference between the conduction velocity slowing of the cold units and the mechanoreceptors after just 6 seconds of stimulation at 20 Hz than after the full 20 seconds. Although the degree of activity-dependent conduction velocity slowing can be used to differentiate between the two types of non-nociceptive afferent C-fibre (i.e., mechanoreceptors and cold thermoreceptors), this approach cannot distinguish the different classes of nociceptive C-fibres present in the rat saphenous nerve.

9.1.5 Recordings from C-fibres without mechanical or thermal fields

In the saphenous nerve, some of the inexcitable C-fibres will be afferent in nature (e.g., the "sleeping" or "silent" nociceptors and the non-cutaneous afferents), whereas others will be efferent fibres (e.g., sympathetic fibres innervating cutaneous and articular blood

vessels) (McMahon and Koltzenburg 1990; Kress *et al.* 1992; Michaelis *et al.* 1994; Karimian *et al.* 1995). The inexcitable units showed a bimodal distribution of conduction velocity slowing following stimulation at 20 Hz for 20 seconds (Figure 6.8a). Since it is known that some of these inexcitable units will be "sleeping" nociceptors and others will be sympathetic efferent units, the behaviour of the inexcitable units was compared to that of identified polymodal nociceptors and spontaneously active sympathetic units (Figure 6.8b). The population of inexcitable C-fibres is consistent with there being 2 broad groups, divided at the point of 20% slowing from resting conduction velocity. Those inexcitable units that slow by greater than 20% show a similar distribution to the units identified as polymodal nociceptors. The inexcitable units that slow by less than 20% show a broadly similar profile to the population of spontaneously active sympathetic efferent fibres. Therefore, it appears that one can differentiate between afferent and efferent inexcitable units by studying their degree of activity-dependent conduction velocity slowing.

The modal conduction velocity slowing of the spontaneously active sympathetic fibres is actually slightly less than that of those inexcitable units slowing in conduction velocity by less than 20%. One possible explanation for this difference could be due to the spontaneous activity of the sympathetic fibres. The continuous background firing of these fibres would, in itself, be sufficient to result in a small degree of conduction velocity slowing, so that what we have called the resting conduction velocity of these units does not reflect their true resting conduction velocity. Therefore, the standard stimulus of 20 seconds at 20 Hz would not produce such a great degree of conduction velocity slowing as it would do if the test had been carried out from their true resting conduction velocity. This also offers an explanation for why the "resting" conduction velocity of the

spontaneous sympathetic units is slower than that of the inexcitable units slowing in conduction velocity by less than 20%.

Additional support for the hypothesis that those inexcitable units that are afferent in nature show greater activity-dependent slowing of conduction velocity than those inexcitable units that are efferent, comes from the more detailed investigation of the mechanically and thermally insensitive units. 23 units for which no fields were found using the standard mechanical and thermal searching techniques were studied using electrical skin stimulation and topical application of 5% or 10% mustard oil. Of the 9 units that slowed in conduction velocity by less than 20%, none showed any sign of afferent properties following the electrical skin stimulation and the topical application of mustard oil. This provides strong support for the theory that inexcitable fibres that slow in conduction velocity by less than 20% following 20 seconds of stimulation at 20 Hz are efferent fibres. Of the 14 insensitive units that slowed in conduction velocity by greater than 20%, afferent properties were observed for 11 of them upon the further investigations using electrical skin stimulation and the topical mustard oil. 7 of these 11 units were affected by the mustard oil in some way (5 were excited and 2 were sensitized). This is similar to the proportion of polymodal nociceptors that responded to the mustard oil (8/12 polymodal nociceptors were excited by the mustard oil). What is the nature of the 3 insensitive units that slowed in conduction velocity by greater than 20% but for which no afferent properties were observed? It is possible that these units could be non-cutaneous afferents innervating, for example, the knee joint or the saphenous vein (Michaelis *et al.* 1994; Karimian *et al.* 1995). Or, since mustard oil did not produce responses in all of the polymodal nociceptors, they could belong to the population of cutaneous nociceptors that are not affected by mustard oil.

9.1.6 How reliably can the different classes of C-fibre be identified solely on the basis of activity-dependent conduction velocity slowing?

The marked differences in the average conduction velocity slowing between the various classes of C-fibre raises the following question. Could the degree of conduction velocity slowing alone be used to differentiate between the different classes of C-fibre? If this was possible, the technique would have good potential as a method allowing identification of the functional class of a C-fibre without having to study the properties of its terminals. The important factor in determining the viability of this technique is the overall distribution of conduction velocity slowing within and between classes (see Figures 6.6 and 6.7).

The optimum cut-off between nociceptive and non-nociceptive fibres is at 20% slowing from resting conduction velocity following 20 seconds of stimulation at 20 Hz. So, if a C-fibre slows in conduction velocity by greater than 20% following 20 seconds of stimulation at 20 Hz, one can be reasonably (about 95%) sure that the fibre will be a nociceptive one. However, it is not possible to differentiate between the different classes of nociceptors found in the rat saphenous nerve, i.e., polymodal nociceptors, heat nociceptors, mechanical nociceptors, sleeping nociceptors. There is a small possibility that the fibre will be a mechanoreceptor (2/17 mechanoreceptors slowed by greater than 20%) or a postganglionic sympathetic unit (1/24 spontaneously active sympathetic fibres slowed by greater than 20%). The fibre will clearly not be a cold thermoreceptor.

If a C-fibre slows in conduction velocity by less than 20% following 20 seconds of stimulation at 20 Hz, one can be reasonably sure that the fibre will be either a cold

thermoreceptor, a mechanoreceptor or a postganglionic sympathetic unit. Two of the 13 mechanical nociceptors found in this study also show less than 20% slowing from resting conduction velocity. However, mechanical nociceptors constitute a minor class of C-fibres and are estimated to account for just 5% of the C-nociceptors that innervate mammalian skin (Lynn 1994). To differentiate between the classes of C-fibre that slow by less than 20% after 20 seconds of stimulation at 20 Hz, one needs to look at the degree of conduction velocity slowing after just 6 seconds. It is likely that a C-fibre that slows by less than 10% after 6 seconds at 20 Hz will be a cold unit, although there is a small chance that it will be a mechanoreceptor. The majority of mechanoreceptors, however, are likely to slow by less than 20% after 20 seconds at 20 Hz and by more than 10% after 6 seconds at 20 Hz.

The difficulty, therefore, comes in distinguishing the postganglionic sympathetic fibres from the cold units and the mechanoreceptors. After 20 seconds of stimulation at 20 Hz, it is not possible to differentiate between the sympathetic efferent fibres and the non-nociceptive afferent fibres, and this differentiation is not any more successful after just 6 seconds of stimulation. However, it is important to remember that in some of the experiments where this kind of diagnostic tool will be useful, the sympathetic fibres will not be present, e.g., in dorsal root ganglion recordings. But if one is to use this technique in experiments where the sympathetic fibres are usually present, such as in peripheral nerve recordings, elimination of the postganglionic sympathetic fibres can be achieved by chronic sympathectomy.

9.2 C-fibre axonal spike shape

The resting conduction velocity and axonal spike shape of 180 C-fibres dissected from the rat saphenous nerve were measured using extracellular recording and under standardized filtering conditions.

9.2.1 Axonal spike shape and resting conduction velocity of cutaneous C-fibres in the rat saphenous nerve

There were three main findings from this study in a rat cutaneous nerve of how axonal spike shape varies with peripheral receptor type:

1) In the whole population, there was a clear trend for the polymodal nociceptors to display wider spikes than the other sub-classes of excitable afferent units. Indeed, this became more evident where spike shapes were measured from filaments containing more than one type of C-fibre. In such filaments the variability in the extent to which the spikes invade a filament is reduced. In all 10 filaments containing at least one polymodal nociceptor and one mechanoreceptor, the polymodal nociceptors consistently displayed the wider spikes.

2) The spontaneously active sympathetic efferent units had wider spikes (both the first peak and the undershoot) than the afferent C-fibres.

3) The spikes of the cold thermoreceptive C-fibres tended to be monophasic.

These 3 findings were independent of resting conduction velocity, i.e. these variations in axonal spike shape between C-fibres with different peripheral receptor types occur within fibres with the same resting conduction velocities.

Within the population of 180 cutaneous C-fibres where spike shape was measured, statistical analysis (ANOVA) on the resting conduction velocities of the different classes of C-fibre revealed that the spontaneously active sympathetic efferent units and the inexcitable units had significantly slower conduction velocities than the other C-fibre classes. The finding that postganglionic sympathetic efferent units conduct more slowly than afferent C-fibres is a consistent finding in our laboratory (see Chapter 6) and has also been reported in the cat sural nerve (Lisney 1988). The likely reason for the inexcitable units having significantly slower conduction velocities than the various classes of afferent C-fibres is that the majority of these units are likely to be sympathetic efferent units, given that 11 of the 17 inexcitable units tested slowed in conduction velocity by less than 20% following 20 seconds of stimulation at 20Hz (see Chapter 6, Chapter 9.1 above, Gee *et al.* 1996a).

One important question that stems from the finding that there is some variation in C-fibre spike shape that is related to receptor type, is whether this phenomenon can be utilised as a tool for identifying C-fibres with particular afferent properties. On the basis of the extracellular recordings reported here, there is too much overlap in the various spike shape measurements and clearly, as the results stand to date, the spike shape alone cannot be used for classification purposes. However, I like to view these results using extracellular recordings as preliminary findings, and think that they give enough of a hint to make further studies into the relationship between C-fibre axonal spike shape and receptor type a viable prospect (see Section 9.2.3 below).

9.2.2 Comparison with previous studies on the spike shapes of identified C-fibre afferent units

There have been several studies questioning the existence of a relationship between action potential shape and sensory receptor type, and these studies have been carried out in a number of species, including leech, snake, cat, rat and mouse (see Section 1.3.1). However, there has only been one study looking at this relationship in dorsal root ganglion cells with unmyelinated (C-fibre) axons, and the finding was that all of the C-fibre afferents studied had broad somatic spikes with inflections on the falling phase, irrespective of modality (Traub and Mendell 1988). This clearly contrasts with the findings from the rat saphenous nerve presented here, where there are some variations in axonal spike shape that are related to C-fibre receptor type. These results from the rat saphenous nerve support the findings of an examination of the axonal spike shape of C-fibres innervating the skin of the pig where a relationship between spike shape and afferent class was demonstrated (Lynn *et al.* 1996a, b). In the pig saphenous nerve, C-fibre nociceptors have wider spikes than mechanoreceptors with the same conduction velocity. Also, heat-sensitive nociceptors tended to have wider spikes than polymodal nociceptors (Lynn *et al.* 1996a, b). The differences between the cat study of Traub and Mendell (1988) and the work on the saphenous nerve of the rat and the pig could be due to species differences (cat vs. rat/pig) and/or differences in the recording methods (intracellular vs. extracellular) and/or the spikes being studied (somal action potential shape vs. axonal action potential shape).

9.2.3 Suggestions for further studies on the relationship between action potential shape and receptor modality in afferent C-fibres

Despite the finding in the cat that somatic action potential shape does not vary with receptor modality in cells with unmyelinated axons, I think that the results from the studies of axonal spike shape of C-fibres in both pig and rat peripheral nerve indicate the need for further studies in this area. Furthermore, this contrast can actually be exploited by studying both somatic and axonal action potentials, and exploring their similarities and differences. I would choose to carry out these further studies in suitable *in vitro* preparations, thereby allowing the use of selective ion channel blockers to examine the ionic currents responsible for producing the different components of the action potentials. For the investigation of axonal spike shapes, the skin-nerve in vitro preparation (Reeh 1986; Kress *et al.* 1992) is not actually required, since one can use the axonal property of activity-dependent slowing of conduction velocity to distinguish nociceptors from non-nociceptors (see Chapter 6 and Section 9.1; Gee *et al.* 1996a). The use of this technique to distinguish nociceptors from non-nociceptors purely on the basis of an axonal property, means that one *in vitro* preparation can be used for studying both somatic and axonal spike shapes. The preparation must have access to both dorsal root ganglion cells and a length of dorsal root sufficient for the positioning of stimulating and recording electrodes, and such preparations in the rat are in use (Harmar and Keen 1982; Waddell *et al.* 1989; Nagy *et al.* 1993).

I would like to pursue the studies of the variation of somatic and axonal spike shapes with peripheral receptor type not only because it could result in a useful technique for the identification of particular classes of afferent fibre without having to study their sensory

properties, but also because I would like to investigate the underlying ionic currents responsible for the differences that occur in spike shape. As outlined in Section 1.3.2 of the introductory chapter, several currents are implicated in the formation of the shape of the action potential. I would like to investigate the presence of these currents in the different functional classes of C-fibre, and to use the blockers available to assess the roles of the different currents in spike shape formation.

CONCLUDING SUMMARY

In this thesis I have reported on experiments carried out to examine the neurogenic vasodilatatory actions and some of the axonal properties of cutaneous C-fibres in the rabbit and the rat.

In both the rabbit and the rat, it seems that a sub-group of polymodal and heat nociceptors are responsible for the efferent action of vasodilatation in the skin. These are the first single C-fibre studies to be carried out on antidromic vasodilatation in these species, and the use of laser Doppler flowmetry and the laser Doppler perfusion imaging system proved to be suitable techniques for measuring skin blood flow in these studies. Taken in conjunction with the studies of plasma extravasation in the rat (Kenins 1981; Bharali and Lisney 1992), the results presented here emphasize the important role of the polymodal nociceptors in neurogenic inflammation. In addition, they also provide an interesting contrast with the single unit study in pig skin which found that the fibres responsible for antidromic vasodilatation in this species were the heat nociceptors, and that the polymodal nociceptors did not have vasodilator actions (Lynn *et al.* 1996a). The laser Doppler perfusion imaging system provided a useful method for studying the flare responses of the skin to noxious heat and mechanical stimuli. The thresholds required to produce flare were similar to the thresholds required to excite the kinds of cutaneous afferent units which have vasodilator actions. Also, a comparison between the size of the flares produced and the size of the afferent and efferent receptive fields of single C-polymodal nociceptors provided strong support for the axon reflex hypothesis for the spread of flare, first proposed by Bruce in 1913 (Bruce 1913).

The phenomenon of activity-dependent slowing of conduction velocity varies greatly between different classes of afferent fibre (Thalhammer *et al.* 1994; Gee *et al.* 1996a). By measuring the extent of conduction velocity slowing in response to a standard tetanus in *all* C-fibre classes, including sympathetic efferent units, it was possible to conclude that this could be used to identify functionally distinct C-fibre types. And so now there is a simple method available to differentiate between nociceptive and non-nociceptive C-fibre afferents. Although this method does not allow for one to distinguish between the different kinds of nociceptive C-fibres (i.e. polymodal nociceptors, heat nociceptors and mechanical nociceptors), it can be used to separate the two kinds of non-nociceptive C-fibres (i.e. mechanoreceptors and cold thermoreceptors). In addition, this technique can also be used to determine if a mechanically and thermally inexcitable C-fibre is afferent or not.

The study of axonal spike shape also revealed that there are variations between the different classes of cutaneous C-fibre in the rat saphenous nerve. However, the differences are not great enough for spike shape to be used as a parameter for identification purposes. But, the finding that there are some differences in C-fibre axonal spike shape that are related to sensory modality shows the need for further investigations into the extent of such differences and of the ionic currents underlying the variations.

In conclusion, although cutaneous afferent C-fibres are usually classed according to their sensory properties, it seems that they have other intrinsic differences, e.g. activity-dependent slowing of conduction velocity and axonal spike shape, and some of these variations can be exploited and used as identification tools. The use of an axonal property to differentiate between the distinct functional classes of cutaneous C-fibres provides a quick method for unit characterization and allows afferent units to be characterized in

experiments where the axons are isolated from their sensory receptors. In addition, it is important to remember that by separating the C-fibres purely on the basis of the sensory stimuli to which they respond, very broad classes are created and further sub-classes do exist, e.g. within the large class of polymodal nociceptors there are some units with vasodilator actions and others which do not possess vasodilator actions.

REFERENCES

1. Andrew D, Matthews B (1996). Properties of single nerve fibres which evoke antidromic vasodilatation in cat dental pulp. *Journal of Physiology* **491**, 27P
2. Andrew D, Matthews B, Coates TW (1996). A method for determining the electrical thresholds of single fibres in dissected nerve filaments. *Journal of Physiology* **493**, 6P
3. Andrews PV, Helme RD, Thomas KL (1989). NK-1 receptor mediation of neurogenic plasma extravasation in rat skin. *Br. J. Pharmacol.* **97**, 1232-1238
4. Asahina A, Hosoi J, Grabbe S, Granstein RD (1995). Modulation of Langerhans cell function by epidermal nerves. *J. Allergy. Clin. Immunol.* **96**(6 Pt 2), 1178-1182
5. Ball DI, Pendry YD, Sheldrick RLG (1993). Characterization of tachykinin receptors mediating vagally-induced bronchoconstriction and plasma-protein extravasation in the guinea-pig. *Neuropeptides.* **24**, 191
6. Baptist G, Marshall JM (1993). Vasodilatation mediated by sensory nerve fibres in the arterioles of skeletal muscle of the anaesthetized rat. *Journal of Physiology* **467**, 35P
7. Barasi S, Lynn B (1986). Effects of sympathetic stimulation on mechanoreceptive and nociceptive afferent units from the rabbit pinna. *Brain Research* **378**, 21-27
8. Barnes PJ (1986). Asthma as an axon reflex. *Lancet.* **1**, 242-245
9. Barnes PJ (1989). Airway neuropeptides: roles in fine tuning and in disease? *News in Physiological Sciences* **4**, 116-120
10. Barnes PJ (1990). Neurogenic inflammation in airways and its modulation. *Arch. Int. Pharmacodyn. Ther.* **303**, 67-82
11. Barnes PJ (1996). Sensory neuropeptides and airway diseases. In *Neurogenic Inflammation*, eds. Geppetti P, Holzer p, 1st edn, pp. 169-185. CRC Press, Boca Raton
12. Bar-Shavit Z, Goldman R, Stabinsky Y, Gottlieb P, Fridkin M, Teichberg VI, Blumberg S (1980). Enhancement of phagocytosis - a newly found activity of substance P residing in its N-terminal tetrapeptide sequence. *Biochem. Biophys. Res. Commun.* **94**, 1445-1451
13. Baumann TK, Simone DA, Shain CN, LaMotte RH (1991). Neurogenic hyperalgesia: the search for the primary cutaneous afferent fibers that contribute to capsaicin-induced pain and hyperalgesia. *Journal of Neurophysiology* **66**, 212-227

14. Bayliss WM (1901). On the origin from the spinal cord of the vaso-dilator fibres of the hind-limb, and on the nature of these fibres. *Journal of Physiology* **26**, 173-209
15. Bayliss WM (1902). Further researches on antidromic nerve-impulses. *Journal of Physiology* **28**, 276-299
16. Beitel RE, Dubner R (1976). Response of unmyelinated (C) polymodal nociceptors to thermal stimuli applied to monkey's face. *Journal of Neurophysiology* **39**, 1160-1175
17. Belmonte C, Gallego R (1983). Membrane properties of cat sensory neurones with chemoreceptor and baroreceptor endings. *J. Physiol. Lond.* **342**, 603-614
18. Belmonte C, Gallar J, Lopez-Briones LG, Pozo MA (1994). Polymodality in nociceptive neurons: Experimental models of chemotransduction. In *Cellular mechanisms of sensory processing*, ed. Urban L, pp. 87-117. Springer-Verlag, Berlin
19. Bessou P, Perl ER (1969). Response of cutaneous sensory units with unmyelinated fibers to noxious stimuli. *Journal of Neurophysiology* **32**, 1025-1043
20. Bharali LA, Lisney SJ (1988). Reinnervation of skin by polymodal nociceptors in rats. *Prog. Brain. Res.* **74**, 247-251
21. Bharali LA, Lisney SJ (1992). The relationship between unmyelinated afferent type and neurogenic plasma extravasation in normal and reinnervated rat skin. *Neuroscience.* **47**, 703-712
22. Bill A, Stjernschantz J, Mandahl A, Brodin E, Nilsson G (1979). Substance P: release on trigeminal nerve stimulation, effects in the eye. *Acta. Physiol. Scand.* **106**, 371-373
23. Birch PJ, Harrison SM, Hayes AG, Rogers H, Tyers MB (1992). The non-peptide NK1 receptor antagonist, (+/-)-CP-96,345, produces antinociceptive and anti-oedema effects in the rat. *Br. J. Pharmacol.* **105**, 508-510
24. Brain SD, Williams TJ (1985). Inflammatory oedema induced by synergism between calcitonin gene-related peptide (CGRP) and mediators of increased vascular permeability. *Br. J. Pharmacol.* **86**, 855-860
25. Brain SD, Williams TJ (1988). Substance P regulates the vasodilator activity of calcitonin gene-related peptide. *Nature.* **335**, 73-75
26. Brain SD, Williams TJ (1989). Interactions between the tachykinins and calcitonin gene-related peptide lead to the modulation of oedema formation and blood flow in rat skin. *Br. J. Pharmacol.* **97**, 77-82

27. Brain SD, Williams TJ, Tippins JR, Morris HR, MacIntyre I (1985). Calcitonin gene-related peptide is a potent vasodilator. *Nature.* **313**, 54-56

28. Brain SD, Tippins JR, Morris HR, MacIntyre I, Williams TJ (1986). Potent vasodilator activity of calcitonin gene-related peptide in human skin. *J. Invest. Dermatol.* **87**, 533-536

29. Brenan A (1986). Collateral reinnervation of skin by C-fibres following nerve injury in the rat. *Brain Research* **385**, 152-155

30. Brenan A, Jones L, Owain NR (1988). The demonstration of the cutaneous distribution of saphenous nerve C-fibres using a plasma extravasation technique in the normal rat and following nerve injury. *J. Anat.* **157**, 57-66

31. Brimijoin S, Lundberg JM, Brodin E, Hökfelt T, Nilsson G (1980). Axonal transport of substance P in the vagus and sciatic nerves of the guinea pig. *Brain Research* **191**, 443-457

32. Brodin E, Gazelius B, Olgart L, Nilsson G (1981). Tissue concentration and release of substance P-like immunoreactivity in the dental pulp. *Acta. Physiol. Scand.* **111**, 141-149

33. Brokaw JJ, White GW (1992). Calcitonin gene-related peptide potentiates substance P-induced plasma extravasation in the rat trachea. *Lung.* **170**, 85-93

34. Bruce AN (1913). Vaso-dilator axon-reflexes. *Quarterly Journal of Experimental Physiology* **6**, 339-354

35. Burgess PR, Perl ER (1967). Myelinated afferent fibres responding specifically to noxious stimulation of the skin. *J. Physiol. Lond.* **190**, 541-562

36. Burgess PR, Petit D, Warren RM (1968). Receptor types in cat hairy skin supplied by myelinated fibers. *Journal of Neurophysiology* **31**, 833-848

37. Cambridge H, Brain SD (1992). Calcitonin gene-related peptide increases blood flow and potentiates plasma protein extravasation in the rat knee joint. *British Journal of Pharmacology* **106**, 746-750

38. Carley LR, Raymond SA (1987). Comparison of the after-effects of impulse conduction on threshold at nodes of Ranvier along single frog sciatic axons. *J. Physiol. Lond.* **386**, 503-527

39. Celander O, Folkow B (1953). The nature and distribution of afferent fibres provided with the axon reflex arrangement. *Acta. Physiol. Scand.* **29**, 259-270

40. Cervero F, Jänig W (1992). Visceral nociceptors: a new world order? [see comments]. *Trends. Neurosci.* **15**, 374-378

41. Chahl LA (1979). The effect of putative peptide neurotransmitters on cutaneous vascular permeability in the rat. *Naunyn. Schmiedebergs. Arch. Pharmacol.* **309**, 159-163

42. Chiba T, Yamaguchi A, Yamatani T, Nakamura A, Morishita T, Inui T, Fukase M, Noda T, Fujita T (1989). Calcitonin gene-related peptide receptor antagonist human CGRP-(8-37). *Am. J. Physiol.* **256**(2 Pt 1), E331-E335

43. Colpaert FC, Donnerer J, Lembeck F (1983). Effects of capsaicin on inflammation and on the substance P content of nervous tissues in rats with adjuvant arthritis. *Life. Sci.* **32**, 1827-1834

44. Cruwys SC, Kidd BL, Mapp PI, Walsh DA, Blake DR (1992). The effects of calcitonin gene-related peptide on formation of intra-articular oedema by inflammatory mediators. *Br. J. Pharmacol.* **107**, 116-119

45. Dalsgaard CJ, Jernbeck J, Stains W, Kjartansson J, Haegerstrand A, Hökfelt T, Brodin E, Cuello AC, Brown JC (1989). Calcitonin gene-related peptide-like immunoreactivity in nerve fibers in the human skin. Relation to fibers containing substance P-, somatostatin- and vasocactive intestinalpolypeptide-like immunoreactivity. *Histochemistry.* **91**, 35-38

46. Darian-Smith I, Johnson KO, LaMotte C, Shigenaga Y, Kenins P, Champness P (1979). Warm fibers innervating palmar and digital skin of the monkey: responses to thermal stimuli. *Journal of Neurophysiology* **42**, 1297-1315

47. Dichter MA, Fischbach GD (1977). The action potential of chick dorsal root ganglion neurones maintained in cell culture. *J. Physiol. Lond.* **267**, 281-298

48. Edvinsson L, Fredholm BB, Hamel E, Jansen I, Verrecchia C (1985). Perivascular peptides relax cerebral arteries concomitant with stimulation of cyclic adenosine monophosphate accumulation or release of an endothelium-derived relaxing factor in the cat. *Neurosci. Lett.* **58**, 213-217

49. Emonds-Alt X, Doutremepuich JD, Heaulme M, Neliat G, Santucci V, Steinberg R, Vilain P, Bichon D, Ducoux JP, Proietto V, et al. (1993). In vitro and in vivo biological activities of SR140333, a novel potent non-peptide tachykinin NK1 receptor antagonist. *European Journal of Pharmacology* **250**, 403-413

50. Escott KJ, Brain SD (1993). Effect of a calcitonin gene-related peptide antagonist (CGRP8-37) on skin vasodilatation and oedema induced by stimulation of the rat saphenous nerve. *British Journal of Pharmacology* **110**, 772-776

51. Ferrell WR, Lam FY (1996). Sensory neuropeptides in arthritis. In *Neurogenic Inflammation*, eds. Geppetti P, Holzer p, 1st edn, pp. 211-227. CRC Press, Boca Raton

52. Ferrell WR, Russell NJ (1986). Extravasation in the knee induced by antidromic stimulation of articular C fibre afferents of the anaesthetized cat. *Journal of Physiology* **379**, 407-416

53. Fewtrell CM, Foreman JC, Jordan CC, Oehme P, Renner H, Stewart JM (1982). The effects of substance P on histamine and 5-hydroxytryptamine release in the rat. *J. Physiol. Lond.* **330**, 393-411

54. Fitzgerald M (1978) The sensitization of cutaneous nociceptors. Ph.D. Dissertation, University College London.

55. Fitzgerald M (1979). The spread of sensitization of polymodal nociceptors in the rabbit from nearby injury and by antidromic nerve stimulation. *Journal of Physiology* **297**, 207-216

56. Fleischer E, Handwerker HO, Joukhadar S (1983). Unmyelinated nociceptive units in two skin areas of the rat. *Brain Research* **267**, 81-92

57. Foreman JC, Jordan CC, Oehme P, Renner H (1983). Structure-activity relationships for some substance P-related peptides that cause wheal and flare reactions in human skin. *J. Physiol. Lond.* **335**, 449-465

58. Fowler JC, Greene R, Weinreich D (1985). Two calcium-sensitive spike after-hyperpolarizations in visceral sensory neurones of the rabbit. *J. Physiol. Lond.* **365**, 59-75

59. Franco-Cereceda A, Lundberg JM, Saria A, Schreibmayer W, Tritthart HA (1988). Calcitonin gene-related peptide: release by capsaicin and prolongation of the action potential in the guinea-pig heart. *Acta. Physiol. Scand.* **132**, 181-190

60. Gallar J, Pozo MA, Tuckett RP, Belmonte C (1993). Response of sensory units with unmyelinated fibres to mechanical, thermal and chemical stimulation of the cat's cornea. *Journal of Physiology* **468**, 609-622

61. Gallego R (1983). The ionic basis of action potentials in petrosal ganglion cells of the cat. *J. Physiol. Lond.* **342**, 591-602

62. Gallego R, Eyzaguirre C (1978). Membrane and action potential characteristics of A and C nodose ganglion cells studied in whole ganglia and in tissue slices. *Journal of Neurophysiology* **41**, 1217-1232

63. Gamse R, Saria A (1985). Potentiation of tachykinin-induced plasma protein extravasation by calcitonin gene-related peptide. *European Journal of Pharmacology* **114**, 61-66

64. Gamse R, Saria A (1987). Antidromic vasodilatation in the rat hindpaw measured by laser Doppler flowmetry: pharmacological modulation. *J. Auton. Nerv. Syst.* **19**, 105-111

65. Gamse R, Holzer P, Lembeck F (1980). Decrease of substance P in primary afferent neurones and impairment of neurogenic plasma extravasation by capsaicin. *British Journal of Pharmacology* **68**, 207-213

66. Gamse R, Posch M, Saria A, Jancsó G (1987). Several mediators appear to interact in neurogenic inflammation. *Acta. Physiol. Hung.* **69**, 343-354

67. Garcia-Caballero T, Gallego R, Roson E, Fraga M, Beiras A (1989). Calcitonin gene-related peptide (CGRP) immunoreactivity in the neuroendocrine Merkel cells and nerve fibres of pig and human skin. *Histochemistry.* **92**, 127-132

68. Garret C, Carruette A, Fardin V, Moussaoui S, Peyronel JF, Blanchard JC, Laduron PM (1991). Pharmacological properties of a potent and selective nonpeptide substance P antagonist. *Proc. Natl. Acad. Sci. U. S. A.* **88**, 10208-10212

69. Gazelius B, Brodin E, Olgart L (1981). Depletion of substance P-like immunoreactivity in the cat dental pulp by antidromic nerve stimulation. *Acta. Physiol. Scand.* **111**, 319-327

70. Gee MD, Lynn B, Cotsell B (1996a). Activity-dependent slowing of conduction velocity provides a method for identifying different functional classes of C-fibre in the rat saphenous nerve. *Neuroscience.* **73(3)**, 667-675

71. Gee MD, Lynn B, Cotsell B (1996b). Identification of the C-fibres responsible for antidromic vasodilatation in the skin of the anaesthetized rat. *Journal of Physiology* **494**, 46P

72. Georgopoulos AP (1976). Functional properties of primary afferent units probably related to pain mechanisms in primate glabrous skin. *Journal of Neurophysiology* **39**, 71-83

73. Geppetti P, Holzer P (eds) (1996) Neurogenic Inflammation, 1st edn. CRC Press, Boca Raton

74. Geppetti P, Tramontana M, Patacchini R, Del-Bianco E, Santicioli P, Maggi CA (1990a). Neurochemical evidence for the activation of the 'efferent' function of capsaicin-sensitive nerves by lowering of the pH in the guinea-pig urinary bladder. *Neurosci. Lett.* **114**, 101-106

75. Geppetti P, Tramontana M, Santicioli P, Del-Bianco E, Giuliani S, Maggi CA (1990b). Bradykinin-induced release of calcitonin gene-related peptide from capsaicin-sensitive nerves in guinea-pig atria: mechanism of action and calcium requirements. *Neuroscience.* **38**, 687-692

76. Geppetti P, Tramontana M, Evangelista S, Renzi D, Maggi CA, Fusco BM, Del-Bianco E (1991). Differential effect on neuropeptide release of different concentrations of hydrogen ions on afferent and intrinsic neurons of the rat stomach. *Gastroenterology.* **101**, 1505-1511

77. Gilliatt RW, Willison RG (1963). The refractory and supernormal periods of the human median nerve. *J. Neurol. Neurosurg. Psychiatry.* **26**, 136-143

78. Görke K, Pierau FK (1980). Spike potentials and membrane properties of dorsal root ganglion cells in pigeons. *Pflugers. Arch.* **386**, 21-28

79. Green PG, Basbaum AI, Levine JD (1992). Sensory neuropeptide interactions in the production of plasma extravasation in the rat. *Neuroscience.* **50**, 745-749

80. Gulbenkian S, Merighi A, Wharton J, Varndell IM, Polak JM (1986). Ultrastructural evidence for the coexistence of calcitonin gene-related peptide and substance P in secretory vesicles of peripheral nerves in the guinea pig. *J. Neurocytol.* **15**, 535-542

81. Häbler HJ, Jänig W, Koltzenburg M (1988). A novel type of unmyelinated chemosensitive nociceptor in the acutely inflamed urinary bladder. *Agents. Actions.* **25**, 219-221

82. Häbler HJ, Jänig W, Koltzenburg M (1990). Activation of unmyelinated afferent fibres by mechanical stimuli and inflammation of the urinary bladder in the cat. *Journal of Physiology* **425**, 545-562

83. Hagermark O, Hökfelt T, Pernow B (1978). Flare and itch induced by substance P in human skin. *J. Invest. Dermatol.* **71**, 233-235

84. Hall JM, Brain SD (1992). Quantification of the vasodilator effects of CGRP, Amylin and [Cys(ACM)2-7]-hCGRPalpha on the microvasculature of the hamster chhek pouch in vivo. *Neuropeptides.* **24**, 207

85. Hall JM, Butt S, Brain SD (1994). SR140333 inhibits NK1-receptor mediated vasodilatation in hamster cheek pouch microvasculature. *Neuropeptides.* **26 (Suppl. 1)**, 39

86. Han SP, Naes L, Westfall TC (1990). Inhibition of periarterial nerve stimulation-induced vasodilation of the mesenteric arterial bed by CGRP (8-37) and CGRP receptor desensitization. *Biochem. Biophys. Res. Commun.* **168**, 786-791

87. Handwerker HO, Anton F, Reeh PW (1987; 65(3)). Discharge patterns of afferent cutaneous nerve fibers from the rat's tail during prolonged noxious mechanical stimulation. *Exp. Brain. Res.*, 493-504

88. Handwerker HO, Kilo S, Reeh PW (1991). Unresponsive afferent nerve fibres in the sural nerve of the rat. *J. Physiol. Lond.* **435**, 229-242

89. Harmar A, Keen P (1982). Synthesis, and central and peripheral axonal transport of substance P in a dorsal root ganglion-nerve preparation in vitro. *Brain Research* **231**, 379-385

90. Harper AA, Lawson SN (1985). Electrical properties of rat dorsal root ganglion neurones with different peripheral nerve conduction velocities. *Journal of Physiology* **359**, 47-63

91. Hartung HP, Toyka KV (1983). Activation of macrophages by substance P: induction of oxidative burst and thromboxane release. *European Journal of Pharmacology* **89**, 301-305

92. Helme RD, Koschorke GM, Zimmermann M (1986). Immunoreactive substance P release from skin nerves in the rat by noxious thermal stimulation. *Neurosci. Lett.* **63**, 295-299

93. Hensel H, Iggo A, Witt I (1960). A quantitive study of sensitive thermoreceptors with C afferent fibres. *Journal of Physiology* **153**, 113-126

94. Higashi H, Morita K, North RA (1984). Calcium-dependent after-potentials in visceral afferent neurones of the rabbit. *J. Physiol. Lond.* **355**, 479-492

95. Hinsey JC, Gasser HS (1930). The component of the dorsal root mediating vasodilatation and the Sherrington contracture. *Am. J. Physiol.* **92**, 679-689

96. Hökfelt T, Kellerth JO, Nilsson G, Pernow B (1975). Substance p: localization in the central nervous system and in some primary sensory neurons. *Science.* **190**, 889-890

97. Hoheisel U, Mense S, Scherotzke R (1994). Calcitonin gene-related peptide-immunoreactivity in functionally identified primary afferent neurones in the rat. *Anat. Embryol. Berl.* **189**, 41-49

98. Holloway GA (1983). Laser-Doppler measurement of cutaneous blood flow. In *Non-invasive Physiological Measurements*, ed. Rolfe P, vol 2, pp. 179-212. Academic Press,

99. Holzer P (1988). Local effector functions of capsaicin-sensitive sensory nerve endings: involvement of tachykinins, calcitonin gene-related peptide and other neuropeptides. *Neuroscience.* **24**, 739-768

100. Holzer P (1993). Capsaicin-sensitive nerves in the control of vascular effector mechanisms. In *Pain*, ed. Wood JN, pp. 191-218. Academic Press, London

101. Holzer P (1996). Sensory neurons in the stomach. In *Neurogenic Inflammation*, eds. Geppetti P, Holzer p, 1st edn, pp. 141-152. CRC Press, Boca Raton

102. Holzer P, Barthó L (1996). Sensory neurons in the intestine. In *Neurogenic Inflammation*, eds. Geppetti P, Holzer p, 1st edn, pp. 153-167. CRC Press, Boca Raton

103. Hosoi J, Murphy GF, Egan CL, Lerner EA, Grabbe S, Asahina A, Granstein RD (1993). Regulation of Langerhans cell function by nerves containing calcitonin gene-related peptide. *Nature.* **363**, 159-163

104. Hua XY, Saria A, Gamse R, Theodorsson-Norheim E, Brodin E, Lundberg JM (1986). Capsaicin induced release of multiple tachykinins (substance P, neurokinin A and eledoisin-like material) from guinea-pig spinal cord and ureter. *Neuroscience.* **19**, 313-319

105. Hughes SR, Brain SD (1994). Nitric oxide-dependent release of vasodilator quantities of calcitonin gene-related peptide from capsaicin-sensitive nerves in rabbit skin. *British Journal of Pharmacology* **111**, 425-430

106. Hughes SR, Buckley TL, Brain SD (1992). Olvanil: more potent than capsaicin at stimulating the efferent function of sensory nerves. *European Journal of Pharmacology* **219**, 481-484

107. Iggo A (1958). The electrophysiological identification of single nerve fibres, with particular reference to the slowest-conducting vagal afferent fibres in the cat. *Journal of Physiology* **142**, 110-126

108.Iggo A, Ogawa H (1971). Primate cutaneous thermal nociceptors. *J. Physiol. Lond.* **216**, 77P-78P

109.Iriuchijima J, Zotterman Y (1960). The specificity of afferent cutaneous C fibres in mammals. *Acta. Physiol. Scand.* **49**, 267-278

110.Jänig W, Lisney SJ (1989). Small diameter myelinated afferents produce vasodilatation but not plasma extravasation in rat skin. *Journal of Physiology* **415**, 477-486

111.Janscó N, Janscó-Gabor A, Szolcsányi J (1967). Direct evidence for neurogenic inflammation and its prevention by denervation and by pretreatment with capsaicin. *Br. J. Pharmacol.* **31**, 138-151

112.Janscó N, Janscó-Gabor A, Szolcsányi J (1968). The role of nerve endings in neurogenic inflammation induced in human skin and in the eye and paw of the rat. *Br. J. Pharmacol.* **33**, 32-41

113.Karimian M, Ferrell WR (1994). Plasma protein extravasation into the rat knee joint induced by calcitonin gene-related peptide. *Neurosci. Lett.* **166**, 39-42

114.Karimian SM, McDougall JJ, Ferrell WR (1995). Neuropeptide and autonomic control of the vasculature of the rat knee joint revealed by laser doppler perfusion imaging. *Experimental Physiology* **80**, 341-348

115.Kenins P (1981). Identification of the unmyelinated sensory nerves which evoke plasma extravasation in response to antidromic stimulation. *Neurosci. Lett.* **25**, 137-141

116.Kidd BL, Mapp PI, Blake DR, Gibson SJ, Polak JM (1990). Neurogenic influences in arthritis. *Ann. Rheum. Dis.* **49**, 649-652

117.Kinnman E, Wiesenfeld-Hallin Z (1993). Time course and characteristics of the capacity of sensory nerves to reinnervate skin territories outside their normal innervation zones. *Somatosens. Mot. Res.* **10**, 445-454

118.Koerber HR, Mendell LM (1992). Functional Heterogeneity of Dorsal Root Ganglion Cells. In *Sensory Neurones: Diversity, Development and Plasticity*, ed. Scott SA, pp. 77-96. Oxford University Press, Oxford

119.Koerber HR, Druzinsky RE, Mendell LM (1988). Properties of somata of spinal dorsal root ganglion cells differ according to peripheral receptor innervated. *Journal of Neurophysiology* **60**, 1584-1596

120.Kolston J, Lisney SJ (1993). A study of vasodilator responses evoked by antidromic stimulation of A delta afferent nerve fibers supplying normal and reinnervated rat skin. *Microvasc. Res.* **46**, 143-157

121.Koltzenburg M, McMahon SB (1986). Plasma extravasation in the rat urinary bladder following mechanical, electrical and chemical stimuli: evidence for a new population of chemosensitive primary sensory afferents. *Neurosci. Lett.* **72**, 352-356

122.Konietzny F, Hensel H (1975). Letters and notes: Warm fiber activity in human skin nerves. *Pflugers. Arch.* **359**, 265-267

123.Kress M, Koltzenburg M, Reeh PW, Handwerker HO (1992). Responsiveness and functional attributes of electrically localized terminals of cutaneous C-fibers in vivo and in vitro. *Journal of Neurophysiology* **68**, 581-595

124.Kumazawa T, Perl ER (1977). Primate cutaneous sensory units with unmyelinated (C) afferent fibers. *Journal of Neurophysiology* **40**, 1325-1338

125.Lam FY, Ferrell WR (1993). Acute inflammation in the rat knee joint attenuates sympathetic vasoconstriction but enhances neuropeptide-mediated vasodilatation assessed by laser Doppler perfusion imaging. *Neuroscience.* **52**, 443-449

126.LaMotte RH, Campbell JN (1978). Comparison of responses of warm and nociceptive C-fiber afferents in monkey with human judgments of thermal pain. *Journal of Neurophysiology* **41**, 509-528

127.Lawson SN (1992). Morphological and biochemical cell types of sensory neurons. , 27-59

128.Lawson SN (1995). Neuropeptides in morphologically and functionally identified primary afferent neurons in dorsal root ganglia: substance P, CGRP and somatostatin. *Prog. Brain. Res.* **104**, 161-173

129.Lawson S (1996). Neurochemistry of cutaneous nociceptors. In *Neurobiology of Nociceptors*, eds. Belmonte C, Cervero F, pp. 71-91. Oxford University Press, Oxford

130.Lawson SN, Waddell PJ (1991). Soma neurofilament immunoreactivity is related to cell size and fibre conduction velocity in rat primary sensory neurons. *J. Physiol. Lond.* **435**, 41-63

131.Lawson SN, Waddell PJ, McCarthy PW (1988). A comparison of the electrophysiological and immunocytochemical properties of rat dorsal root ganglion neurones with A and C fibers. In *Fine Afferent Nerve Fibers and Pain*, eds. Schmidt RF, Schaible HG, Vahle-Hinz C, pp. 195-203. VCH Verlagsgesellschaft, Berlin

132.Lawson SN, Crepps B, Bao JJ, Brighton BW, Perl ER (1993). Differential correlation of substance P-like immunoreactivity (SP-LI) with the type of C-fiber sensory receptor. *Society for Neuroscience Abstracts* **19**, 136.6

133.Lawson SN, Crepps BA, Bao J, Brighton BW, Perl ER (1994). Substance P-like immunoreactivity (SP-LI) in dorsal root ganglia (DRGs) of anaesthetized guinea-pigs is related to sensory receptor type in A- and C-fibre neurones. *Journal of Physiology*, 476p

134.Lawson SN, Crepps B, Buck H, Perl ER (1996). Correlation of CGRP-like immunoreactivity (CGRP-LI) with sensory receptor properties in dorsal root ganglion (DRG) neurones in guinea pigs. *Journal of Physiology* **493**, 45P

135.Leah JD, Cameron AA, Snow PJ (1985). Neuropeptides in physiologically identified mammalian sensory neurones. *Neurosci. Lett.* **56**, 257-263

136.Lee TJ, Saito A, Berezin I (1984). Vasoactive intestinal polypeptide-like substance: the potential transmitter for cerebral vasodilation. *Science.* **224**, 898-901

137.Lee Y, Kawai Y, Shiosaka S, Takami K, Kiyama H, Hillyard CJ, Girgis S, MacIntyre I, Emson PC, Tohyama M (1985a). Coexistence of calcitonin gene-related peptide and substance P-like peptide in single cells of the trigeminal ganglion of the rat: immunohistochemical analysis. *Brain Research* **330**, 194-196

138.Lee Y, Takami K, Kawai Y, Girgis S, Hillyard CJ, MacIntyre I, Emson PC, Tohyama M (1985b). Distribution of calcitonin gene-related peptide in the rat peripheral nervous system with reference to its coexistence with substance P. *Neuroscience.* **15**, 1227-1237

139.Lembeck F (1983). Sir Thomas Lewis's nocifensor system, histamine and substance P-containing primary afferent nerves. *Trends in Neuroscience* **6**, 106-108

140.Lembeck F, Donnerer J, Tsuchiya M, Nagahisa A (1992). The non-peptide tachykinin antagonist, CP-96,345, is a potent inhibitor of neurogenic inflammation. *Br. J. Pharmacol.* **105**, 527-530

141.Levine JD, Moskowitz MA, Basbaum AI (1985). The contribution of neurogenic inflammation in experimental arthritis. *J. Immunol.* **135**(2 Suppl), 843s-847s

142.Levine JD, Coderre TJ, Basbaum AI (1988). The peripheral nervous system and the inflammatory process. *Proc. 5th. Cong. Pain.*, 33-43

143.Lewis T (1927) The blood vessels of the human skin and their responses. Shaw & Sons, London

144.Lisney SJW (1987). Functional aspects of the regeneration of unmyelinated axons in the rat saphenous nerve. *Journal of the Neurological Sciences* **80**, 289-298

145.Lisney SJ (1988). The proportions of sympathetic postganglionic and unmyelinated afferent axons in normal and regenerated cat sural nerves. *J. Auton. Nerv. Syst.* **22**, 151-157

146.Lisney SJW, Bharali LAM (1989). The axon reflex: an outdated idea or a valid hypothesis. *News. in. Physiol. Sci.* **4**, 45-48

147.Lou YP, Franco-Cereceda A, Lundberg JM (1992). Different ion channel mechanisms between low concentrations of capsaicin and high concentrations of capsaicin and nicotine regarding peptide release from pulmonary afferents. *Acta. Physiol. Scand.* **146**, 119-127

148.Lundberg JM (1993). Capsaicin-sensitive nerves in the airways - implications for protective reflexes and disease. In *Neuroscience perspectives: capsaicin in the study of pain*, ed. Wood JN, pp. 219-227. Academic press, London

149.Lundberg JM, Brodin E, Hua X, Saria A (1984). Vascular permeability changes and smooth muscle contraction in relation to capsaicin-sensitive substance P afferents in the guinea-pig. *Acta. Physiol. Scand.* **120**, 217-227

150.Lundberg JM, Franco-Cereceda A, Alving K, Delay-Goyet P, Lou YP (1992). Release of calcitonin gene-related peptide from sensory neurons. *Ann. N. Y. Acad. Sci.* **657**, 187-193

151.Lynn B (1979). The heat sensitization of polymodal nociceptors in the rabbit and its independence of the local blood flow. *J. Physiol. Lond.* **287**, 493-507

152.Lynn B (1988). Neurogenic inflammation. *Skin. Pharmacol.* **1**, 217-224

153.Lynn B (1990). Capsaicin: actions on nociceptive C-fibres and therapeutic potential. *Pain.* **41**, 61-69

154.Lynn B (1994). The fibre composition of cutaneous nerves and the classification and response properties of cutaneous afferents, with particular reference to nociception. *Pain Reviews* **1**, 172-183

155.Lynn B (1995). The design of nociceptive sensory systems at the body surface for detecting hazardous environmental conditions. *Environmental Medicine* **39**, 93-105

156.Lynn B (1996a). Efferent functions of nociceptors. In *Neurobiology of Nociceptors*, eds. Carlos Belmonte, Fernando Cervero, 1st edn, pp. 418-438. Oxford University Press, Oxford

157.Lynn B (1996b). Principles of classification and nomenclature relevant to studies of nociceptive neurones. In *Neurobiology of Nociceptors*, eds. Belmonte C, Cervero F, 1st edn, pp. 1-2. Oxford University Press, Oxford

158.Lynn B, Baranowski R (1987). A comparison of the relative numbers and properties of cutaneous nociceptive afferents in different mammalian species. In *Fine afferent nerve fibres and pain*, eds. Schmidt RF, Schaible HG, Vahle-Hing C, pp. 85-94. VCH Verlagsgesellschaft, Weinheim

159.Lynn B, Carpenter SE (1982). Primary afferent units from the hairy skin of the rat hind limb. *Brain Research* **238**, 29-43

160.Lynn B, Cotsell B (1991). The delay in onset of vasodilator flare in human skin at increasing distances from a localized noxious stimulus. *Microvasc. Res.* **41**, 197-202

161.Lynn B, Cotsell B (1992a). Blood flow increases in the skin of the anaesthetized rat that follow antidromic sensory nerve stimulation and strong mechanical stimulation. *Neurosci. Lett.* **137**, 249-252

162.Lynn B, Cotsell B (1992b). The use of a Laser-doppler perfusion imager to study flare in the skin of anaesthetized rats and rabbits. *Journal of Physiology*, 29p

163.Lynn B, Cotsell B (1993). Spread of flare around injuries compared with the size of nociceptor receptive fields in the same skin area in anaesthetized rats and rabbits. *XXXII Congress of the International Union of Physiological Sciences* **Glasgow Meeting**, 256.6

164.Lynn B, Shakhanbeh J (1988). Neurogenic inflammation in the skin of the rabbit. *Agents. Actions.* **25**, 228-230

165.Lynn B, Cotsell B, Faulstroh K, Pierau F-K (1992). Flare and C-fibre receptive fields in three mammalian species. *14th European Workshop on Inflammation* **London**, p6

166.Lynn B, Faulstroh K, Pierau FK (1995). The classification and properties of nociceptive afferent units from the skin of the anaesthetized pig. *Eur. J. Neurosci.* **7**, 431-437

167.Lynn B, Schütterle S, Pierau F-K (1996a). The vasodilator component of neurogenic inflammation is caused by a special class of heat-sensitive nociceptors in the skin of the pig. *Journal of Physiology* **492(2)**, 587-593

168.Lynn B, Schütterle S, Pierau F-K, Faulstroh K, Basile S (1996b). The duration of axonal action potentials varies with the afferent type for C-fibres innervating the skin of the anaesthetized pig. *Japanese Journal of Physiology* **45 Supp.2**, S243

169.Maggi CA (1991a). Capsaicin and primary afferent neurons: from basic science to human therapy? *J. Auton. Nerv. Syst.* **33**, 1-14

170.Maggi CA (1991b). The pharmacology of the efferent function of sensory nerves. *J. Auton. Pharmacol.* **11**, 173-208

171.Maggi CA (1993). The pharmacological modulation of neurotransmitter release. In *Capsaicin in the study of pain*, ed. Wood JN, pp. 161-189. Academic Press, London

172.Martling CR, Saria A, Fischer JA, Hökfelt T, Lundberg JM (1988). Calcitonin gene-related peptide and the lung: neuronal coexistence with substance P, release by capsaicin and vasodilatory effect. *Regul. Pept.* **20**, 125-139

173.McMahon SB, Koltzenburg M (1990). Novel classes of nociceptors: beyond Sherrington [news] [see comments]. *Trends. Neurosci.* **13**, 199-201

174.Meech RW (1978). Calcium-dependent potassium activation in nervous tissues. *Annu. Rev. Biophys. Bioeng.* **7**, 1-18

175.Meyer RA, Davis KD, Cohen RH, Treede RD, Campbell JN (1991). Mechanically insensitive afferents (MIAs) in cutaneous nerves of monkey. *Brain Research* **561**, 252-261

176.Michaelis M, Göder R, Häbler HJ, Jänig W (1994). Properties of afferent nerve fibres supplying the saphenous vein in the cat. *J. Physiol. Lond.* **474**, 233-243

177.Morita K, Katayama Y (1989). Bullfrog dorsal root ganglion cells having tetrodotoxin-resistant spikes are endowed with nicotinic receptors. *Journal of Neurophysiology* **62**, 657-664

178.Moskowitz MA, Buzzi MG (1991). Neuroeffector functions of sensory fibres: implications for headache mechanisms and drug actions. *J. Neurol.* **238 Suppl 1**, S18-S22

179.Moskowitz MA, Brody M, Liu-Chen LY (1983). In vitro release of immunoreactive substance P from putative afferent nerve endings in bovine pia arachnoid. *Neuroscience.* **9**, 809-814

180.Moskowitz MA, Lee WS, Cutrer FM (1996). Sensory neuropeptides in migraine. In *Neurogenic Inflammation*, eds. Geppetti P, Holzer p, 1st edn, pp. 187-199. CRC Press, Boca Raton

181.Nagahisa A, Kanai Y, Suga O, Taniguchi K, Lowe JA, Hess HJ (1992). Anti-inflammatory and analgesic activity of a non-peptide substance P receptor antagonist. *European Journal of Pharmacology* **217**, 191-195

182.Nagy I, Urban L, Woolf CJ (1993). Morphological and membrane properties of young rat lumbar and thoracic dorsal root ganglion cells with unmyelinated axons. *Brain Research* **609**, 193-200

183.Nicholls JG, Baylor DA (1968). Specific modalities and receptive fields of sensory neurons in CNS of the leech. *Journal of Neurophysiology* **31**, 740-756

184.Nong YH, Titus RG, Ribeiro JM, Remold HG (1989). Peptides encoded by the calcitonin gene inhibit macrophage function. *J. Immunol.* **143**, 45-49

185.Nordin M (1990). Low-threshold mechanoreceptive and nociceptive units with unmyelinated (C) fibres in the human supraorbital nerve [published erratum appears in J Physiol (Lond) 1991 Dec;444:777]. *J. Physiol. Lond.* **426**, 229-240

186.O'Brien C, Woolf CJ, Fitzgerald M, Lindsay RM, Molander C (1989). Differences in the chemical expression of rat primary afferent neurons which innervate skin, muscle or joint. *Neuroscience.* **32**, 493-502

187.Ohlen A, Lindbom L, Staines W, Hökfelt T, Cuello AC, Fischer JA, Hedqvist P (1987). Substance P and calcitonin gene-related peptide: immunohistochemical localisation and microvascular effects in rabbit skeletal muscle. *Naunyn. Schmiedebergs. Arch. Pharmacol.* **336**, 87-93

188.Olgart L, Gazelius B, Brodin E, Nilsson G (1977). Release of substance P-like immunoreactivity from the dental pulp. *Acta. Physiol. Scand.* **101**, 510-512

189.Payan DG, Brewster DR, Goetzl EJ (1983). Specific stimulation of human T lymphocytes by substance P. *J. Immunol.* **131**, 1613-1615

190.Payan DG, Levine JD, Goetzl EJ (1984). Modulation of immunity and hypersensitivity by sensory neuropeptides. *J. Immunol.* **132**, 1601-1604

191.Perl ER (1968). Myelinated afferent fibres innervating the primate skin and their response to noxious stimuli. *J. Physiol. Lond.* **197**, 593-615

192.Pini A, Lynn B (1991). C-fibre function during the 6 weeks following brief application of capsaicin to a cutaneous nerve in the rat. *European Journal of Neuroscience* **3**, 274-284

193.Pini A, Baranowski R, Lynn B (1990). Long-term reduction in the number of C-fibre nociceptors following capsaicin treatment of a cutaneous nerve in adult rats. *European Journal of Neuroscience* **2**, 89-97

194.Ransom BR, Holz RW (1977). Ionic determinants of excitability in cultured mouse dorsal root ganglion and spinal cord cells. *Brain Research* **136**, 445-453

195.Raymond SA (1979). Effects of nerve impulses on threshold of frog sciatic nerve fibres. *J. Physiol. Lond.* **290**, 273-303

196.Raymond SA, Lettvin JY (1978). Aftereffects of activity in peripheral axons as a clus to nervous coding. In *Physiology and pathobiology of axons*, ed. Waxman SG, pp. 203-225. Raven Press, New York

197.Reeh PW (1986). Sensory receptors in mammalian skin in an in vitro preparation. *Neurosci. Lett.* **66**, 141-146

198.Ritter AM, Mendell LM (1990). The somal spike of physiologically identified high threshold mechanoreceptors is insensitive to TTX. *Pain.* **Suppl. 5**, S110

199.Ritter AM, Mendell LM (1992). Somal membrane properties of physiologically identified sensory neurons in the rat: effects of nerve growth factor. *Journal of Neurophysiology* **68**, 2033-2041

200.Rose RD, Koerber HR, Sedivec MJ, Mendell LM (1986). Somal action potential duration differs in identified primary afferents. *Neurosci. Lett.* **63**, 259-264

201.Rosenfeld MG, Mermod JJ, Amara SG, Swanson LW, Sawchenko PE, Rivier J, Vale WW, Evans RM (1983). Production of a novel neuropeptide encoded by the calcitonin gene via tissue-specific RNA processing. *Nature.* **304**, 129-135

202.Ruff MR, Wahl SM, Pert CB (1985). Substance P receptor-mediated chemotaxis of human monocytes. *Peptides.* **6 Suppl 2**, 107-111

203.Sah P (1996). Ca(2+)-activated K+ currents in neurones: types, physiological roles and modulation. *Trends. Neurosci.* **19**, 150-154

204.Saria A (1988). Neuroimmune interactions in the airways: implications for asthma, allergy, and other inflammatory airway diseases. *Brain. Behav. Immun.* **2**, 318-321

205.Saria A, Lundberg JM, Skofitsch G, Lembeck F (1983). Vascular protein linkage in various tissue induced by substance P, capsaicin, bradykinin, serotonin, histamine and by antigen challenge. *Naunyn. Schmiedebergs. Arch. Pharmacol.* **324**, 212-218

206.Saria A, Martling CR, Theodorsson-Norheim E, Gamse R, Hua XY, Lundberg JM (1987). Coexisting peptides in capsaicin-sensitive sensory neurons: release and actions in the respiratory tract of the guinea-pig. *Acta. Physiol. Hung.* **69**, 421-424

207.Saria A, Martling CR, Yan Z, Theodorsson-Norheim E, Gamse R, Lundberg JM (1988). Release of multiple tachykinins from capsaicin-sensitive sensory nerves in the lung by bradykinin, histamine, dimethylphenyl piperazinium, and vagal nerve stimulation. *Am. Rev. Respir. Dis.* **137**, 1330-1335

208.Schaible HG, Schmidt RF (1983). Responses of fine medial articular nerve afferents to passive movements of knee joints. *Journal of Neurophysiology* **49**, 1118-1126

209.Schaible HG, Schmidt RF (1985). Effects of an experimental arthritis on the sensory properties of fine articular afferent units. *Journal of Neurophysiology* **54**, 1109-1122

210.Schmelz M, Schmidt R, Ringkamp M, Handwerker HO, Torebjörk HE (1994). Sensitization of insensitive branches of C nociceptors in human skin. *J. Physiol. Lond.* **480**(15 Oct Pt 2), 389-394

211.Schmidt R, Schmelz M, Forster C, Ringkamp M, Torebjörk E, Handwerker H (1995). Novel classes of responsive and unresponsive C nociceptors in human skin. *J. Neurosci.* **15**(1 Pt 1), 333-341

212.Scroggs RS, Fox AP (1991). Distribution of dihydropyridine and omega-conotoxin-sensitive calcium currents in acutely isolated rat and frog sensory neuron somata: diameter-dependent L channel expression in frog. *J. Neurosci.* **11**, 1334-1346

213.Scroggs RS, Fox AP (1992a). Calcium current variation between acutely isolated adult rat dorsal root ganglion neurons of different size. *J. Physiol. Lond.* **445**, 639-658

214.Scroggs RS, Fox AP (1992b). Multiple Ca2+ currents elicited by action potential waveforms in acutely isolated adult rat dorsal root ganglion neurons. *J. Neurosci.* **12**, 1789-1801

215.Shakhanbeh JM (1989) Physiological studies on rabbit C-fibres including their role in neurogenic inflammation in the skin. Ph.D. Dissertation, Univeristy of London.

216.Shea VK, Perl ER (1985). Sensory receptors with unmyelinated (C) fibers innervating the skin of the rabbit's ear. *Journal of Neurophysiology* **54**, 491-501

217.Shin HC, Raymond SA (1991). Excitability changes in C fibers of rat sciatic nerve following impulse activity. *Neurosci. Lett.* **129**, 242-246

218.Shin HC, Lee YL, Kwon HY, Park HJ, Raymond SA (1994). Activity-dependent variations in conduction velocity of C fibers of rat sciatic nerve. *Neurosci. Res.* **19**, 427-431

219.Stöhr M (1981). Activity-dependent variations in threshold and conduction velocity of human sensory fibers. *Journal of the Neurological Sciences* **49**, 47-54

220.Stys PK, Ashby P (1990). An automated technique for measuring the recovery cycle of human nerves. *Muscle Nerve*, 750-758

221.Sugiura Y, Lee CL, Perl ER (1986). Central projections of identified, unmyelinated (C) afferent fibers innervating mammalian skin. *Science.* **234**, 358-361

222.Sugiura Y, Hosoya Y, Ito R, Kohno K (1988). Ultrastructural features of functionally identified primary afferent neurons with C (unmyelinated) fibers of the guinea pig: classification of dorsal root ganglion cell type with reference to sensory modality. *J. Comp. Neurol.* **276**, 265-278

223.Szolcsányi J (1988). Antidromic vasodilatation and neurogenic inflammation. *Agents. Actions.* **23**, 4-11

224.Terashima SI, Liang YF (1994). Touch and vibrotactile neurons in a crotaline snake's trigeminal ganglia. *Somatosens. Mot. Res.* **11**, 169-181

225.Thalhammer JG, Raymond SA, Popitz-Bergez FA, Strichartz GR (1994). Modality-dependent modulation of conduction by impulse activity in functionally characterized single cutaneous afferents in the rat. *Somatosens. Mot. Res.* **11**, 243-257

226.Tokimasa T, Shiraishi M, Akasu T (1990). Morphological and electrophysiological properties of C-cells in bullfrog dorsal root ganglia. *Neurosci. Lett.* **116**, 304-308

227.Torebjörk HE (1974). Afferent C units responding to mechanical, thermal and chemical stimuli in human non-glabrous skin. *Acta. Physiol. Scand.* **92**, 374-390

228.Tornebrandt K, Nobin A, Owman C (1987). calcitonin gene-related peptide (CGRP): perivascular distribution and vasodilatory effects. *Regulatory Peptides* **15**, 1-23

229.Traub RJ, Mendell LM (1988). The spinal projection of individual identified A-delta- and C-fibers. *Journal of Neurophysiology* **59**, 41-55

230.Vallbo A, Olausson H, Wessberg J, Norrsell U (1993). A system of unmyelinated afferents for innocuous mechanoreception in the human skin. *Brain Research* **628**, 301-304

231.Van HJ, Gybels J (1981). C nociceptor activity in human nerve during painful and non painful skin stimulation. *J. Neurol. Neurosurg. P.* **44**, 600-607

232.Vongsavan N, Matthews B (1992). The vascularity of dental pulp in cats. *J. Dent. Res.* **71**, 1913-1915

233.Vongsavan N, Matthews B (1993). Some aspects of the use of laser Doppler flow meters for recording tissue blood flow. *Experimental Physiology* **78**, 1-14

234.Waddell PJ, Lawson SN, McCarthy PW (1989). Conduction velocity changes along the processes of rat primary sensory neurons. *Neuroscience.* **30**, 577-584

235.Wahlestedt C, Beding B, Ekman R, Oksala O, Stjernschantz J, Hakanson R (1986). Calcitonin gene-related peptide in the eye: release by sensory nerve stimulation and effects associated with neurogenic inflammation. *Regul. Pept.* **16**, 107-115

236.Wårdell K (1992). Laser Doppler perfusion imaging. *Linkop. Stud. Sci. Tech.* **308**, 107

237.Wårdell K, Naver HK, Nilsson GE, Wallin BG (1993). The cutaneous vascular axon reflex in humans characterized by laser Doppler perfusion imaging. *Journal of Physiology* **460**, 185-199

238.Weinreich D, Wonderlin WF (1987). Inhibition of calcium-dependent spike after-hyperpolarization increases excitability of rabbit visceral sensory neurones. *J. Physiol. Lond.* **394**, 415-427

239.White DM, Helme RD (1985). Release of substance P from peripheral nerve terminals following electrical stimulation of the sciatic nerve. *Brain Research* **336**, 27-31

240.Wiesenfeld-Hallin Z (1988). Partially overlapping territories of nerves to hindlimb foot skin demonstrated by plasma extravasation to antidromic C-fiber stimulation in the rat. *Neurosci. Lett.* **84**, 261-265

241.Wiesenfeld-Hallin Z, Kinnman E, Aldskogius H (1988). Studies of normal and expansive cutaneous innervation territories of intact and regenerating C-fibres in the hindlimb of the rat. *Agents. Actions.* **25**, 260-262

242.Wiesenfeld-Hallin Z, Kinnman E, Aldskogius H (1989). Expansion of innervation territory by afferents involved in plasma extravasation after nerve regeneration in adult and neonatal rats. *Exp. Brain. Res.* **76**, 88-96

243.Williams TJ (1982). Vasoactive intestinal polypeptide is more potent than prostaglandin E2 as a vasodilator and oedema potentiator in rabbit skin. *Br. J. Pharmacol.* **77**, 505-509

244.Xu XJ, Hao JX, Wiesenfeld-Hallin Z, Hakanson R, Folkers K, Hökfelt T (1991). Spantide II, a novel tachykinin antagonist, and galanin inhibit plasma extravasation induced by antidromic C-fiber stimulation in rat hindpaw. *Neuroscience.* **42**, 731-737

245.Xu XJ, Dalsgaard CJ, Maggi CA, Wiesenfeld-Hallin Z (1992). NK-1, but not NK-2, tachykinin receptors mediate plasma extravasation induced by antidromic C-fiber stimulation in rat hindpaw: demonstrated with the NK-1 antagonist CP-96,345 and the NK-2 antagonist Men 10207. *Neurosci. Lett.* **139**, 249-252

246.Yoshida S, Matsuda Y (1979). Studies on sensory neurons of the mouse with intracellular-recording and horseradish peroxidase-injection techniques. *Journal of Neurophysiology* **42**, 1134-1145

247.Yoshida S, Matsuda Y, Samejima A (1978). Tetrodotoxin-resistant sodium and calcium components of action potentials in dorsal root ganglion cells of the adult mouse. *Journal of Neurophysiology* **41**, 1096-1106

248.Zhang S, Hoffert M (1987). Substance P is contained in myelinated nociceptor primary afferents. *Pain.* **Suppl. 4**, S281

249.Scott DT, Lam FY, Ferrell WR (1991). Time course of substance P-induced protein extravasation in the rat knee joint measured by micro-turbidimetry. *Neurosci. Lett.* **129**, 74-76

250.Scott DT, Lam FY, Ferrell WR (1992). Acute inflammation enhances substance P-induced plasma protein extravasation in the rat knee joint. *Regul. Pept.* **39**, 227-235

APPENDIX I - Laser Doppler flowmetry and laser Doppler perfusion imaging

The laser Doppler flowmeters (MBF2 and MBF3D, Moor Instruments, UK) use a near infra-red laser diode (wavelength = 780nm), and the time constant was set at the minimum (0.1sec). The diameter of the optical fibres used ranged from 0.2 to 0.25mm and the separation of the emitting and collection fibres ranged from 0.4mm to 0.6mm.

The laser Doppler perfusion imager (Lisca Developments, Linkoping, Sweden) uses a He-Ne laser (wavelength = 633nm). Care had to be taken when setting the scan parameters to ensure that the entire area of interest was scanned and that the scan time was not so great that any vasodilatation response was missed. For the single unit antidromic vasodilatation studies, the scan times varied from 20-65secs in the rabbit and from 10-30secs in the rat. The vasodilatation produced by antidromic stimulation of a single vasoactive unit lasts for longer than the time to take a single scan. Indeed, responses were usually seen in several consecutive scans, and to make Figures 3.3-3.6 and Figures 4.3-4.5 the response from 2-6 individual scans has been averaged (see below). Also, information about the time course of vasodilator responses of single C-fibres can be gathered from experiments using laser Doppler flowmetry (e.g. see Figure 4.6).

For the flare studies, scan times ranged from 14-18secs (mechanical stimulation of rat skin), 44secs-1min16secs (mechanical stimulation of rabbit skin) and 1min32sec-1min52sec (heat stimulation of rabbit skin). The flare responses to mechanical stimulation of rabbit and rat skin could be seen on consecutive scans (see Figures 5.1 and 5.4), and so it seems unlikely that any flare responses were missed. The flare response to heat stimulation of rabbit skin tends to peak within 30secs-1min, and recovers to baseline within about 2-3minutes (Shakhanbeh, 1989). Taking into account the time taken to remove the heat probe, mid-scan would have been at around 1 minute, and therefore the peak response should have been seen in the first scan. However, it is appreciated that by using the imaging system to assess the spatial properties of vasodilatation, the temporal resolution is compromised, especially when large scans are needed. Therefore, for detailed temporal information about blood flux in a tissue (e.g. time to peak, duration of response, recovery time) the laser Doppler flowmetry method is preferred since it provides a continual record of blood flux at a single point.

The Lisca software can perform image subtraction (e.g., Figure 4.7). However, it is not capable of averaging a number of such "difference" images. To produce images that show *average* blood flow responses from a number of individual scans (e.g., Figures 3.3-3.6 and 4.3-4.5) the following steps were followed:

1. Image subtraction (response image minus baseline image) was performed using the Lisca software (Data Analysis option; Image Subtraction option) resulting in a "difference" image. For each responsive unit, several of these "difference" images were made.
2. The Lisca software was used to make ASCII files of the "difference" images and of the baseline images (File handling option; Create ASCII File option)
3. The ASCII files of the "difference" images were opened into a spreadsheet (Excel), and they were averaged.
4. The ASCII file of the baseline image was opened in Excel, and the average baseline PIM value within the responsive area was calculated.
5. The maximum PIM value within the responsive area was calculated from the averaged ASCII file produced in step 3.
6. From steps 4 and 5, the maximum percentage increase in skin blood flow within the area of vasodilatation can be calculated.
7. The average ASCII file produced in step 3 was cut and pasted into CorelChart, and a spectral map using 4 colours was produced.
8. The spectral range was set so that each colour represented a band of percentage increase in skin blood flow from the baseline.
9. The chart was cut and pasted into CorelDraw for annotation and to draw on the afferent receptive fields when known.
10. To create a figure containing several difference images (e.g. Figures 5.1, 5.4 and 5.7), several ASCII files were pasted into CorelChart and one spectral map was produced.